ANALYSIS OF BUILDING-INTEGRATED RENEWABLE ENERGY SYSTEMS IN MODERN UK HOMES

A THESIS SUBMITTED TO THE UNIVERSITY OF MANCHESTER FOR THE DEGREE OF DOCTOR OF ENGINEERING IN THE FACULTY OF ENGINEERING AND PHYSICAL SCIENCES

2010

By

Alexander Glass

Mechanical, Aerospace and Civil Engineering

Contents

Abstract **7**
Declaration **8**
Copyright **9**
Acknowledgment **10**
List of Figures **14**
Nomenclature **18**
1 Aims and Objectives **23**
2 Introduction **25**
2.1 The Need for Reducing CO_2 Emissions 25
2.1.1 Climate Change 25
2.1.2 Depletion of Fossil Fuels 29
2.1.3 UK Carbon Emissions 30
2.1.4 The UK Domestic Sector 31
2.1.5 Summary 32
2.2 The Code for Sustainable Homes (CSH) 33
3 Literature Review **36**
3.1 Achieving Sustainability in Urban Developments in the UK 36
3.2 Review of Existing Zero-Carbon Homes in the UK 43
3.3 Summary 49
4 Barratt Developments PLC **51**
4.1 The History of Barratt Developments 51
4.2 Market Position 52
4.3 Marketing Strategy and Philosophy 55
5 The EcoSmart Show Village **58**
6 Methodology **68**
6.1 Monitoring Strategy and Apparatus 68
6.1.1 Simulated Living Conditions 69
6.1.3 Measuring Apparatus 69
6.1.4 Data Capture 73
6.2 Data Conditioning 75
6.2.1 Data Normalisation and Interpolation 75
6.2.2 Time Stamp Correction 77
6.3 Data Validation 78
6.3.1 Energy Readings 78
6.3.2 IButton Sensors 79
6.4 Statistical Methods for Data Analysis 81

6.5 Payback Calculation Method 83
6.5.1 Feed-in Tariffs (FIT) 84
6.5.2 Renewable Heat Incentive (RHI) 85
6.5.3 Calculating Simple Financial Payback 86
6.5.4 Calculating Energy and Carbon Payback 88
7 Support Systems 91
7.1 The Inverter 91
7.1.1 Theoretical Background 91
7.1.2 Efficiency Losses 92
7.1.3 Inverter Energy Consumption 95
7.1.4 Inverter Model 96
7.2 The Heat Store 97
8 Preliminary Modelling 99
8.1 Estimating Beam and Diffuse Components of Global Solar Radiation 99
8.2 Estimating Dew Point Temperature 103
8.3 Estimating Air Density 104
8.4 Finding Wind Direction Difference 106
9 Estimating Space Heating Requirements 107
9.1 Input Data 107
9.1.1 Internal Temperature 107
9.1.2 Ventilation Losses 108
9.2 Building Energy Models 111
9.2.1 Simple Heat Loss Model 111
9.2.2 SAP Calculations 112
9.2.3 Software Simulation – CASAnova 113
9.2.4 Model Comparison 114
9.2.5 Modelling Limitations 115
9.2.6 Model Validation 115
10 Photovoltaic Systems 117
10.1 Introduction 117
10.1.1 Background Theory 117
10.1.2 Capital Cost, Embodied Energy and Carbon 119
10.1.3 EcoSmart Village Set-up 121
10.2 Availability of Solar Energy 122
10.3 Photovoltaic Energy Prediction 123
10.3.1 PV GIS 123
10.3.2 PV Watts 125
10.3.3 PV SYST 125
10.3.4 SAP 2005 126
10.4 Measured Results 126
10.5 System Reliability 129
10.6 PV System Modelling 129
10.6.1 Angle Transformation 129
10.6.2 Calculating Cell Temperature 130
10.6.3 Inverter Model 135
10.6.4 The PV Model 136
10.7 Model Validation 136
10.8 Evaluation and Comparison of PV Estimation Tools 139
10.8.1 Quantitative Comparison 140
10.8.2 Qualitative Comparison 142
10.9 Considerations for the Integration of PV Systems 142

10.9.1 Minimum and Maximum Yields 143
10.9.2 Effect of Varying Latitude 143
10.9.3 UK Benchmark – Look-up Chart for Estimating PV Output 145
10.9.4 Effect of PV Inclination and Orientation 145
10.9.5 Effect of Longitude 147
10.9.6 Summary 147
10.10 Financial, Energy and Carbon Savings 148
10.11 Conclusion 150
11 Solar Thermal Systems 152
11.1 Introduction 152
11.1.1 Background Theory 152
11.1.2 EcoVillage Set-up 155
11.1.3 Set-up Problems 157
11.1.4 Capital cost, Embodied Energy and Embodied CO_2 157
11.2 Initial Energy Generation Estimate 159
11.3 Measured Output from EcoSmart Systems 168
11.4 Domestic Control Systems 172
11.4.1 Methodology 172
11.4.2 Test System 1 172
11.4.3 Test System 2 176
11.4.4 Control System Set-up 179
11.5 Solar Thermal Model 184
11.5.1 Modelling Options 184
11.5.2 Solar Collector Model 185
11.5.3 Control System and Heat Transfer Model 188
11.5.4 Cylinder Model 189
11.6 Model validation 191
11.6.1 Finding U-value of the Storage Cylinder 191
11.6.2 Steady-state Validation of Cylinder Model 193
11.6.3 Input Data for Model Validation 195
11.6.4 Detailed Model Validation - April 2010 198
11.7 Modelling Domestic Solar Thermal Systems 204
11.7.1 Analysing Test System 1 204
11.7.2 Analysing Test System 2 208
11.7.3 Analysing EcoSmart Alderney System 209
11.7.4 Improving EcoSmart Alderney System 213
11.7.5 Analysis Vertical Solar Thermal Panel 215
11.8 Financial, Energy and Carbon Savings 216
11.9 Visitor Feedback 219
11.10 Conclusion 219
12 Micro Wind Turbine Systems 222
12.1 Introduction 222
12.1.1 Background Theory 223
12.1.2 EcoSmart Village Set-up 225
12.1.3 Capital Cost, Embodied Energy and Embodied CO_2 227
12.2 Urban Wind Potentials 230
12.2.1 Average Wind Speed 230
12.2.2 Turbulence Considerations 231
12.3 Predicting Wind Generation 235
12.3.1 Estimating Average Wind Speed 235
12.3.2 Weibull and Rayleigh Distribution 236
12.3.3 Estimated Annual Yield 237

12.4 Measured Data 238
12.4.1 Wind Data 238
12.4.2 Inverter Losses and Energy Consumption 242
12.4.3 Measured Energy Output 242
12.5 Reliability 243
12.6 System Modelling 245
12.6.1 Modelling Options 245
12.6.2 Micro Wind Turbine Model 246
12.6.3 Model Results and Discussion 248
12.7 Detailed Analysis of Turbulence 249
12.7.1 Micro Wind Turbine Response to Turbulence 250
12.7.2 Detailed Analysis of Turbulence at the Test Site 252
12.7.3 Corroboration with Other Research 255
12.8 Payback rate and carbon savings 256
12.9 Visitor Feedback 258
12.10 Conclusion 259
13 Ground Source Heat Pump Systems 261
13.1 Introduction 261
13.1.1 Theoretical Background 262
13.1.2 EcoSmart Village Set-up 264
13.1.3 Set-up Problems 266
13.1.4 Capital Cost and Embodied CO_2 266
13.2 Available Energy from the Ground 267
13.3 Theoretical Output 270
13.4 Measured Results and Discussion 271
13.4.1 Adjusting Ventilation Losses 271
13.4.2 Electricity Consumption 272
13.4.3 Coefficient of Performance 274
13.4.4 Temperature and Humidity Control 275
13.5 System Reliability 277
13.6 Performance Assessment 278
13.7 Visitor Feedback 280
13.8 Financial and Carbon Savings 281
13.9 Conclusion 282
14 Micro Combined Heat and Power Systems 284
14.1 Introduction 284
14.1.1 Theoretical Background 284
14.1.2 EcoSmart Village Set-up 285
14.1.3 Capital Cost and Embodied Carbon 287
14.2 Results from Other Research 288
14.3 Theoretical Output 289
14.4 Measured Output 290
14.4.1 Buckingham System 290
14.4.2 Edinburgh System 295
14.4.3 Summary and Discussion 298
14.5 System Reliability 300
14.6 Visitor Feedback 300
14.7 Financial and Carbon Savings 301
14.8 Conclusion 302

15 EcoSmart Village Performance and Recommendations 304
15.1 Performance of Renewable Energy Systems..... 304
15.2 Recommendations of EcoSmart Village systems and possible improvements 305
16 Conclusion 307
16.1 Availability of Resources 307
16.2 Predicting Realistic Performance..... 308
16.3 Actual System Performance at the EcoSmart Test Site 309
16.4 Lessons Learnt..... 310
16.5 Recommendation 311
17 Further Work 313
References..... 314
Appendices 329
A. PV Watts and PV SYST Comparison 329
B. Visitor Feedback Questionnaire 334

Abstract

Driven by climate change and the impending depletion of fossil fuels, the UK Government has set the great challenge to UK builders to produce zero-carbon homes as of 2016. Due to a lack of experience the merits of integrating onsite micro renewable energy systems were largely unknown. Barratt Development PLC, UK's largest builder, set out in 2006 to investigate how these new building regulations can best be tackled. The key points to be investigated are: how much CO_2 can be offset using renewable energy systems in standard homes and at what cost; how reliable are these systems; and how can their performance be improved? At the EcoSmart village several systems were tested under realistic conditions, including PV, Solar Thermal, Micro Wind Turbines, GSHPs and microCHP.

The systems were tested over a 12-month period, integrated into standard Barratt homes, and running under near real-life conditions. Data was recorded from the test-site, including heat and electrical energy generation and consumption, temperature data and weather data. This data was used to establish the theoretical performance of the systems at the test site, and by doing so simple methods were found and tested that can be used by builders or architects to gain a better understanding of the expected performance of a particular system. The estimated energy generation was then compared to the measured performance. Detailed modelling and analysis of observations was carried out to provide explanations for any discrepancies, and based on this general recommendations were made on how the performance of the systems could be improved.

Given the commercial drivers behind carrying out this research project, a high emphasis was given to financial implications of installing the systems. For this purpose payback periods and life-time savings were estimated, based on measured performance and other influences such as feed-in tariffs. This was also done for embodied energy and embodied carbon, as this will ultimately determine how the systems can help to fulfil the purpose of Government legislation, which is to reduce the carbon footprint of the UK domestic sector. The table below provides a summary of the performance that can be achieved by some of the systems at the EcoSmart village, provided that the recommendations for simple improvements given in this thesis are followed.

System	Net Life-time Savings			Specific cost per tCO_2
	No. years	Financial	Carbon (tCO_2)	
PV (1kWp)	30	£4,690	8.0	-£586
Solar Thermal	25	-£68	4.1	£17
GSHP (vertical)	23	£2.479 to £12,804	12.2 to 22.2	-£203 to -£577

Declaration

No portion of the work referred to in the thesis has been submitted in support of an application for another degree or qualification of this or any other university or other institute of learning.

Copyright

i. The author of this thesis (including any appendices and/or schedules to this thesis) owns certain copyright or related rights in it (the "Copyright") and s/he has given The University of Manchester certain rights to use such Copyright, including for administrative purposes.

ii. Copies of this thesis, either in full or in extracts and whether in hard or electronic copy, may be made **only** in accordance with the Copyright, Designs and Patents Act 1988 (as amended) and regulations issued under it or, where appropriate, in accordance with licensing agreements which the University has from time to time. This page must form part of any such copies made.

iii. The ownership of certain Copyright, patents, designs, trade marks and other intellectual property (the "Intellectual Property") and any reproductions of copyright works in the thesis, for example graphs and tables ("Reproductions"), which may be described in this thesis, may not be owned by the author and may be owned by third parties. Such Intellectual Property and Reproductions cannot and must not be made available for use without the prior written permission of the owner(s) of the relevant Intellectual Property and/or Reproductions.

iv. Further information on the conditions under which disclosure, publication and commercialisation of this thesis, the Copyright and any Intellectual Property and/or Reproductions described in it may take place is available in the University IP Policy (see http://www.campus.manchester.ac.uk/medialibrary/policies/intellectual-property.pdf), in any relevant Thesis restriction declarations deposited in the University Library, The University Library's regulations (see http://www.manchester.ac.uk/library/aboutus/regulations) and in The University's policy on presentation of Theses.

Acknowledgment

I would like to take this opportunity to thank my two supervisors Prof. Geoff Levermore and Dr. Tony Sung for their invaluable help and support. Tony regularly went out of his way to help me and used every opportunity to pass on his wealth of knowledge and experience. He actively encouraged me to improve all my skills, academic and personal, and I am very thankful for that. Geoff was always there for me whenever support or advice was needed, providing great academic as well as moral guidance. Both Geoff and his wife Carolyn have been very helpful and accommodating, and did whatever they could to ensure that I was able to carry out this research with the best available resources. I am very grateful for being given the opportunity to work with both Geoff and Tony, I have learnt many valuable things from both of them.

I also thank Barratt Developments PLC for providing the testing facilities and making this research possible. Mr. Terry Ritchie in particular was always helpful to provide whatever was required.

I would also like to acknowledge the support given by the University of Manchester, in particular Dr. David Stanley and Paul Townsend, who have both been extremely helpful and have given me much of their time. My special thanks also goes to Rebecca Warren, who has put in a great amount of effort to set up the solar thermal test rig, despite the many unexpected challenges we encountered along the way. Thank you to families Levermore and Handley for allowing me to take measurements from their domestic solar thermal systems, the data and lessons learnt from this makes up a significant part of my thesis. Alan Williamson has provided great advice on some electrical systems including inverters, and Frances Hill often gave me valuable inspiration in the meetings we had with Geoff and undergraduate students.

I'm grateful for my parents and the freedom they have given me. Things weren't easy in the past, but I'm very happy for being given the opportunity to make my own decisions early on in life. I am very pleased to see that the outcome of my decisions has now made everyone happy.

Last but not least I would also like to thank all my dear friends, Joe Dalton, Gemma Warrington, Lucy Silman, Amy Crawford, Paul Cryer, Dee Richardson, Lauren Hurley, John 'bumbaclot' Linklater, Sian Connell and in particular Craig Hale who has spent many hours proof-reading this thesis while at the same time putting our plans of taking over the world into action. I will never forget some of the amazing times I had with you guys including Ibiza, the New Years Cabin extravaganza, skiing in Bulgaria, trotting in the fields around Lake Bala, the many crazy nights out we had, and the list goes on. I would also like to thank Kathryn Griffiths & Dooch, the thought of you two never fails to make me smile. Although challenging at times you have become a cherished part of my life, and hopefully will be for a long time to come. Thanks to each and every one of you the last 4 years have truly been 'the time of my life'.

List of Tables

TABLE 3.A: DCLG[63] ESTIMATED COSTS IN 2008 OF ACHIEVING CSH LEVEL 6 RATING 42
TABLE 4.A: BARRATT DEVELOPMENTS 2009 ESTIMATED MARKET SHARE[92] 55
TABLE 5.A: LATITUDE AND LONGITUDE OF ECOSMART VILLAGE (SOURCE: GOOGLE EARTH) 58
TABLE 5.B: SHOWING DETAILED INFORMATION FOR ALDERNEY 61
TABLE 5.C: SHOWING DETAILED INFORMATION FOR PALMERSTON 62
TABLE 5.D: SHOWING DETAILED INFORMATION FOR WASHINGTON 63
TABLE 5.E: SHOWING DETAILED INFORMATION FOR EDINBURGH 64
TABLE 5.F: SHOWING DETAILED INFORMATION FOR BUCKINGHAM 65
TABLE 5.G: SHOWING DETAILED INFORMATION FOR MALVERN 66
TABLE 5.H: SHOWING DETAILED INFORMATION FOR WINDERMERE 67
TABLE 6.A: ACCURACY OF DAVIS VANTAGE PRO 2 PLUS WEATHER STATION 70
TABLE 6.B: UNIT CONVERSIONS OF WEATHER DATA 76
TABLE 6.C: INTERPOLATION OF WEATHER DATA 76
TABLE 6.D: INTERPOLATION OF INTERNAL IBUTTON DATA 76
TABLE 6.E: COMPARISON OF VARIOUS METER READINGS FOR MALVERN PV SYSTEM 78
TABLE 6.F: ELECTRICITY MEASUREMENT BALANCE FOR PALMERSTON, FEBRUARY 2007 79
TABLE 6.G: 2010 FEED-IN TARIFFS[113] 84
TABLE 6.H: PROPOSED RHI TARIFFS[115] 85
TABLE 6.I: ESTIMATED AVERAGE ENERGY PRICES[116] OVER PAYBACK PERIOD 87
TABLE 6.J: CAPITAL COST FOR ALL SYSTEMS INSTALLED AT ECOSMART SHOW VILLAGE 87
TABLE 6.K: CARBON FOOTPRINT OF GRID ENERGY AND AVERAGE HOUSEHOLD NEAR MANCHESTER 88
TABLE 7.A: INVERTER ENERGY CONSUMPTION ON DAYS WITH NEGLIGIBLE WIND SPEEDS 96
TABLE 8.A: CALCULATED VALUES FOR DIFFUSE FACTOR AND COMPONENTS OF SOLAR RADIATION 101
TABLE 8.B: COMPARISON OF DIFFUSE FRACTION BETWEEN MODEL AND CONTROL DATA 103
TABLE 8.C: WIND DIRECTION CONVERSION 106
TABLE 9.A: MEASURED AVERAGE INTERNAL TEMPERATURES OVER A 12-MONTH PERIOD 107
TABLE 9.B: RESULTS FROM PRESSURISATION TEST 110
TABLE 9.C: SAP ESTIMATED VENTILATION RATE 110
TABLE 9.D: RESULTS FOR SIMPLIFIED HEAT LOSS MODEL 112
TABLE 9.E: SPACE HEATING DEMAND ACCORDING TO SAP CALCULATIONS 112
TABLE 9.F: ANNUAL ENERGY DEMAND FOR SPACE HEATING FROM CASANOVA SIMULATION 113
TABLE 9.G: COMPARISON BETWEEN ALL THREE MODELS 114
TABLE 9.H: HEATING SYSTEMS AT THE ECOSMART VILLAGE 115
TABLE 9.I: COMPARISON OF CASANOVA ESTIMATE WITH MEASURED HEAT SUPPLY 116
TABLE 10.A: CAPITAL COST OF THE ECOSMART PV SYSTEMS IN 2006 120
TABLE 10.B: SUMMARY OF ESTIMATES FOR EMBODIED ENERGY OF PV SYSTEMS 120
TABLE 10.C: ESTIMATED EMBODIED CARBON OF BUILDING-INTEGRATED PV SYSTEMS 120
TABLE 10.D: SPECIFICATIONS OF SOLARCENTURY PV SYSTEM 121
TABLE 10.E: SUMMARY OF ECOSMART VILLAGE PV SYSTEMS 121
TABLE 10.F: PV GIS ESTIMATES FOR ECOSMART VILLAGE 124
TABLE 10.G: PV WATTS ESTIMATES FOR ECOSMART SHOW VILLAGE 125
TABLE 10.H: PV SYST ESTIMATION FOR ECOSMART SHOW VILLAGE 125
TABLE 10.I: SAP 2005 ESTIMATE FOR ECOSMART VILLAGE 126
TABLE 10.J: MONTHLY BREAKDOWN OF MEASURED PV GENERATION FROM ALL METERS 127
TABLE 10.K: DISCREPANCIES OF PV GIS RESULTS COMPARED TO MEASURED DATA 141
TABLE 10.L: DISCREPANCIES OF PV WATTS RESULTS COMPARED TO MEASURED DATA 141
TABLE 10.M: DISCREPANCIES OF PV SYST RESULTS COMPARED TO MEASURED DATA 141
TABLE 10.N: COMPARISON OF PV ESTIMATION TOOLS 142
TABLE 10.O: ESTIMATED ANNUAL PV GENERATION AT EXTREME WEATHER CONDITIONS 143
TABLE 10.P: PV GIS ESTIMATES FOR REFERENCE LOCATIONS THROUGHOUT THE UK 144
TABLE 10.Q: PV ESTIMATES FOR LOCATIONS AT DIFFERENT LONGITUDE 147
TABLE 10.R: CAPITAL COST AND EMBODIED CARBON FOR ROOF-INTEGRATED 1KWP PV SYSTEM 148
TABLE 10.S: PERFORMANCE OF ECOSMART SYSTEMS AND UK PV BENCHMARK 148
TABLE 10.T: AVERAGE FINANCIAL SAVINGS ASSUMING THE SYSTEMS ARE NEW-BUILDS, INSTALLED BEFORE APRIL 2012 149
TABLE 10.U: PAYBACK RATES AND LIFETIME SAVINGS; FINANCIAL, ENERGY AND CO_2 149
TABLE 11.A: SYSTEM PARAMETERS FOR FLAT PANEL AND EVACUATED TUBE SYSTEM 156

TABLE 11.B: CAPITAL COST FOR ECOSMART VILLAGE SOLAR THERMAL SYSTEMS 157
TABLE 11.C: EMBODIED ENERGY AND CO_2 IN SOLAR THERMAL SYSTEM LIFE-CYCLE[209] 158
TABLE 11.D: GENERIC $F_R(\tau\alpha)_n$ AND $F_R U_L$ VALUES FOR SOLAR THERMAL COLLECTORS 160
TABLE 11.E: MONTHLY PARAMETERS REQUIRED FOR *F*-CHART CALCULATIONS 160
TABLE 11.F: RESULTS FROM BEAM TRANSMITTANCE-ABSORPTION LOSSES CALCULATIONS 163
TABLE 11.G: PARAMETERS REQUIRED FOR *F*-CHART CALCULATION, BASED ON FLAT PANEL SYSTEM 164
TABLE 11.H: X AND Y VALUE CALCULATIONS REQUIRED FOR *F*-CHART CALCULATION, BASED ON FLAT PANEL SYSTEM 165
TABLE 11.I: X AND Y VALUE CALCULATIONS REQUIRED FOR *F*-CHART CALCULATION, BASED ON EVACUATED TUBE SYSTEM 165
TABLE 11.J: *F*-CHART FRACTION, POTENTIAL ENERGY GENERATION AND EFFICIENCY OF SOLAR THERMAL SYSTEMS AT ECOSMART SHOW VILLAGE 166
TABLE 11.K: MEASURED ENERGY GENERATION FROM EVACUATED TUBE SYSTEM 168
TABLE 11.L: COMPARISON OF *F*-CHART ESTIMATE AND MEASURED GENERATION FROM HEAT METER AND IBUTTONS 169
TABLE 11.M: ANNUAL YIELD OF ECOSMART VILLAGE SOLAR THERMAL SYSTEMS 169
TABLE 11.N: GAS CONSUMPTION FOR ALDERNEY AND WINDERMERE HOMES 170
TABLE 11.1.4.O: ENERGY CONSUMPTION OF SOLAR THERMAL PUMPS 171
TABLE 11.P: DESIGN PARAMETERS OF TEST SYSTEM 1 173
TABLE 11.Q: CONTROL TEMPERATURES AND RESPECTIVE IBUTTON VALUES, WITH REFERENCE TO FIGURE 11.11 175
TABLE 11.R: DESIGN PARAMETERS OF TEST SYSTEM 2 177
TABLE 11.S: FLOW CONTROL PROFILE BASED ON TEMPERATURE DIFFERENCE BETWEEN CYLINDER AND COLLECTOR 178
TABLE 11.T: MODEL INPUT PARAMETERS FOR TEST SYSTEM 1 196
TABLE 11.U: DRAW-OFF PATTERN FOR 14TH APRIL 2010 197
TABLE 11.V: TYPICAL DRAW-OFF PATTERN FOR TEST SYSTEM 1 198
TABLE 11.W: COMPARISON BETWEEN MEASURED AND MODELLED GENERATION OF TEST SYSTEM 1 199
TABLE 11.X: ESTIMATING ANNUAL YIELD OF TEST SYSTEM 1, USING MODEL AND MEASURED RESULTS 205
TABLE 11.Y: ANNUAL YIELD OF TEST SYSTEM 1 206
TABLE 11.Z: MODELLED ANNUAL YIELD BETWEEN JULY 2009 AND JUNE 2010 209
TABLE 11.AA: INPUT PARAMETERS FOR ECOSMART VILLAGE ALDERNEY SYSTEM MODELLING 210
TABLE 11.BB: PERFORMANCE OF ALDERNEY EVACUATED TUBE SYSTEM WITH OPTIMISED BOILER 214
TABLE 11.CC: SUMMARY OF SYSTEM COST, ENERGY AND CARBON 217
TABLE 11.DD: FINANCIAL ANNUAL SAVINGS 217
TABLE 11.EE: PAYBACK RATES AND LIFETIME SAVINGS; FINANCIAL, ENERGY AND CARBON 217
TABLE 11.FF: ENERGY AND CO_2 ESTIMATES FROM OTHER RESEARCH 218
TABLE 12.A: WIND TURBINE SPECIFICATIONS 225
TABLE 12.B: CAPITAL COST OF THE MICRO WIND TURBINE SYSTEMS 227
TABLE 12.C: ESTIMATED EMBODIED ENERGY OF ECOSMART TURBINES, BY COMPONENT 228
TABLE 12.D: ESTIMATED EMBODIED ENERGY OF ECOSMART TURBINES, BY COMPONENT 229
TABLE 12.E: DIFFERENCE BETWEEN MEASURED AVERAGE WIND SPEED AND NOABL DATABASE (DATA SOURCE: NOABL AND TURAN ET AL.[258]) 231
TABLE 12.F: ROUGHNESS LENGTH AND DRAG COEFFICIENT FOR DIFFERENT TERRAIN TYPES (SOURCE: AUSTRALIAN STANDARD AS1170.2) 233
TABLE 12.G: ANNUAL AVERAGE WIND SPEED PREDICTIONS COMPARED TO MEASUREMENTS 235
TABLE 12.H: INITIAL ESTIMATES FOR MICRO WIND GENERATION AT THE ECOSMART TEST SITE 237
TABLE 12.I: KEY FOR FIGURE 12.8 238
TABLE 12.J: RESULTS FROM WIND DATA ANALYSIS (SOURCE: WINDOGRAPHER) 239
TABLE 12.K: AVERAGE DAILY INVERTER ENERGY CONSUMPTION 242
TABLE 12.L: SUMMARY OF ANNUAL WIND TURBINE PERFORMANCE AT ECOSMART VILLAGE 243
TABLE 12.M: INVERTER ENERGY CONSUMPTION USED FOR INVERTER MODELLING 248
TABLE 12.N: RESULTS FROM MICRO WIND TURBINE MODEL 248
TABLE 12.O: RESULTS FROM WINDOGRAPHER SIMULATION 248
TABLE 12.P: TURBINE GENERATION AND INVERTER LOSSES DURING COINCIDING GENERATING PERIODS 252
TABLE 12.Q: CAPITAL COST AND EMBODIED ENERGY AND CARBON, COMPARED TO ESTIMATED ANNUAL DC YIELD 257

TABLE 12.R: ANNUAL SAVINGS EXPECTED AT ECOSMART TEST SITE BASED ON OPTIMUM CONDITIONS (NO INVERTER, TURBINE LOCATED AWAY FROM ROOF EDGES) 257
TABLE 12.S: PAYBACK RATES FROM ECOSMART SYSTEMS BASED ON OPTIMUM CONDITIONS (NO INVERTER, TURBINE LOCATED AWAY FROM ROOF EDGES) 257
TABLE 12.T: ESTIMATED PAYBACK RATES FOR OPTIMUM PLACEMENT BUT USING AN INVERTER 258
TABLE 13.A: ECOSMART VILLAGE GSHP SYSTEM SPECIFICATIONS 265
TABLE 13.B: CAPITAL COST OF GSHP SYSTEMS AT THE ECOSMART VILLAGE 266
TABLE 13.C: ESTIMATED EMBODIED CO_2 OF GSHP UNITS AT ECOSMART VILLAGE 267
TABLE 13.D: ESTIMATED SPACE HEATING REQUIREMENTS 270
TABLE 13.E: ELECTRICAL ENERGY REQUIRED FOR SPACE HEATING USING GSHP, ASSUMING CP=3 270
TABLE 13.F: ADJUSTED AIR CHANGE RATES 272
TABLE 13.G: MONTHLY SUMMARY OF GSHP RELATED DATA FOR PALMERSTON AND MALVERN 273
TABLE 13.H: ADJUSTED ANNUAL HEAT DEMAND AND RESULTING ANNUAL CP VALUES 274
TABLE 13.I: RESULTS FROM MANUAL HEAT ENERGY CALCULATIONS BASED ON TEMPERATURE 275
TABLE 13.J: ANNUAL AVERAGE INTERNAL TEMPERATURES 276
TABLE 13.K: ANNUAL SAVINGS OF THE THREE GSHP SYSTEMS, BASED ON 2011 RHI TARIFFS 281
TABLE 13.L: FINANCIAL AND CARBON PAYBACK PERIODS AND LIFE-TIME SAVINGS 281
TABLE 14.A: MANUFACTURER SPECIFICATIONS OF WHISPERGEN MCHP SYSTEM 286
TABLE 14.B: CAPITAL COST OF MCHP SYSTEM AT ECOSMART VILLAGE 287
TABLE 14.C: ESTIMATED EMBODIED CO_2 OF THE WHISPERGEN MCHP UNITS 288
TABLE 14.D: ESTIMATED HEATING REQUIREMENTS 289
TABLE 14.E: ESTIMATED GAS CONSUMPTION AND ELECTRICITY GENERATION OF MCHP SYSTEMS 289
TABLE 14.F: MONTHLY BREAKDOWN OF MEASURED RESULTS FOR BUCKINGHAM MCHP SYSTEM 290
TABLE 14.G: ELECTRICAL EFFICIENCY AND OVERALL SYSTEM EFFICIENCY FOR BUCKINGHAM 294
TABLE 14.H: MONTHLY BREAKDOWN OF MEASURED RESULTS FOR EDINBURGH MCHP SYSTEM 295
TABLE 14.I: ELECTRICAL EFFICIENCY AND OVERALL EFFICIENCY FOR EDINBURGH SYSTEM 297
TABLE 14.J: ANNUAL SAVINGS FOR THE MCHP SYSTEMS AT THE ECOSMART VILLAGE 301
TABLE 14.K: PAYBACK RATES AND LIFE-TIME SAVINGS OF THE MCHP SYSTEMS 301
TABLE 15.A: ESTIMATED LIFE-TIME FINANCIAL AND CARBON SAVINGS BASED ON ECOSMART VILLAGE MEASUREMENTS 304
TABLE 15.B: EXPECTED LIFE-TIME SAVINGS OF IMPROVED ECOSMART VILLAGE SYSTEMS 306

List of Figures

FIGURE 2.1: OBSERVED AND MODELLED TEMPERATURE, COMPARING NATURAL VARIATIONS AND VARIATIONS ACCOUNTING FOR HUMAN INTERVENTION (SOURCE: IPCC AR4[14]) 27
FIGURE 2.2: SECTORAL BREAKDOWN OF POTENTIAL CO_2 EMISSION REDUCTIONS BY 2030 (SOURECE: IPCC AR4[14]) 28
FIGURE 2.3: 2008 GREENHOUSE GAS EMISSION DISTRIBUTION BY SECTOR (BASED ON 2010 DECC FIGURES FOR 2008 EMISSIONS[25]) 30
FIGURE 2.4: THE RECENT TREND IN UK GREENHOUSE GAS EMISSIONS (SOURCE: DECC 2010[25]) 31
FIGURE 2.5: BREAKDOWN OF ENERGY USE IN UK DOMESTIC SECTOR IN 2000 (SOURCE: DTI 2002) 32
FIGURE 2.6: CSH POINT SCORING SYSTEM AND CATEGORIES (SOURCE: CSH[28], 2006) 34
FIGURE 2.7: CSH LEVEL RATING SYSTEM (SOURCE: CSH[28], 2006) 34
FIGURE 2.8: REQUIRED REDUCTION OF DESIGN EMISSIONS RATE FOR DIFFERENT CODE LEVELS (SOURCE: CSH[28], 2006) 35
FIGURE 3.1: COST AND SAVINGS ASSOCIATED WITH REDUCING CO_2 EMISSIONS BY 60% BY 2050 (SOURCE: SHORROCK ET AL[33]. 2005) 37
FIGURE 3.2: ESTIMATED COST OF CO_2 SAVINGS PER YEAR FROM VARIOUS LOW OR ZERO CARBON TECHNOLOGIES (SOURCE: MAUNSELL & CAPENER[39], 2007) 38
FIGURE 3.3: CAPITAL COST FOR CO_2 SAVING FOR VARIOUS LOW AND ZERO CARBON TECHNOLOGIES (SOURCE: RAB[43], 2007) 39
FIGURE 3.4: INTERACTION BETWEEN SUPPLY CHAIN, TECHNOLOGY AND BEHAVIOUR TO ACHIEVE ZERO-CARBON HOMES (SOURCE: THEOBALD ET AL[48], 2008) 41
FIGURE 3.5: BARRATT GREEN HOUSE (LEFT) AND KINGSPAN LIGHTHOUSE (RIGHT) 44
FIGURE 3.6: PHOTOGRAPH OF BEDZED DEVELOPMENT 45
FIGURE 3.7: SCHEMATIC DIAGRAM SHOWING BEDZED FEATURES (SOURCE: TWINN[77] 2003) 46
FIGURE 3.8: MODEL OF HANHAM HALL HOUSING DESIGN (SOURCE: BARRATT DEVELOPMENTS) 47
FIGURE 3.9: MODEL OF GREENWATT WAY DEVELOPMENT (SOURCE: INSIDE HOUSING) 48
FIGURE 4.1: HOUSING (NEW BUILD) STARTS AND COMPLETIONS IN ENGLAND SINCE 1997 (SOURCE: DCLG HOUSING STATISTICS[95] 2009) 53
FIGURE 4.2: AGE STRUCTURE OF THE UK WITH 2010 AS BASELINE (SOURCE: OFFICE FOR NATIONAL STATISTICS) 54
FIGURE 4.3: REGIONAL BREAKDOWN OF HOUSE PRICES IN AUGUST 2009 AND 2010 (SOURCE: DCLG PRICE INDEX[97] 2010) 54
FIGURE 4.4: THE LATEST BARRATT DEVELOPMENTS INNOVATION; ECO-TOWN HANHAM HALL (SOURCE: BARRATT DEVELOPMENTS) 57
FIGURE 5.1: MAP SHOWING LOCATION OF BUCKSHAW ECOSMART VILLAGE (SOURCE: ECOSMART VILLAGE BROCHURE) 58
FIGURE 5.2: PHOTOGRAPH SHOWING A MODEL OF THE TEST SITE 59
FIGURE 5.3: SCHEMATIC LAYOUT OF THE TEST HOMES 59
FIGURE 5.4: EFFICIENCY MEASURES AND RENEWABLE ENERGY SYSTEMS INCORPORATED AT THE ECOSMART VILLAGE 60
FIGURE 5.5: SCHEMATIC DIAGRAMS OF ALDERNEY SYSTEMS 61
FIGURE 5.6: SCHEMATIC DIAGRAMS OF PALMERSTON SYSTEMS 62
FIGURE 5.7: SCHEMATIC DIAGRAMS OF WASHINGTON SYSTEMS 63
FIGURE 5.8: SCHEMATIC DIAGRAMS OF EDINBURGH SYSTEMS 64
FIGURE 5.9: SCHEMATIC DIAGRAMS OF BUCKINGHAM SYSTEMS 65
FIGURE 5.10: SCHEMATIC DIAGRAMS OF MALVERN SYSTEMS 67
FIGURE 5.11: SCHEMATIC DIAGRAMS OF WINDERMERE SYSTEMS 67
FIGURE 6.1: DAVIS VANTAGE PRO 2 PLUS WEATHER STATION AT ECOSMART VILLAGE 70
FIGURE 6.2: IMPORT/EXPORT SINGLE PHASE CREDIT METER 5235 71
FIGURE 6.3: ELECTRICITY METER METERMAID 71
FIGURE 6.4: SUPERCAL 539 PLUS HEAT METER 72
FIGURE 6.5: IBUTTON TEMPERATURE/HUMIDITY RECORDER 72
FIGURE 6.6: EXAMPLE OF PV GENERATION AND SOLAR IRRADIATION ALIGNMENT 77
FIGURE 6.7: TESTING THERMAL EFFECTS OF USING BLU-TACK TO ATTACH IBUTTONS 80

FIGURE 6.8: TEMPERATURE VARIATION OF IBUTTONS ATTACHED WITH DIFFERENT LAYERS OF BLU-TACK 80
FIGURE 6.9: LINEAR EQUATION DERIVED USING LEAST SQUARES TECHNIQUE TO CORRELATE IBUTTON READINGS AND CONTROL READINGS 81
FIGURE 6.10: ESTIMATED CARBON CONTENT OF RENEWABLE ENERGY GENERATION (SOURCE: POSTNOTE[120] 2006) 89
FIGURE 7.1: EFFICIENCY VARIATION WITH POWER LOAD OF TYPICAL INVERTER (SOURCE: MONDOL[127], 2007) 93
FIGURE 7.2: MALVERN PV INVERTER EFFICIENCY VARIATION WITH RESPECT TO DC LOAD 93
FIGURE 7.3: PV INVERTER EFFICIENCY WITH 15W DC CORRECTION FOR SWITCHING LOSSES 94
FIGURE 7.4: CONTROL INVERTER EFFICIENCY DISTRIBUTION 95
FIGURE 7.5: LINEAR MODEL TO REPRESENT INVERTER EFFICIENCY DISTRIBUTION 96
FIGURE 7.6: GLEDHILL HEAT STORE SYSTEM FOR SOLAR THERMAL 'BOILERMATESOL' (SOURCE: GLEDHILL BROCHURE) 98
FIGURE 8.1: DIAGRAM SHOWING THE DECLINATION ANGLE AS A RESULT OF EARTH TILT 100
FIGURE 8.2: MONTHLY DISTRIBUTION OF DIFFUSE AND BEAM COMPONENTS 102
FIGURE 8.3: MODELLED VARIATION OF RADIATION FRACTION WITH CLEARNESS INDEX (SOURCE: DUFFIE & BECKMANN[131]) 102
FIGURE 8.4: DIFFERENCE BETWEEN MEASURED AND MODELLED DEW POINT TEMPERATURE 104
FIGURE 9.1: THERMAL IMAGE OF THE ALDERNEY HOME AT THE ECOSMART SHOW VILLAGE 108
FIGURE 9.2: PRESSURISATION FAN UNIT 109
FIGURE 9.3: GRAPHICAL COMPARISON BETWEEN SPACE HEATING MODELS 114
FIGURE 10.1: SCHEMATIC DIAGRAM SHOWING HOW EXCITED ELECTRONS MOVE INTO CONDUCTION BAND 118
FIGURE 10.2: EXPECTED VARIATION OF CAPITAL COST WITH TIME (SOURCE: DCLG[154], 2010) 119
FIGURE 10.3: PHOTOGRAPHS MALVERN (LEFT), PALMERSTON (CENTRE) AND WASHINGTON (RIGHT) PV SYSTEMS 121
FIGURE 10.4: SUN-PATH DIAGRAM FOR THE LOCATION OF THE ECOSMART VILLAGE (SOURCE: UNIVERSITY OF OREGON) 122
FIGURE 10.5: COMPARISON OF PV METER READINGS, SHOWING MEASURED ANNUAL OUTPUT 127
FIGURE 10.6: MEASURED DISTRIBUTION OF GENERATING HOURS AT VARIOUS POWER LEVELS 128
FIGURE 10.7: BROKEN PV PANEL WAS ABLE TO RETAIN THE SHATTERED GLASS 129
FIGURE 10.8: DIAGRAM SHOWING THE ANGLES FOR THE DIRECT BEAM CALCULATIONS 130
FIGURE 10.9: RELATION BETWEEN IRRADIANCE AND TEMPERATURE DIFFERENCE BETWEEN PV CELL AND AMBIENT FOR ROOF-INTEGRATED PV (SOURCE: DAVIS ET AL. 2001[184]) 134
FIGURE 10.10: TEMPERATURE – IRRADIANCE RELATION OF TEMPERATURE MODEL COMPARED TO NOCT MODEL 135
FIGURE 10.11: PV MODEL VALIDATION, SAMPLE DATA FOR 4TH JUNE 2007 136
FIGURE 10.12: PV MODEL WITH ADJUSTED INVERTER EFFICIENCY, SAMPLE DATA FOR 11TH MAY 137
FIGURE 10.13: MONTHLY COMPARISON OF PV MODEL WITH METER READINGS FOR PALMERSTON 138
FIGURE 10.14: MONTHLY COMPARISON OF PV MODEL WITH METER READINGS FOR WASHINGTON 138
FIGURE 10.15: MONTHLY COMPARISON OF PV MODEL WITH METER READINGS FOR MALVERN 138
FIGURE 10.16: ANNUAL COMPARISON OF PV MODEL WITH METER READINGS FROM ALL TEST SYSTEMS 139
FIGURE 10.17: ANNUAL YIELD ESTIMATED FOR THE TEST SITE USING VARIOUS TOOLS, COMPARED WITH MEASURED OUTPUT 140
FIGURE 10.18: WEEKLY PV GENERATION (MAXIMUM, MINIMUM, & AVERAGE WEEKLY OUTPUT) .. 143
FIGURE 10.19: DISTRIBUTION OF LATITUDE REFERENCES THROUGHOUT THE UK 144
FIGURE 10.20: PERCENTAGE DIFFERENCE BETWEEN PV GIS RESULTS AND BENCHMARK VALUE .. 145
FIGURE 10.21: SHOWING PERCENTAGE DIFFERENCES, FOCUSING ON MODULE INCLINATION 146
FIGURE 10.22: PERCENTAGE DIFFERENCES OF ANNUAL OUTPUT, FOCUSING ON MODULE ORIENTATION 146
FIGURE 11.1: SIMPLE SCHEMATIC DIAGRAM OF A TYPICAL FLAT PANEL SOLAR THERMAL COLLECTOR 153
FIGURE 11.2: SIMPLE SCHEMATIC DIAGRAM OF A TYPICAL EVACUATED TUBE SOLAR THERMAL COLLECTOR 153
FIGURE 11.3: VARIATION OF TANK TEMPERATURE AND HEAT EXCHANGER TEMPERATURE FOR PARALLEL AND COUNTER-FLOW 154
FIGURE 11.4: EVACUATED TUBE SYSTEM (LEFT) AND FLAT PANEL SYSTEM (RIGHT) 155
FIGURE 11.5: SOLAR THERMAL SCHEMATIC DIAGRAM (SOURCE: SOLARPANELSYSTEMS LTD.) ... 156

FIGURE 11.6: REFERENCE GRAPH FOR TRANSMITTANCE-ABSORPTION RATIO CALCULATIONS (SOURCE: DUFFIE AND BECKMAN[131], 2006) 162
FIGURE 11.7: REFERENCE GRAPH FOR AVERAGE ANGLE OF INCIDENCE ($\overline{\theta}_b$) CALCULATIONS (SOURCE: DUFFIE AND BECKMAN[131], 2006) 162
FIGURE 11.8: *F*-CHART BASED OUTPUT IN RELATION TO HOT WATER DEMAND 167
FIGURE 11.9: COMPARISON OF SYSTEM EFFICIENCY BETWEEN FLAT PANEL AND EVACUATED TUBE SYSTEM 168
FIGURE 11.10: IBUTTONS ON DOMESTIC SOLAR THERMAL SYSTEM (TEST FAMILY 1) 174
FIGURE 11.11: TEMPERATURE VARIATIONS OF 1-MINUTE IBUTTON SAMPLING TEST, SHOWING DRAW-OFF EVENTS 175
FIGURE 11.12: TEST SYSTEM 2 HOT WATER CYLINDER AND SENSOR ARRANGEMENT 177
FIGURE 11.13: COMPARISON OF IRRADIANCE ON A 45° INCLINED PLANE AND VERTICAL PLANE (SOURCE: PV GIS) 179
FIGURE 11.14: SIMPLIFIED LAYOUT OF SOLAR THERMAL SHED 180
FIGURE 11.15: LAYOUT OF SOLAR THERMAL CYLINDERS 181
FIGURE 11.16: SCHEMATIC DIAGRAM OF HOT WATER CYLINDER SHOWING 3 MODELLED LAYERS 189
FIGURE 11.17: SCHEMATIC DIAGRAM OF SOLAR HOT WATER CYLINDER (SOURCE: ALBION SUPERDUTY TECHNICAL DOCUMENTATION) 191
FIGURE 11.18: VARIATION OF AVERAGE TEMPERATURE OF SOLAR CYLINDER DURING HOLIDAY PERIOD 192
FIGURE 11.19: TEMPERATURE VARIATION OF CYLINDER MODEL UNDER STEADY-STATE CONDITIONS 193
FIGURE 11.20: STRATIFICATION EFFECT AFTER VARIOUS DIFFERENT DRAW-OFF EVENTS FROM THE MODELLED CYLINDER 194
FIGURE 11.21: BOTTOM CYLINDER TEMPERATURE VARIATION ON 14TH APRIL 2010 197
FIGURE 11.22: MEASURED ENERGY INPUT TO CYLINDER (BASED ON TOP AND BOTTOM TEMPERATURES) COMPARED TO MODELLED INPUT INCLUDING BOILER TOP-UP 200
FIGURE 11.23: COMPARISON OF MEASURED CYLINDER TEMPERATURES AND TEMPERATURES EXPORTED FROM MODEL FOR WEEK 1; 2ND TO 8TH APRIL 2010 201
FIGURE 11.24: COMPARISON OF MEASURED CYLINDER TEMPERATURES AND TEMPERATURES EXPORTED FROM MODEL FOR WEEK 2; 9TH TO 15TH APRIL 2010 201
FIGURE 11.25: COMPARISON OF MEASURED CYLINDER TEMPERATURES AND TEMPERATURES EXPORTED FROM MODEL FOR WEEK 3; 16TH TO 22ND APRIL 2010 202
FIGURE 11.26: COMPARISON OF MEASURED CYLINDER TEMPERATURES AND TEMPERATURES EXPORTED FROM MODEL FOR WEEK 4; 23RD TO 29TH APRIL 2010 202
FIGURE 11.27: TEMPERATURE DISTRIBUTIONS FOR 12TH APRIL 2010, TEST SYSTEM 1 203
FIGURE 11.28: COMPARISON OF AVERAGE CYLINDER TEMPERATURE IN APRIL 2010, MEASURED VS. MODEL 204
FIGURE 11.29: MONTHLY COMPARISON OF MODEL AND MEASURED RESULTS, TEST SYSTEM 1 205
FIGURE 11.30: COMPARISON OF MODELLED GENERATION FOR DIFFERENT BOILER SETTINGS AND ESTIMATES BASED ON MEASURED DATA 208
FIGURE 11.31: COMPARISON BETWEEN F-CHART METHOD, SOLAR THERMAL MODEL AND MEASURED RESULTS OVER A 12 MONTH PERIOD 211
FIGURE 11.32: COMPARISON BETWEEN MONTHLY AVERAGE EFFICIENCY OF THE ALDERNEY EVACUATED TUBE SYSTEM, USING F-CHART, MODEL AND MEASURED RESULTS. 211
FIGURE 11.33: COMPARISON OF EFFECTS OF BOILER SETTING ON ANNUAL YIELD OF ECOSMART ALDERNEY SOLAR SYSTEM 214
FIGURE 11.34: COMPARISON BETWEEN SOLAR THERMAL GENERATION OF COLLECTOR INCLINED AT 45° AND VERTICAL COLLECTOR WITH TWICE THE AREA 215
FIGURE 11.35: STATISTICS FROM FEEDBACK QUESTIONNAIRE. SOURCE: SMS MARKET RESEARCH SUMMARY REPORT 219
FIGURE 12.1: FORCES ACTING ON SINGLE TURBINE BLADE 223
FIGURE 12.2: STEALTHGEN WIND TURBINE (LEFT) AND WINDSAVE WIND TURBINE (RIGHT) 225
FIGURE 12.3: POWER CURVE FOR WINDSAVE WS1000 (SOURCE: WINDSAVE WS1000 DATASHEET) 226
FIGURE 12.4: POWER CURVE FOR STEALTHGEN D400 (SOURCE: STEALTHGEN D400 USER'S MANUAL) 226
FIGURE 12.5: SCHEMATIC DIAGRAM OF WIND TURBINE SYSTEM LAYOUT 227
FIGURE 12.6: TYPICAL RATIOS OF COMPONENT WEIGHT AND SPECIFIC ENERGY CONTENT OF THEIR RAW MATERIALS (SOURCE: LENZEN & MUNKSGAARD[254], 2002) 228

FIGURE 12.7: RAYLEIGH DISTRIBUTION OF ESTIMATED WIND SPEEDS AT ECOSMART VILLAGE TEST SITE 236
FIGURE 12.8: MODEL OF THE TEST SITE, SHOWING WIND TURBINES AND WEATHER STATION 238
FIGURE 12.9: MONTHLY VARIATION OF WIND SPEEDS (SOURCE: WINDOGRAPHER) 240
FIGURE 12.10: FREQUENCY AND WEIBULL DISTRIBUTIONS (SOURCE: WINDOGRAPHER) 240
FIGURE 12.11: WIND ROSE PLOT SHOWING WIND SPEED DISTRIBUTION 241
FIGURE 12.12: WIND ROSE PLOT SHOWING ENERGY DISTRIBUTION 241
FIGURE 12.13: DAMAGED TURBINE BLADE WHICH HAD DETACHED DURING THE STORM ON 18TH JANUARY 2007 244
FIGURE 12.14: RETRACTABLE WIND TURBINE (SOURCE: STEALTHGEN D400 MANUAL) 244
FIGURE 12.15: CP VARIATION WITH WIND SPEED 247
FIGURE 12.16: CFD DIAGRAM OF WIND VELOCITY PROFILE OVER A MODELLED ISOLATED HOUSE (SOURCE: HEATH ET AL[275], 2007) 250
FIGURE 12.17: LATERAL TURBULENCE (HOURLY STANDARD DEVIATION OF WIND DIRECTION) DURING GENERATING TIMES OF BOTH TURBINES OVER A 4-WEEK SAMPLE PERIOD IN 2007 253
FIGURE 12.18: LONGITUDINAL TURBULENCE (HOURLY STANDARD DEVIATION OF WIND SPEED) DURING GENERATING TIMES OF BOTH TURBINES OVER A 4-WEEK SAMPLE PERIOD IN 2007 253
FIGURE 12.19: LATERAL TURBULENCE FOR COMBINED PERIODS OF ENERGY GENERATION ONLY, OVER A 4-WEEK SAMPLE PERIOD IN 2007 254
FIGURE 12.20: LATERAL TURBULENCE FOR COMBINED PERIODS OF ZERO GENERATION ONLY, OVER A 4-WEEK SAMPLE PERIOD IN 2007 254
FIGURE 12.21: STATISTICS FROM FEEDBACK QUESTIONNAIRE (SOURCE: SMS MARKET RESEARCH SUMMARY REPORT) 259
FIGURE 13.1: VERTICAL U SYSTEM (LEFT) AND HORIZONTAL SLINKY-TYPE SYSTEM (RIGHT) (SOURCE: CURTIS[288], 2001) 262
FIGURE 13.2: COMPRESSION / EXPANSION CIRCUIT OF GSHP SYSTEM (SOURCE: CALOREX GSHP USER MANUAL) 263
FIGURE 13.3: GSHP UNIT (LEFT) AND BOREHOLE/PILING OPERATIONS (RIGHT) 264
FIGURE 13.4: MODELLED SOIL TEMPERATURE VARIATION IN UK (SOURCE: DOHERTY ET AL[294], 2004) 268
FIGURE 13.5: SOIL TEMPERATURE VARIATIONS IN BRITAIN (SOURCE: BS EN15450[293]) 268
FIGURE 13.6: TEMPERATURE PROFILE IN °C NEAR BOREHOLE (BHE) AT BEGINNING [LEFT] AND AFTER 3 MONTHS OPERATION DURING WINTER IN GERMANY [RIGHT] (SOURCE: RAYBACH & SANNER[286], 2000) 269
FIGURE 13.7: PALMERSTON INTERNAL TEMPERATURE VARIATIONS DURING WINTER PERIOD 276
FIGURE 13.8: PALMERSTON INTERNAL HUMIDITY VARIATIONS DURING WINTER PERIOD 276
FIGURE 13.9: MALVERN HEAT PUMP POWER CONSUMPTION AND TEMPERATURE VARIATIONS 277
FIGURE 13.10: TEMPERATURE DIFFERENCE BETWEEN MALVERN GSHP FLOW AND RETURN PIPES 279
FIGURE 13.11: STATISTICS FROM FEEDBACK QUESTIONNAIRE (SOURCE: SMS MARKET RESEARCH SUMMARY REPORT) 280
FIGURE 14.1: WHISPERGEN MCHP SYSTEM AT ECOSMART SHOW VILLAGE 285
FIGURE 14.2: WHISPERGEN MCHP SYSTEM (SOURCE: WHISPERGEN TECHNICAL SPECIFICATION BROCHURE) 286
FIGURE 14.3: COMPARISON OF BUCKINGHAM DATA 291
FIGURE 14.4: BUCKINGHAM HEAT AND ELECTRICITY OUTPUT COMPARED TO GAS CONSUMPTION 292
FIGURE 14.5: INTERNAL TEMPERATURE OF MCHP-CONTROLLED HOMES, APRIL-JULY 2007 292
FIGURE 14.6: INTERNAL TEMPERATURE OF MCHP-CONTROLLED HOMES, JANUARY-APRIL 2007 293
FIGURE 14.7: ELECTRICAL EFFICIENCY AND OVERALL EFFICIENCY OF BUCKINGHAM SYSTEM 294
FIGURE 14.8: HEAT AND ELECTRICITY OUTPUT COMPARED TO GAS CONSUMPTION OF EDINBURGH SYSTEM 296
FIGURE 14.9: ELECTRICAL EFFICIENCY AND OVERALL EFFICIENCY OF EDINBURGH SYSTEM 298
FIGURE 14.10: GAS CONSUMPTION AND ELECTRICITY GENERATION OVER ONE CYCLE 299
FIGURE 14.11: STATISTICS FROM FEEDBACK QUESTIONNAIRE (SOURCE: SMS MARKET RESEARCH SUMMARY REPORT) 300

Nomenclature

A_C	Collector area (m²)
A_P	Pipe surface area (m²)
A_T	Surface area of hot water tank (m²)
c_1	Heat loss coefficient at ($T_m - T_a$) = 0
c_2	Temperature dependence of the heat loss coefficient
c_3	Wind speed dependence of the heat loss coefficient
c_4	Sky temperature dependence of the heat loss coefficient
c_5	Effective thermal capacity
c_6	Wind dependence in the zero loss efficiency
cp	Performance coefficient (wind turbine)
c_{temp}	Temperature correction coefficient for PV (K^{-1})
C	Cost (£)
CO_2	CO_2 equivalent emissions (kg)
C_P	Specific heat capacity (J/Kg°K)
CP	Coefficient of Performance (GSHP)
df	t-value degrees of freedom
D	Density (kg/m^3)
E_L	Long-wave irradiance (W/m²)
E_β	Long-wave irradiance on an inclined surface outdoors (W/m²)
E_s	Long-wave sky irradiance (W/m²)
ET	Equation of time

f	Solar fraction
F_R	Collector efficiency factor
FIT	Feed-in Tariff (£)
VF_{sky}	Sky view factor
G	Hemispherical solar irradiance (W/m²)
G^*	Global hemispherical solar irradiance (W/m²)
G''	Net irradiance (W/m²)
$h_{c,\,forced}$	Forced convection coefficient (W/m²K^{-1})
$h_{c,\,free}$	Free convection coefficient (W/m²K^{-1})
$\overline{H}_T$	Monthly average daily irradiation incident on collector surface (J/ m²)
I_0	Extraterrestrial radiation (W/m²)
j	Scale parameter of Rayleigh wind distribution (m/s)
k_T	Clearness index
k_{temp}	Temperature correction factor (for PV)
K_θ	Incidence angle modifier
L	Monthly total heating load for hot water requirements (J)
m	Mass (Kg)
$\dot{m}$	Mass flow rate (Kg/s)
n	Julian date, meaning the sum of days after 1st January
N	Air change rate (ach)
N_{50}	Number of air changes per hour at 50 Pa pressure (ach)
P	Pressure (Pa)

P_0	Wind power (W)
P_T	Wind turbine power output (W)
P_{AC}	Alternating current electrical power (W)
P_{DC}	Direct current electrical power (W)
P_{PV}	PV generation power (W)
Q_{50}	Specific rate of air volume leakage at 50 Pa pressure (m³/hr.m²)
Q	Energy (J)
Q_R	Radiation energy losses (J)
$\dot{Q}_{loss}$	Rate of heat loss (W)
r_{LS}	Least Squares method residuals
$\overline{R}_b$	Ratio between irradiation on horizontal surface and tilted surface
R	Gas constant (J/kg°K)
R^2	Ratio of residual errors of Least Squares method
RH	Relative humidity (%)
RHI	Renewable Heat Incentive tariff (£)
$\overline{S}$	Average absorbed solar irradiation (J/m²)
S_r	Sum of Least Squares method residuals
Δt	Total number of seconds in month (s)
$t_{payback(C)}$	Carbon payback period (years)
$t_{payback(E)}$	Energy payback period (years)
$t_{payback(F)}$	Financial payback period (years)
t_{sol}	Solar time (hr)
t_{value}	t-value of t-test
T_a	Ambient air temperature (°C)
$\overline{T}_a$	Monthly average ambient temperature (°C)

T_{dp}	Atmospheric dew point temperature (°C)
T_e	Collector outlet (exit) temperature (°C)
T_{cell}	PV cell temperature (°C)
T_{in}	Collector inlet temperature (°C)
T_m	Mean temperature of heat transfer liquid (°C)
T_{ref}	Empirically derived reference temperature (100°C)
T_s	Sky temperature (°C)
U	Heat loss coefficient (W/m²K)
U_L	Collector overall loss coefficient (W/m²K)
$\overline{U}$	Mean wind speed (m/s)
u	Wind speed (m/s)
u_*	Friction velocity (m/s)
V	Volume (m^3)
z_0	Roughness length (m)
Z_{PV}	SAP over-shading factor
α	Solar absorptance
β	Tilt angle of collector surface (°)
ε	Hemispherical emittance
θ	Angle of incidence (°)
κ	Surface drag coefficient
λ	Wavelength (m)
η	System efficiency
η_0	Zero-loss collector efficiency
η_H	Heat exchanger efficiency
$\eta_{inverter}$	Efficiency of inverter
σ	Stefan-Bolzmann constant (J/s m² K^4)

σ_{SD}	Standard Deviation
τ	Transmittance
τ_C	Heat loss time constant (s)
$(\overline{\tau\alpha})$	Monthly average transmittance-absorption product
$(\tau\alpha)_e$	Effective transmittance-absorptance product
$(\tau\alpha)_{en}$	Transmittance-absorptance product for radiation at normal incidence
ψ	Longitude of location (°)
$(\ )_b$	Subscript identifying direct solar beam components
$(\ )_d$	Subscript identifying solar diffuse components
$(\ )_{embodied}$	Subscript for embodied values
$(\ )_E$	Subscript referring to electrical energy (Wh)
$(\ )_H$	Subscript referring to heat energy (Wh)
$(\ )_g$	Subscript identifying ground reflection components

1 Aims and Objectives

As climate change becomes an ever more important cause for concern, many countries worldwide have responded to this and are actively trying to reduce their greenhouse gas emissions. In the UK, the domestic sector in particular has been identified as a main target for emission reductions, and UK house builders are facing great challenges set by impending legislation.

Barratt Developments PLC, the UK's largest builder, has taken the lead in investigating practical and cost-effective ways of meeting these challenges. In 2006 it was anticipated that renewable energy systems would have a significant role to play, but it remained to be tested how exactly some of the available systems would perform. To do this, an elaborate test site, the EcoSmart show village, was built by Barratt Developments PLC where several renewable energy systems were tested in standard Barratt homes. This research project will set out to establish how on-site micro-generation of energy can help to offset the carbon footprint of a modern UK home, and how these systems can be improved for best performance. More specifically, this research will try to answer the following questions:

1) How much CO_2 can be displaced by the integration of micro-generation systems in standard UK homes, and what are the financial implications?

2) Do all of the tested systems work reliably and perform as expected?

3) How can the performance of micro-generation systems be improved?

Throughout the course of the research it was discovered that the lack of reliable information available to builders and architects appears to be a major barrier for the successful integration of micro renewable energy systems. It was therefore decided to also explore the following point:

4) How can a builder or architect easily obtain reliable information about the realistic performance of micro renewable energy systems?

Thesis Structure

In order to provide the background to answer the questions outlined above, this thesis will be set out in the following structure:

In chapter 2 an introduction will be given to the drivers for recent legislation, which has ultimately caused Barratt to undertake this research. This includes climate change, the impending depletion of fossil fuels, and considerations from a financial point of view. Chapter 3, the literature review, will give an overview of other work done in this area that provides the foundations for the analyses.

Chapters 4 and 5 will give a more detailed introduction to Barratt Developments, focussing on their role in the UK housing market, and to the EcoSmart village test site.

The research methodology, a description of support systems and some preliminary modelling including space heating estimates will be presented in chapters 6-9. This will provide the background for the analysis of the renewable energy systems.

Chapters 10-14 will describe the analyses of the five systems that were tested at the EcoSmart village in detail, exploring available resources, any reasons for discrepancies between expected and measured performance, and a prediction of financial and carbon emission savings. After preliminary data analysis it was decided to focus the research on the solar technologies and wind power in particular, as these systems showed the most promising or the most surprising results.

Chapters 15 and 16 will summarise the conclusions drawn from this research, and based on this will present answers to the questions set out above. Finally, chapter 17 will provide suggestions for further work that may be necessary to provide additional evidence in support of the conclusions drawn during this research.

2 Introduction

This chapter will outline the underlying reasons why UK builders such as Barratt Developments face the challenges of vastly reducing the carbon emissions of new homes.

2.1 The Need for Reducing CO_2 Emissions

The following sections provide an overview of research that identifies a widely accepted causal link between CO_2 concentration in the atmosphere and global warming. The burning of fossil fuels is shown to be the highly probable cause for measured increases in atmospheric CO_2 content. During the recent Copenhagen Climate Conference in 2009 it was agreed that everything must be done to limit the global temperature rise to a maximum of 2°C over the next century. Beyond this a chain reaction is triggered that causes further release of greenhouse gases through the warming of the oceans, leading to highly significant and irreversible climate change. This scenario is expected to have catastrophic consequences, including extreme weather, a global rise in sea level and a shift in climate patterns that could potentially result in mass starvations, destruction of eco-systems, acidified oceans and extensive uninhabitable regions.

Even if the widely accepted climatic models are proven to be wrong, and the CO_2 emissions are not the leading cause for global warming, the sources of energy that are responsible for these emissions (fossil fuels) are expected to deplete within a matter of decades. Based purely on this perspective it will soon become imperative to reduce CO_2 emissions. Energy must be conserved in the short term, and alternative sources of energy must be established in a cost-efficient way to ensure long term energy security for an ever more demanding world.

2.1.1 Climate Change

Inspired by revelations in ice age theory, John Tyndall believed in the mid-nineteenth century that he had found a possible explanation for the dramatic changes in Earths' climate. He realised that some molecules within the atmosphere could absorb thermal radiation, and concluded that changes in atmospheric composition could be the leading cause for all climate changes[1]. In 1965, the issue of 'man-made' climate change first appeared in a report from the President's Science Advisory Committee to US President Lyndon Johnson[2], after the first carbon dioxide measurements[3] and up-to-date temperature reconstruction[4] became available.

The 1970's Perception of Global Cooling – A Myth?

Some publications[5,6], even as recent as 2004[7], 2007[8] and 2008[9], suggest that during the 1970's there were widespread fears of an impending ice age, but a more thorough review[10] of other publications from 1965-1979 confirmed that a general consensus amongst leading scientists in the late 1970's emerged, agreeing that global warming was a far greater issue than potential global cooling. After modelling aerosols from a volcanic eruption in Bali (1963) it was widely agreed in 1978 that global warming through greenhouse gasses was the dominant force[11] in climate change. This view was reflected in a report produced by a panel of experts, who were brought together in 1979 under the US National Research Council to clarify the view on climate change[12]. The panel concluded that the potential damage of carbon dioxide was real, and while there were still huge uncertainties, urgent action should be taken to address the issue.

IPCC Fourth Assessment Report - Climate Change 2007

In 1988 the IPCC was founded to provide an independent body to assess climate change in an open, transparent way, based on peer-reviewed scientific publications. The IPCC has established itself as the leading reference for climate change.[13]

In 2007, the most recent IPCC report was released, receiving huge publicity and recognition amongst scientists around the world. In this report the IPCC has concluded[14] that it is now evident that the warming of the climate is unequivocal. This is based on trends in measured global temperature, sea level and snow cover of the northern hemisphere. Figure 2.1 shows an extract of modelled and measured inter-continental temperature increases with and without CO_2 emissions.

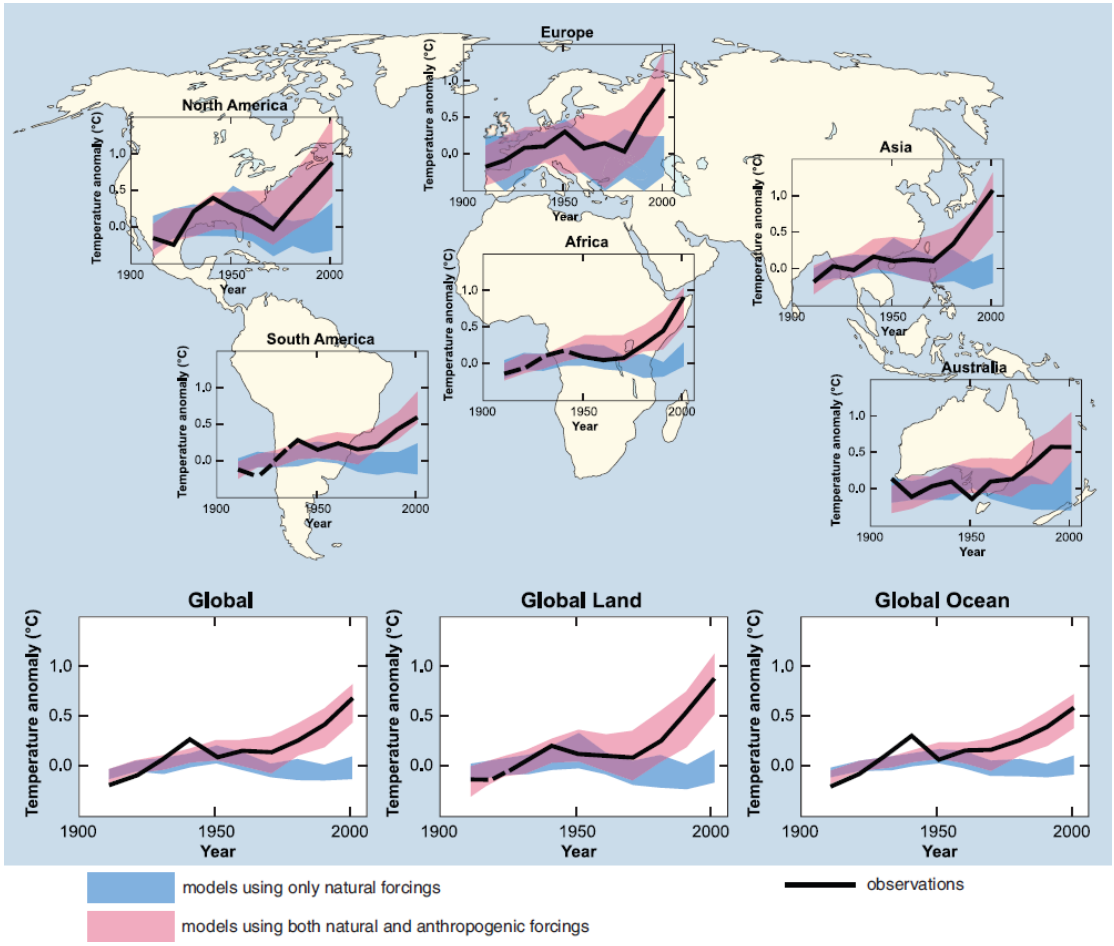

Figure 2.1: Observed and modelled temperature, comparing natural variations and variations accounting for human intervention (Source: IPCC AR4[14])

Continued greenhouse gas emissions at or beyond current levels will cause further warming and other climate changes.

For climate change mitigation, different options are discussed. It is suggested that mitigation options exist that can reduce the 2030 emissions by around 30% at a net negative cost. Also, timely investments in the energy infrastructure have long term impacts on CO_2 emissions. Figure 2.2 shows a sectoral breakdown of the potential emission reductions by 2030 for the cases of investing US$20, US$50 or US$100 per tCO_2-eq/yr.

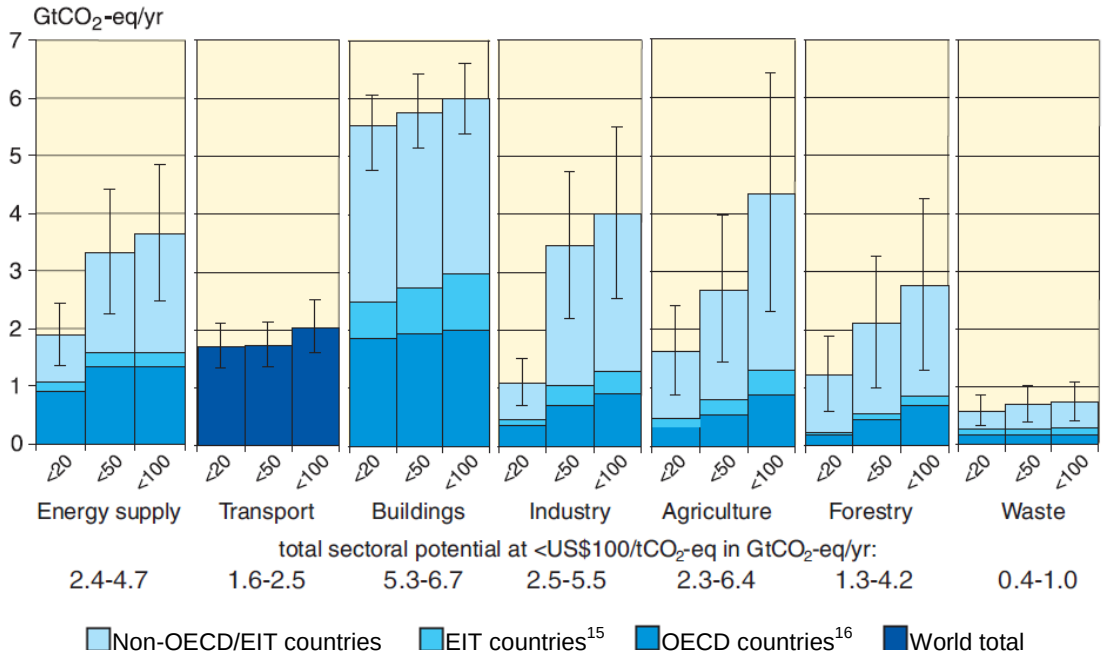

Figure 2.2: Sectoral breakdown of potential CO_2 emission reductions by 2030 (Sourece: IPCC AR4[14])

Based on Figure 2.2, an investment of US$100 per tCO_2-eq/yr in every sector would result in bringing 2030 emissions to just below 2005 values. The total global investment would need to be in the region of US$3 trillion ($3x10^{12}$) annually.

Figure 2.2 also shows clearly that by far the greatest reductions in greenhouse gas emissions can be achieved in the buildings sector. Even with relatively little investment significant savings can be achieved. Given this evidence, it is important to focus all efforts on reducing greenhouse gas emissions in this sector first to achieve the greatest 'value for money'.

Stern Review - The Economics of Climate Change

In 2005, the UK government asked economist Sir Nicholas Stern to lead a review of the economics of climate change[17]. In its conclusion the review makes a clear statement that there is overwhelming evidence that climate change is a serious global threat, which will affect basic elements of life for people[18]. Dealing with these consequences will effectively reduce the global Gross Domestic Product (GDP) by 5-20% annually, now and forever. To avoid this scenario, the report urges strong and sharp intervention. It is found that investments in the order of 1% of GDP now could avert a vast majority of the costs of dealing with climate change later. Other conclusions include:

- A stabilisation of atmospheric CO_2 content at 500-550ppm would limit further warming at 2°C by the end of the 21st century. This could be achieved by investing 1% of GDP now.

- A delay in actions may result in the opportunity of CO_2 stabilisation at 550ppm slipping by.

- The transition to low-carbon energy will bring challenges for competitiveness but also opportunities for growth. Strong action is required to motivate the uptake of low carbon technologies.

When asked about his Review in 2008, in light of the IPCC 4th Assessment Report that was released the year before, Nicholas Stern said: "We underestimated the risks, we underestimated the damage associated with temperature increases, and we underestimated the probabilities of temperature increases"[19]. He also added that based on the findings from the IPCC Report, he estimates that the cost involved in reducing carbon levels to non-dangerous levels would have doubled, to about 2% of global GDP.

2.1.2 Depletion of Fossil Fuels

Fossil fuels have a wide variety of uses in today's world. On top of providing large amounts of energy to power the modern world life-styles we have come to take for granted, fossil fuels are also required to produce a wide range of sub-products including polymers, pesticides and fertilisers.

It is widely accepted that crude oil is a finite resource, and that sooner or later an oil production peak is reached[20]. When this happens further oil extraction will subsequently become more and more difficult and expensive, with higher risks and technical challenges involved. Currently there is some debate over when exactly the oil production peak will be reached, with forecasts[21] from recent years ranging from 2007-2030. Many of these models show a production peak that is imminent, expected to occur within the next 5-10 years at the latest.

From an economic point of view the oil production peak is associated with significant consequences, as without timely intervention the demand in oil will remain high while the supply becomes more difficult and more costly. Experts[22] expect that demand side intervention will be required ideally 20 years before, but at least 10 years before the oil peak to avoid significant oil deficits and resulting economic complications. It has also been shown that the global GDP is directly linked (approximately 1:1) to oil production[23], meaning any action taken after the oil production peak will effectively become even more expensive.

2.1.3 UK Carbon Emissions

In 1997 the UK signed the Kyoto Protocol, thereby committing to a greenhouse gas emission reduction of 12.5% over 1990 levels by 2012. The aspirational target set by the UK government at the time was a reduction of 20%[24]. By 2008, the UK emissions show that the country is currently well underway to achieving even its voluntary target. Nonetheless, the total greenhouse gas emissions are still in the order of 0.63GtCO_2-eq/yr[25], which accounts for over 1.5% of world wide greenhouse gas emissions based on IPCC figures. A sectoral breakdown of the UK 2008 greenhouse gas emissions is shown in Figure 2.3.

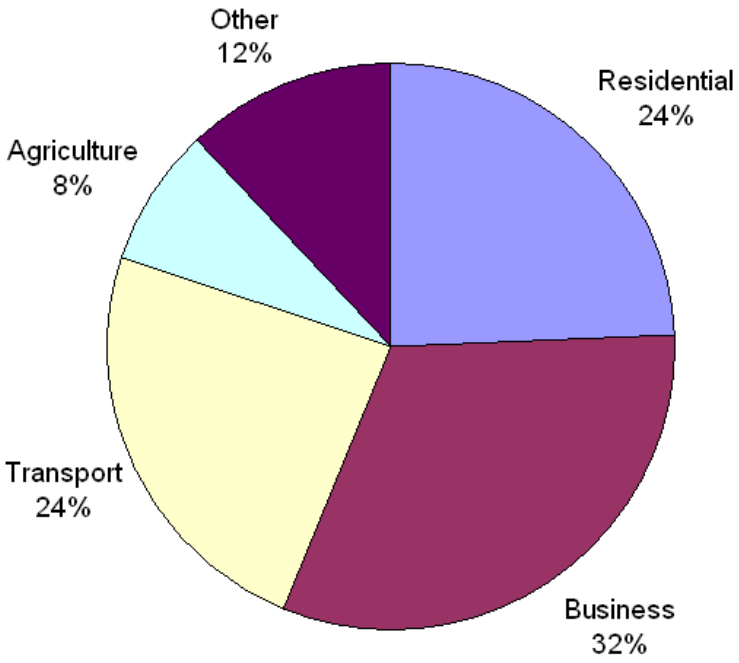

Figure 2.3: 2008 Greenhouse gas emission distribution by sector (Based on 2010 DECC figures for 2008 emissions[25])

For the future, promising trends can already be seen. Recent emission reductions from 2008-2009 showed decreases for all major sectors, in particular Business and Energy Supply, which both achieved more than 10% reductions. This was put down to an overall fall in energy consumption, combined with fuel switching from coal to nuclear electricity generation[25]. Figure 2.2 shows UK greenhouse gas emissions since 1990.

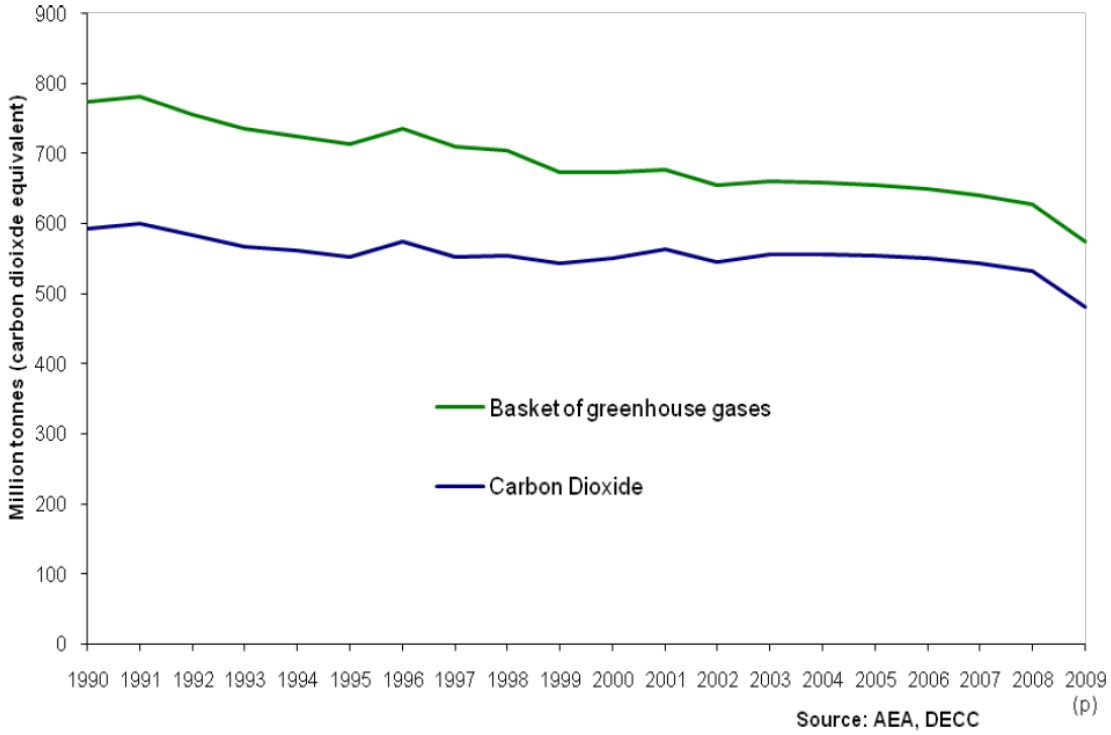

Figure 2.4: The recent trend in UK Greenhouse Gas Emissions (Source: DECC 2010[25])

2.1.4 The UK Domestic Sector

It was previously shown by the IPCC 4th Assessment Report that the highest potential for reducing greenhouse gas emissions exists in the residential sector. Even small investments in this sector are expected to make a significant difference.

In 2008 the UK residential sector accounted for 24% of national greenhouse gas emissions[25]. A further breakdown of this value reveals the distribution shown in Figure 2.5.

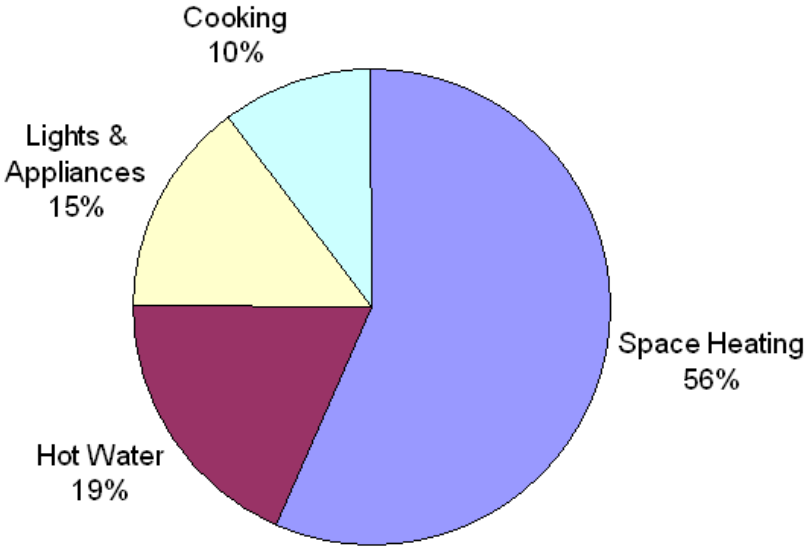

Figure 2.5: Breakdown of energy use in UK domestic sector in 2000 (Source: DTI 2002)

The UK government has set targets to reduce greenhouse gas emissions significantly in the future. The currently set out milestone targets, which have been described as ambitious[26], are as follows:

- An 80% reduction over 1990 emissions of domestic sector by 2050
- A 29% reduction over 2008 emissions of domestic sector by 2020[27]

2.1.5 Summary

Most acknowledged research today leads to the conclusion that climate change is an undisputable fact, and greenhouse gas emissions are largely responsible. There is worldwide agreement that something needs to be done to minimise the vastly damaging effects. Evidence is presented that suggests immediate action is the best, if not the only option available. This evidence includes, but is not limited to:

- Findings presented in the IPCC 4th Assessment Report
- The Stern Review on the Economics of Climate Change
- The link between the impending oil production peak and global GDP

While worldwide action is required, this action must begin on a small, local scale. The UK Government has recently taken ambitious steps in setting out legislation that is intended to lead to rigorous reductions in UK greenhouse gas emissions,

most predominantly from the domestic sector. Academia and Industry are currently working hand-in-hand to present technically and economically feasible solutions.

2.2 The Code for Sustainable Homes (CSH)

To reduce the domestic sector carbon emissions, builders have been challenged to provide eco-home excellent rated and low carbon houses now, CSH[28] level 5 in 2013 and zero carbon homes as of 2016[29]. There is currently some debate over the definition of "zero-carbon" homes. The Government had published a consultation[30] on the definition of zero carbon homes, in particular an approach based on:

- high levels of energy efficiency in the home
- a minimum level of carbon reduction to be achieved on-site
- a list of allowable solutions for off-site energy generation

The current definition[31] of a "zero-carbon home" set by the DCLG in 2008 states:

Zero Carbon Home: "Where net carbon dioxide emissions resulting from ALL energy used in the dwelling are zero or better. This includes the energy consumed in the operation of the space heating/cooling and hot-water systems, ventilation, all internal lighting cooking and all electrical appliances. The calculation can take account of contributions from onsite renewable/low carbon installations.

Off-site renewable contributions can only be used where these are directly supplied to the dwellings by private wire arrangement."

This definition emphasises the fact that in order to be classed as zero-carbon, a new-built home must rely on carbon reduction and offset solutions that are on-site or supplied by private-wire. While it is widely expected that a review of the definition will at least result in communal heating arrangements being accepted, a final definition has still not been reached. In March 2010 the UK Housing Minister, Grant Shapps, released a press statement[32] to inform developers about his intentions to finalise the definition within "a matter of weeks".

The CSH point-scoring system is shown in Figure 2.6, consisting of mandatory and 'tradable' categories. Figure 2.7 provides a summary on how many points are required for the various code levels. Details on the point scoring system and the various requirements for the different categories can be found in the CSH technical guide.

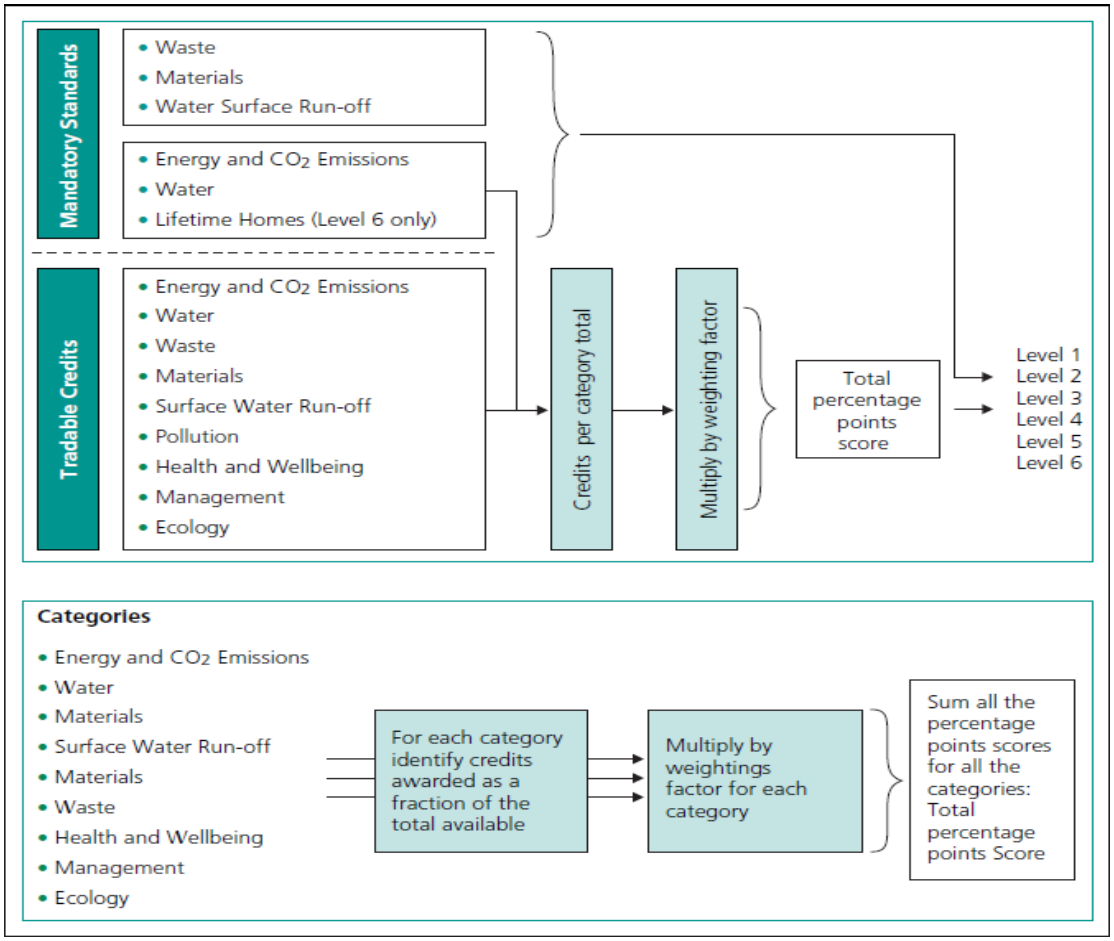

Figure 2.6: CSH point scoring system and categories (Source: CSH[28], 2006)

Total percentage points score (equal to or greater than)	Code Levels
36 Points	Level 1 (★)
48 Points	Level 2 (★★)
57 Points	Level 3 (★★★)
68 Points	Level 4 (★★★★)
84 Points	Level 5 (★★★★★)
90 Points	Level 6 (★★★★★★)

Figure 2.7: CSH level rating system (Source: CSH[28], 2006)

The point system is based on the percentage carbon reduction of the design emission rate (DER) over the target emission rate (TER), which is zero for code levels 5 and 6. The TER refers to the legal requirement in terms of annual carbon emission per square meter, and DER refers to the predicted emissions based on Standard Assessment Procedure (SAP) calculations. Figure 2.8 provides an overview of the requirements in terms of carbon reduction for each code level.

Percentage improvement (reduction) of the DER over TER associated to each Code Level	
% reduction	Level
⩾10	1
⩾18	2
⩾25	3
⩾44	4
⩾100	5

Figure 2.8: Required reduction of design emissions rate for different code levels (Source: CSH[28], 2006)

In order to calculate the reduction of the design emission rate for the CSH, SAP 2005 must be used. SAP 2005 provides carbon emissions factors for different building features, such as mechanical cooling systems, as well as for various low or zero carbon technologies. These carbon emission factors are multiplied by the amount of energy that is expected from the system in order to calculate the total amount of carbon offset. This is then subtracted from the design emission rate, which must also be established using SAP 2005. Un-regulated emissions can also be estimated by SAP 2005.

The CSH heavily encourages on-site energy generation. While creating some controversy, it must therefore be investigated how these systems can help to offset carbon and save energy and to achieve a CSH level 6 rating.

3 Literature Review

This literature review will provide the background information on other related research, which will be used as a basis for the analyses described in this thesis, and show that this research has resulted in a valuable contribution to knowledge.

3.1 Achieving Sustainability in Urban Developments in the UK

In 2005, Shorrock et al.[33] reviewed options of reducing carbon emissions from UK housing stock for BRE. It was assessed how emissions could be reduced by existing stock, how effective the existing energy efficiency policies are, and what possible scenarios of carbon emissions might lead us to 2050. The review of existing measures showed that in 2010 potentially 17.5Mt of carbon could be saved, with 6-13.5MtCO_2/yr being saved cost-effectively. While by 2020 only 13.5MtCO_2/yr may be saved, in 2050 this figure could increase to 29.5MtCO_2/yr due to new technological innovations. Improved insulation and energy efficiency measures are considered most cost-effective, while Solar Thermal provides a commercially non-viable option of saving carbon. PV was considered too expensive at the time. Using government grants, the cost of saving 1 tonne of CO_2 had dropped to £74 by 2001. Using the BREHOMES model, future scenarios were explored. It was found that assuming at least 50% of buildings are equipped with heat pumps it would be possible to achieve 60.7% carbon savings by 2050, based on 2005 technology and modelling. This scenario would cost £55bn, but its cumulative savings would begin to outweigh costs after about 2012, taking 2001 as a starting point. As shown in Figure 3.1, by 2050 this scenario would bring great financial benefits to society.

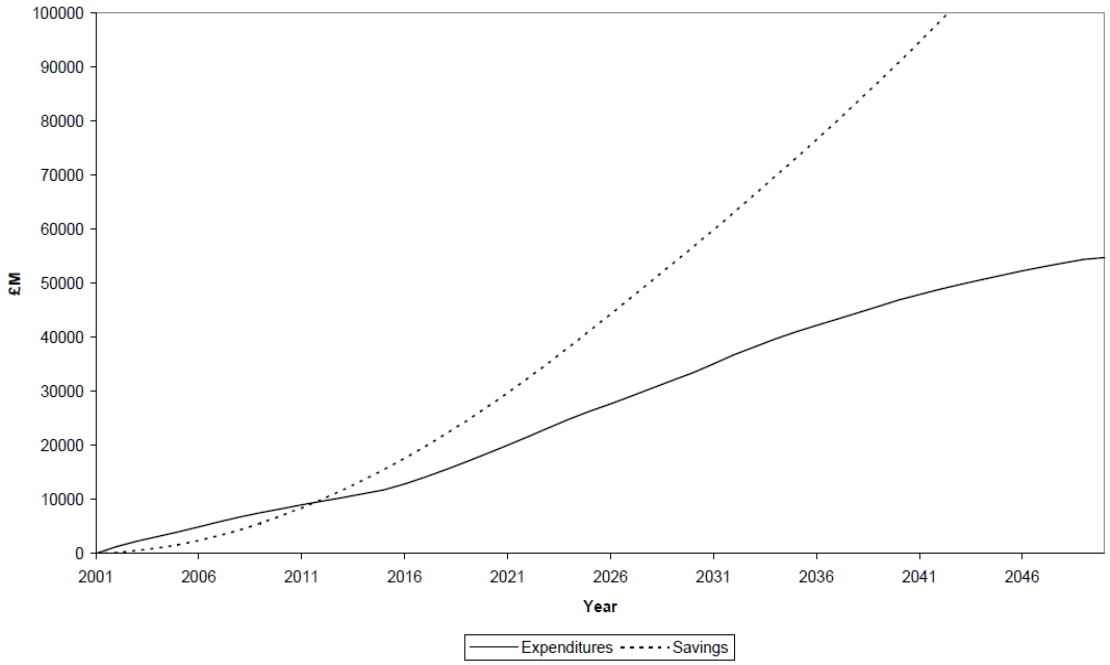

Figure 3.1: Cost and savings associated with reducing CO_2 emissions by 60% by 2050 (Source: Shorrock et al[33]. 2005)

The 40% House report[34] (2005) set out to investigate what challenges would need to be overcome to reach the original government target of CO_2 emission reduction by 60%[35] of 1990 values by 2050. The target emission reduction was later revised and increased to 80%. It was already suggested that all new build homes are designed to have a zero-space heating demand[36]. While the report is mainly concerned with improving existing housing stock, the effect of micro generation on the national power grid was also explored. It was thought that given the centralised nature of the UK grid, micro generation of electricity on a large scale could lead to power instabilities. However, more recent studies suggested that the network is more stable than previously thought, being able to tolerate up to 50% micro-generating households. An investigation[37] of network fault levels showed that the impact of micro-generation is not significant, as the faults were not severe enough to melt standard size network cabling. In a different study it is estimated that by 2050 30-40% of the UK's domestic sector electricity demand could be satisfied by micro-generation.[38]

A technical consultancy report[39] was prepared in 2007 for the South West Regional Development Agency and Government Office, exploring the viability as well as potential costs and benefits of regional zero-carbon developments. A brief review of government policy is given, looking at the Energy White Paper[40] 2003, The Energy Challenge: Energy Review[41] 2006, Climate Change and Sustainability Act 2006, the proposed changes to Part L of the building regulations and an early

version of the Code for Sustainable Homes. Emissions are perceived to be split between regulated (e.g. space heating) and non-regulated (e.g. appliances), with weighting for residential buildings of roughly 50:50. Several options were explored to achieve a zero-carbon rating, including energy efficiency, PV, communal biomass heating, GSHP and wind technology. It was found that 'zero carbon' in terms of regulated emissions is achievable for about 14% extra cost for small urban developments using communal biomass and PV. While wind power theoretically gives a better cost/benefit ratio, it is recognised that wind is unlikely to work well in urban areas. Achieving zero carbon in terms of total emissions was not found to be technically viable without using large scale wind power. Energy efficiency, PV and biomass would only be able to offset 61% of total emissions. A cost benefit analysis was carried out, determining how much it would cost to offset one tonne of CO_2 using various different technologies. Results are summarised in Figure 3.2. For comparison, reducing the external wall U-value from 0.25 to 0.21 for a detached building is expected to cost £27,000 per tonne CO_2 saved annually.

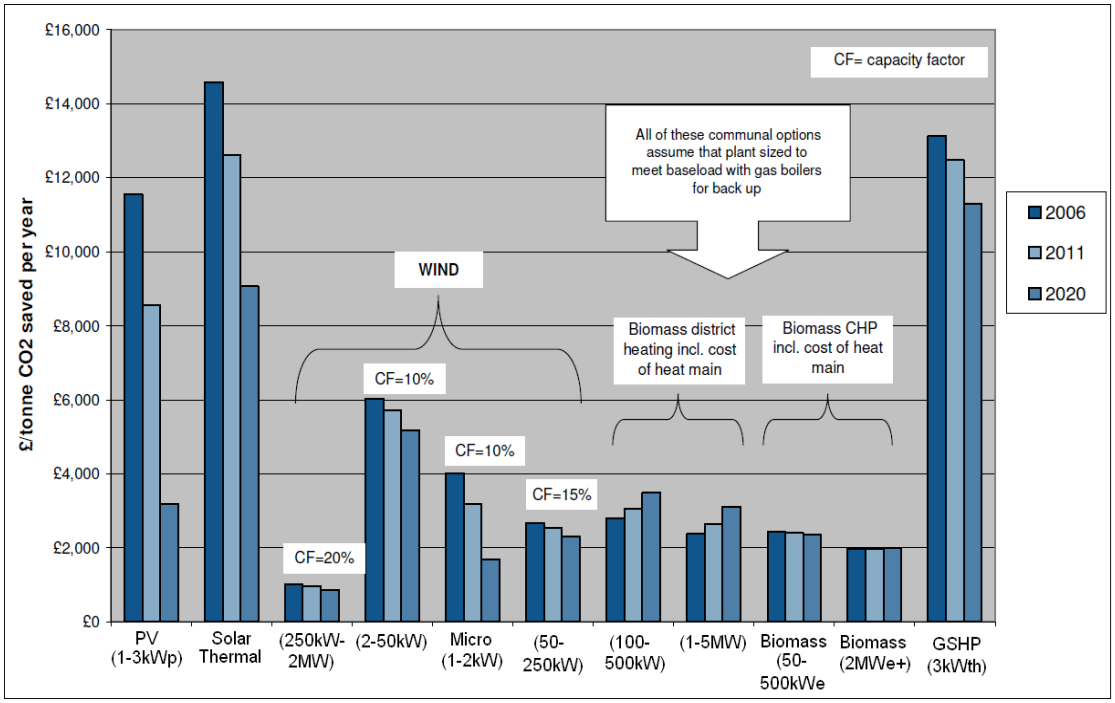

Figure 3.2: Estimated cost of CO_2 savings per year from various low or zero carbon technologies (Source: Maunsell & Capener[39], 2007)

Energy and carbon payback of low or zero-carbon systems is also considered, with CO_2 paybacks achieved after 1-5 years for all technologies. Carbon payback of energy efficiency measures is found to take around 10 years[42]. It is envisaged that by 2026, 97% of CO_2 reduction is achieved by renewable energy systems and only 3% by energy efficiency measures as energy efficiency measures are included in future building regulations. It is further concluded that a key technology to

satisfying zero-carbon ratings is biomass CHP, despite being somewhat unproven on a small scale.

The Renewables Advisory Board (RAB) released a report in 2007[43] in which they assessed the role of onsite energy generation in delivering zero-carbon homes. It recommends that onsite generation is enforced wherever possible to stimulate the market for micro renewable energy technology. This could create a new market for micro renewable systems worth £2.3 billion per year. Overall it is expected that PV plays the biggest role in fulfilling CSH Level 6 requirements, being fitted to 70% of all new homes built after 2016. Micro CHP is expected to have the second largest share, with systems being found in around 30% of all new zero-carbon homes. Micro wind turbines are expected in around 10% of zero-carbon homes, while Solar Thermal systems are only expected in less than 5% of new builds. Modelling has also predicted that 12% of newly built homes after 2016 will not be able to meet the stringent requirements set out by the CSH. It is further discussed how the cost of low or zero carbon technology compares with estimated CO_2 savings, with results summarised in Figure 3.3.

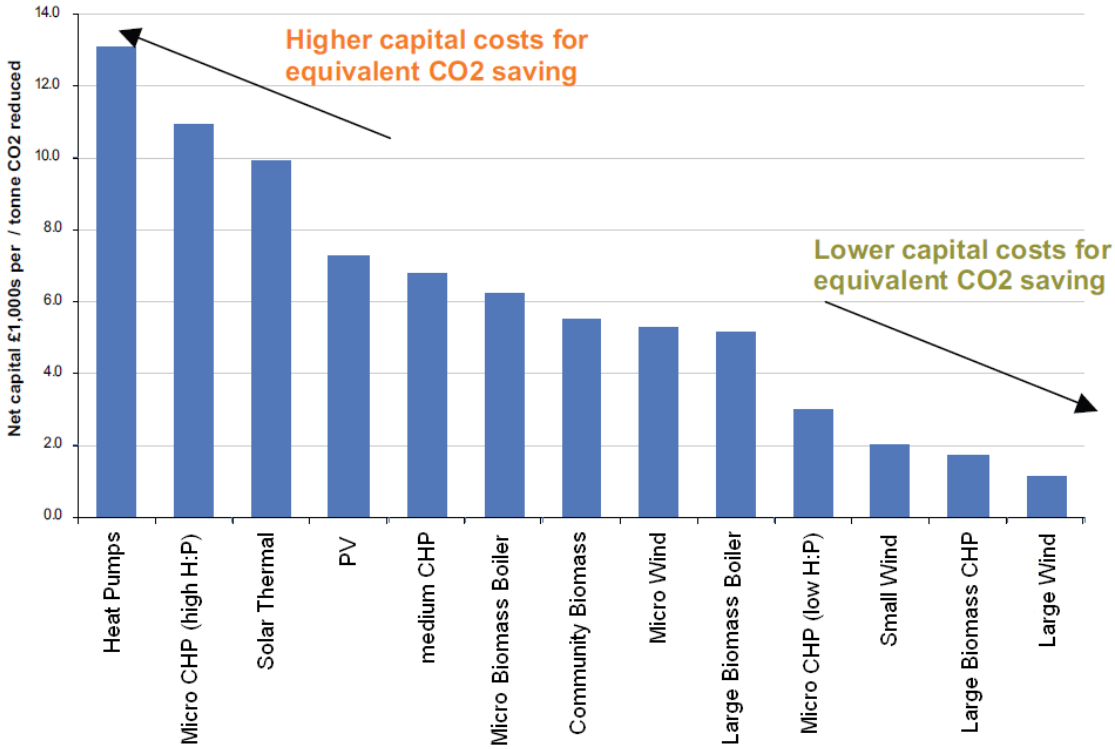

Figure 3.3: Capital cost for CO_2 saving for various low and zero carbon technologies (Source: RAB[43], 2007)

For the case of single dwellings the lowest estimated cost of achieving CSH Level 6 through renewable energy systems is around £13,000, while the cost drops to £7,000 for large developments in urban areas and £4,000 in rural areas. For single

dwellings the lowest cost is achieved using a 1.3kW micro CHP system and a 2.3kW PV system.

In 2008 Moloney et al.[44] investigated housing and sustainability from a different view by looking at the gap between technical solutions and householder behaviour in Australia, which is also applicable to other countries such as the UK. A knowledge gap was identified in the socio-technical factors influencing the uptake of new technical innovations[45]. After reviewing two case studies, it was concluded that the interaction between technology and householder behaviour can best be described as a relationship, which is a result of social practice. People's perception will strongly depend on social standards and norms, therefore to successfully mitigate climate change, more will need to be done than simply setting regulations.

A knowledge gap has also been identified on the supply side of zero-carbon homes in the UK by Chen et al[46] in 2008. Using a system for value judgement used in BRE's EcoHomes 2006[47], the knowledge about sustainability was assessed on a group of Architectural students. It was found that while many young Architects are aware of the sustainability issues, very few have been equipped with the technical knowledge that is required to address them.

An assessment on meeting the challenge of building zero carbon homes was presented by Northumbria University in 2008[48], which discusses a holistic approach to meeting the 2016 targets. It suggests that zero-carbon homes can only be achieved through an interaction of regulations, supply chain, technology and behaviour, illustrated by Figure 3.4.

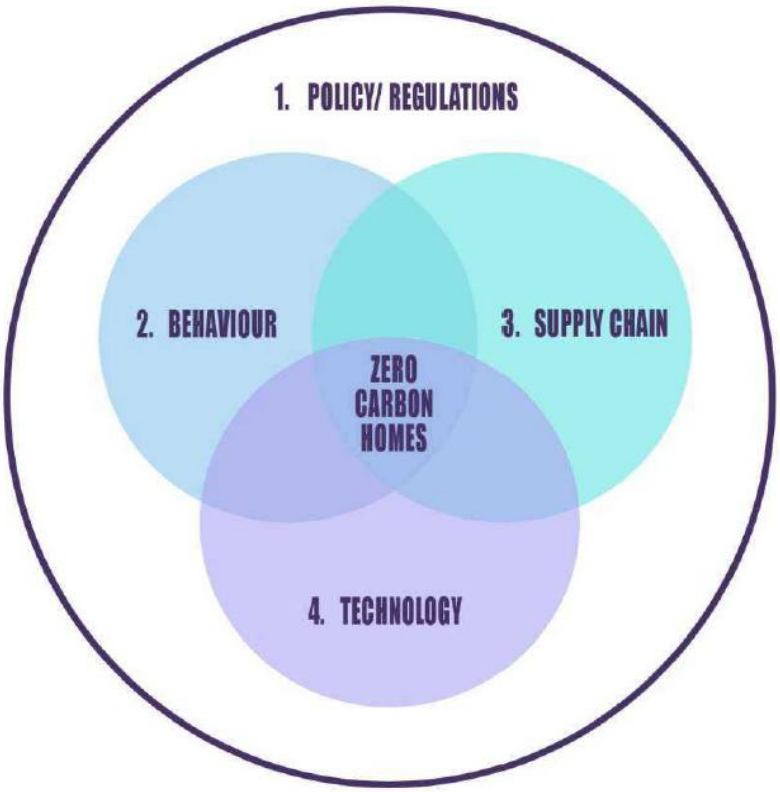

Figure 3.4: Interaction between supply chain, technology and behaviour to achieve zero-carbon homes (Source: Theobald et al[48], 2008)

Due to adequate regulations including CSH at least 2050 targets can be considered feasible[49]. Behavioural changes however are much more difficult to achieve. Only 44% of the UK population is actively trying to save energy[50], and only 4% feel that they personally can make a difference[51]. While there are recognised barriers for the general public to actively reduce their carbon footprint[52], carbon taxing is largely opposed[53] and even perceived to increase fuel poverty[54]. In terms of the supply chain it is observed that industry has adapted well so far, bringing various professionals closer together[55]. Currently good progress has been made with methods to deliver individual zero-carbon homes, but the next step is delivering eco-towns. This would provide the opportunity to bring together environmental, economic and social sustainability, but require a change in the planning system[56]. While some feel that achieving the 2016 CSH target is an insurmountable task from a supply chain perspective[57], others believe it is achievable[58] given political urgency and a strong will for implementation in a set timescale. The available technology to improve the thermal performance of existing buildings includes retrofitted insulation, double or triple glazing, and phase change materials[59] to improve the thermal mass, where increasing thermal mass in particular can be very beneficial[60]. The application of the renewable energy systems Micro Wind, PV and Solar Thermal are also discussed. It is identified that existing methods of predicting wind energy generation are highly inadequate for urban environments, as wind speed variations and surface roughness are not considered. For both Wind and PV generation, there is a considerable mismatch between supply and demand, with about 70% of

renewable energy having to be exported for either system. In future, the use of smart metering is expected to improve energy exporting as well as behavioural changes. PV is perceived as the most versatile and promising technology, but there may be a shortage in the supply chain if demand begins to grow with the introduction of zero-carbon homes[57].

In 2008, a Zero-Carbon Task Group Report[61] by the UK Green Building Council set out to revise the definition of 'zero-carbon' set out in the Code for Sustainable Homes. After reviewing case studies and modelling a variety of scenarios, it was concluded that 10-80% of new builds would not be able to satisfy the original definition of zero-carbon. Instead, it was recommended that the definition is changed to also allow near-site energy generation, provided it can be demonstrated that these offsite solutions were installed specifically to provide for the particular development. This view is also shared by other researchers[62]. It was further found that the additional cost per dwelling for renewable energy systems would range on average from £13,000 for single urban dwellings to £800 for large rural developments, with the overall average being around £6,000.

To take the financial analysis one step further, the Department for Communities and Local Government released a cost analysis[63] of the Code for Sustainable Homes in 2008. This report assesses the estimated cost involved in achieving CSH Level 6 rating for different types of dwellings. Building Regulations 2006 compliant buildings are used as a basis. The cost for achieving the minimum energy requirements varies largely depending on building type, while the cost of achieving a full CSH Level 6 rating will also depend on the ecological value and the flood risk associated with the development. Results are summarised in Table 3.A. Zero stamp duty is not accounted for by this analysis, which could reduce the cost implied with achieving CSH Level 6 ratings by up to £15,000.

Table 3.A: DCLG[63] Estimated costs in 2008 of achieving CSH Level 6 rating

		Min. Energy for Level 6		**Full Level 6 rating**	
		Excluding Micro Wind	Including Micro Wind	Best Case	Worst Case
Small Development	Detached	£40,200	£36,600	-	£47,500
	Mid terraced	£29,200	£24,800	-	-
	End terraced	£29,400	£24,700	-	£37,700
Market Town	Detached	£32,800	£13,100	£37,800	-
	Mid terraced	£24,700	£9,000	-	-
	End terraced	£24,800	£8,800	£31,200	-

The additional cost of achieving CSH Level 6 standards is expected to reduce by 15% in 2010, 26% in 2016 and 35% by 2025.

This cost assessment was revised[64] in 2010 (based on 2009 costs) with improved modelling and cost data validation. According to the revised assessment, the overall average cost of improving 2006 Building Regulation dwellings to CSH Level 6 ratings is around £38,500 in 2009, £34,800 in 2012 and £33,500 in 2017. This does not account for potential wind energy generation, but does assume communal biomass heating schemes.

In 2009 Gupta and Chandiwala[65] concluded that Industry is currently struggling to achieve CSH Level 6 requirements due to the barriers cost, skill and knowledge. To facilitate the CSH assessment of buildings in the design stage, a model was created, based on Passiv Haus[66] and AECB Energy Standards[67]. Cost was found to be the key barrier[68] to achieving CSH level 6. Modelling of different scenarios has shown that while achieving CSH Level 5 would cost around £26,000 more than CSH Level 3, achieving Level 6 could mean extra costs up to £46,500. Based on this it is concluded that energy requirements should be reduced as much as possible before considering the integration of renewable energy systems in zero-carbon homes.

Considering the high cost involved with building CSH Level 6 dwellings using onsite solutions, in 2009 Chow explored the option of using district energy systems as a more cost effective measure[69]. A building energy model[70], which is based on SAP 2005 and BREDEM, was used to estimate energy requirements. Based on modelled results it is estimated that 40m^2 PV and a 10kW biomass boiler is required to satisfy the energy of a potential CSH Level 6 dwelling. This results in total cost of around £28,000. When looking at a larger development of 50 identical dwellings, it is proposed that a 225kW Wind turbine and a 500kW biomass boiler are able to provide all the required energy. A CHP system is mentioned as an alternative, but not considered for analysis. The estimated wind turbine output is based on an average of manufacturer predictions and measurements from similar case study systems[71]. While running costs are unchanged, capital costs are shown to reduce by 74% to an estimated £7,300 per dwelling. It is also noted that the use of large wind turbines may not be suitable in urban areas due to regulatory space constraints and their high audiovisual impact. Financial payback for the individual solution is estimated to be 25 years, compared to 10 years for the district energy system.

3.2 Review of Existing Zero-Carbon Homes in the UK

Apart from several low-carbon developments such as in Leeds[72], several zero-carbon buildings have been completed in the UK. Some privately built homes include the zero-carbon house in Birmingham[73], or the zero-carbon home on Britain's most northern island of Unst[74]. These buildings are built to the highest standards of insulation and air tightness and make use of low energy appliances and natural day lighting where possible. They typically use PV, air or ground source heat pumps and large onsite heat storage capacities.

Other zero-carbon homes have also been built to provide proof of concept and experimental data. The BRE Innovation Park in Watford houses two of them, the Kingspan Lighthouse and the Barratt Green House, which is based on preliminary findings from the EcoSmart Village in Buckshaw. Both are shown in Figure 3.5.

Figure 3.5: Barratt Green House (left) and Kingspan Lighthouse (right)

The Kingspan Lighthouse[75] features extensive use of renewable energy systems, including a large area (46m^2) PV and solar thermal system, a wind catcher for ventilation with heat recovery system, and a biomass boiler. The Barratt Green House[76] design is slightly more focussed on preserving energy, designed with high thermal mass to dampen heating and cooling needs in extreme weather. Large windows with shutters provide an active balance between natural day lighting and solar gain, while a mechanical ventilation system with heat recovery provides fresh air. Onsite energy is generated using a PV system, while some roof area is used for roof-top planting to further improve insulation and offset some carbon.

BedZED in Beddington, Sutton

Figure 3.6: Photograph of BedZED development

The most important development in recent years, and the only one of its kind in the UK at the time the EcoSmart Show Village was built, is the Beddington Zero Energy Development (BedZED)[77]. It comprises several conceptual homes ranging from CSH Level 3 to Level 6. The final cost of the development is estimated at £15M, which is relatively affordable, especially considering it was later found that 80% of the sustainability measures could have been realised at 20% of the cost[78]. Being developed throughout 1999 and completed in 2002, the 83 buildings were built with the following features:

- Wind driven ventilation with heat recovery
- Passive solar heating
- PV system and low energy appliances
- Rainwater harvesting
- Communal biomass CHP
- High insulation and air tightness
- Locally sourced materials to reduce embodied energy
- Office space to encourage and shared communal car schemes to encourage home working and reduce vehicle dependence[79]

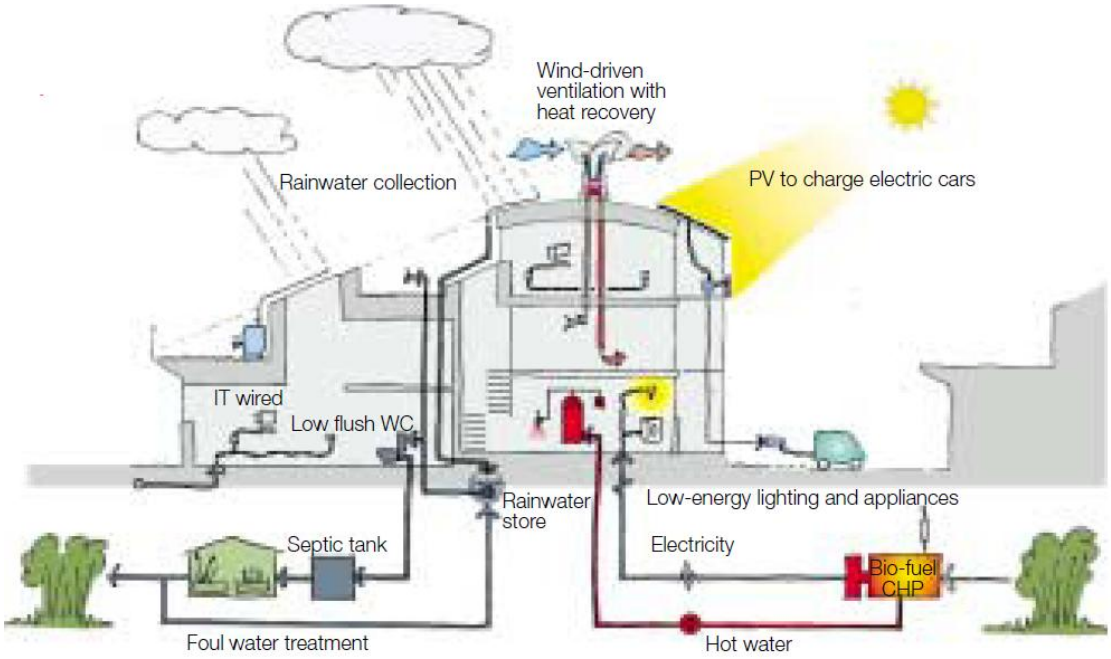

Figure 3.7: Schematic diagram showing BedZED features (Source: Twinn[77] 2003)

The BedZED development has been tried and tested for many years, realising its target of being a net zero-carbon development[80]. Throughout its first year of operation, the development surpassed its target reduction in energy demand for hot water, mains water and fossil fuel car mileage, and reached its target reduction for space heating. The only target reduction not reached by a margin of 25% was that of electricity demand[81].

Hanham Hall in Bristol

Figure 3.8: Model of Hanham Hall housing design (Source: Barratt Developments)

This is another zero carbon development from Barratt Homes, comprising a zero-carbon village with 178 homes that are built to CSH Level 6 standard, as well as several shops and offices. The development[82] was initiated in 2009, the first homes are due to become available early 2011. This extensive development is expected to lay the foundations for future zero-carbon developments. Its features include:

- Embodied energy conscious construction
- Highest level of energy saving construction, including high levels of insulation and triple glazed windows, as well as high levels of air tightness
- Natural day lighting and energy saving appliances
- Communal biomass CHP system
- Walking & cycling routs and extensive public transport to discourage use of cars
- Greenhouses and allotments for growing own produce

The development will consist of a mix of flats different size houses. Several partners were used as consultants, including BRE, Communities and Local Government and NHBC.

Greenwatt Way in Slough

Figure 3.9: Model of Greenwatt Way development (Source: Inside Housing)

This most recent development[83] consists of 10 test homes that are designed to achieve CSH Level 6. The project was initiated by Scottish and Southern Energy (SSE), designed by PRP Architects and AECOM, and built by Bramall Construction. It will be monitored between 2010 and 2012 to assess the actual energy savings and the potential application after 2016. Features of the Greenwatt Way development include:

- Highly energy efficient building design, high air tightness, triple glazed windows
- Natural ventilation system with heat recovery
- PV roof
- Grey water recycling
- Energy saving appliances and lighting
- Smart metering
- District heating from central plant room

While electricity is largely offset using PV generation, all heat and hot water is supplied from a central plant room that uses a biomass CHP and solar hot water technology. During the monitoring phase the houses are being rented out. The development cost approximately £3.5M, and will be monitored and tested by BRE. The development cost of zero-carbon buildings appears to be decreasing considerably, with Bramall Construction, part of the Keepmoat Group and leading the construction of the Greenwatt development, reportedly being able to build zero-carbon homes for under £130,000[84].

3.3 Summary

The review of existing literature and prototype zero-carbon developments has shown that meeting zero-carbon, and in particular CSH Level 6 standards, is a great but surmountable challenge. It was shown that currently energy efficiency measures are very useful to improve building standards and reduce overall energy demand, in particular for existing buildings. However, their effectiveness and viability will decrease dramatically over time as overall standards improve. In the medium to long term the integration of renewable energy systems is essential to offset any carbon emission of the remaining energy requirement.

The integration of micro renewable systems is not as difficult as anticipated by some, with tests showing that the grid could currently tolerate up to 50% of all UK households feeding energy into the grid. The market for micro renewable systems is expected to grow to £2.3bn per year, and any investments in reducing carbon emissions now will result in long term net savings. The most promising low and zero carbon technologies appear to be PV and biomass CHP or Boiler systems, with wind generation being perceived as being too constrained in urban environments. From a financial and energy point of view, it is undisputed that larger scale renewable energy systems perform significantly better than micro-generation systems.

It was further identified that urban developments play a critical role in achieving national emission targets, and these are the areas that are both most challenging and most important. The anticipated cost involved for these cases ranges between £25,000 and £40,000 in 2010, and around £16,000 to £33,000 in 2016, which has also been identified as one of the most significant barriers to achieving CSH Level 6. Some concerns have been raised about the original definition of 'zero-carbon' which only allows off-site generation if supplied by private wire arrangement. It has been shown that communal or district energy generation could result in cost savings of up to 74% for individual households, and it is suggested that the next step in designing zero-carbon developments should be a move towards eco-towns rather than focussing on individual dwellings.

Further barriers to zero-carbon development that have been identified include behaviour of the general public on the demand side, and a lack of appropriate education about technical solutions for architects on the supply side. Efforts will need to be undertaken in both areas to ensure that the technical potential and feasibility of zero-carbon developments can be fully exploited in practice.

Several private and public prototype developments in the UK how shown that achieving a CSH Level 6 is feasible in practice. The most noticeable existing developments are BedZED, as well as the concept studies Barratt Green House and Kingspan Lighthouse at the BRE Innovation Park. All three have achieved their zero-carbon rating by using innovative building design that is aimed to integrate energy efficiency and renewable energy as much as possible. Common features include high insulation and air tightness, natural ventilation, consideration for solar gains, rainwater harvesting, PV and private or communal biomass heating solutions. Two further developments, Hanham Hall and Greenwatt Way, are due to be completed very shortly. They have been designed to test zero-carbon development on a larger scale, in eco-towns. Both developments feature a combination of individual micro-generation such as PV, and communal solutions such as biomass heating.

4 Barratt Developments PLC

To understand Barratt's motivation in building the EcoSmart village and initiating this research project, background information will be presented on the company, its position in the market and the general marketing strategy.

4.1 The History of Barratt Developments

Barratt Developments PLC has its origins in 1958, when the residential property development company was founded as Greensitt Bros. Being founded in Newcastle upon Tyne, it was taken over by Lewis Greensitt, a local Newcastle builder, and Lawrie Barratt, a former accountant, in 1962. The company was renamed as Greensitt & Barratt.

Sir Lawrie Barratt was frustrated at the high price of houses for first time buyers and decided to build his own house in 1953[85]. Based on this experience he adopted a market-driven approach, which was to "figure out how much low- and middle-wage people could afford and design homes that fit their budgets".

After completing rigorous expansion[86] in 1968, Greensitt & Barratt was floated on the London Stock Exchange. Shortly after the floatation Lewis Greensitt left, and the company was renamed as Barratt Developments PLC[87] in 1973.

As a result of the baby-boom[88] after World War 2, the 1970's saw an unprecedented increase in first-time buyers, and Barratt expanded rapidly into all areas of the UK[89]. The strategic expansion moves were accompanied by a high profile marketing campaign including national television advertisement. Most famously, a campaign was run to promote £7,000 starter homes (around £30,000 in today's worth[90]) featuring actor Patrick Allen and the Barratt Helicopter in 1977[85].

In 1983 Barratt sold 16,500 houses, making the company by far the largest builder in the country. In the mid-1980's the company successfully diversified into upmarket housing, and by 1999 Barratt had sold a total of over 250,000 homes, with around 27,000 plots awaiting development[85].

By 2004 Barratt had achieved annual average sales of around 6,400 houses since the founding of the company, meaning that out of all homes that are in existence today in England and Wales more than 1 out of 70 is a Barratt Home. The year 2007 provided another landmark for Barratt with the acquisition of Wilson Bowden PLC for £2.2bn in 2007[91] in response to similar actions taken by their largest rivals, George Wimpey and Taylor Woodrow. Arguably this investment was

made at an unfortunate time for Barratt, with the 2008 recession subsequently taking its toll.

Today the Barratt group has become profitable again, with an operating profit of £34m recorded in 2009[92]. Barratt Developments currently consists of a network of 25 house building divisions throughout Britain with an estimated 4000 direct employees[89].

4.2 Market Position

In order to gain an idea of the implications of reduced carbon emissions from Barratt homes, it is important to first understand how many new homes are built in the UK and what share Barratt have in this market. Barratt's marketing techniques will also be explored in more detail, as they play a role in assessing what difference the actions taken by Barratt will make to the future UK housing stock.

Market Dynamics

The current housing stock in the UK is estimated to consist of around 25.6 million homes[34]. In 2007, as a result of the lack of affordable homes for first-time buyers, the UK Government announced aspirations to build 240,000 new homes in England every year as of 2016[93]. A projection of annual completions[94] scaled up for the whole of the UK suggests around 320,000 new homes would be built as of 2016 if this challenge was to be fulfilled.

However, due to the economic recession during 2008 there was a sharp decrease in housing completions instead. A historical variation of housing starts and completions over the last 12 years is shown in Figure 4.1.

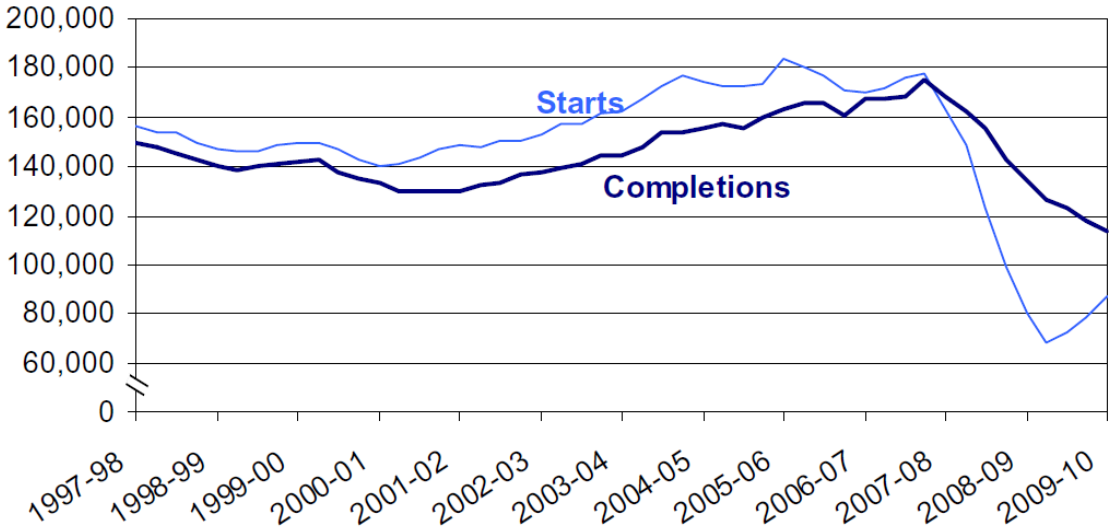

Figure 4.1: Housing (new build) starts and completions in England since 1997 (Source: DCLG Housing Statistics[95] 2009)

With annual completions currently in the region of 113,000[95] for 2009, the market is currently under 50% of the target set out by the Government. However, given time, the market should regain its previous strength, and proposed levels of 240,000 new builds in England might still be reached by 2016 provided there are no further economic strains on the supply chain.

Figure 4.2 shows the current (2010) age structure of the UK. While immigration may result in slight alterations, the current age structure can still be used to form the basis for future demand estimates. Assuming that first time buyers are typically aged late 20's to early 30's, a new peak demand can be expected for this age group around 2016. After this the housing demand for first-time buyers is expected to steadily decrease until 2030. However, similar to the situation experienced with 'WW2 baby boomers' during the 1980's, it can be expected that the 2016 first-time buyers will be looking to move up the property ladder and invest in bigger, better homes, thus increasing the demand for higher quality homes by 2030.

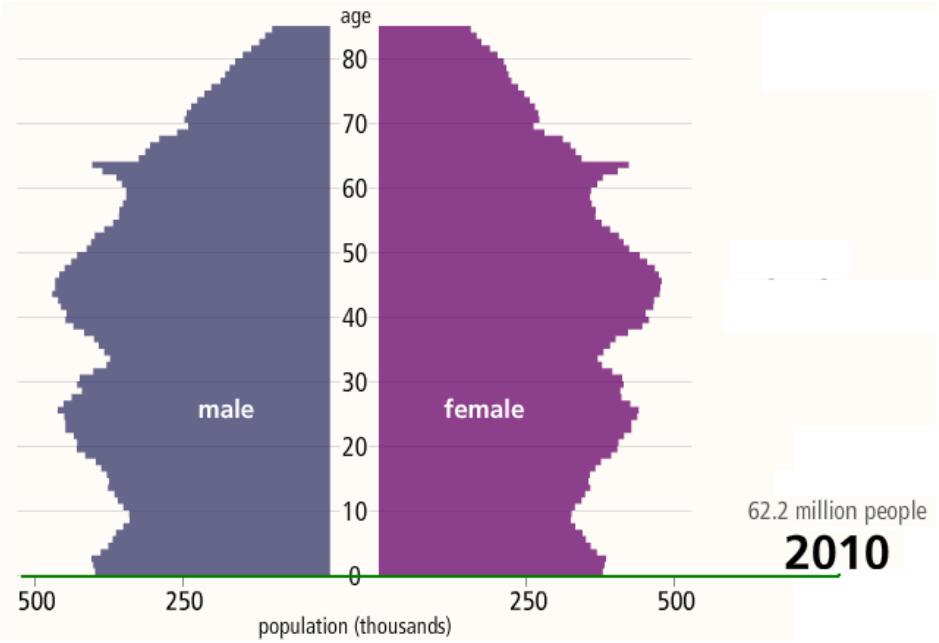

Figure 4.2: Age Structure of the UK with 2010 as baseline (Source: Office for National Statistics)

Barratt's Position in the Current UK Market

The current market of an estimated 113,000 completions can be broken down into flats and houses based on NHBC estimates. In 2007 the market share of flats was predicted to be 51% of all new-builds, which is an increase over historic figures. 22% of new builds would be terraced[96], the remaining 27% detached housing.

The average selling price of new build houses in the UK in August 2010 was around £213,100, with August 2009 selling prices averaging around £196,800[97]. The regional breakdown for both years is shown in Figure 4.3.

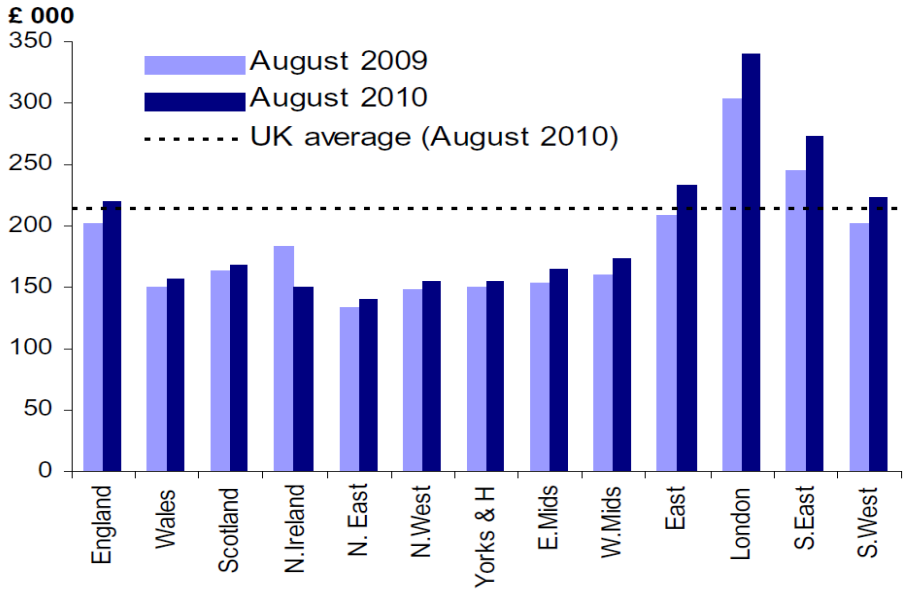

Figure 4.3: Regional breakdown of house prices in August 2009 and 2010 (Source: DCLG Price Index[97] 2010)

According to the most recent Busniess Report[92], Barratt Developments sold over 13,200 homes in the UK in 2009, 50.5% of which consisted of houses and 49.5% of flats. This leads to the 2009 statistics presented in Table 4.A.

Table 4.A: Barratt Developments 2009 estimated market share[92]

	Barratt Sales	UK Total Sales	Market Share
Houses	6700	55,000	12.2%
Flats	6500	58,000	11.2%
Total	13,200	113,000	**11.7%**

The average price of a Barratt home in 2009 was £157,000, which is 20% below the national average of August 2009. While the actual difference will be smaller as many Barratt developments are based in the northern regions of the UK, it still highlights Barratt's underlying strategy to offer affordable homes.

4.3 Marketing Strategy and Philosophy

Historically, Barratt Developments has always been a company who had a high emphasis on marketing. They were one of the first companies, certainly in the building sector, to treat marketing as an integrated process in product development. To put the marketing ingenuity of early days into perspective, a brief review of marketing developments is outlined below.

In 1954, only shortly before Barratt Development was founded, the actual concept of marketing was introduced by Drucker[98], stating that "Marketing is the unique function of business, it is the whole business seen from the customer's point of view. Concern and responsibility for marketing must permeate all areas of the enterprise." During the 1950's and 1960's marketing was then further defined[99] in detail. During the 1970's and 1980's a range of markets began to segment, leading to increased customer power and the wish to obtain more individualised products.[100] Only then were customer opinions and wishes really taken into account, eventually leading to a consideration of treating marketing as a process rather than a function[101]. Using this philosophy meant every part of a company would essentially be concerned with marketing by constantly keeping the customer in mind.[102] Sir Barratt has effectively done just this from the outset – he started off

in the early 1960's with the aim to create a product that is designed to fit the needs and wants of customers, being both affordable and of high quality.

Another rather innovative marketing concept is presented by experiential marketing. This type of marketing focuses on marketing a product by exciting people and creating a subconscious link between a product and a positive experience. It can be argued that Barratt Developments already implemented an early form of experiential marketing in the late 1970's. Their 1977 high profile campaign where a Barratt helicopter and a well known actor featured in TV advertisements reportedly received huge publicity at the time, creating an impressive Brand image. Again, Barratt Developments had shown that their marketing strategy was well applied and ahead of its time.

Today the marketing process remains a key cornerstone of the company, and Barratt make continuous efforts to develop their brand image to reflect this. In 2007 it was recognised that product development based on customer feedback has become increasingly important across all industries, and it was decided to emphasise this with a new marketing campaign. The Barratt slogan was changed to "built around you", and a high profile advertisement campaign was launched, including frequent TV and newspaper advertisement.

During the 1980's the Barratt range was increased to also satisfy the up-market for high quality homes, which has been a successful diversification to this date. Throughout most of its history Barratt had adopted the slogan "Britains Premier Housebuilder" to reflect its market position as well as its future aspirations. Today, the declared philosophy of Barratt Developments is both broadened and generalised to address all aspects of the business. While high levels of quality and customer satisfaction continue to be seen as core strengths, the philosophy now includes the 5 key areas Performance, Customer, People (staff), Partners and Planet (sustainability). The latter now plays a more important role than ever before.

To reflect their ambitions Barratt have now taken the next step in being at the forefront of development. After the announcement of the CSH, Barratt Development initiated several pioneering projects to develop their understanding of the task ahead. This will also ensure they maintain their leading position in the UK housing market.

- In 2006 the EcoSmart show village was built to test the performance of several low and zero carbon energy systems under real weather conditions.
- In 2008 Barratt built the Green House in the BRE Innovation Park, one of the first zero-carbon concept homes in the UK.
- In 2011 the company will complete the largest zero-carbon development in the UK, the Hanham Hall eco-town in Bristol. It comprises 195 units that are designed to meet CSH Level 6 standards, shown in Figure 4.4.

Barratt Development's persistent efforts to remain innovative in both marketing and product development is likely to ensure that they will be well prepared to enter a new era of zero-carbon development in the UK as of 2016. Barratt hope that this approach will enable them to continuously strengthen their market position in the foreseeable future.

Figure 4.4: The latest Barratt Developments innovation; Eco-town Hanham Hall (Source: Barratt Developments)

5 The EcoSmart Show Village

This chapter will provide a detailed overview of the EcoSmart village test site.

The Barratt EcoSmart show village was constructed in 2006, located in the residential estate Buckshaw near Chorley, Lancashire. Figure 5.1 shows its location on a map, between the M6 and M61 motorways. Table 5.A gives the Latitude and Longitude of the test site.

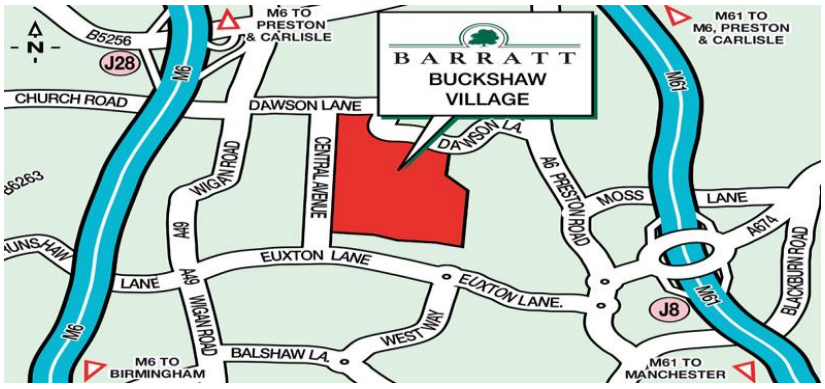

Figure 5.1: Map showing location of Buckshaw EcoSmart Village (Source: EcoSmart village brochure)

Table 5.A: Latitude and Longitude of EcoSmart village (Source: Google Earth)

Latitude	53.39° North
Longitude	2.38° West

The EcoSmart Village consisted of seven test homes which featured 2006 energy-efficiency and renewable energy technologies. The test houses are based on popular conventional houses, as sold in large numbers by Barratts Development PLC every year. These standard houses were deliberately chosen to test the performance and of the systems without modifying existing designs to incorporate them. Figure 5.2 and Figure 5.3 provide an overview of the layout of the EcoSmart show village, where Figure 5.3 shows the names given to each house. Throughout the monitoring period the test houses were used as show homes.

Figure 5.2: Photograph showing a model of the test site

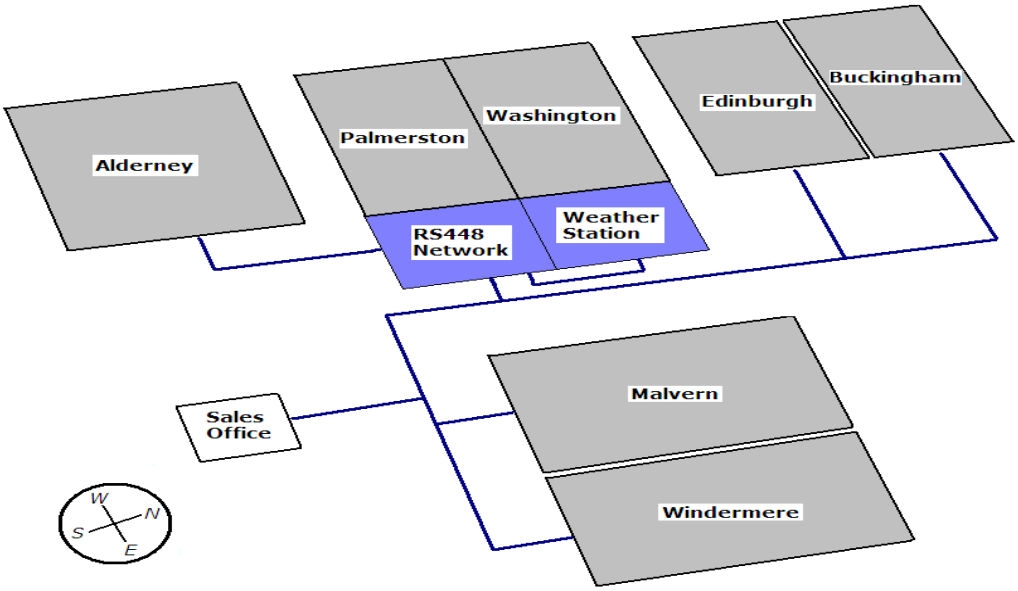

Figure 5.3: Schematic layout of the test homes

The test houses have been built to meet SAP 2001 standards, with improved U-values for additional insulation and energy efficiency. They incorporate some of the following low or zero carbon systems:

- Micro Wind Turbine (MWT)
- Solar photovoltaic panel (PV)
- Solar thermal collector panel (flat panel or evacuated tube)
- Geothermal ground source heat pump (GSHP)
- Micro combined heat and power unit (μCHP)

- Rainwater harvesting and recycling system
- Energy efficient lighting
- Under-floor heating and 'smart' Heat Store systems

Figure 5.4 provides an overview of the energy efficiency or generation features of the EcoSmart Village homes. Below is a detailed description of each building.

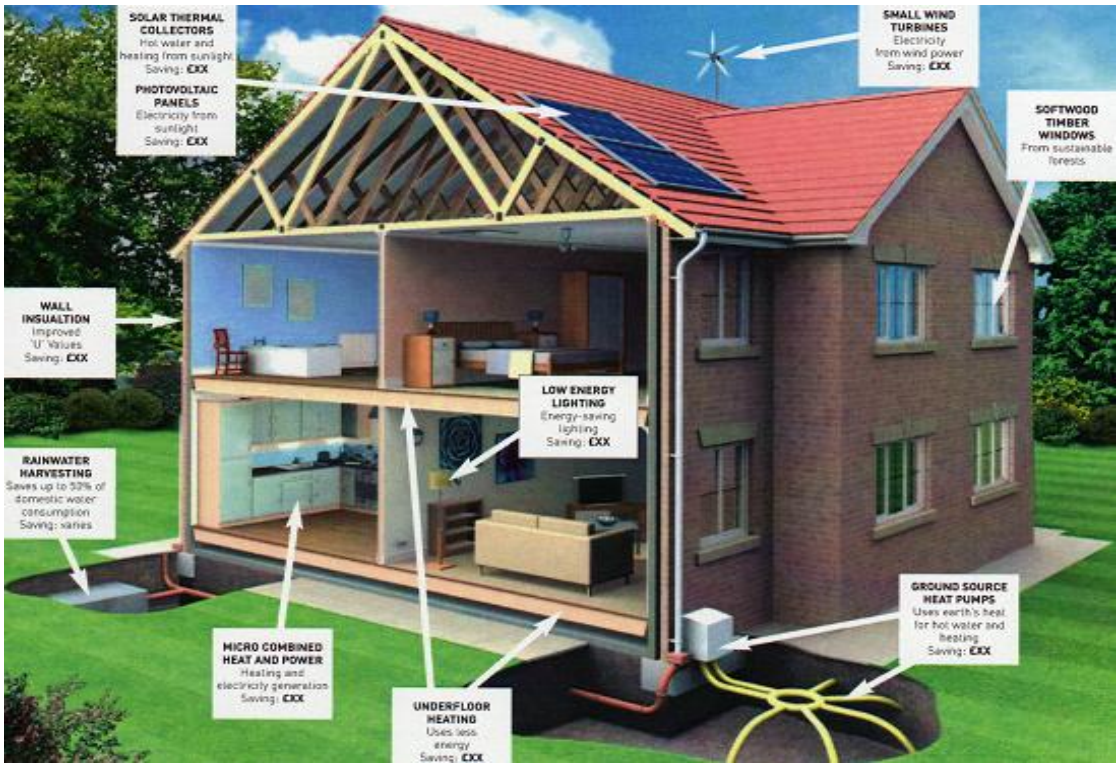

Figure 5.4: Efficiency measures and renewable energy systems incorporated at the EcoSmart village

Alderney

The House of the type "Alderney" is a fully detached property in the upper-class range of houses, consisting of two floors. The ground floor contains a large kitchen, dining room and separate lounge. The upstairs area consists of 4 bedrooms and 2 bathrooms. Detailed information about the building is given in Table 5.B below.

Table 5.B: Showing detailed information for Alderney

Ground Floor Area (m^2)	56.4
First Floor Area (m^2)	47.8
Total Floor Area (m^2)	104.3
Total Volume of Building (m^3)	253.4
Insulation Walls (U-value, W/m^2K)	0.28
Insulation Roof (U-value, W/m^2K)	0.16
Insulation Ground (U-value, W/m^2K)	0.24
Insulation Windows (U-value, W/m^2K)	1.57
Insulation Doors (U-value, W/m^2K)	1.59
Space Heating Demand (kWh)	5278
Hot Water Demand (kWh)	3500
SAP Rating	98

The energy saving lighting system has total power of 426 Watts. The building also contains several lights and appliances, which use power from sockets. The Alderney is equipped with a 2.5m² flat panel Solar Thermal system and a 400W rated Micro Wind Turbine. The wind turbine is mounted on the west side of the roof, the direction of prevailing wind, while the Solar Thermal system is south-facing. An inverter and import/export meter are used to export the generated electricity. Schematic diagrams of the systems are shown Figure 5.5.

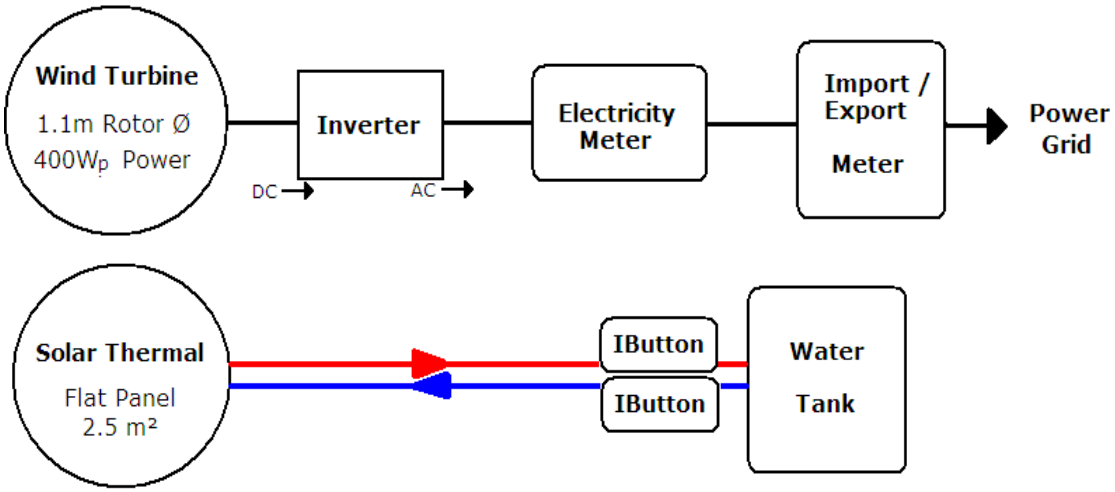

Figure 5.5: Schematic diagrams of Alderney systems

Palmerston

The "Palmerston" house is a semi-detached property in the lower-class range, again consisting of two floors. The ground floor contains a lounge, and a compact kitchen / dining-area combination. The upstairs area consists of 3 bedrooms and 1 bathroom. Detailed information is given in Table 5.C below.

Table 5.C: Showing detailed information for Palmerston

Ground Floor Area (m²)	36.3
First Floor Area (m²)	34.9
Total Floor Area (m²)	71.2
Total Volume of Building (m³)	173.6
Insulation Walls (U-value, W/m²K)	0.28
Insulation Roof (U-value, W/m²K)	0.22
Insulation Ground (U-value, W/m²K)	0.24
Insulation Windows (U-value, W/m²K)	1.58
Insulation Doors (U-value, W/m²K)	0.89
Space Heating Demand (kWh)	3194
Hot Water Demand (kWh)	2917
SAP Rating	102

The Palmerston lighting system has combined power of 320W. The building also contains several lamps and appliances, which use power from sockets. The Palmerston uses a PV and a GSHP system. The 1.04kW PV system with area of 7.8m² is south-facing with 45º inclination, and is interfaced with an inverter to allow AC electricity export. The 4.8kW$_e$ GSHP is a vertical borehole system and is combined with a smart heat-store system, which uses under-floor heat distribution. The schematic diagrams of both systems are shown in Figure 5.6.

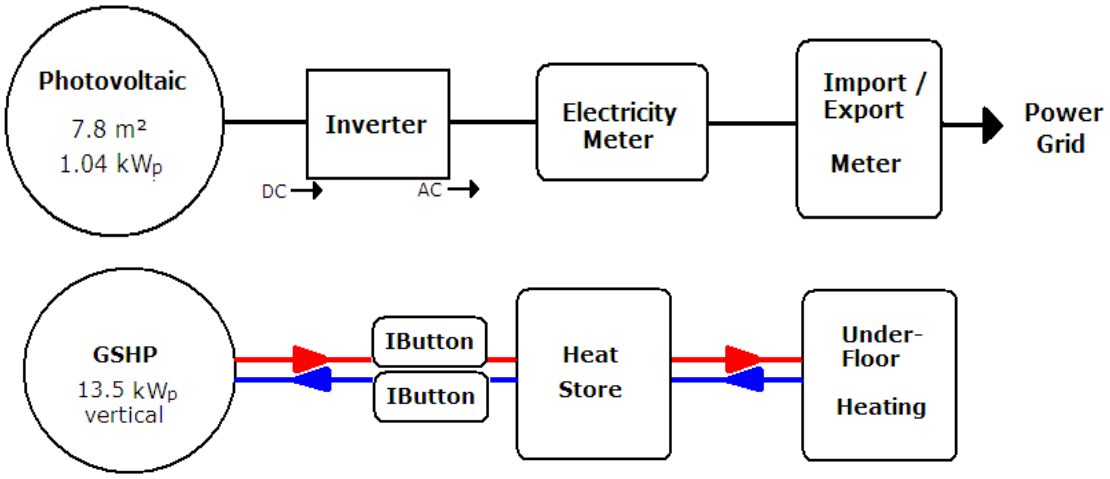

Figure 5.6: Schematic diagrams of Palmerston systems

Washington

The "Washington" is a semi-detached property in the lower-class range, again consisting of two floors, similar in build but slightly smaller than the Palmerston. The ground floor contains a small kitchen and lounge / dining-room combination. The upstairs area consists of 2 bedrooms and 1 bathroom. Detailed information about the building is provided in Table 5.D.

Table 5.D: Showing detailed information for Washington

Ground Floor Area (m^2)	29.0
First Floor Area (m^2)	29.0
Total Floor Area (m^2)	58.0
Total Volume of Building (m^3)	141.6
Insulation Walls (U-value, W/m^2K)	0.28
Insulation Roof (U-value, W/m^2K)	0.16
Insulation Ground (U-value, W/m^2K)	0.24
Insulation Windows (U-value, W/m^2K)	1.59
Insulation Doors (U-value, W/m^2K)	0.89
Space Heating Demand (kWh)	2556
Hot Water Demand (kWh)	2667
SAP Rating	106

The building contains a 245W lighting system, as well as lamps and appliances, which use power from the sockets. Its systems are very similar to the Palmerston layout, comprising the same size and type of PV and GSHP systems. The GSHP is also interfaced with the same smart heat store and under-floor distribution system, and the PV system with an inverter and import/export meter. However, the Washington PV system faces east at an inclination of 45º. The schematic layout of the systems is shown in Figure 5.7.

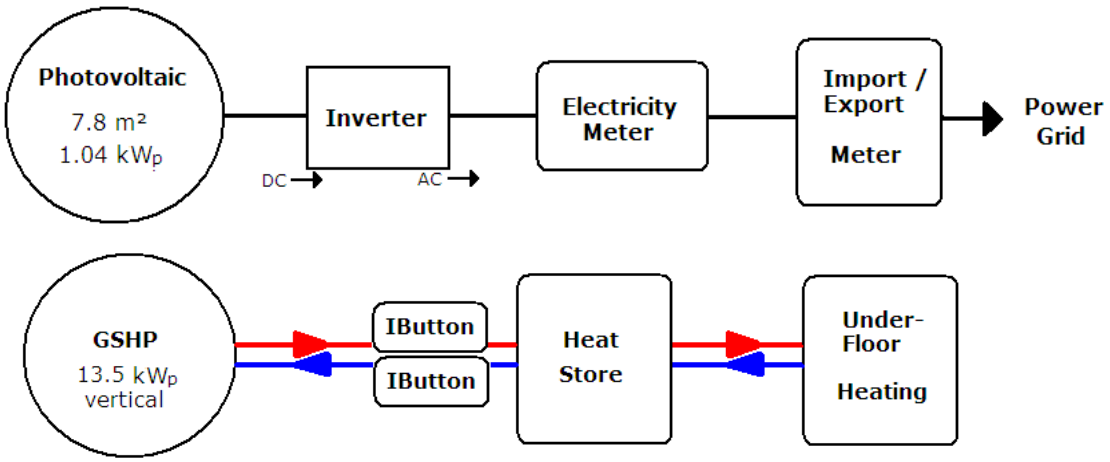

Figure 5.7: Schematic diagrams of Washington systems

Edinburgh

The "Edinburgh" is a stand-alone property in the mid-class range, consisting of two floors. The ground floor contains a lounge, dining room and a kitchen with an adjacent utility room. The upstairs area comprises 3 bedrooms and 1 bathroom. Detailed information is given in Table 5.E.

Table 5.E: Showing detailed information for Edinburgh

Ground Floor Area (m^2)	48.6
First Floor Area (m^2)	38.9
Total Floor Area (m^2)	87.4
Total Volume of Building (m^3)	212.3
Insulation Walls (U-value, W/m^2K)	0.28
Insulation Roof (U-value, W/m^2K)	0.18
Insulation Ground (U-value, W/m^2K)	0.24
Insulation Windows (U-value, W/m^2K)	1.56
Insulation Doors (U-value, W/m^2K)	1.38
Space Heating Demand (kWh)	5361
Hot Water Demand (kWh)	3222
SAP Rating	94

The energy-saving lighting system requires 418W in total, and the building also contains other lamps and appliances using socket power. This building uses a gas-fired µCHP system and a Micro Wind Turbine. The 1kW rated wind turbine is mounted at the highest point of the roof, and uses and inverter to allow electricity export. The µCHP system has a rated power output of up to $12kW_t$ /$1kW_e$, and like GSHP it is also interfaced with a smart heat store and under-floor heating. Schematic diagrams are provided in Figure 5.8.

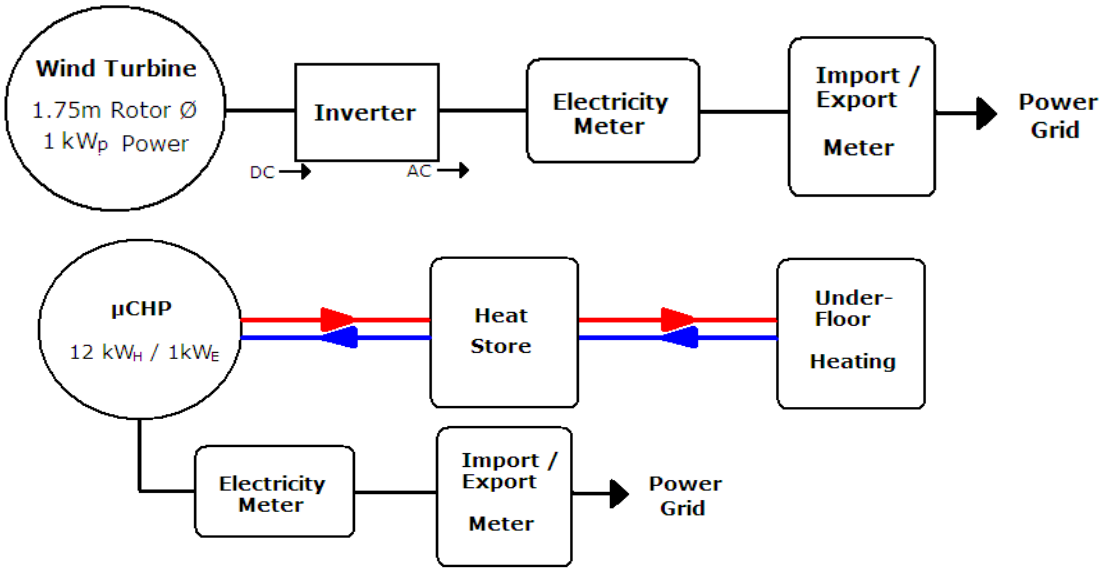

Figure 5.8: Schematic diagrams of Edinburgh systems

Buckingham

The "Buckingham" is a stand-alone property in the mid-class range, comprising two floors. It is very similar to the Edinburgh albeit slightly larger. The ground floor contains a lounge, separate dining room and a kitchen with attached utility room, while there are 4 bedrooms and 2 bathrooms upstairs. Details of the Buckingham are given in Table 5.F.

Table 5.F: Showing detailed information for Buckingham

Ground Floor Area (m^2)	44.2
First Floor Area (m^2)	53.7
Total Floor Area (m^2)	97.8
Total Volume of Building (m^3)	239.7
Insulation Walls (U-value, W/m^2K)	0.28
Insulation Roof (U-value, W/m^2K)	0.18
Insulation Ground (U-value, W/m^2K)	0.24
Insulation Windows (U-value, W/m^2K)	1.55
Insulation Doors (U-value, W/m^2K)	1.38
Space Heating Demand (kWh)	5860
Hot Water Demand (kWh)	3389
SAP Rating	94

The Buckingham lighting systems has total power of 360W and the building uses some socket-powered lamps and appliances. Just like Edinburgh, the Buckingham also contains a µCHP system and a Micro Wind Turbine of the same size and make. Again, the µCHP uses a smart heat store for improved performance as well as under-floor heat distribution, while the wind turbine is connected to an inverter. Schematic diagrams of the Buckingham systems are shown in Figure 5.9.

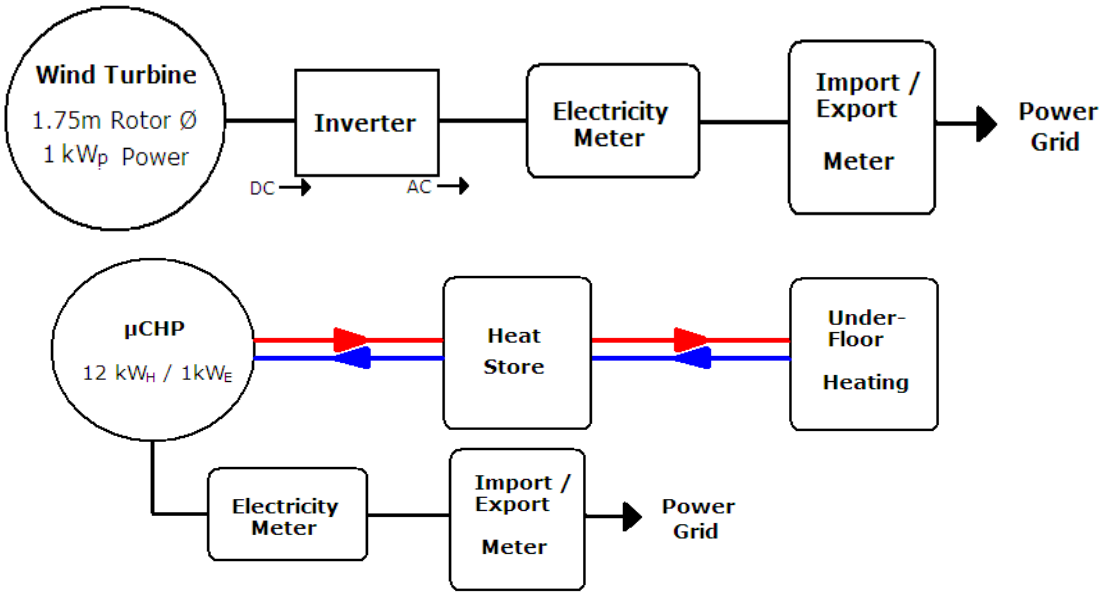

Figure 5.9: Schematic diagrams of Buckingham systems

Malvern

The "Malvern" is fully detached and represents the most luxurious of the houses, consisting of three floors. The ground floor contains a large kitchen with utility room, spacious lounge and dining room. The first floor comprises 2 bedrooms, a bathroom and a study. The top floor contains 2 bedrooms and a bathroom. More details are summarised in Table 5.G.

Table 5.G: Showing detailed information for Malvern

Ground Floor Area (m²)	63.5
First Floor Area (m²)	60.6
Second Floor Area (m²)	45.1
Total Floor Area (m²)	169.3
Total Volume of Building (m³)	420.9
Insulation Walls (U-value, W/m²K)	0.28
Insulation Roof (U-value, W/m²K)	0.19
Insulation Ground (U-value, W/m²K)	0.24
Insulation Windows (U-value, W/m²K)	1.54
Insulation Doors (U-value, W/m²K)	0.89
Space Heating Demand (kWh)	8250
Hot Water Demand (kWh)	4111
SAP Rating	99

The lighting system has total power of 690W, and apart from the usual lamps and appliances the Malvern also incorporates an integrated Lutron entertainment system. A 400W rated Micro Wind Turbine, a GSHP system, and PV system were all tested at the Malvern. The PV system faces east at 60º inclination and the GSHP is a combined horizontal and vertical system, each rated at 3.6kW$_e$. Support systems are the same as for all other houses. Schematic diagrams are shown in Figure 5.10.

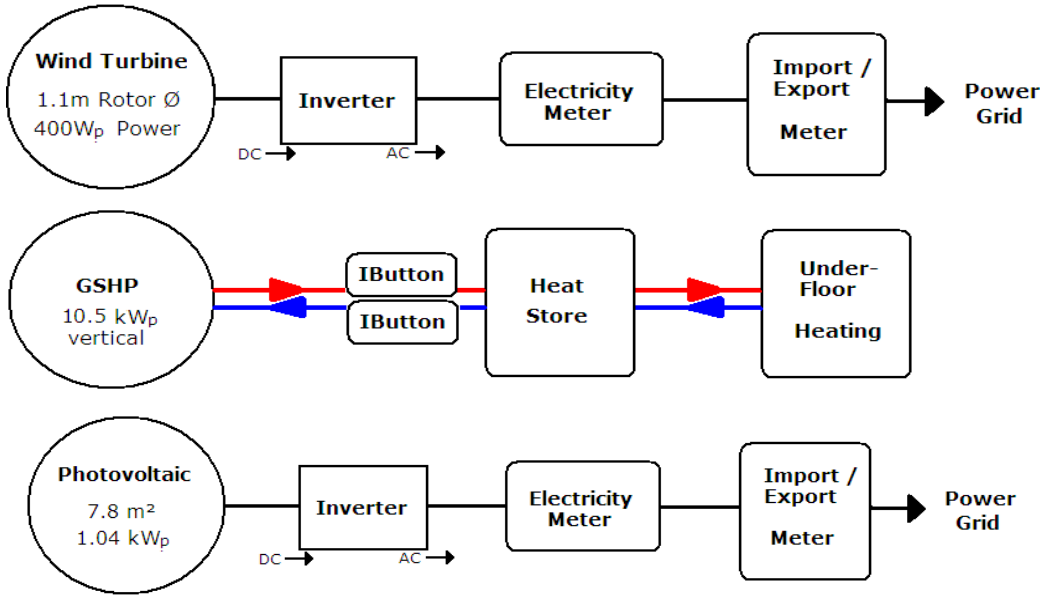

Figure 5.10: Schematic diagrams of Malvern systems

Windermere

The "Windermere" is a fully detached property in the upper-class range of houses offered by Barratts, consisting of two floors. The ground floor contains a spacious kitchen, lounge and dining area. The upstairs area consists of 4 bedrooms and 2 bathrooms. Further details are given in Table 5.H.

Table 5.H: Showing detailed information for Windermere

Ground Floor Area (m^2)	48.6
First Floor Area (m^2)	59.1
Total Floor Area (m^2)	107.7
Total Volume of Building (m^3)	263.9
Insulation Walls (U-value, W/m^2K)	0.28
Insulation Roof (U-value, W/m^2K)	0.18
Insulation Ground (U-value, W/m^2K)	0.24
Insulation Windows (U-value, W/m^2K)	1.55
Insulation Doors (U-value, W/m^2K)	2.07
Space Heating Demand (kWh)	6444
Hot Water Demand (kWh)	3583
SAP Rating	94

The Windermere energy-saving lighting system consumes 406W in total and also has several lamps and appliances using power from sockets. This building incorporates a $3m^2$ Evacuated Tube Solar Thermal system and a 400W rated Micro Wind Turbine. The wind turbine is mounted on the west side of the roof, and its downstream path is partially obstructed by the Malvern house. The Solar Thermal system is facing south at an inclination of 45º. Further details are shown in the schematic diagrams in Figure 5.11.

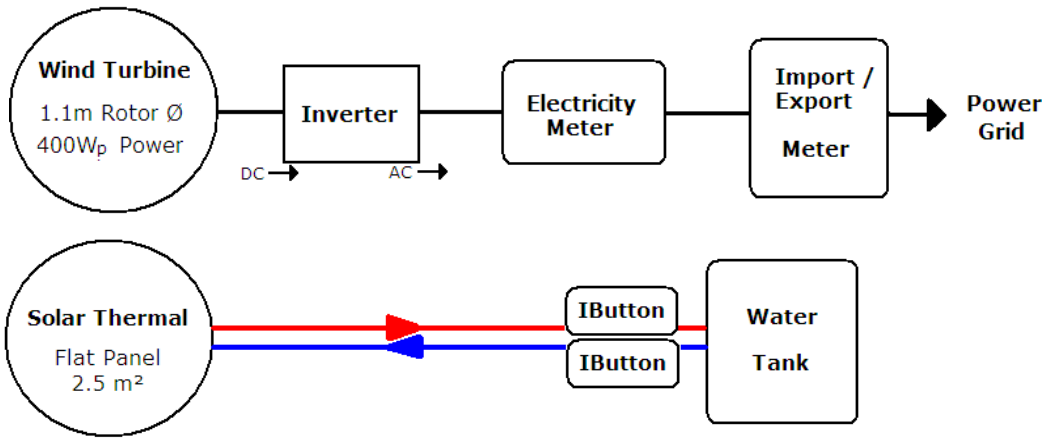

Figure 5.11: Schematic diagrams of Windermere systems

6 Methodology

The EcoSmart village set-up, described in the previous chapter, was used as a test rig to measure and analyse the performance of several micro-generation renewable energy systems. The quality and quantity of data that is gathered from the test site is the key to making this analysis as robust and meaningful as possible. This chapter will provide an overview of the tools and methods used to evaluate energy resources and assess the theoretical and actual performance of all integrated energy systems.

6.1 Monitoring Strategy and Apparatus

Part of the uniqueness of this research project comes from the fact that these systems are monitored in near real-life conditions, installed in standard houses and under real weather conditions. The monitoring period lasted 15 months, during which the homes were used as show homes, open to visits by the general public.

The monitoring strategy involved gathering as much data as possible in order to provide a true picture of the performance of the systems and account for any discrepancies between measured output and expectations. To provide a complete picture, the following data was gathered:

- Weather data
- Energy output data from the systems
- Supplementary energy supplied to the building
- Energy consumption of the buildings
- Temperature within the buildings

It was envisaged that this data would be sufficient to analyse the performance of each individual system. The buildings themselves were also analysed in detail to establish their energy demand. Based on these analyses it will be concluded what impact the renewable systems have had and at what cost/benefit ratio.

6.1.1 Simulated Living Conditions

In order to allow the systems to function under realistic conditions and to simulate energy loads, it was attempted to simulate realistic living conditions as far as possible. As the houses at the EcoSmart village were used as show homes, which were open to visitors from 11:00 until 16:00 every day of the week, all lights and appliances such as desk lamps and televisions were switched on during opening hours.

All heating systems throughout the show homes were controlled by thermostats, which were constantly set to 21°C. Some time into the recording phase all thermostats were fitted with anti-tampering devices to stop visitors from changing the temperature settings.

The EcoVillage staff was asked to draw off hot water from the homes that were fitted with solar thermal systems. This was done during mid-day, long enough to empty the hot water cylinders entirely.

6.1.2 Visitor Feedback

All visitors to the EcoSmart village were asked to fill in a questionnaire in order to gain an understanding of the levels of appeal for the various systems, and how much people were generally willing to pay for these systems. The feedback questionnaires (shown in Appendix B, page 338) were analysed by Survey & Marketing Services Ltd. Extracts of the Summary Research Report are given for each of the systems.

6.1.3 Measuring Apparatus

The following section will describe the apparatus used to collect data at the EcoSmart village.

Weather Station

Figure 6.1: Davis Vantage Pro 2 Plus Weather Station at EcoSmart village

The weather station that was used to monitor on-site weather conditions was the UK version of the Vantage Pro 2 Plus from Davis Instruments Corp. It houses a solar powered integrated sensor suite and uses wireless technology to transmit data. The data was transmitted to the Davis WeatherLink data logger. Its integrated memory can store up to 4000 interval readings in case contact to the logging PC is interrupted. It samples weather data every second and then provides average values over the chosen sampling period. The weather station was mounted on the roof of the Washington building. The range of measurement parameters and their estimated accuracy provided by the distributor Ambient Weather Inc. are given in Table 6.A. However, given the mounting arrangement shown in Figure 6.1 the accuracy of the anemometer and attached wind vane must be questioned. Despite being some way above the actual weather station, it is still mounted in relatively close proximity to some of the other integrated instruments, which is likely to provide some distortions in the wind flow.

Table 6.A: Accuracy of Davis Vantage Pro 2 Plus weather station

Measurement Parameter	Maximum Error
Wind speed	2%
Wind direction	7º
Outdoor Temperature	1ºC
Indoor Temperature	1ºC
Outdoor Humidity	3%
Barometric Pressure	1 mbar
Rainfall	4%
UV	5%
Global Solar Radiation	5%

Import/Export meter

Figure 6.2: Import/Export Single Phase Credit Meter 5235

The electricity that was generated by the renewable energy systems was exported to the grid. The two-way link to the grid was established using an import/export meter. The meter used for this project is the British Standard Single Phase Credit Meter, model 5235, shown in Figure 6.2. The meter is tested to IEC 62053-21 Class 1 or 2 standard[103], and has an estimated error of ±1%. These are predominantly used to measure PV and Wind generation and are referred to as 'fixed' meters, and are usually treated as the benchmark meter.

Electricity meter

Figure 6.3: Electricity meter Metermaid

The electricity meters used to measure all electricity generation and consumption were the Metermaid[104] din-rail mounted AC kWh meters from the manufacturer Microcustom International Ltd., shown in Figure 6.3. They have a digital output allowing connection to the data logger, and are built to conform to EN61036 standards, with accuracy rating given as ±1%. They were used to monitor PV and

Wind generators, μCHP, heat-store system, GSHP, as well as house lights and appliances. Readings from these meters will be referred to as 'logger' readings, or 'mobile' readings if taken manually by EcoVillage staff. They will usually be used for control and validation purposes.

Heat meter

Figure 6.4: Supercal 539 Plus Heat Meter

The heat meters that were used to monitor all heat generating devices are the Supercal 539 Plus Heat and Cooling energy meters from the manufacturer Sontex, shown in Figure 6.4. These battery powered thermal energy meters comply with EN1434 (Class 3) and work by measuring the flow rate, using a small turbine, and temperature. They provide data on a display and through M-Bus and pulse output. The meter must be permanently connected directly into the pipe work.

IButtons

Figure 6.5: IButton temperature/humidity recorder

IButtons[105] are small portable sensors with integrated flash memory, developed by Maxim Integrated Products Inc. These devices are battery powered and do not

require a permanent data link. There are two different IButton models with different sensors and storage capacity:

IButton type A - temperature and humidity: capacity for 4096 readings
IButton type B - temperature only: capacity for 2048 readings

According to the manufacturer, the IButton recording devices have accuracy limits of ±0.5º C. They are programmable, and data is retrieved using a USB link to a PC or Laptop. A picture of the IButton is shown in Figure 6.5. The IButtons were used to measure internal temperature and humidity. Due to metering problems described later, they were also used to measure the output of some of the heat generating systems.

6.1.4 Data Capture

The metering set-up and data capture phase was scheduled to continue for 15 months after the EcoSmart village was constructed, with the aim of obtaining 12 months of quality data under the strategy set out previously.

List of Measurements

The following list shows all energy readings that were taken from the EcoSmart Village, excluding weather data:

- Electricity output of all PV systems
- Electricity output of all Micro Wind Turbine systems
- Electricity output of all µCHP systems
- Electricity consumption of GSHP
- Electricity consumption of Heat Store
- Electricity consumption of all downstairs lights
- Electricity consumption of all upstairs lights (if applicable)
- Electricity consumption of all sockets (appliances)
- Electricity consumption of all Malvern entertainment system
- Heat output of all GSHP systems
- Heat output of all µCHP systems
- Gas consumption for all houses without low carbon heating system
- Internal temperatures of every room in every house
- Internal relative humidity of every house (measured in Lounge)
- Flow rates from solar thermal systems using standard integrated flow meters (rotameter type)
- Rain Harvest Tank meter

In addition to this, several readings were taken manually on a daily basis to provide control readings for the data logger readings. The list of manual readings is as above, with the following additions:

- Total energy import of building
- Total energy export of building
- PV readings from a separate meter provided by PV supplier

Logging Interval

To provide a detailed dynamic picture of the performance of the renewable energy systems, an adequate time interval had to be chosen.

For weather data it was anticipated that the measurement with most frequent variation is wind speed. The British Standard BS EN 61400-21:2002 was reviewed, which set out a framework for wind turbine testing. It suggested that wind data readings taken at 10-minute intervals would be adequate for the analysis of micro wind turbines. Consequently the weather data was logged at 10-minute intervals. This interval provided a 2-week safety buffer for the data logger if the uplink to the PC was interrupted. In 2008 the British Standard was reviewed, and the updated version BS 61400-21:2008 now suggests that 1-minute sampling intervals would be more appropriate.

The data logger interval for all electricity meters was set slightly lower, at 5 minutes, to allow a more in-depth analysis of any unexpected power fluctuations. In relation to this a study[106] of the effects of analysin demand patterns at different time intervals revealed that 5-minute intervals are significantly more accurate than longer intervals, such as 1 hour.

IButton sampling intervals needed to be considered differently. Ambient temperatures were not expected to vary significantly or frequently. With the added constraint of a limited memory, it was decided to use 20-minute intervals. This would provide enough memory for 28 days worth of data, allowing data retrieval during monthly visits.

Manual readings were taken once every day by the EcoSmart village staff whenever it was possible.

Metering Problems

It was found that the heat meters for all GSHP and Solar Thermal systems were not working. Error messages were shown on the display, the technical manual suggested the solution ‘send back to manufacturer’. Unfortunately this was not

possible, as they had already been integrated into the pipe work of the systems. As an emergency solution it was decided to attach IButton temperature sensors to the flow and return pipes of these systems to obtain temperature readings. This data could then be used indirectly to obtain energy generation estimates.

6.2 Data Conditioning

After taking measurements from the EcoSmart village it was required to prepare the data for accurate and efficient analysis. In order to condition the data, the format of the different data sets needed to be normalised. Initially the data which was recorded from the EcoSmart village had various different time intervals as previously justified. These are summarised below.

Weather Station: 10-minute interval
Energy readings (data-logger): 5-minute interval
IButtons: 20-minute interval

For analysis, the data had to be changed to equal intervals and the time stamp corrected and aligned.

6.2.1 Data Normalisation and Interpolation

MS Excel was chosen as a general platform for data analysis. The powerful platform contains appropriate tools to carry out different forms of analysis and is widely compatible with other systems.

To analyse and compare all data efficiently and correctly it needs to be in a compatible format. It was therefore decided to change all data to 5 minute intervals by means of linear interpolation.

Energy Data: This data was already recorded at 5-minute intervals using the wireless data logger. The data was manually exported into an MS Excel spreadsheet, where date and time stamps were aligned and any gaps in the data were sized to represent the appropriate number of 5-minute intervals.

Weather Data: This data was recorded using the software Weatherlink 5.3. Using the export function, a spreadsheet was created from various txt files. Some of the units of the data measurements had to be converted, as shown in Table 6.B

Table 6.B: Unit conversions of weather data

Parameter	Original Unit	Converted Unit	Conversion Equation
Temperature	Degree Fahrenheit (°F)	Degree Celsius (°C)	$°C = (°F - 32) \times (5 \div 9)$
Wind speed	Miles per hour (mph)	Meters per second (m/s)	$m/s = 0.447 \times mph$
Pressure	Inches of mercury (inHG)	Millibar (mb)	$mb = 33.8639 \times \text{inHG}$

Once this was done, any gaps in the data were extended to provide continuous time and date values. Having aligned the data, a Visual Basic Macro was used to space out the data. Linear interpolation, outlined in Table 6.C, was deemed to be appropriate given the nature of the data.

Table 6.C: Interpolation of weather data

0	Actual Reading	x
5	Interpolated Reading	$z = (x + y) \div 2$
10	Actual Reading	y

Internal Temperature: Data was imported to spreadsheets from the IButton sensors. After combining all data, all time stamps were aligned and synchronised as well as possible. Some time differences remained in the order of 1-2 minutes. After all data had been aligned and spaced out to account for data gaps, the data was interpolated linearly as shown in Table 6.D.

Table 6.D: Interpolation of internal Ibutton data

0	Actual Reading	x
5	Interpolated Reading	$u = (x + z) \div 2$
10	Interpolated Reading	$z = (x + y) \div 2$
15	Interpolated Reading	$v = (y + z) \div 2$
20	Actual Reading	y

Solar Thermal & GSHP Temperatures: The IButton sensors were also set to 20-minute recording interval to allow for the same 28-day buffer. The data was aligned and interpolated using the same method as for internal temperature readings.

6.2.2 Time Stamp Correction

During the monitoring phase a problem was encountered with the energy data readings that were recorded using the data logger. The system clock of the PC seemed to be faulty, causing the time to jump randomly every couple of hours. All attempts to rectify this problem during the recording stage, including the use of third party time-keeping software, failed.

After the recording stage was completed and all data was retrieved and normalised, there were two sets of data that could be used to rectify this problem:

1. The continuous energy data at 5-minute intervals with a wrong time and date scale, showing the energy output for a south-facing PV system
2. The continuous weather data at 5-minute intervals (interpolated) with a correct time scale, showing global solar radiation

To adjust the time and date of the energy data, the solar irradiation data with its corresponding time and date stamp was graphically compared on a day by day basis, and adjusted to match up. An example of this is shown in Figure 6.6. Once the solar radiation was consistently in line with the energy readings from the PV system, the date and time stamp was copied into the spreadsheet containing the energy readings.

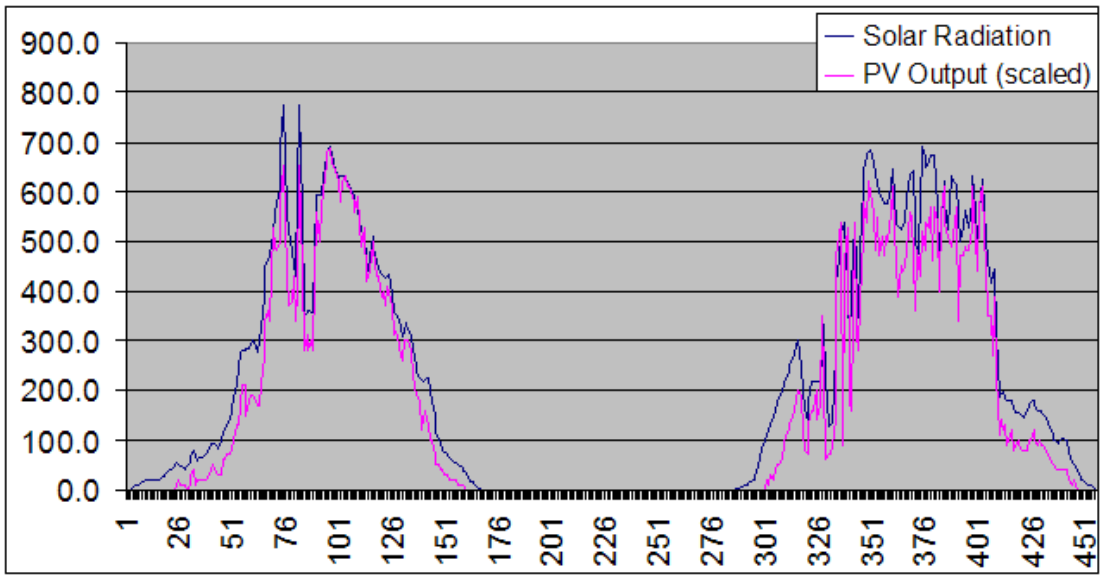

Figure 6.6: Example of PV generation and solar irradiation alignment

6.3 Data Validation

Before detailed analysis can commence the accuracy of the recorded data needs to be verified. For this reason measurements were taken from different sources to provide control readings. The most valuable source of control readings is provided be the manual readings that were taken by the EcoVillage staff on a daily basis. These were typically read off from secondary control meters, referred to as 'mobile' meters. Additionally, PV readings for Malvern system were available from an independent system from the manufacturer Fronius, who also supplied the inverters used for the PV systems. This will be referred to as 'Fronius' data.

6.3.1 Energy Readings

To verify the accuracy of the energy data, three sets of available data for the Malvern PV system were analysed and compared. Monthly and annual results are shown in Table 6.E below.

Table 6.E: Comparison of various meter readings for Malvern PV system

	Malvern PV (kWh)		
	Fronius	Mobile	Fixed
Nov-06	16.1	15	10
Dec-06	8.0	8	5
Jan-07	12.2	12	8
Feb-07	23.3	24	17
Mar-07	61.6	63	53
Apr-07	90.9	88	72
May-07	93.3	85	73
Jun-07	101.6	96	83
Jul-07	85.1	76	64
Aug-07	89.2	88	76
Sep-07	62.0	51	45
Oct-07	35.0	29	22
Annual	**678.2**	**635**	**528**

When comparing the datasets in Table 6.E the most noticeable thing is that the fixed meter readings appear to be considerably lower than the other two sets, in the order of around 20%. This can be explained by the fact that the meters used were the import/export meters, which register a net value of energy generation and consumption. As will be explored in more detail later, the inverters used for PV and Wind Turbine systems require some external power to run. Therefore while the Fixed reading accounts for inverter consumption, the Fronius and Mobile readings

do not. When comparing the Fronius and Mobile readings, differences are insignificant for most months. Annually, there is a difference of about 6%. Considering that the Fronius readings were taken straight from the inverter, a difference in cable losses can account for part of the difference, while the remaining error between the two meters is at an acceptable level.

To further validate the energy readings, the energy balance was checked on a monthly basis for every building. An extract of this analysis is shown in Table 6.F for the Palmerston building. Data is shown for the month of February 2007, about half way through the monitoring period.

Table 6.F: Electricity measurement balance for Palmerston, February 2007

	Meter Readings (all in kWh)							
	Import	PV	GSHP	Heat Store	Lights	Sockets	Kitchen	**Net**
01/02/2007	4910	618.71	1644.5	982.6	624.2	1001.1	193.1	
28/02/2007	5546	655.18	2007.9	1103.5	689.6	1106.1	206.0	
Difference	-636	-36.5	363.4	120.9	65.4	105	12.9	**-4.9**

Table 6.F provides evidence that the metering and logging apparatus work within acceptable ranges of accuracy. The 'import' reading was taken manually from the building's electricity meter while all other devices were metered as described. The net energy balance shows a difference of 4.9kWh for the entire month. This is a very small cumulative error considering that this is based on close to 50,000 readings (6 sets over 28 days at 5-minute intervals), all of which consist of 3-4 figure readings.

6.3.2 IButton Sensors

The maximum error specified by the manufacturer is ±0.5ºC. To verify this, 25 IButtons that were used for measurements during this project were calibrated at the University of Manchester. Calibration was done using a low temperature oven with very accurate temperature settings. It was confirmed that none of the IButtons showed any deviation from the control temperature, or each other, of more than 0.5ºC**.**

In order to attach the IButton sensors to the pipe work of heating systems the pressure sensitive adhesive Blu-Tack was used. The adhesive was applied in layers of approximately 1mm thickness, with no layer exceeding 2mm. The thermal effects resulting from the layer of Blu-Tack between the pipe and the sensor were investigated in a controlled set-up. For this purpose IButton sensors were attached to the outside of a glass of hot water with different thicknesses of Blu-Tack, using

very thin (<1mm), moderate (1-2mm) and very thick (~5mm) layers, shown in Figure 6.7.

Figure 6.7: Testing thermal effects of using Blu-Tack to attach IButtons

To provide a control reading, a fourth IButton was attached to the inside of the glass to measure water temperature. The control IButton was attached at the same height as the external IButtons. Results are summarised in Figure 6.8.

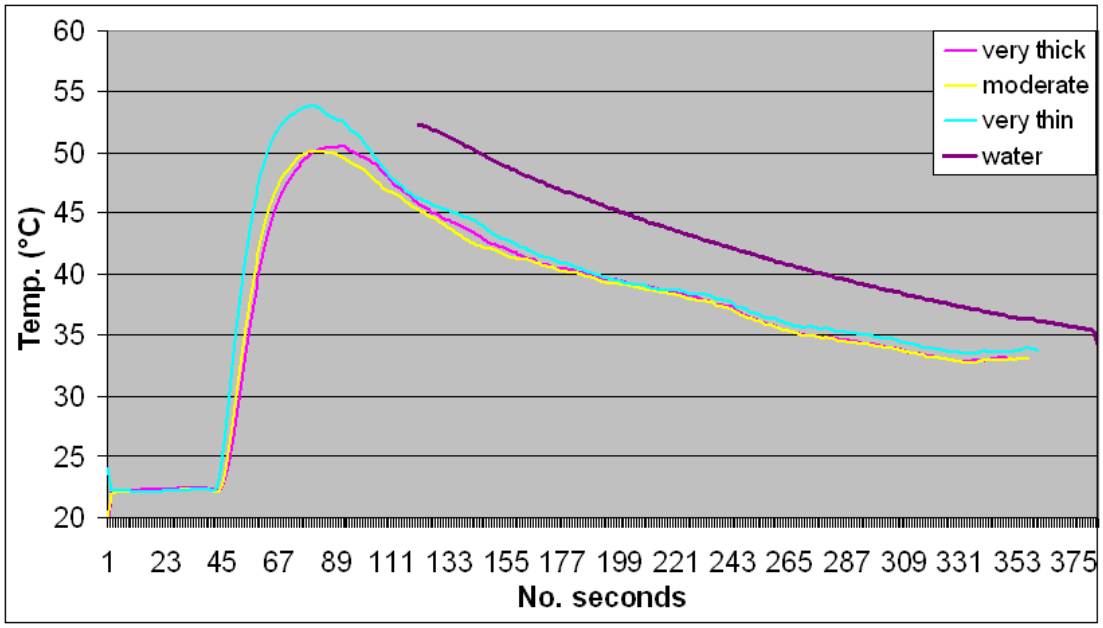

Figure 6.8: Temperature variation of IButtons attached with different layers of Blu-Tack

Figure 6.8 shows that there is increased latency as a result of using a thicker layer of Blu-Tack. While the very thin layer, which is not a very secure option in practice, picks up the temperature changes of the glass very quickly, the thicker layers take

slightly longer. However, after approximately 1 minute the temperatures of all three layers converge and show a very similar variation in readings throughout the rest of the cooling phase of the glass. The significant difference between water temperature and IButton temperature can be attributed to the thermal losses from the relatively thick layer of glass.

The temperature difference between the IButtons and the water appears to decrease as the water cools, and can be expected to eventually converge at room temperature. It was decided to explore this further on a solar thermal system, where control temperatures from calibrated thermocouple sensors were available. A scatter graph was plotted, and the least squares method applied to find a linear equation that correlates IButton values to control values at minimal residual error. Results are show in Figure 6.9.

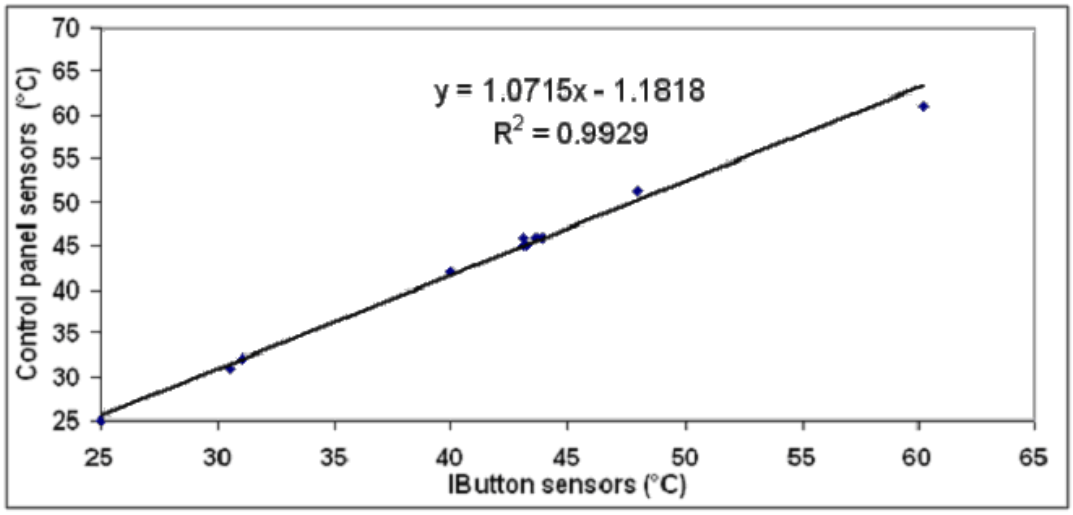

Figure 6.9: Linear equation derived using least squares technique to correlate IButton readings and control readings

The derived relationship is:

$$y = 1.0715x - 1.1818 \qquad (6.1)$$

At IButton temperature of 25°C, the corrected temperature using equation (6.1) is equal to 25.6°C. This is an acceptable error, as it is of similar magnitude to the IButton error of ±0.5°C. The linear equation (6.1) is used to adjust all IButton readings.

6.4 Statistical Methods for Data Analysis

A large part of analysis carried out for this research involves comparing data sets, for example of data comparing theoretical system performance and measured system performance. Statistics will be applied to provide a meaningful quantitative comparison. The most commonly used methods for this purpose are set out below.

Mean and Standard Deviation

The mean average will be used predominantly to determine the expected values of a distribution. The standard deviation of the data set will provide an indication of the expected data spread[107], which provides an indication to the magnitude of error that can be expected. The standard deviation is found using equation (6.2), where (X) is the variable and (n) the number of variables.

$$\sigma_{SD} = \sqrt{\frac{\Sigma(X - \overline{X})^2}{n}} \tag{6.2}$$

The standard deviation of the data set accounts for about 68% of the data, assuming a normal distribution.

Least Squares Method

The least squares method is used on numerous occasions for curve fitting purposes. It is used to fit a linear or polynomial equation to a set of data points, with the aim of minimising the sum of squares of the residual errors. The term 'residual error' refers to the difference between the observed value and the value according to the linear or polynomial model[108]. Equation (6.3) presents the least squares method, where (r_{LS}) refers to residuals and (S_r), their sum, must be minimised. In equation (6.4) the term (y) refers to the observed value.

$$S_r = \sum_{i=1}^{n} r_{LS(i)}^2 \tag{6.3}$$

$$r_{LS(i)} = y_{(i)} - f(x_{(i)}, b) \tag{6.4}$$

For linear least squares the model function is given by:

$$f(x_{(i)}, b) = b_0 + b_1 x \tag{6.5}$$

For the purposes of analysis the Excel-integrated function for curve fitting is used to minimise (S_r) and to find the resulting line of best fit with a minimal sum of residuals squared.

To evaluate how well the model relates to the data set, the (R^2) value is found. This value relates the sum of residual squares to the sum of total squares, where (R^2) converges to 1 as the sum of residual errors approaches zero.

The t-test

The t-test[109] is a valuable tool when comparing two data sets[110]. It can be used to find the probability of two sample values within two similar datasets showing a statistically significant difference. The expression used to calculate the t-value is given by equation (6.6).

$$t_{value} = \frac{\bar{x}_1 - \bar{x}_2}{\sqrt{\frac{\sigma_{SD1}^{\ 2}}{n_1} + \frac{\sigma_{SD2}^{\ 2}}{n_2}}} \qquad (6.6)$$

In order to relate the t-value to a statistical probability, the degree of freedom of the data must be determined. This is given by equation (6.7):

$$df = n_1 + n_2 - 2 \qquad (6.7)$$

Using the t-value and the degree of freedom, the Student's t distribution table[111] can be used to determine the relevant probability of two random samples having a statistically significant difference.

6.5 Payback Calculation Method

Determining the value of a system based on payback period can be approached in three different ways; financial payback of capital investment, energy payback and carbon payback, where the term 'carbon' refers to CO_2 equivalent emissions. Energy and carbon payback are strongly related, while all three approaches are important. The financial payback will influence the motivation for consumers to opt for a specific system which can ultimately affect the product choice when buying a house. The energy payback, and the related carbon payback, will determine the viability from an environmental point of view as it will determine a systems' effectiveness in helping to mitigate climate change.

6.5.1 Feed-in Tariffs (FIT)

In November 2008 the Planning and Energy Act[112] set out a series of requirements for the UK government to meet its commitments to combat climate change, in particular by encouraging the use of renewable energy systems to generate power. In response to this, and after a period of industry consultation[113], feed-in tariffs on renewable electricity generation have been introduced in April 2010[114].

The feed-in tariffs (FIT's) are fixed rates at which energy generated by renewable energy systems will be valued. These tariffs are incentives for installing renewable energy systems and do not require electricity to be exported to the national grid. However, if electricity is exported, an additional 5p/kWh will be paid on top of the nominal tariff. The model of the FIT's is such that initial tariffs are available for installations commissioned in or after April 2010. This tariff depends on the type of installation and is fixed for a certain period; 25 years for PV installations, 10 years for MicroCHP and a 20-year period for all other systems.

For any installation commissioned after April 2012, there will be a 'degression' value for the initial tariff, which is a reduction of the tariff to be received over the entire period. The degression is also linked to inflation, making it slightly flexible. Table 6.G provides an extract of tariffs for electricity generating renewable energy systems up to April 2020.

Table 6.G: 2010 Feed-in tariffs[113]

	Size	Annual Tariff (pence/kWh), starting in										
		April 2010	April 2011	April 2012	April 2013	April 2014	April 2015	April 2016	April 2017	April 2018	April 2019	April 2020
µCHP	≤2kW	10	10	10	10	10	10	10	10	10	10	10
PV	≤4 kW (new build)	36.1	36.1	33	30.2	27.6	25.1	22.9	20.8	19	17.2	15.7
PV	≤4 kW (retrofit)	41.3	41.3	37.8	34.6	31.6	28.8	26.2	23.8	21.7	19.7	18
PV	>4-10kW	36.1	36.1	33	30.2	27.6	25.1	22.9	20.8	19	17.2	15.7
PV	>10-100kW	31.4	31.4	28.7	26.3	24	21.9	19.9	18.1	16.5	15	13.6
PV	>100kW-5MW	29.3	29.3	26.8	24.5	22.4	20.4	18.6	16.9	15.4	14	12.7
PV	Stand alone system	29.3	29.3	26.8	24.5	22.4	20.4	18.6	16.9	15.4	14	12.7
Wind	≤1.5kW	34.5	34.5	32.6	30.8	29.1	27.5	26	24.6	23.2	21.9	20.7
Wind	>1.5-15kW	26.7	26.7	25.5	24.3	23.2	22.2	21.2	20.2	19.3	18.4	17.6
Wind	>15-100kW	24.1	24.1	23	21.9	20.9	20	19.1	18.2	17.4	16.6	15.9
Wind	>100-500kW	18.8	18.8	18.8	18.8	18.8	18.8	18.8	18.8	18.8	18.8	18.8
Wind	>500kW-1.5MW	9.4	9.4	9.4	9.4	9.4	9.4	9.4	9.4	9.4	9.4	9.4
Wind	>1.5MW-5MW	4.5	4.5	4.5	4.5	4.5	4.5	4.5	4.5	4.5	4.5	4.5

These tariffs have been set out to allow a real rate of return on investment of 5-8%, allowing it to be seen as an ethical investment opportunity. As the tariffs are linked to inflation, the nominal rate of return can be as high as 7-10%, allowing electricity generating renewable systems to achieve financial payback within a 20-year period.

6.5.2 Renewable Heat Incentive (RHI)

Similar to electricity generating systems, heat generating systems will also be subsidised under the Renewable Heat Incentive (RHI) scheme. A consultation document[115] was released in February 2010 by the Department of Energy & Climate Change, responses to which are currently being analysed. The proposed tariffs are shown in Table 6.H.

Table 6.H: Proposed RHI tariffs[115]

Technology	Size	Tariff (pence/kWh)	Tariff type	Lifetime (years)
Ground source heat pumps	≤45kW	7	deemed	23
Ground source heat pumps	>45-350kW	5.5	deemed	20
Ground source heat pumps	>350kW	1.5	metered	20
Air source heat pumps	≤45kW	7.5	deemed	18
Air source heat pumps	>45-350kW	2	deemed	20
Solar thermal	≤20kW	18	deemed	20
Solar thermal	>20-100kW	17	deemed	20

These proposed tariffs were calculated based on a rate of return of 6% for solar, and 12% for all other systems to reflect the level of risk and effort involved.

Unlike electricity generating systems it is rather difficult to meter heat generating systems. Metering heat generation could also encourage surplus heat generation in order to benefit from the RHI scheme. It is therefore proposed that tariffs for small/medium size systems, in particular for domestic applications, are fixed. This will be based on a 'deemed' (reasonable heat requirement that the installation is intended to serve) number of kWh generated, rather than actual energy generated. It is yet to be decided what method or model this deemed requirement will be based on. The RHI scheme is set to start in April 2011, but it has been proposed that all installations commissioned after July 2009 are eligible to receive RHI tariffs.

6.5.3 Calculating Simple Financial Payback

Financial payback is achieved when the capital investment of installing a system has been redeemed through savings generated over time. Savings are based on a comparison to likely alternatives, for example a grade A condensing gas boiler, or electricity that is imported from the national power grid. However, the capital cost of alternatives will not be considered for the purpose of this analysis.

In order to provide a method of analysis that is widely applicable, while at the same time providing a robust and justifiable estimation of payback period, several assumptions were made. These include the following:

1. No opportunity cost, possible interest payments or cost of alternatives are considered as it is outside the scope of this research to consider all options and rates that may apply. Instead, this research will provide a base-line case which can be adjusted for individual cases.

2. Maintenance costs for the systems are assumed to equal estimates presented by the Department for Communities and Local Government in 2010[64]. While these estimates are rather generic, they should adequately reflect the vast majority of cases.

3. It is expected that systems reach their expected life-time, and performance does not vary throughout the system's lifetime. While in practice performance will reduce over time, it can be argued that for most cases, given the appropriate maintenance, this reduction becomes negligible.

4. The effect of expected climate change throughout the expected system life-time is assumed to have a negligible effect on system output. While this may ultimately prove to be wrong, this is an area which is currently too unpredictable.

5. Energy prices are expected to vary over estimated system lifetime. Estimates for 2020 energy prices have been published by the Department for Energy and Climate Change[116] (DECC) for different scenarios. For the purpose of payback calculations the prices for the 'high' scenario are adopted, which predicts 3.6p/kWh for gas and 14.3p/kWh for electricity.

6. Inflation has not been considered. The fact that FIT's and RHI's are linked to inflation should negate any effects of inflation on payback estimates.

7. 2011 tariffs will be used for all payback estimates. This is done as capital investment costs are used from 2010 or previously, and the regression values of the tariffs are designed to account for expected variations in capital costs.

8. For electricity generation, it is expected that 50% of energy is used directly, and 50% is exported to the national grid[117]

The assumed average prices for gas and electricity import are summarised in Table 6.I, where the gas price has been adjusted to account for efficiency losses of using a 90% efficient A-rated condensing gas boiler.

Table 6.I: Estimated average energy prices[116] over payback period

Electricity (per kWh)	Heat from Gas (per kWh)
£0.143	£0.04*

*adjusted to account for 90% efficient boiler

The capital costs will need to be considered to calculate payback rates, as well as any known maintenance expenses. The capital costs of the EcoSmart village systems, provided by Barratt Developments, are summarised in Table 6.J. Capital costs will be adjusted later based on other research, where appropriate.

Table 6.J: Capital cost for all systems installed at EcoSmart show village

Renewable / Energy Efficiency System	Installation Cost (£)
Wind turbine (1.75m)	1500
Wind turbine (1.1m)	2250
Photovoltaic	4500
Flat panel solar thermal collector	2600
Evacuated tube solar thermal collector	3500
GSHP (1)	7800
GSHP (2)	12250
µCHP	2700

Equation (6.8) will be used to calculate payback periods for all systems, where the term (C) refers to capital cost and the subscripts 'H' and 'E' refer to annual heat and electricity generation respectively. The values £0.04 and £0.143 are the assumed average prices for gas and electricity, and £0.05 is the FIT mark-up for electricity export to the grid.

$$t_{payback(F)} = \frac{C_{capital} + C_{maint}}{0.04Q_{Gas} + Q_H RHI + 0.143\left(\frac{Q_E}{2}\right) + Q_E FIT + 0.05\left(\frac{Q_E}{2}\right)} \quad (6.8)$$

6.5.4 Calculating Energy and Carbon Payback

In order to calculate the carbon savings from the use of renewable energy systems, the typical carbon generation from burning fossil fuels must be established to provide comparative values. These values for gas and electricity are based on SAP 2009 CO_2 emission factors.

It is also important to know the carbon footprint of an average household to estimate the carbon offset in terms of a percentage contribution. According to a British Gas report[118] released in 2006 by Centrica PLC, there is a great variation of average domestic carbon footprint in cities throughout the UK, ranging from 3255kgCO_2 to 8092kgCO_2 per annum. Due to the proximity of the test site and near average value, the average carbon footprint for Manchester will be used as a reference value for carbon calculations. This is given as 4862kgCO_2.

The carbon content for grid electricity and natural gas, as well as the average annual carbon footprint for a dwelling near Manchester are summarised in Table 6.K.

Table 6.K: Carbon footprint of grid energy and average household near Manchester

	per	value
$CO_{2(gas)}$ [119]	kWh	0.198 kgCO_2
$CO_{2(electricity)}$ [119]	kWh	0.517 kgCO_2
$CO_{2(annual)}$ [118]	dwelling	4,862 kgCO_2

It must be noted that the carbon content shown in Table 6.K is based on the current situation. It is recognised that in future the carbon content of national energy grid is expected to decrease, as the proportion of large scale renewable

electricity generation and bio gas are increased in the electricity and gas networks. However, for carbon payback calculations the following assumption is made:

1. As carbon payback periods are generally fairly short, the current estimates of carbon footprint are deemed as being sufficiently accurate for this analysis.

Embodied Energy and Carbon

With the carbon content of electricity and gas that will be offset by renewable energy generation accounted for, it must also be considered that the systems contain a certain amount of embodied energy and carbon.

Materials, manufacturing, transport and installation all contribute to the embodied energy of a system. Depending on what type of energy (heat, electricity or fuel for transport) is required for each of these processes, the amount of embodied carbon will vary. To provide an indication of magnitude, Figure 6.10 summarises[120] the estimated carbon content of the energy generated over the life-time of several renewable energy systems. This is based on estimated generation and the embodied carbon of the individual systems. For comparison, the average life-time carbon content of PV generation is approximately 10% of the carbon content of electricity from the national grid.

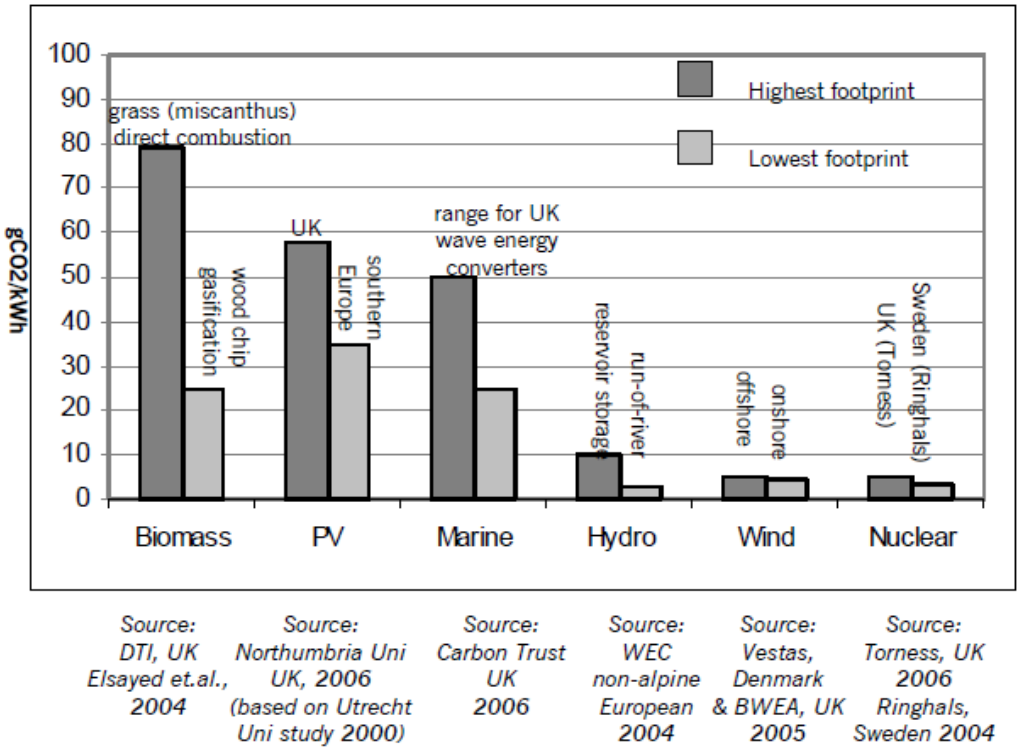

Figure 6.10: Estimated carbon content of renewable energy generation (Source: POSTnote[120] 2006)

As substantial research has already been done in this area the embodied energy and carbon for each individual system will be analysed in detail based on literature reviews.

Should no literature be available that provides a conclusive extimate for the embodied carbon of a particular system, this will be estimated based mainly on materials and their assembly. For the typical embodied energy and carbon of raw materials in the UK, the peer-reviewed[121] Inventory of Carbon and Energy (ICE) database[122] will be used as a reference. For assembly and any other processes that involve primary electricity, a carbon content factor of 0.23kgCO_2/kWh was used, which was adopted from a 2007 UK Government consultancy report[39].

Having established the estimated embodied energy and carbon, the payback periods for energy and carbon will be calculated using equations (6.9) and (6.10) respectively.

$$t_{payback(E)} = \frac{Q_{embodied}}{Q_H + Q_E} \tag{6.9}$$

$$t_{payback(C)} = \frac{CO_{2(embodied)}}{CO_{2(gas)}Q_H + CO_{2(electricity)}Q_E} \tag{6.10}$$

7 Support Systems

Many of the renewable energy systems tested at the EcoSmart village require support systems to provide energy more efficiently or in a useful form. The GSHP and μCHP systems for example are connected to a smart heat store that acts as a buffer between energy supply and demand.

The electrical systems also require a support system. Apart from the μCHP Stirling engine all on-site electricity generation is DC, which needs to be converted to AC for grid-integration by using an inverter.

This section will describe the support systems in detail, identify any implications they have on energy generation, and develop models where appropriate to account for any losses that may result from their use.

7.1 The Inverter

All small-scale wind turbine systems use a permanent-magnet generator, the output of which is rectified to give a DC voltage which varies with speed. Photovoltaic semiconductors generate a flow of electrons in one direction, also resulting in DC generation. For both cases inverters are required to change the DC power to AC power that can either be exported to the grid, or be used directly by appliances.

7.1.1 Theoretical Background

In its simplest form, an inverter uses a transformer and a switch on the primary coil to allow current to flow in opposite directions, causing the induction of alternating current in the secondary coil. The switching mechanism in inverters, which is required to change the direction of DC current, is called 'commutation'. This can be controlled in two ways, by self commutation or forced commutation. The main difference is that forced commutation allows the switch to control the 'on' setting by using a device such as a thyristor, while the 'off' setting is controlled by a supplementary circuit[123].

A self commutated inverter on the other hand can control both 'on' and 'off' settings. Using modern semi-conductor switching devices high switching frequencies exceeding several kHz are reached, which makes it much easier to filter harmonics, resulting in low network disturbances[124]. This property makes

self-commutated inverters more applicable to small-scale, grid-connected renewable energy systems. They can either be voltage commutated or current commutated, meaning the switching is controlled by either voltage or current levels. A survey has shown that practically all inverters used for peak loads of 1kWh or less are self-commutated voltage type inverters[125].

Any inverter, whatever its type, requires a low-voltage control system, and most modern systems will employ a microprocessor. The power needed to drive the electronics is usually obtained from the AC mains by transforming down and rectifying, and using further devices to give a stabilised low-voltage power supply. It is unlikely that this can be done without consuming at least 5W, so that, even if the inverter is not switching it will consume at least 120Wh per day if it is left connected and operational. If the inverter starts to switch, then losses occur in each switching operation additional to those already mentioned. It is impossible to generalise but some feel for magnitudes can be obtained from the fact that if operating at its rated output, the inverter is unlikely to be more than about 90% efficient, with most of the losses being attributable to switching. Hence it is quite possible that the DC link needs to input a power of about 2% of the inverter rating before any measurably significant power is fed into the mains.[126] Based on this assessment, there are two types of losses involved when using inverters:

- Efficiency losses across all power ranges, which have a greater overall effect on low power loads as a minimum 'switching loss' needs to be overcome. This may be as much as 2% of the inverter rating

- Energy consumption by the inverter for control (microprocessor) system when switched on, expected to be at least 5W, even while zero load is applied

7.1.2 Efficiency Losses

Inverters have varying efficiencies, which are usually rather low under low load levels, and increase as the input (DC) power approaches the rated power of the inverter. The typical efficiency curve of a generic inverter[127] is as shown in Figure 7.1.

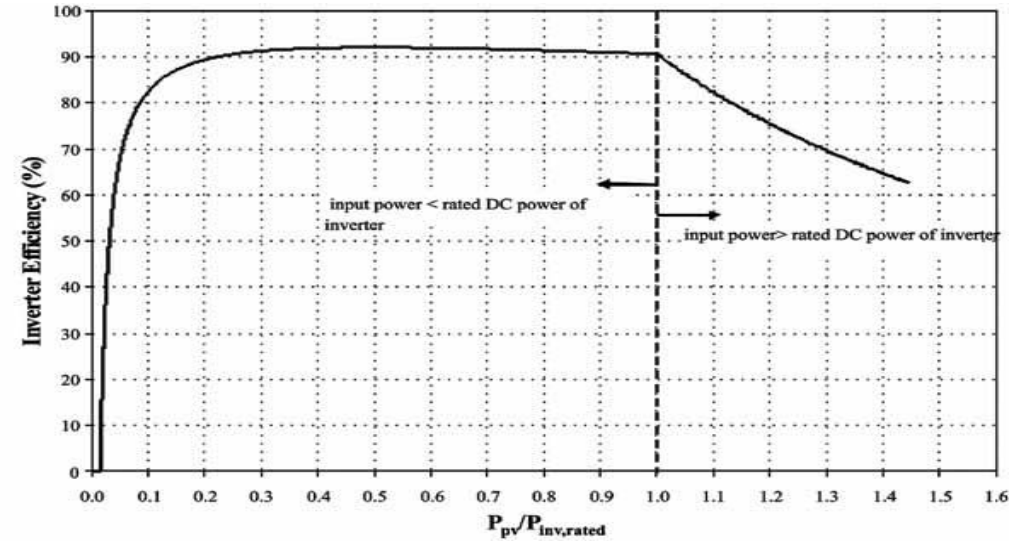

Figure 7.1: Efficiency variation with power load of typical inverter (Source: Mondol[127], 2007)

The efficiency curves for the inverters used at the EcoSmart village were unobtainable, but the third party Fronius logger that was connected to the Malvern PV system measured both DC and AC power across the inverter. To obtain an efficiency variation based on the measurements a simple ratio was used, shown in equation (7.1). Results of these calculations up to a DC load of 700W are shown in Figure 7.2.

$$\eta_{inverter} = \frac{P_{AC}}{P_{DC}} \tag{7.1}$$

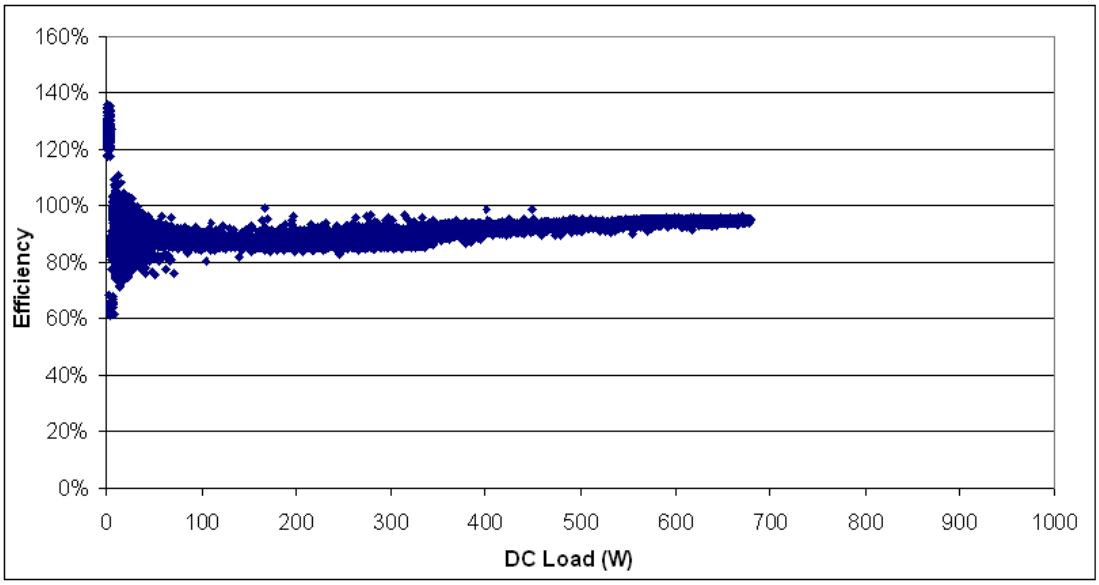

Figure 7.2: Malvern PV inverter efficiency variation with respect to DC load

Based on this analysis the inverter shows a different behaviour than the generic inverter shown in Figure 7.1. Some of the efficiency values at low loads are greater than 100%, confirming that this is wrong.

As mentioned before, a certain minimum power level needs to be reached to overcome relay switching losses. It was estimated that these losses could be as much as 2% of the rated power, in the case of the PV inverters around 20W. It is possible that the DC load is measured after these losses occur.

After an iterative process a moderate value of 15W (1.5% of inverter rating) was assumed. When adding this value of 15W to the DC load in equation (7.1), the resulting distribution is shown in Figure 7.3. This corrected efficiency curve is now much closer to the generic efficiency curve shown previously.

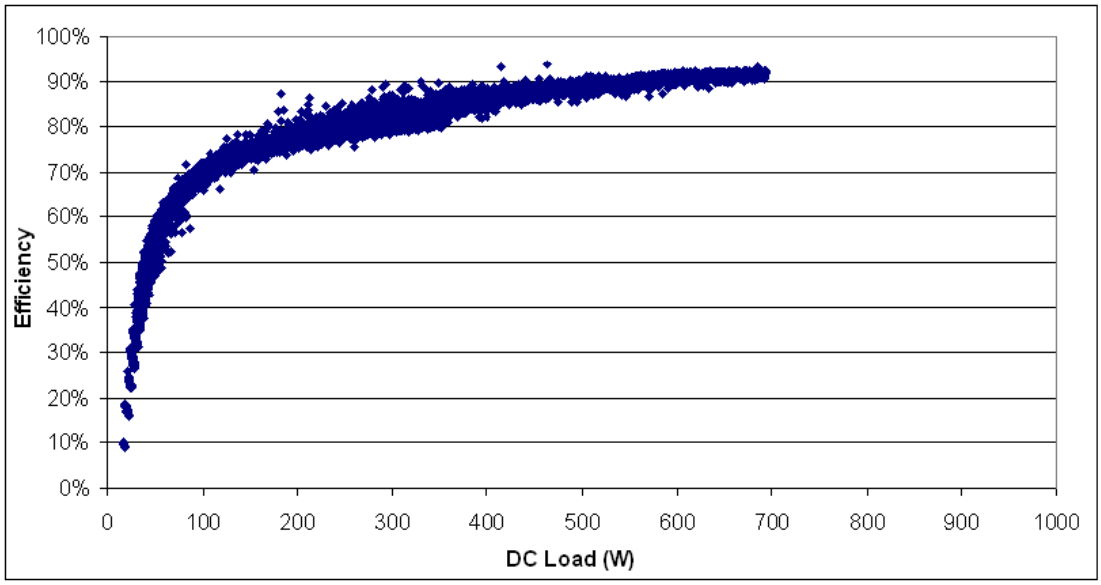

Figure 7.3: PV Inverter efficiency with 15W DC correction for switching losses

Validation

As the inverter efficiency curve is based on an estimated correction factor, its accuracy must be validated. For this purpose a 2.7kWp domestic PV system was analysed, which uses a 2.8kW rated inverter. This control inverter is a Diehl Platinum 2800S model, which incorporates electricity meters and a data logger that is able to give values for DC load before switching losses and AC output. Using equation (7.1) the efficiency curve is calculated, which is shown in Figure 7.4.

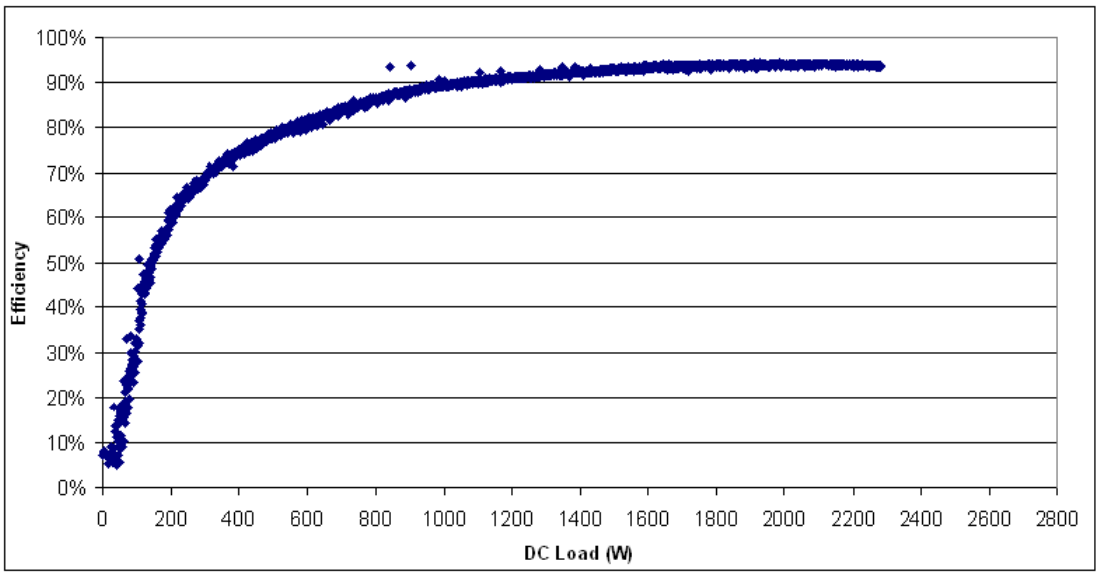

Figure 7.4: Control inverter efficiency distribution

The comparison of Figure 7.3 and Figure 7.4 shows very little difference. The good correlation between the adjusted efficiency curve for the EcoSmart systems and the control inverter suggests that the methods applied are sufficiently accurate for further use in system modelling.

7.1.3 Inverter Energy Consumption

The inverters consume energy when switched on, regardless of the DC load. While PV inverters were automatically switched off when zero DC load was applied, the unpredictable nature of wind meant that wind turbine inverters were constantly switched on. As previously described the electricity meters used to monitor the wind turbine systems were designed to measured electricity flowing both ways, hence recording both power consumption and power generation as a positive output.

In order to determine the electric energy consumption of the inverters, three days were analysed which were known to have wind speeds consistently below the turbine cut-in speed of 2.5m/s. After analysing the weather data, the 8th, 19th and 21st of July 2007 were chosen for this analysis. The total daily energy readings for the wind turbine meters on those particular days are shown in Table 7.A.

Table 7.A: Inverter energy consumption on days with negligible wind speeds

		Daily inverter energy consumption (Wh)			
Eco Home	**System**	**08/07/2007**	**19/07/2007**	**21/07/2007**	**Average**
Buckingham	Windsave	169.5	170.5	170.0	**170.0**
Edinburgh	Windsave	181.0	180.5	180.5	**180.7**
Alderney	StealthGen	159.5	159.5	159.5	**159.5**
Malvern	StealthGen	119.5	120.5	118.0	**119.3**
Windermere	StealthGen	122.5	130.0	130.0	**127.5**

The values in Table 7.A can now be used to account for the annual inverter energy consumption of the wind turbine inverters.

For the PV inverters, similar energy consumption levels were assumed as for the 1kW rated inverter used for the Windsave turbines. It can be assumed that the PV inverters consume 7.3Wh of energy during every hour of daylight.

7.1.4 Inverter Model

To summarise the analysis on inverter losses, the simplified linear model given by equation (7.2) will be used. The resulting distribution is shown in Figure 7.5.

$$\eta_{inverter} = \begin{cases} 0.0171P_{DC} - 0.257 & when \quad 0 < P_{DC} \le 50W \\ 0.00133P_{DC} + 0.533 & when \quad 50 < P_{DC} \le 200W \\ 3.3\times10^{-4}P_{DC} + 0.733 & when \quad 200 < P_{DC} \le 500W \\ 10^{-4}P_{DC} + 0.85 & when \quad 500 < P_{DC} \le 1000W \end{cases} \qquad (7.2)$$

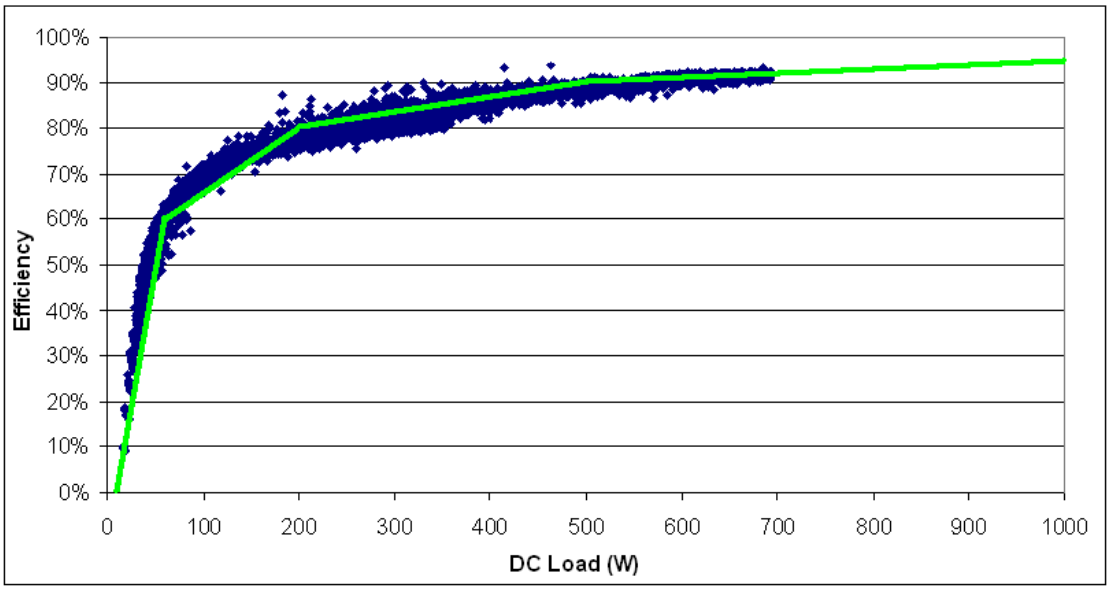

Figure 7.5: Linear model to represent inverter efficiency distribution

The derived model for the inverter will be used for PV and wind turbine inverters. The ranges given in equation (7.2) will be adjusted for the smaller inverter of the 400W rated wind turbines. In addition to the efficiency model, a value for the inverter energy consumption will be subtracted from the annual yield, based on the method described above.

7.2 The Heat Store

The smart heat store systems used in conjunction with the GSHP and µCHP systems are the Gledhill BoilerMate systems. In this case the term 'smart' refers to the ability to control the space heating system, being able to control when they are switched on and for how long. They were specifically designed for each of the space heating systems, taking into account what demand profiles would be best suited to ensure smooth and efficient running. The different versions include the 'BoilerMateHP' for use with heat pumps, the 'BoilerMatemCHP' designed specifically for µCHP systems, as well as the 'BoilerMateSol', which is intended to be used in conjunction with Solar Thermal systems. They are controlled by an integrated microprocessor control system, which is able to monitor temperature levels and automatically call on the heating system when required. At the same time the integrated storage tank provides a valuable buffer, which means the heating systems can run for longer periods at a time.

The heat-store system also consumes a significant amount of energy, although the exact amount is not specified by the manufacturer. Electricity meters have been connected to the heat store systems. The energy consumed by the heat-stores at the EcoSmart village were recorded and will be shown for each individual system. The exact algorithms of the heat store control were not investigated in detail, as this is outside the scope of this research project Figure 7.6 shows a general schematic layout of the Gledhill system, in this case for the 'BoilerMateSol' system.

.

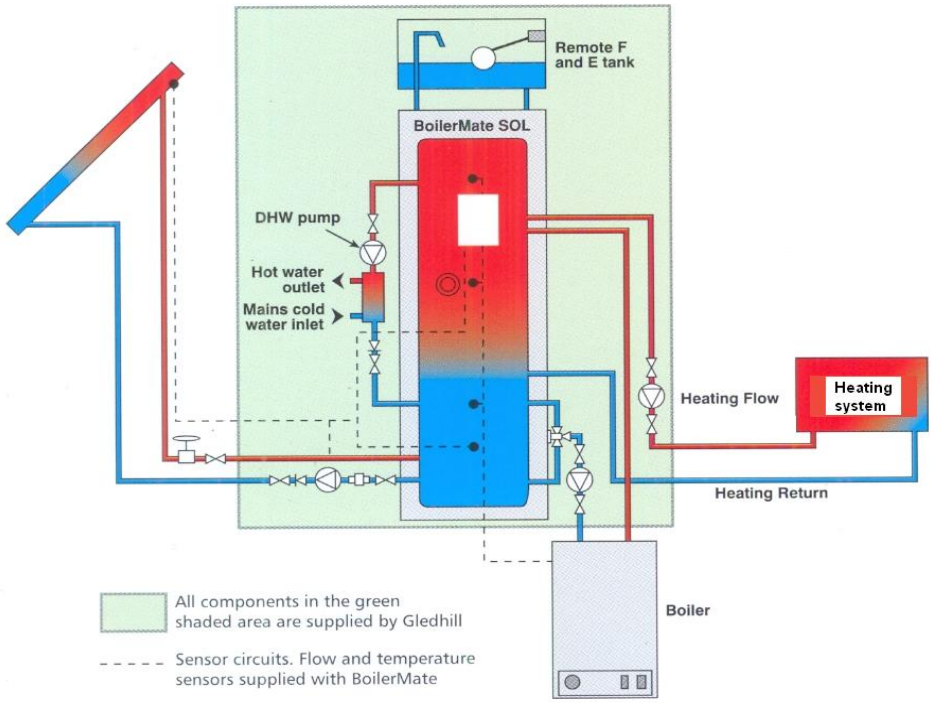

Figure 7.6: Gledhill heat store system for solar thermal 'BoilerMateSol' (Source: Gledhill brochure)

8 Preliminary Modelling

In order to use the weather data that was gathered for analysis and modelling purposes, in particular for determining the theoretical performance of some of the renewable energy systems, some preliminary modelling was required. During preliminary analysis it was found that some data was required which was unavailable, or it was required in a different format. This section outlines and validates the methods used for conversions and derivations of the parameters required for system modelling.

8.1 Estimating Beam and Diffuse Components of Global Solar Radiation

For modelling of solar systems is it necessary to know the amount of direct beam and indirect diffuse solar radiation.

Several recognised methods are known that can be used to divide the values for global solar radiation into beam and diffuse components. Methods have been empirically derived by Orgill & Hollands[128], Erbs et al[129] and Reindl et al[130]. These methods were reviewed and compared by Duffie & Beckmann[131], who concluded that for practical purposes the Erbs method and the Orgill & Hollands method produce the same outcome. The Erbs method was chosen. It works on the basis that the diffuse and beam components of global solar radiation can be related to the intensity of the radiation measured on ground compared to the extraterrestrial radiation as seen outside the atmosphere.

The instantaneous extraterrestrial radiation (I_0) on a horizontal surface is found using equation (8.1), where (δ), (φ) and (ω) and angles of declination, Latitude and solar hour angle respectively and (n) is the Julian date:

$$I_0 = G\left(1 + 0.033\cos\frac{360n}{365}\right) \times \left(\cos\phi\sin\delta\cos\omega + \sin\phi\sin\delta\right) \qquad (8.1)$$

For analysis over discrete time intervals, in this case 1 hour, the relationship can be expresses as shown in equation (8.2).

$$I_0 = \frac{12 \times 3600}{\pi} G \left(1 + 0.033 \cos \frac{360n}{365}\right) \times \left(\cos\phi \sin\delta (\sin\omega_1 + \sin\omega_2) + \frac{\pi(\omega_1 - \omega_2)}{180} \sin\phi \sin\delta\right) \quad (8.2)$$

Equation (8.2) requires the hour angle and declination angle to be found on an hourly basis. The solar hour angle can be calculated using equation (8.3), for which the solar time (t_{sol}) can be found using equation (8.4) and the difference in longitude (ψ) between the location and that of the standard time zone.

$$\omega = 15(t_{sol} - 12) \quad (8.3)$$

$$t_{sol} = t + 4(\psi_{st} - \psi_{loc}) + ET \quad (8.4)$$

The term (*ET)*, the equation of time, is given by equation (8.5):

$$ET = 229.2(0.000075 + 0.001868\cos B - 0.032077\sin B - 0.014615\cos 2B - 0.04089\sin 2B) \quad (8.5)$$

$$B = (n-1)\frac{360}{365} \quad (8.6)$$

The solar declination angle referred to in equation (8.1) defines the angular position of the sun at solar noon as a result of the earth tilt with respect to the plane of the equator, where north is taken as positive. As shown in Figure 8.1 the declination angle ranges –23.5º < δ < 23.5º. The declination angle can be found using equation (8.7).

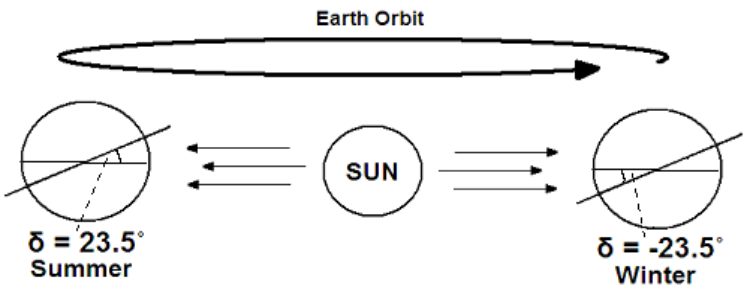

Figure 8.1: Diagram showing the declination angle as a result of earth tilt

$$\delta = 23.45 \times \sin\left[360 \times \frac{(284+n)}{365}\right] \tag{8.7}$$

The clearness index (k_T) can be found using equation (8.8), where the term (I) refers to measured solar radiation on the ground.

$$k_T = \frac{I}{I_0} \tag{8.8}$$

Equation (8.9) derived empirically by Erbs et al[129] can now be used to estimate the fraction of the diffuse radiation (I_d) component using the clearness index derived previously. This equation was derived to calculate components of hourly radiation.

$$\begin{aligned}
\frac{I_d}{I} &= 1 - 0.09k_T && \text{for } k_T \le 0.22 \\
\frac{I_d}{I} &= 0.9511 - 0.1604k_T + 4.388k_T^{\,2} - 16.638k_T^{\,3} + 12.336k_T^{\,4} && \text{for } 0.22 < k_T < 0.8 \\
\frac{I_d}{I} &= 0.165 && \text{for } k_T \ge 0.8
\end{aligned} \tag{8.9}$$

Using this method the diffuse and direct beam components of measured radiation on a horizontal surface have been estimated for the EcoSmart village. Monthly averages of these values have been summarized in Table 8.A and Figure 8.2.

Table 8.A: Calculated values for diffuse factor and components of solar radiation

	Total monthly values (Wh/m²)			**Average daily values (Wh/m²)**			
	Global Radiation	Beam	Diffuse	Global Radiation	Beam	Diffuse	$\frac{I}{I_0}$
Jan-07	17107	5311	11795	552	171	380	0.69
Feb-07	33370	13169	20201	1192	470	721	0.61
Mar-07	73615	34922	38693	2375	1127	1248	0.53
Apr-07	115195	60567	54628	3840	2019	1821	0.47
May-07	93544	43216	50328	3018	1394	1623	0.54
Jun-07	128901	51279	77623	4297	1709	2587	0.60
Jul-07	92528	30614	61914	2985	988	1997	0.67
Aug-07	95171	34048	61122	3070	1098	1972	0.64
Sep-07	74901	24979	49922	2497	833	1664	0.67
Oct-07	47495	14319	33175	1532	462	1070	0.70
Nov-06	22442	6248	16194	748	208	540	0.72
Dec-06	11994	2736	9258	387	88	299	0.77
Annual	806261	321409	484852	2209	881	1328	0.60

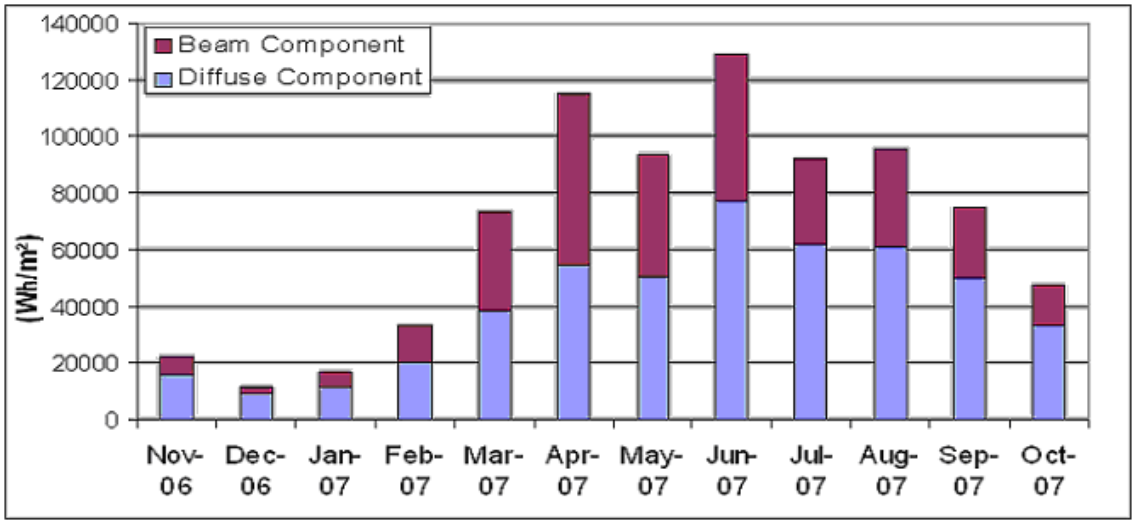

Figure 8.2: Monthly distribution of Diffuse and Beam components

These results show that during the test year, the annual proportion of diffuse radiation at the test site is around 60%. As expected this value varies throughout the year, being much lower in the summer months than winter months. This can be explained by the fact that the beam radiation is much less intense during winter months, meaning the proportion of radiation that reaches the ground due to atmospheric scattering becomes greater.

Validation

The method presented by Erbs et al. has been derived from field data, tested vigorously, and compared to other models as shown in Figure 8.3.

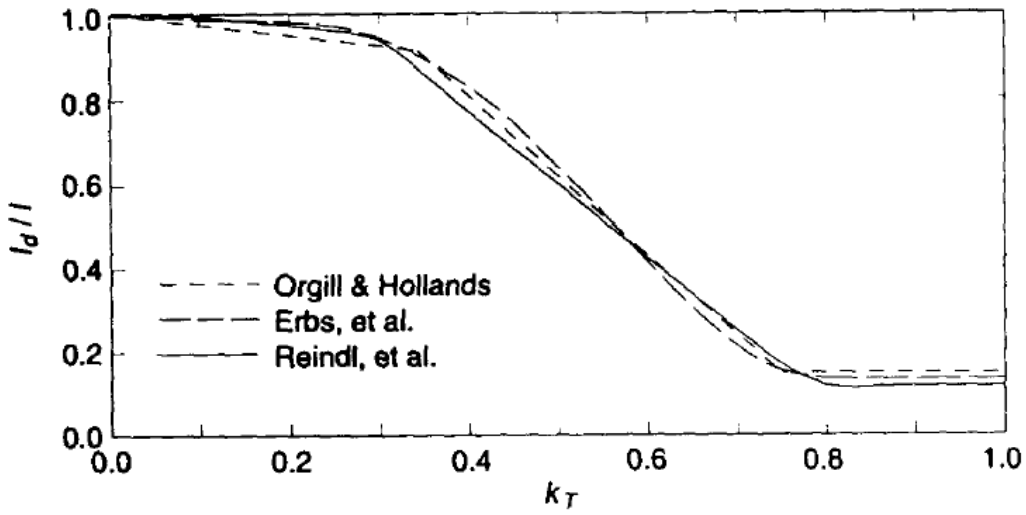

Figure 8.3: Modelled variation of Radiation Fraction with Clearness Index (Source: Duffie & Beckmann[131])

Although there should be little need for further validation, the results obtained using the method were compared to several other available data sets. These data sets include measured solar data from the Manchester area (Ringway weather station) from June 2009 until July 2010, as well as the CIBSE Test Reference Year[132] for Manchester. To provide a simple verification the annual diffuse fractions of global solar radiation are compared, as shown in Table 8.B.

Table 8.B: Comparison of diffuse fraction between model and control data

	Annual Diffuse Fraction
EcoSmart Village 2006/2007	60%
CIBSE Manchester TRY	65%
Manchester Ringway 2009/2010	58%

Table 8.B shows that the ratio of diffuse radiation is rather similar to those of the control data sets. While the comparison of different years may not be entirely robust, as shown by the difference between TRY and Ringway data, it still adds to the existing evidence that this model produces results of acceptable correctness and accuracy.

8.2 Estimating Dew Point Temperature

Estimating the dew point temperature is required to calculate the sky emittance, which is used to determine radiant heat losses from solar thermal systems for modelling purposes. Dew point temperature was measured at the EcoSmart village, but measurements were not available for the modelling of other Solar Thermal systems. After methods for determining the dew point temperature were reviewed[133], a relatively simple linear relationship[134] between dew point temperature and relative humidity was found to be adequate for the purposes of this research. The mathematically derived relationship is expected to provide results with less than 1ºC error based on experimental trials[134]. The relationship is given in equation (8.10).

$$T_{dp} = T_a - \left(\frac{100 - RH}{5} \right) \qquad (8.10)$$

Validation

To provide independent validation, the weather data from November 2006 to November 2007 recorded at the EcoSmart village was used to assess the accuracy of the simplified linear model. For this purpose the differences between measured dew point temperature and results from the model were calculated for each of the 5-minute data intervals. Figure 8.4 shows the 32,000 greatest differences for the overall 105,000 interval readings.

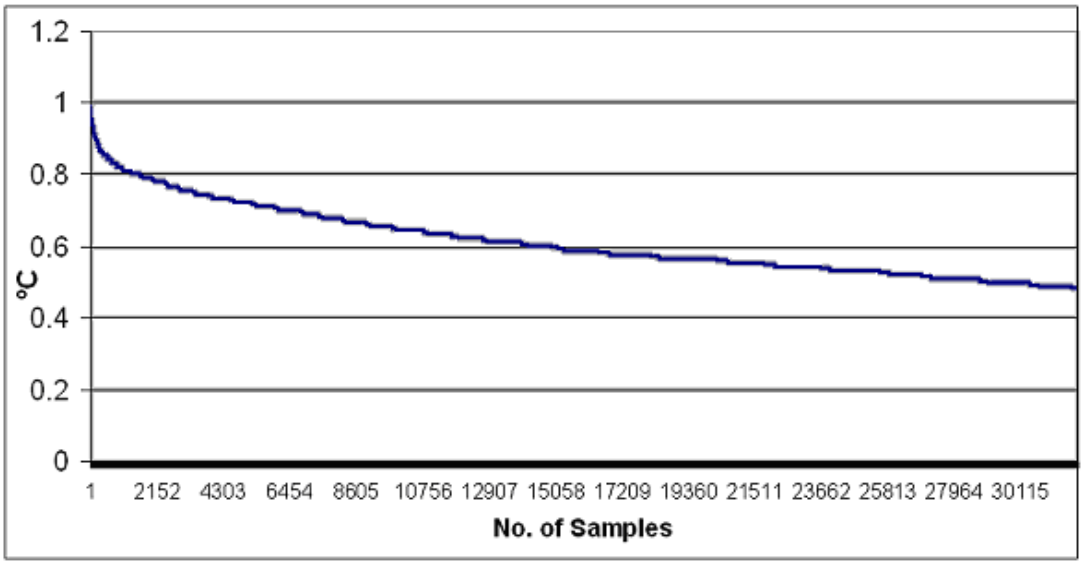

Figure 8.4: Difference between measured and modelled dew point temperature

Figure 8.4 provides an independent verification that the simplified model is able to estimate the dew point temperature to an accuracy of <1ºC error. The average error was found to be 0.41ºC over the 12-month period. Considering the accuracy of the weather station, given as 1ºC, the error of this simplified relationship is deemed acceptable for modelling purposes.

8.3 Estimating Air Density

Air density is an important factor when calculating the power output of a wind turbine. After modelling, variations up to 30% throughout the test period were found between warm, humid days and cold, dry days. Air density was not measure directly and must therefore be determined using other properties.

To determine[135] the density of air it can be considered as an ideal gas for simplicity[136]. Based on the ideal gas equation, equation (8.11) defines the density of air, consisting of a mix of dry air (subscript 'd') and water vapour (subscript 'v').

$$D = (\frac{P_d}{R_d T}) + (\frac{P_v}{R_v T}) \quad (8.11)$$

The gas constants are known[137] to be:

$$R_d = 287.05 J / Kg°K$$
$$R_v = 461.495 J / Kg°K$$

The vapour pressure can be related to saturation pressure (subscript 's') and humidity as shown in equation (8.12).

$$P_v = P_s \times RH \quad (8.12)$$

The saturation pressure of water vapour can be found using equation (8.13) [138].

$$P_s = a_0 \times 10^{\left(\frac{a_1 T}{a_2 + T}\right)} \quad (8.13)$$

where: a_0 = 6.1078
a_1 = 7.5
a_2 = 237.3

Having found the vapour pressure, the dry air pressure can be found by means of subtraction. After finding both the water vapour pressure and the dry air pressure, the air density can now be calculated using equation (8.11).

Validation

No weather data could be found that contains measurements for air pressure, relative humidity and air density. Therefore the accuracy of calculations cannot be validated using real data. The two main sources of uncertainty come from assuming air can be treated as an ideal gas, and the algorithm to find saturation pressure based on temperature described by equation (8.13). The validity and accuracy has been established in the relevant reference documents, which lead to assume that while there are more accurate methods available, the presented solutions provide simple and fairly accurate approximations. On the whole,

accuracy for these calculations is not critical, but merely helps to improve the data input to other models. These models will also have other, more significant sources of uncertainty.

8.4 Finding Wind Direction Difference

The wind direction measured by the weather station was given in alphabetic terms, where N = north, S= south, etc. For numerical analysis this had to be converted to degrees. This conversion then allowed finding the wind direction change that would represent the smallest angular difference.

The wind direction was converted from alphabetical to numeric values as shown in Table 8.C.

Table 8.C: Wind direction conversion

Alphabetic	Numeric (º)
N	0
NNE	22.5
NE	45
ENE	67.5
E	90
ESE	112.5
SE	135
SSE	157.5
S	180
SSW	202.5
SW	225
WSW	247.5
W	270
WNW	292.5
NW	315
NNW	337.5

Difference in wind direction was assessed by finding the modulus (absolute value) of subtraction of the numeric values from two consecutive time intervals. However, when the wind direction changed from say 350° to 10°, an algorithm was written to give this as a difference of 20° as opposed to the unlikely value of 340°. The algorithm essentially prevented computed changes that were greater than 180°, as this case was considered to be unlikely to occur in practice over the period of 10 minutes sampling time.

9 Estimating Space Heating Requirements

The energy demands of the dwellings at the EcoSmart village must be determined as accurately as possible to establish their carbon footprint and the energy loads for the space heating systems. Space heating typically accounts for more than half of the energy consumption in a domestic building[139].

Several methods will be compared to simulate the energy performance of the buildings as accurately as possible. To ensure that input data for simulation is also as accurate as possible, a pressurisation test was carried out on two of the buildings to quantify the ventilation losses. The energy models will also be adjusted for average measured internal temperatures. The following section will present the results of this analysis, and provide a realistic indication to the space heating requirements of the buildings.

9.1 Input Data

All modelling methods require the specification of two important input variables:

- Average internal temperature
- Average ventilation losses

9.1.1 Internal Temperature

The heating systems of all houses were controlled by thermostat, which were all set to 21°C. The temperatures of every room in every house were measured and recorded throughout the trial period. The resulting average temperatures, taking into account the approximate sizes of the rooms, are given in Table 9.A.

Table 9.A: Measured average internal temperatures over a 12-month period

	Average internal temp. (°C)
Palmerston	21.1
Windermere	19.7
Washington	21.3
Malvern	20.9
Edinburgh	21.9
Buckingham	20.2
Alderney	20.3

Table 9.A shows that the temperatures of all houses are fairly well controlled. All buildings apart from Windermere are within 1°C of the temperature that was set on the thermostat. These averages for measured temperature over a 12-month period will be used as a basis for modelling the heating requirement of each building.

9.1.2 Ventilation Losses

When considering the source of thermal losses from a domestic property, ventilation losses have a large part to play. Figure 9.1 shows the thermal image of one of the properties at the EcoSmart village. It can clearly be seen that the highest losses originate from trickle vents above the windows. Warm areas are also seen along roof edges. Given the roof structure it is likely that warm air from the vents is collecting there, although it is also possible that the edges themselves are areas of leakage. The wooden window frames also appear to act as thermal bridges.

Figure 9.1: Thermal image of the Alderney home at the EcoSmart show village

According to CIBSE Guide B2[140] the recommended air change rate is 0.5-1.0 Air Changes per Hour (ach). This is related to the entire building volume. To minimise heat losses the ventilation rate should be reduced as much as possible. However, if the ventilation rate is too low, there is a high risk that the lack of fresh air can lead to sick building syndrome[141]. The test houses were designed to have ventilation rates of around 0.7-0.8ach. However, designed ventilation rates are rarely achieved in practice[142] as there is much room for error during the construction phase.

In order to obtain a feel for the difference between designed and actual ventilation rate, should there be any, a standard pressurisation test was carried out on two of the test homes. An alternative method of measuring the ventilation rate is provided by the tracer gas technique[143], which involves measuring the flow of a unique gas to or from the test volume. This technique was unavailable to the research team.

Pressurisation test

The pressurisation test was carried out on the Windermere and the Palmerston. The Air Change Rate (ach) is the rate at which the entire volume of the building is replaced. The test is carried out by fitting a fan unit to the door of the dwelling, as shown in Figure 9.2, making sure that the surrounding frame is air-tight.

Figure 9.2: Pressurisation fan unit

After switching the fan on and while varying its speed, the pressure difference across the fan as well as air flow rate through the fan are measured. Using this data, the effective air change rate at a pressure of 50Pa can be calculated using methods and equations outlined in British Standard BS EN13829:2001. These two factors are related by the internal volume of the building, as shown by equation (9.1):

$$Q_{50} = N_{50}V \qquad (9.1)$$

As these values only apply for the reference pressure difference of 50Pa, they must be converted to values which are representative of typical atmospheric conditions, with pressure differences related to wind speed.

Sherman[144] developed a simple approximation in 1987 for this conversion, based on the LBL infiltration model[145]. It is suggested that a conversion factor of 20 can be used. This $N_{50}/20$ method assumes average wind speed of 4m/s, whereas

the average wind speed recorded during the test period was 3.1m/s, which is likely to cause minor inaccuracies. The complete results from the pressurisation tests are shown in Table 9.B. Both results are within the recommended 0.5-1.0ach range.

Table 9.B: Results from pressurisation test

	Palmerston	Windermere
Mean Q50 (m^3/hr)	2746	3136
Q50specific ($m^3/hr.m^2$)	17.42	11.13
Building volume (m^3)	173.6	263.9
Mean N50 (ach)	15.82	11.88
Q50/20 (m^3/hr)	137.3	156.8
N50/20 (ach)	**0.79**	**0.59**

Theoretical Estimate

For all buildings where the pressurisation test was not performed the SAP 2005 estimate will be used. The SAP method is based on a combination of generic values for various building features and properties. Estimates for the EcoSmart village are summarised in Table 9.C.

Table 9.C: SAP estimated ventilation rate

	***N* (ach)**
Palmerston	0.76 (0.79)*
Windermere	0.77 (0.59)*
Washington	0.74
Malvern	0.83
Edinburgh	0.81
Buckingham	0.79
Alderney	0.75

* Measured values shown for comparison

The comparison between SAP estimated ventilation rate and measured ventilation rate using the standard 50Pa pressurisation test is not fully conclusive. While the Palmerston values are very close with 4% difference, the Windermere values show a much greater difference of over 23%. The main conclusion to be drawn from this is that actual air change rates can be significantly different to estimated rates, and should ideally be assessed by testing for each individual case. Unfortunately this was not possible for the case of the EcoSmart village due to the limited resources available to the research team.

For further analysis the SAP estimated values will be used, except for the case of Palmerston and Windermere, where measured values were available. The previously found error of up to 23% may also apply to all other buildings.

9.2 Building Energy Models

Having determined the average internal temperatures and ventilation rates, the buildings' space heating requirements can be modelled. Three different methods were used to gain a broad range of comparable estimates:

- Simple heat loss model
- SAP calculations
- Software simulation

9.2.1 Simple Heat Loss Model

A good approximation of the heat losses of a building at a given time interval is provided by the steady state equation (9.2), where (A) is total external surface area, (N) is the air change rate and (V) is the total volume of the building.

$$\dot{Q}_{loss} = \left(\Sigma UA + \frac{1}{3} NV \right) \times \left(T_i - T_a \right) \qquad (9.2)$$

This simplified method neglects heat gains from solar radiation, internal gains from other heat sources, and additional heat losses from wind-chill effects. These effects can be expected to cancel each other out to some extent, but significant inaccuracies will inevitably remain.

The advantage of this method is that it can be used to calculate the theoretical energy loss for each of the 5-minute intervals of the recorded temperature data, although it must be noted that reasonable accuracy can only be ensured when using average values over several days or longer. For comparison, SAP uses yearly average values, and the building energy simulation software uses hourly data.

The design U-values were used for the simulation, which may result in minor errors. Internal and external temperatures for the buildings were recorded during the test period as described previously. The modelling time-step was chosen as 5 minutes, in accordance with the available interpolated temperature data. The air change rates of the buildings are taken from Table 9.C.

Results for the 12 month test period are shown in Table 9.D. Average internal temperature is also given for reference.

Table 9.D: Results for simplified heat loss model

	Annual thermal energy losses (kWh)	Avg. internal temp. (°C)
Palmerston	7,611	21.1
Windermere	11,531	19.7
Washington	7,481	21.3
Malvern	20,433	20.9
Edinburgh	13,133	21.9
Buckingham	10,489	20.2
Alderney	13,406	20.3

9.2.2 SAP Calculations

The SAP calculations were used to assess the buildings during the design stage. SAP[146] uses generic values for heat loss, heat gain and ventilation losses together with building dimensions and other parameters such as U-values to estimate the annual energy requirement.

The SAP calculations are not very flexible in accounting for variations in weather data or more detailed construction properties, but it does allow for the manual adjustment of some values. Two of these values are the average internal temperature of the dwelling and the ventilation losses.

Table 9.E shows a comparison of the initially estimated space heating energy requirements based on generic values, and the space heating requirements after the internal temperature and ventilation rate had been adjusted manually.

Table 9.E: Space heating demand according to SAP calculations

	Initial estimates (kWh/yr)	**Adjusted estimates (kWh/yr)**
Palmerston	3,772	**4,576**
Windermere	7,589	**6,285**
Washington	2,975	**3,628**
Malvern	9,717	**10,821**
Edinburgh	6,297	**7,800**
Buckingham	6,881	**7,070**
Alderney	6,222	**6,445**

The adjusted values in Table 9.E differ by around 10-20% from the initial estimates. With the exception of Windermere, all buildings show a space heating demand that is greater than initially anticipated. Windermere's adjusted demand is mainly affected by the 23% lower measured air change rate.

9.2.3 Software Simulation – CASAnova

The simulation software CASAnova[147] was developed at the University of Siegen, Germany, and is freely available. It provides an academically verified and easy to use solution. It uses a single zone dynamic temperature model, and the calculation of heating demand is based on European norm BS EN832:2000. The model is based on an approximated representation of the building and it allows the import of third party hourly weather data. The input data for the energy simulation includes:

- Geometry: building dimensions including area, number of floors, internal volume and orientation

- Windows: orientation and size of windows, type, U-values, and shading

- Insulation: independent U-values of walls, roof and floor, absorption coefficient, heat bridges and doors

- Building: indoor set temperature, internal gains, mechanical and natural ventilation, air conditioning, type of construction

- Climate: The ability to chose from several weather data sets, or import weather data

- Energy: the type of heating and heat distribution systems, type of fuel used

Despite only generating an approximated building model, the range of considered variables suggests that CASAnova is able to analyse the energy performance of a given building to a relatively high degree of accuracy.

The energy losses for the buildings were simulated for measured average internal temperatures. Results are shown in Table 9.F.

Table 9.F: Annual energy demand for space heating from CasaNova simulation

	Estimated Heating Demand (kWh/yr)
Palmerston	7,638
Windermere	7,151
Washington	6,066
Malvern	14,936
Edinburgh	10,207
Buckingham	8,753
Alderney	7,504

9.2.4 Model Comparison

Table 9.G and Figure 9.3 show a comparison between all three methods for each individual building to provide a basis for meaningful analysis and validation.

Table 9.G: Comparison between all three models

	SAP (adjusted) (kWh)	CASAnova (kWh)	Heat Loss Model (kWh)
Palmerston	4,576	7,638	7,611
Windermere	6,285	7,151	11,531
Washington	3,628	6,066	7,481
Malvern	10,821	14,936	20,433
Edinburgh	7,800	10,207	13,133
Buckingham	7,070	8,753	10,489
Alderney	6,445	7,504	13,406

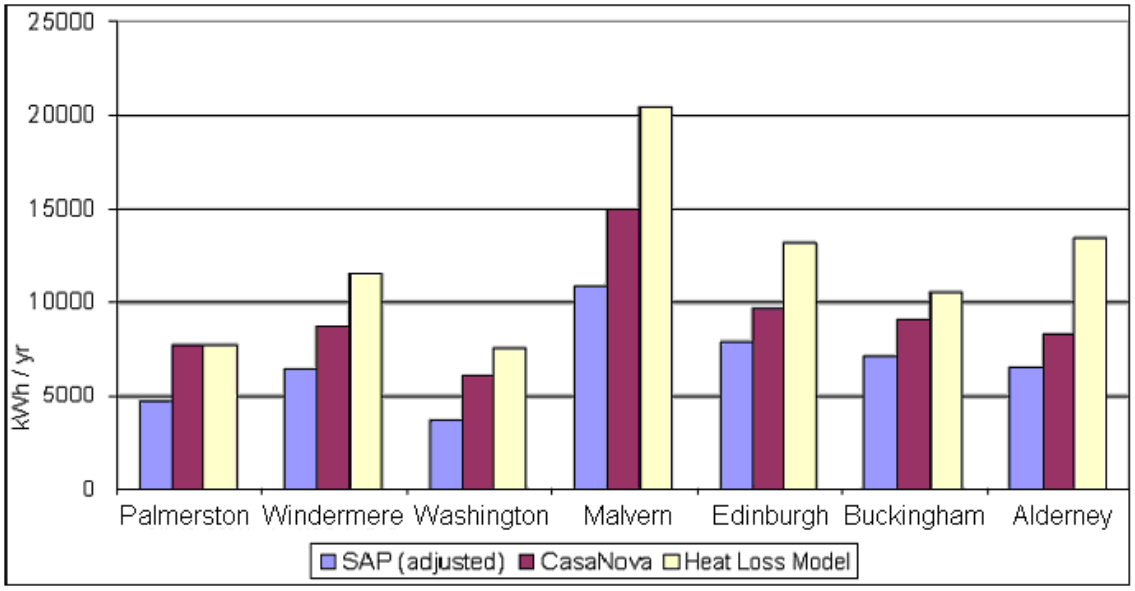

Figure 9.3: Graphical comparison between space heating models

As shown by Table 9.G and Figure 9.3, there are significant differences between all estimates. SAP generally gives a much lower estimate for space heating demand than the two other methods. Perhaps the excessive use of generic values, which are unable to account for any weather variations, can be held partially responsible for this. The simplified heat loss model generally provides significantly higher estimates, which might be expected due to the inaccuracies discussed previously.

Based on the presented analysis it appears that CASAnova can be expected to provide the most realistic estimate. This is concluded after a process of elimination, as SAP calculations involve too many assumptions and generic values

to be considered accurate, and the simplified heat loss model completely neglects solar gains and wind effects.

9.2.5 Modelling Limitations

The main modelling limitation is given by the ventilation losses. It was shown that the measured value of air change rate can be significantly different to the theoretical value. In one of two tests the difference was found to be over 23%.

Another important thing to consider is that the ventilation rate, measured or simulated, only accounts for passive ventilation of the building under steady conditions, meaning when windows and doors remain shut. However, as these homes were used as show homes, doors in particular were opened randomly and frequently from the many visitors as well as staff of the EcoSmart show village. Therefore, no matter how good the simulation may be, there will always remain a significant and unquantifiable error.

9.2.6 Model Validation

Based on the comparison of three different models and a qualitative assessment, it was concluded that the CASAnova simulation program is expected to provide the most accurate estimates for space heating demand. For validation, the CASAnova results can be compared to measured energy supply for space heating. The space heating systems throughout the EcoSmart village are shown in Table 9.H.

Table 9.H: Heating systems at the EcoSmart village

	Heating System
Palmerston	GSHP
Washington	GSHP
Malvern	GSHP
Edinburgh	µCHP
Buckingham	µCHP
Alderney	Boiler + Solar Thermal
Windermere	Boiler + Solar Thermal

At the EcoSmart village all buildings have variable input from low or zero carbon systems. As the heat meters for solar thermal and GSHP systems did not work, the only remaining buildings for comparison are Edinburgh and Buckingham. A comparison between CASAnova heat demand estimates and measured heat supply by the μCHP systems is shown in Table 9.I.

Table 9.I: Comparison of CASAnova estimate with measured heat supply

	CASAnova Estimate (kWh)	**Measured Heat Supply** (kWh)	**Difference** (%)
Edinburgh	10207	10790	**5.7%**
Buckingham	8753	8256	**-6.0%**

At first glance Table 9.I shows good correlation between the CASAnova estimate and the measured space heating demand of the two buildings. However, it must be stressed that these results may not be very accurate, as the uncertainties for ventilation losses including visitors opening doors can be quite significant. This effect may not have been as significant as for other homes as the Edinburgh and Buckingham were two of the smaller and arguably least interesting homes in terms of their energy systems, and they were located furthest from the entrance (sales office). Nonetheless, the small differences of 5.7% and -6% seem to confirm that the CASAnova simulation is sufficiently accurate to provide a suitable tool for estimating space heating demands.

10 Photovoltaic Systems

PV systems are able to generate electricity from direct sunlight, and are often roof-mounted to maximise solar potentials. With electricity being the most expensive and also most carbon intensive form of energy we use in the domestic sector, the prospects of generating 'free, green electricity' are very promising. The following sections will assess the viability of building-integrated PV systems in the UK, both in energy and in financial terms. In addition to this, there will be a focus on finding a simple and accurate method that allows architects and builders to anticipate the performance of these systems without any technical background knowledge.

10.1 Introduction

Photovoltaic is the term used to describe materials or devices that are able to convert the energy that is contained by photos of light into electrical current and voltage.

The integration of PV systems in the built environment in the UK has been contemplated and assessed for some time[148], and over the last few years test sites such as the BRE Innovation Park have been constructed to demonstrate feasibility and effectiveness. Other countries, such as the Netherlands[149] and Germany[150] have also had positive experiences with energy generation using roof-mounted PV systems, and are looking to continuously expand the use of this technology.

10.1.1 Background Theory

The following section will outline some of the physics behind photovoltaic electricity generation. Other literature[151] provides more detailed descriptions.

Semi-conductors and Band Gap Energy

The materials used to convert light into electrical energy are semiconductors, predominately Silicone. On an atomic level, there is an outer valance band, where electrons are held in fixed positions, and a conduction band, where electrons are essentially free to move around. These bands are separated by a band gap, which represents a certain amount of energy (band gap energy). As electrons, excited by photon energy, move into the conduction band, they form negative charges and

effectively leave positive charges (described as holes) behind in the valence band. Figure 10.1 is used to illustrate this process.

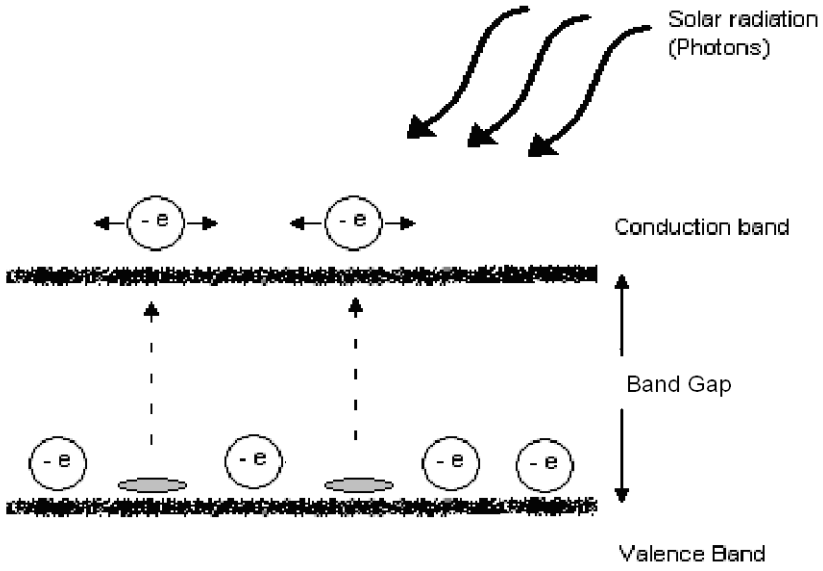

Figure 10.1: Schematic diagram showing how excited electrons move into conduction band

The p-n Junction Diode

To direct the flow of electrons, the semi-conductor is doped with other atoms that cause impurities and form an electric field within the crystals. These impurities are formed using so-called n-type materials (such as phosphorous). At the same time, the other side of the semi-conductor now becomes positively charged, forming the p-type material. This method effectively creates the so-called 'p-n diode' and allows a potential difference to be created across the semi-conductor as electrons become excited.

The I-V Curve and Internal Resistance

The current and voltage characteristics of the PV cells are influenced by different factors, including air mass, solar radiation and cell temperature. Air mass describes the thickness of the atmosphere and affects the intensity of solar radiation, as well as the distribution of the solar spectrum[152]. Temperature also has a significant effect on power output by causing a variation in voltage across the PV cell. For silicone semi-conductors the voltage will typically drop around 0.37% per degree Celsius.

Shading on PV Cells

PV cells are very sensitive to shading. Being connected in series, the internal resistance induced by shading can be very significant, reducing the overall output power by around 50% for 1 shaded cell (in an array of typically 32). To mitigate this effect bypass diodes can be used, which effectively form a bypass for individual modules if they are shaded.

Standard Testing Conditions

In order to provide a fair comparison between solar PV systems Standard Testing Conditions[153] (STC) have been established for PV performance testing. These conditions include the following:

- Solar radiation of 1000W/m^2
- Air mass of 1.5
- Cell temperature of 25°C

10.1.2 Capital Cost, Embodied Energy and Carbon

Considering that PV technology has been around for a relatively long time, the cost in terms of money and energy is fairly well understood. The Department for Communities and Local Government released a cost projection[154] for PV systems, which is based on market tested and peer reviewed data. The results of this projection are shown in Figure 10.2.

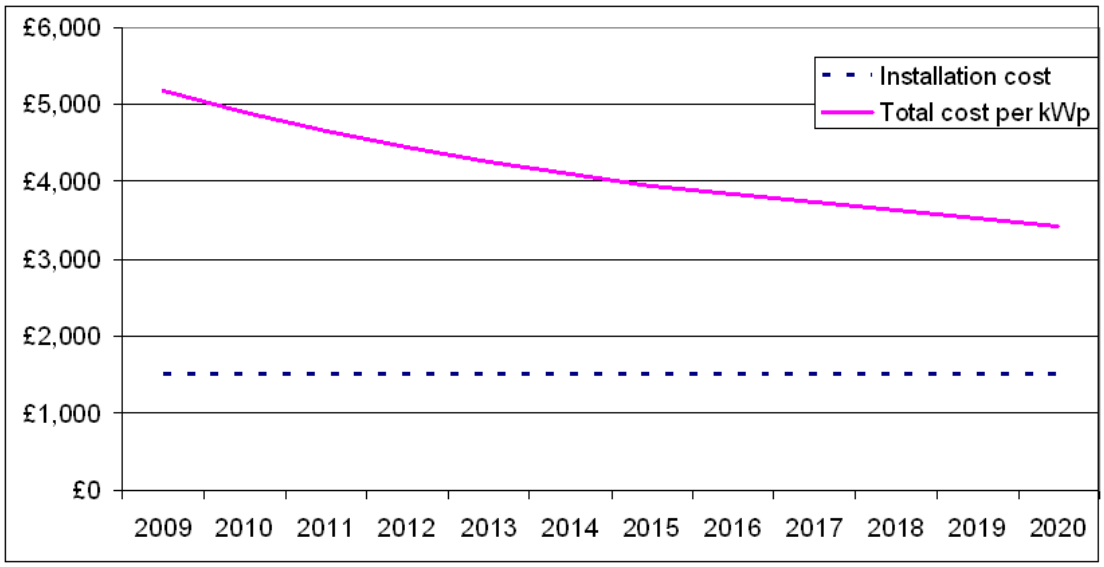

Figure 10.2: Expected variation of capital cost with time (Source: DCLG[154], 2010)

For comparison, the system capital cost for the EcoSmart Village systems in early 2006 is given in Table 10.A.

Table 10.A: Capital cost of the EcoSmart PV systems in 2006

Size	System cost
1kWp	£4,500

The system cost for the EcoSmart Village refers to system capital cost only. As the systems are installed during the construction phase of the dwelling, and the installation method is similar to that of conventional roof-tiles, no additional installation costs were incurred. However, with reference to Figure 10.2 this value does provide a representative estimate for PV capital cost over the next 2-3 years and will therefore be used for analysis.

Much literature is available that has assessed the embodied energy and carbon in modern PV systems, with a differentiation for building-integrated solutions. Estimates can vary significantly[155], depending on whether the silicone is classed as recycled waste[156] or not. Some critically reviewed estimates are summarised in Table 10.B.

Table 10.B: Summary of estimates for embodied energy of PV systems

Source	Embodied Energy (kWh/m2)	
	standalone	roof-integrated
Alsema & Nieuwlaar[157]	1300	1380
Nawaz & Tiwari[158]	1710	
Wilson & Young[159]	2500	
Average	1837	**1482***

*based on average for standalone systems and the ratio found by Nawaz & Tiwari

As shown in Table 10.B, the value that will be adopted for embodied energy of building-integrated systems is 1482kWh/m^2, which is based on a literature review.

All of the reviewed documents suggest that the energy required for the PV manufacturing process consists predominantly of electrical energy. All embodied carbon estimates are based on afore mentioned CO_2 content factor for primary electricity. The resulting estimate for embodied carbon is shown in

Table 10.C. This value is well in line with other estimates[39], ranging from 101-599 kgCO_2/m^2.

Table 10.C: Estimated embodied carbon of building-integrated PV systems

Size	Embodied CO_2
1 m^2	341 Kg

10.1.3 EcoSmart Village Set-up

Figure 10.3: Photographs Malvern (left), Palmerston (centre) and Washington (right) PV systems

There are 3 similar mono-crystalline PV panels installed at the EcoSmart show village, shown in Figure 10.3, each having a different orientation and tilt. The systems were manufactured by SolarCentury Ltd. and have been installed in accordance with the Construction, Design and Management (CDM) regulations[160]. Each panel consists of 20 individual solar roof tiles, with a combined area of 7.8m², able to generate a peak output of 1.04 kW. The module efficiency at standard test conditions (STC) is stated as 14.9%. These parameters are summarised in Table 10.D, while Table 10.E summarises orientation and tilt angles.

Table 10.D: Specifications of SolarCentury PV system

Type	mono-crystalline
Rated power	1.04 kW
Surface Area	7.8 m²
Efficiency	14.9 %

Table 10.E: Summary of EcoSmart village PV systems

System	**Orientation**	**Inclination**
1 - Palmerston	South	45°
2 - Washington	East	45°
3 - Malvern	East	60°

The DC power that is generated by the PV systems is converted to AC power using an inverter, and exported to the power grid using an import/export meter. While there is no explicit warranty for the PV system, the manufacturer gives a guarantee that the system performance will not drop below 80% of its initial efficiency within 25 years of commissioning.

10.2 Availability of Solar Energy

The availability of solar radiation varies significantly with latitude. In the UK, during June and July daylight is experienced[161] during 69% of the total number of hours, while in December this value drops to 32%. The path of the sun also varies significantly in northern latitudes, on a daily as well as an annual basis. This has a profound effect on the intensity of solar radiation on the earths' surface and on specific collector planes. This variation can be calculated using standard equations[162]. The resulting sun-path diagram[163] for the EcoSmart village test site is shown by Figure 10.4.

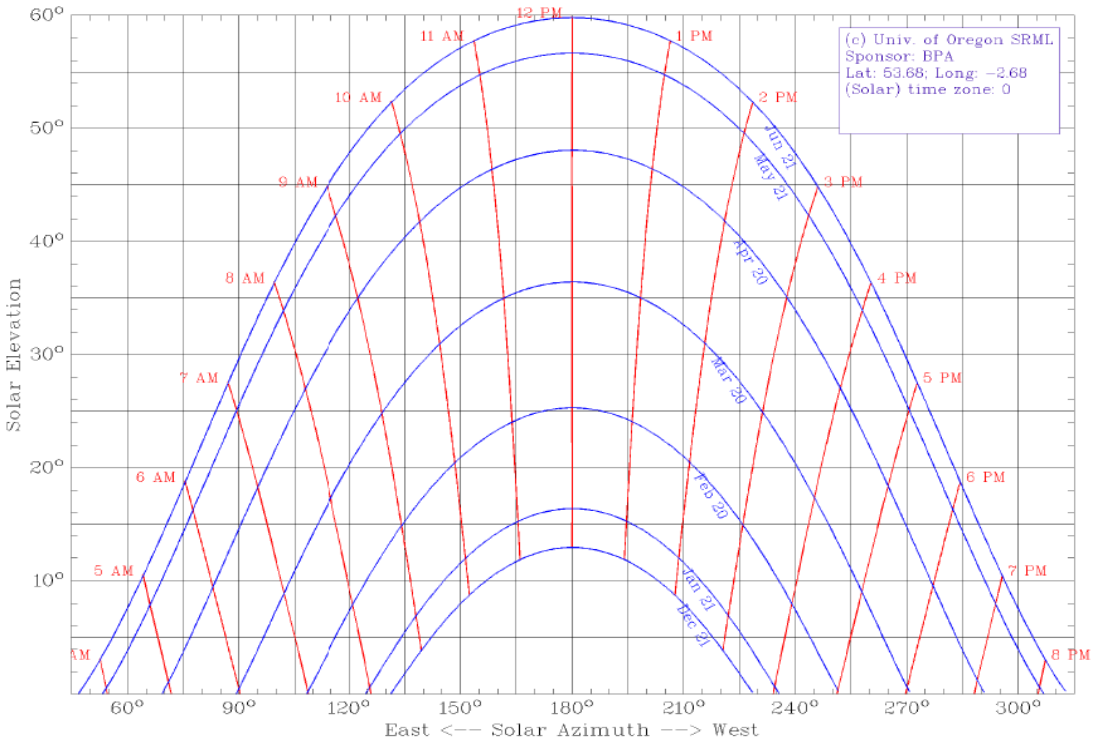

Figure 10.4: Sun-path diagram for the location of the EcoSmart village (Source: University of Oregon)

Having established the predictable variations in availability, some relatively unpredictable variations are presented by weather and cloud cover. To account for this, the measured weather data must be used, which was previously split into beam and diffuse components of solar radiation using the method outlined in section "8.1 – Estimating beam and diffuse components of global solar radiation".

10.3 Photovoltaic Energy Prediction

Despite being shown to have questionable accuracy[164], the Standard Assessment Procedure (SAP 2005) is the government recommended method for estimating PV generation. However, with PV being a very mature technology, many other simple and user-friendly models are available to predict the performance of PV systems throughout the world. Three of these models are:

- **PV GIS**
- **PV Watts**
- **PV Syst**

These PV estimation tools were used to predict PV generation at the EcoSmart village, and their predictions compared to the measured results and SAP 2005 estimates. Based on this, a recommendation is made as to which of these tools is generally best suited to provide PV output estimates throughout the UK.

10.3.1 PV GIS

PV GIS (Geographical Information System) is a freely available web-based estimation tool. It was developed by the European Commission Joint Research Centre and requires little user input, including:

- Location (using Google maps)
- PV technology (e.g. mono-crystalline, thin film, etc.)
- Rated size of the system (in kWh_p)
- System inclination and orientation
- System integration (free-standing or roof-integrated) for temperature calculations

Other than energy output for a given system the PV GIS tool provides several output options, including:

- optimum inclination / orientation
- PV generation from sun-tracking system
- Solar irradiance on different planes

These output options give PV GIS great flexibility and allow it to be used for design optimisation as well as evaluation of proposed designs.

To provide indications of estimation accuracy, the following parameters are also provided:

- Distance between the chosen location and the location which the weather data is taken from
- Estimated losses due to temperature affects
- Estimated losses due to angular reflectance
- In-plane irradiance as average daily and average monthly values
- Sun-path diagrams

PV GIS Method

The PV GIS tool comprises vast amounts of data[165] which has been spatially interpolated. This data includes:

- Weather data[166] from over 800 ground meteorological stations interpolated to 15-minute intervals
- Linke Turbidity (haziness of the atmosphere due to aerosols) from 611 locations[167]
- A Digital Elevation Model[168] to account for terrain shading

Data modelling[169,170] and interpolation techniques[171] have been thoroughly validated[172]. The model also accounts for temperature losses, cable losses and inverter losses, which are largely adjustable by the user.

PV GIS Results

Input parameters were selected that most accurately represent the EcoVillage set-up. All estimated losses were left at default values. Results are shown in Table 10.F.

Table 10.F: PV GIS estimates for EcoSmart village

	Palmerston (kWh)	**Washington** (kWh)	**Malvern** (kWh)
Jan	31	14	13
Feb	47	26	24
Mar	71	50	46
Apr	96	78	71
May	119	107	97
Jun	107	102	92
Jul	113	105	94
Aug	99	84	76
Sep	82	59	54
Oct	57	34	32
Nov	32	16	14
Dec	21	9	9
Annual Yield	**874**	**685**	**622**

10.3.2 PV Watts

The results of the PV Watts[173] estimate are summarized in Table 10.G. A detailed review can be found in Appendix A, page 331.

Table 10.G: PV WATTS estimates for EcoSmart show village

	Palmerston (kWh)	**Washington** (kWh)	**Malvern** (kWh)
	22	6	5
Feb	44	20	18
Mar	70	43	37
Apr	105	73	63
May	126	101	88
Jun	110	88	75
Jul	112	89	76
Aug	107	80	69
Sep	86	56	49
Oct	54	28	24
Nov	30	12	10
Dec	17	5	5
Annual Yield	**882**	**598**	**520**

10.3.3 PV SYST

Results for PV SYST analysis are summarized in Table 10.D. Details are given in Appendix B, page 332.

Table 10.H: PV SYST estimation for EcoSmart show village

	Standard (NASA) weather data			EcoVillage data
	Palmerston (kWh)	**Washington** (kWh)	**Malvern** (kWh)	**Malvern** (kWh)
Jan	38	16	15	12
Feb	44	24	23	21
Mar	70	47	43	49
Apr	96	74	68	71
May	118	103	94	78
Jun	111	104	94	79
Jul	112	103	93	70
Aug	99	83	76	70
Sep	83	59	54	49
Oct	52	32	30	32
Nov	35	17	16	15
Dec	33	13	12	8
Annual Yield	**891**	**675**	**618**	**554**

10.3.4 SAP 2005

The Standard Assessment Procedure (SAP 2005) is currently the standard compliance tool for designers and PV suppliers to estimate the potential generation from a PV system.

The SAP methodology is highly simplified. One location, Sheffield, was chosen to represent the whole of the UK. As Sheffield has very similar Latitude to the test site the results should be fairly representative. Weather data for this location is represented by an average over the years 1960-1979[119], giving a value (G) for annual irradiance. Solar data for three typical ranges of inclination, as well as orientations in 45° steps from north to south are available. An empirical factor (0.8) is used to account for angle changes throughout the year and any losses including inverter, and an over-shading factor (Z_{pv}) is used to account for any shading. The SAP equation is given in equation (10.1), where (kWp) refers to the DC rating of the system.

$$Q_E = 0.8 * kWp * G * Z_{PV} \qquad (10.1)$$

Table 10.I shows the relevant values of irradiance and the annual yield based on SAP 2005. As there is no shading, the over-shading factor was set to 1.

Table 10.I: SAP 2005 estimate for EcoSmart Village

System	Orientation	Inclination	Irradiance (kWh/m^2)	Annual Yield (kWh)
Palmerston	South	45°	1023	**851**
Washington	East	45°	829	**690**
Malvern	East	60°	753	**626**

10.4 Measured Results

Several readings are available for the PV output at the EcoSmart village, comprising 'fixed' (import/export meter) readings, 'mobile' (electricity meter) readings, and 'Fronius' (independent inverter meter) readings for Malvern. Results are shown in Table 10.J:

Table 10.J: Monthly breakdown of measured PV generation from all meters

	Palmerston (kWh)		Washington (kWh)		Malvern (kWh)		
	Mobile	**Fixed**	Mobile	**Fixed**	Fronius	Mobile	**Fixed**
Jan-07	16	13	9	6	12	12	8
Feb-07	42	37	22	16	23	24	17
Mar-07	81	75	56	49	62	63	53
Apr-07	113	104	84	77	91	88	72
May-07	101	93	83	74	93	85	73
Jun-07	97	88	94	84	102	96	83
Jul-07	72	64	76	65	85	76	64
Aug-07	94	85	82	73	89	88	76
Sep-07	66	60	46	41	62	51	45
Oct-07	46	42	24	20	35	29	22
Nov-06	25	21	14	8	16	15	10
Dec-06	10	8	7	4	8	8	5
Annual	763	**690**	597	**515**	678	635	**528**

Table 10.J shows that there are some discrepancies between the different meters that were used. The difference in the measured yearly total PV generation, for the period from 01/11/06 until 30/10/07, is shown in Figure 10.5.

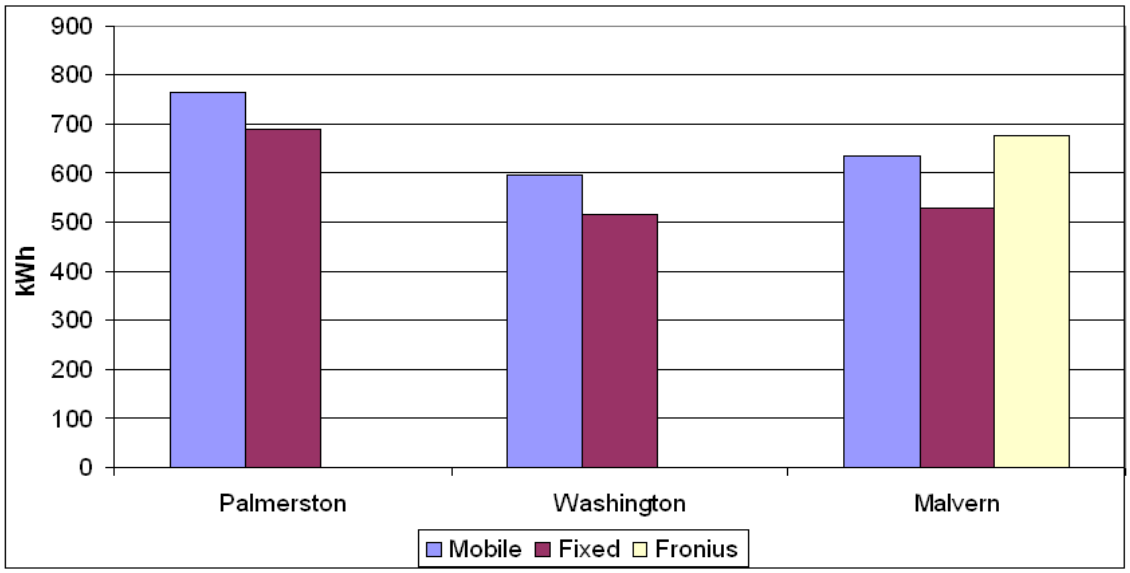

Figure 10.5: Comparison of PV meter readings, showing measured annual output

Figure 10.5 shows that that the readings from some meters show significantly higher outputs than the 'fixed' meter, by up to 20% from the 'mobile' meter and 28% from the third party Fronius meter installed by the supplier. The reason for this discrepancy is that the import/export meter measures power generation and consumption, giving a net value. As was previously explored in detail, inverters consume energy while they are running, which accounts for the 20% difference in registered output. As the 'fixed' (import/export) meter would be used as a reference by energy supply companies for determining the energy offset, this meter will be assumed to give the correct reading and will be used for further analysis.

Energy distribution

Figure 10.6 shows the measured PV energy distribution as recorded from the east facing PV panel at 60° inclination (Malvern). The generating hours were grouped into different power bands:

- P < 50W
- 50W <P< 100W
- 101W <P< 200W
- 201W <P< 400W
- P > 400W

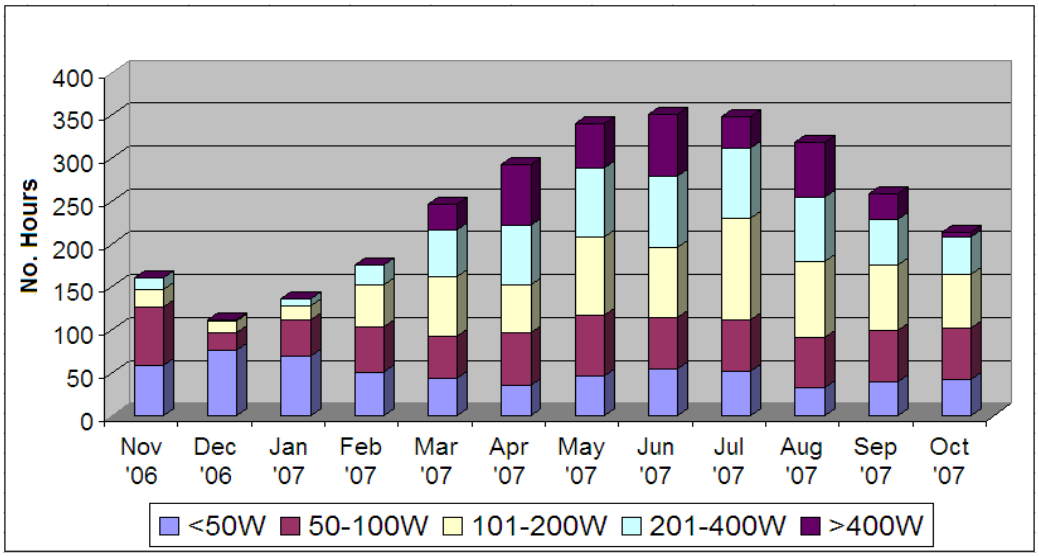

Figure 10.6: Measured distribution of generating hours at various power levels

The results shown in Figure 10.6 provide a valuable indication of the usefulness of the energy generated by the 1.04kW rated PV system. While the frequency of low-power (below 100W) generation is fairly steady throughout the year, high-power generation (above 400W) is only achieved during the summer months. In total, the system was able to generate electricity for 2953 hours during the year, which equates to 34% of all hours and 66% of all daylight hours of the test year.

10.5 System Reliability

The PV systems can be described as very reliable. During the entire project no problems were encountered with any of the three systems installed at the EcoSmart village. All systems consistently showed an energy output throughout every month, and the annual output was reasonably close to the expected output.

After the end of the project, the PV systems were dismantled and transported to the University of Manchester. During transportation, one of the PV panels was broken, but it was found that the panel was able to retain the pieces of broken glass, as shown in Figure 10.7. This indicates that even if the PV panel should shatter, either as a result of vandalism or extreme weather conditions, the risk of falling debris is very low.

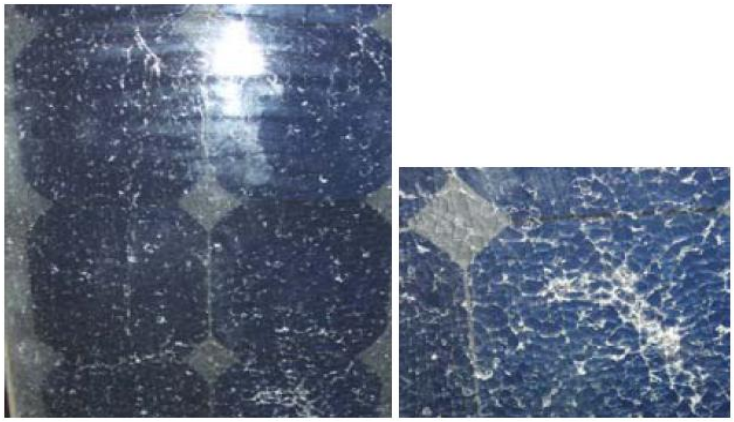

Figure 10.7: Broken PV panel was able to retain the shattered glass

10.6 PV System Modelling

To provide a basis for simulation and to verify the measured results from first principles a model for the PV systems was created. This model is verified and used with the recorded weather data to simulate all three systems and gain a better understanding of where losses originate from and how sensitive the systems are to external influences such as temperature.

10.6.1 Angle Transformation

Having previously found the beam component of solar radiation on a horizontal surface, this must now be adjusted for other planes using angle transformations. These equations will determine the angle (θ) between the sun and the surface in

question at a given time. This angle can then be related to the intensity of beam radiation on the surface in question. The relevant equations are outlined below with reference to Figure 10.8.

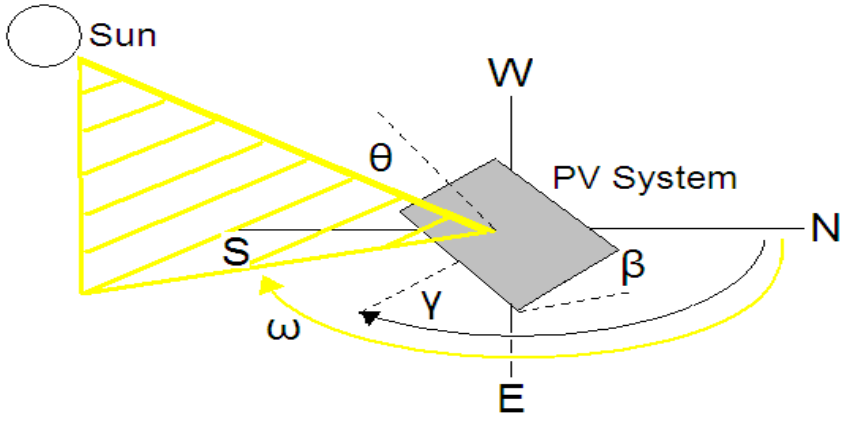

Figure 10.8: Diagram showing the angles for the direct beam calculations

It was previously shown how the hour angle (ω) and declination angle (δ) can be calculated using equations (8.4) and (8.7). In order to find the angle (θ) between the direct beam direction and the plane normal to the collector surface, equation (10.2) is used. The inclination angle (β), orientation (γ) and hour angle (ω) are shown in Figure 10.8. The term (φ) refers to the latitude of the location.

$$\begin{aligned}\cos\theta &= \sin\delta\sin\phi\cos\beta - \sin\delta\cos\phi\sin\beta\cos\gamma \\ &+ \cos\delta\cos\phi\cos\beta\cos\omega + \cos\delta\sin\phi\sin\beta\cos\gamma\cos\omega \\ &+ \cos\delta\sin\beta\sin\gamma\sin\omega\end{aligned} \qquad (10.2)$$

Equation (10.2) is a standard equation[174] that has been widely used and tested in the past, and therefore will not require validation. The term cos(θ), when multiplied by the value of the beam component of solar radiation, defines the intensity of beam radiation that reaches the surface in question. To further refine the model, temperature variation of the PV system as well as any inverter losses must also be considered.

10.6.2 Calculating Cell Temperature

As explained previously, the performance of PV cells varies with cell temperature. Typically, the cell efficiency decreases around 0.3-0.5% per degree Celsius, where 25°C (from STC) is used as a baseline. The following section will outline the methods that are used to determine cell temperature and verify their accuracy.

The NOCT Method

Traditionally, the cell temperature is calculated using the Nominal Operating Cell Temperature, or NOCT. The NOCT temperature is derived during testing, given the following conditions:

Solar irradiation = 800W/m^2
Ambient temperature = 20°C
Wind speed = 1m/s

The NOCT can then be used to estimate the cell temperature using equation (10.3), where the number 20 refers to the testing temperature (in °C) and 800 to the solar irradiance (in W/m^2).

$$T_{cell} = T_a + G\left(\frac{NOCT - 20}{800}\right) \qquad (10.3)$$

However, while being easy to use, the NOCT temperature model does have some severe limitations. It assumes that heat losses are linear and are not affected by changes in ambient temperature, which is not a very good approximation for radiation heat losses. The wind speed is assumed to be 1m/s constantly, which does not allow for any consideration of increased forced convection from the panel at higher wind speeds. Also, this simplified model was derived for rack-mounted PV panels, and does not account for the case of roof-mounting. When panels are roof-integrated with not air gap, there cannot be any convection or radiation losses from the rear.

Dynamic Temperature Model

A more comprehensive temperature model is given by Eicker[175], considering an energy balance including thermal losses from radiation and convection. However, this iterative model makes many assumptions and simplifications which are not explained in detail, verified, or justified. An earlier model, first published by Jones & Underwood in 2001[176], was found to be more accurate. This model approaches finding the cell temperature based on the same energy balance as Eicker, but using differential equations and heat loss factors that are derived from first principles. Its accuracy was verified using measured data from a site in Northumbria.

The energy balance for the Jones & Underwood temperature model is given by equation (10.4), where subscripts 'lw', 'sw' and 'conv' refer to long-wave radiation, short-wave radiation and convection respectively.

$$C_p \frac{dT}{dt} = Q_{lw} + Q_{sw} - Q_{conv} - P_{PV} \qquad (10.4)$$

Using empirical data, the estimated time constant for a PV module was found to be 7 minutes. This module was similar in size and composition to the SolarCentury PV module tested at the EcoSmart Village. The specific heat capacity was also estimated, based on the comprised materials. Results are shown below.

$C_p =$ 2918 J/°K

The components of the energy balance can be found using equations (10.5) to (10.11):

$$Q_{sw} = \alpha G A \qquad (10.5)$$

The absorption coefficient (α) is given as 0.77 for silicon[177]. However, reflection from the glass cover must also be accounted for. As will be described later with reference to Figure 11.7, a good incidence angle approximation for UK latitudes is around 50°, which relates to an angle correction factor of around 0.9. It can therefore be assumed that the glass cover effectively reduces the absorption coefficient by 10%, giving[178]:

α = 0.7

The long-wave radiation accounts for interactions with sky and ground, where β is the inclination angle of the module.

$$Q_{lw} = A\sigma\left(\frac{1+\cos\beta}{2}\varepsilon_{sky}T_{sky}^4 + \frac{1-\cos\beta}{2}\varepsilon_{ground}T_{ground}^4 - \varepsilon_{PV}T_{PV}^4\right) \qquad (10.6)$$

With reference to equation (10.6) the ground temperature is taken as ambient temperature, and the subscript PV refers to module parameters. The sky emittance relative to ambient temperature is approximated using the relationship outlined in equations (11.15) and (11.16). The first value for module temperature is found

using the simplified NOCT model, all subsequent time steps use the temperature from the previous time-step.

$$Q_{conv} = -A(h_{c,forced} + h_{c,free})(T_{PV} - T_a) \quad (10.7)$$

The subscripts 'forced' and 'free' in equation (10.7) refer to forced convection by wind at the front of the panel, and free natural convection by buoyancy at its rear respectively. An approximation for free convection was developed by Holman[179], but can be taken as zero for the roof-integrated case, as there is no air gap to allow any kind of convection.

After a literature review showed approximations for forced convection taking a wide range of values from 1.2[180] to 9.6[181] W/m^2K^{-1} for a wind speed of 1m/s, it was decided to adopt an empirical relationship derived from test results presented by Jones & Underwood[176]. The resulting simple linear model is given by equation (10.8).

$$h_{c,forced} = 0.5 + \frac{v_w}{1.85} \quad (10.8)$$

The electrical power output of the PV module is given by equation (10.9). The electrical efficiency is adjusted using a cell temperature approximation based on the NOCT method. The efficiency is adjusted using equation (10.10), where the subscript *'std'* refers to standard testing conditions. Equation (10.11) gives the temperature correction factor, where 'c_{temp}' is the temperature coefficient and 25 is the standard testing temperature in ºC.

$$P_{PV} = \eta_{el} G A \quad (10.9)$$

$$\eta_{el} = k_{Temp} \times \eta_{el,std} \quad (10.10)$$

$$k_{Temp} = 1 + c_{temp}(T_{PV} - 25) \quad (10.11)$$

From experimental results by Nishioka[182] the temperature coefficient (c_{temp}) can be taken as –0.4% K^{-1} for mono-crystalline silicon modules. This is verified by manufacturer specifications[183] for the SolarCentury C21 roof tiles, which states a coefficient of -0.38% K^{-1}.

To solve the temperature differential equation (10.4), it can be multiplied by the number of seconds in the time step using the Euler approximation for integrating differential equations. However, while results are expected to be reasonably accurate, this approximation does have some limitations as the model time step of 5 minutes is relatively high compared to the time constant of the panel of 7 minutes.

Temperature Model Validation

Empirical data is used to validate the temperature model. Such data was collected by the US National Institute of Standards and Technology in 2001[184], showing the difference between measured cell temperature and ambient temperature in relation to solar irradiance for several rear-insulated PV modules. This was done to simulate a case of PV roof-integration. While wind speeds are not given, a clear correlation can be seen. The NOCT model is also plotted for comparison, as shown in Figure 10.9.

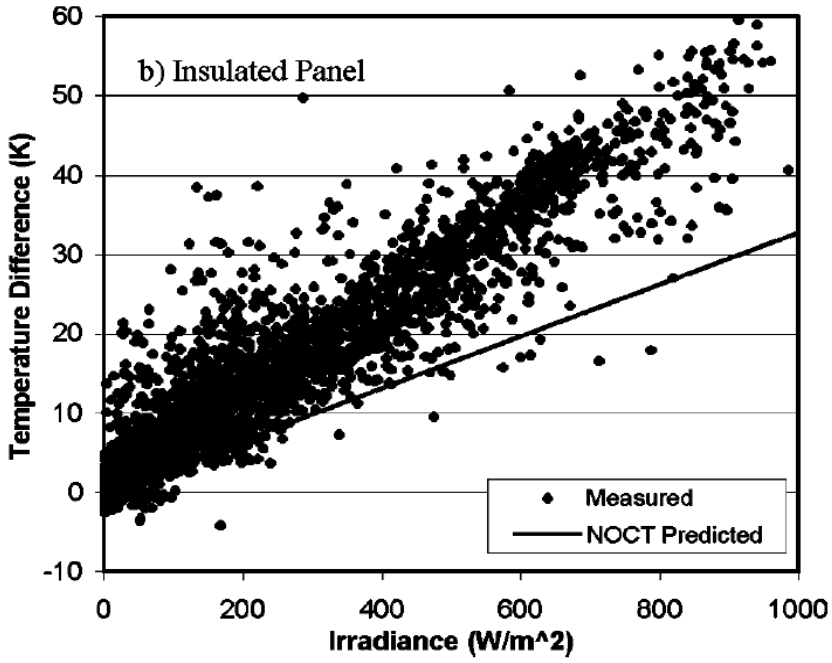

Figure 10.9: Relation between irradiance and temperature difference between PV cell and ambient for roof-integrated PV (Source: Davis et al. 2001[184])

Figure 10.10 shows a similar comparison for the temperature model. For consistency and to allow a direct comparison, the wind speed of the model was set to 1m/s, and ambient temperature to a constant 20ºC. These are the same values which the NOCT model is based on.

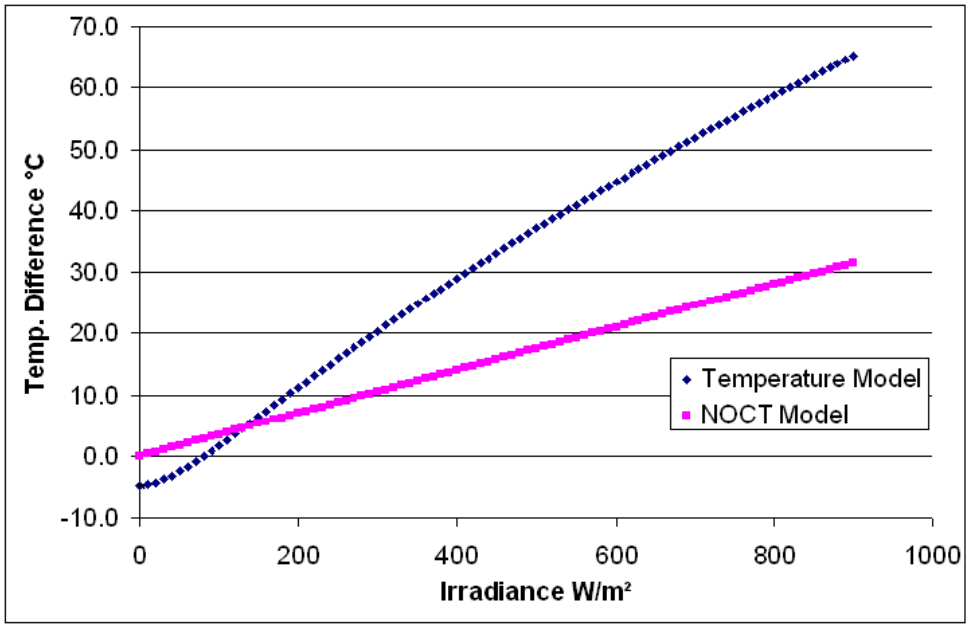

Figure 10.10: Temperature – Irradiance relation of temperature model compared to NOCT model

Figure 10.9 and Figure 10.10 show a good correlation. The temperature model appears to accurately simulate the PV cell temperature in comparison to the measured values. Although the model gives slightly higher temperatures (maximum difference to measured values is around 15%), this can be expected, as the modelled wind speed of 1m/s is set quite low. Compared to NOCT model results both measured and modelled temperatures are significantly higher (approximately by 70-100%), providing evidence that the NOCT method does not provide a valid approximation for the case of roof-integrated PV systems. The difference between NOCT prediction and actual temperatures can be as much as 30ºC, which equates to a difference in PV efficiency of 12%.

10.6.3 Inverter Model

Inverters have varying efficiencies, which is usually rather poor at low load levels, and increases as the input (DC) power approaches the rated power of the inverter. To account for this, an inverter model was previously derived from test data, and will be used for the PV system model. Details on inverter modelling are given in section "7.1.4 – Inverter model".

10.6.4 The PV Model

When combining all the sub-models described above, the complete PV model now considers the following:

- Differentiation of beam and diffuse radiation components
- Angle adjustments for beam irradiance for each time step
- Module efficiency adjustment due to temperature variation for each time step
- Efficiency losses from the inverter for each time step

The comprehensive model is summarised by equation (10.12), where η_{el} is the effective module efficiency based on cell temperature, and subscripts 'b' and 'd' refer to beam and diffuse components of solar irradiance respectively.

$$P_{PV} = \eta_{el}\eta_{inverter}A\left(I_b \cos\theta + I_d\right) \qquad (10.12)$$

10.7 Model Validation

In order to validate the PV model, its results were compared to measured data from the south-facing Palmerston system at 5-minute intervals. Several sample days were compared, including the 4th June 2007, which is shown in Figure 10.11.

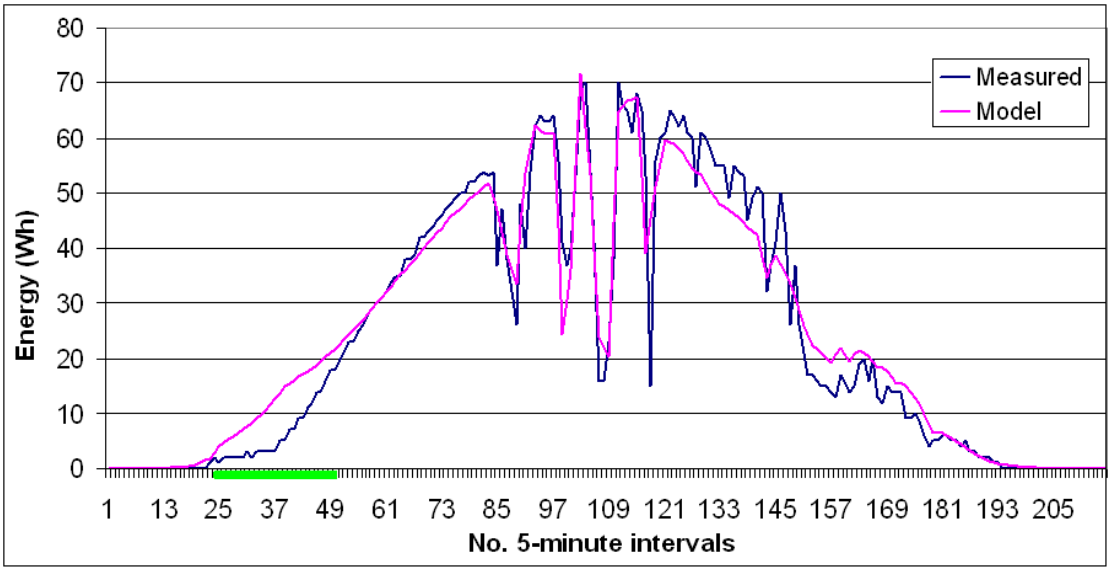

Figure 10.11: PV model validation, sample data for 4th June 2007

Figure 10.11 shows a very good correlation between the model and measured values. During intervals number 120 and 150 the model is slightly lower than the measurements and several spikes do not appear in the model. This can be explained by the fact that weather data was interpolated from 10-minute average values, and the fact that the beam and diffuse splitting model is not 100% accurate. Another area of minor concern is shortly after sunrise (marked in green), where the model estimates are slightly higher than the measured values. It appears that there is some slight shading to the east of the Palmerston module. This is confirmed when looking at other sunny days in June, which show the same pattern. However, this only has a minor effect on mid-summer PV generation and can therefore be neglected for analysis.

To verify the inverter model, periods of low power generation were observed and found to give a very good correlation with the measured results. An example for this is presented in Figure 10.12, in particular the period marked in green.

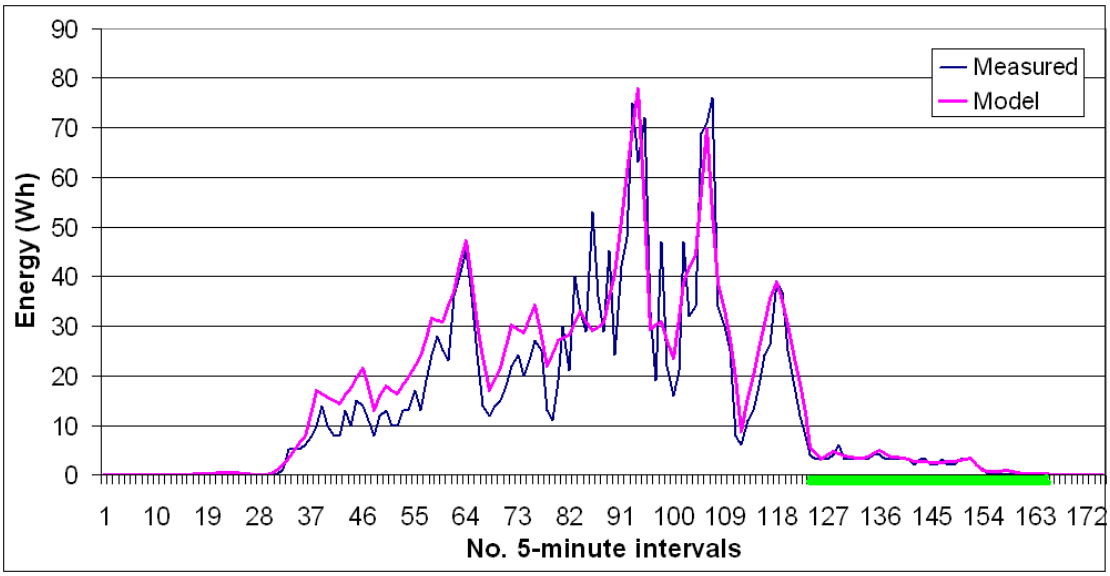

Figure 10.12: PV model with adjusted inverter efficiency, sample data for 11th May

Using the model, monthly generation was estimated and compared to all available meter readings. These are summarised in Figure 10.13, Figure 10.14, and Figure 10.15 for Palmerston, Washington and Malvern respectively.

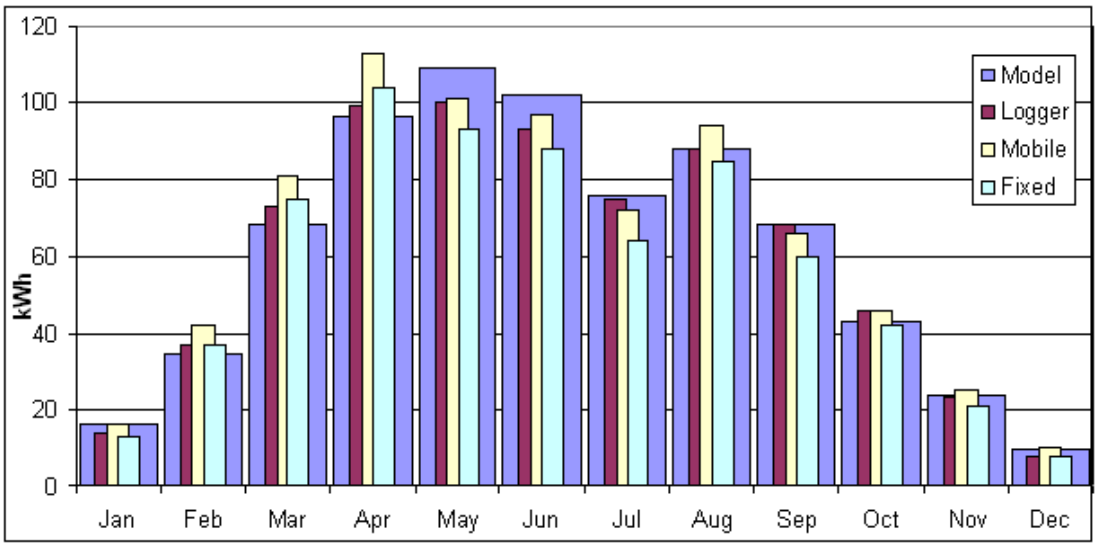

Figure 10.13: Monthly comparison of PV model with meter readings for Palmerston

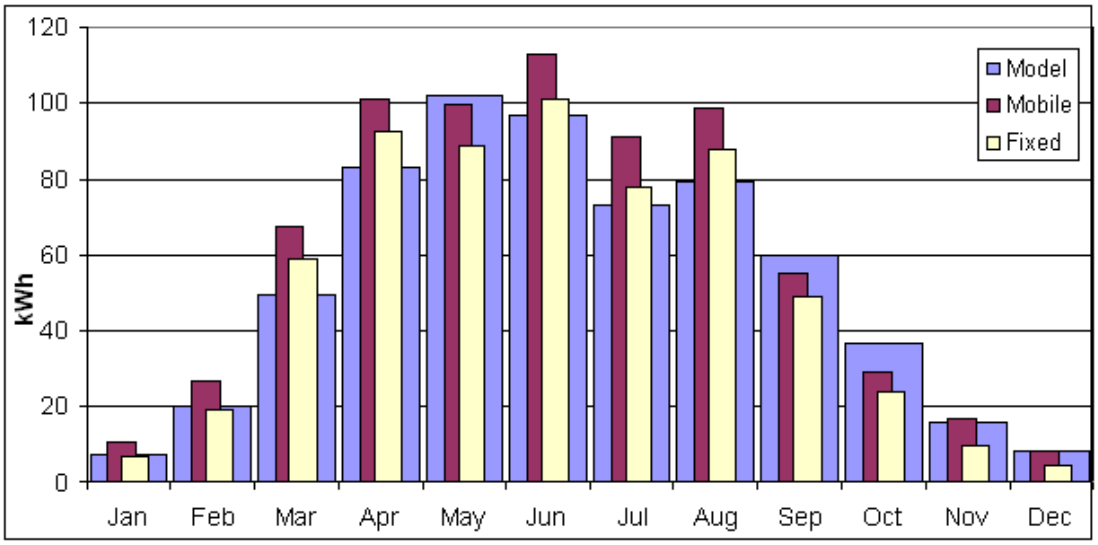

Figure 10.14: Monthly comparison of PV model with meter readings for Washington

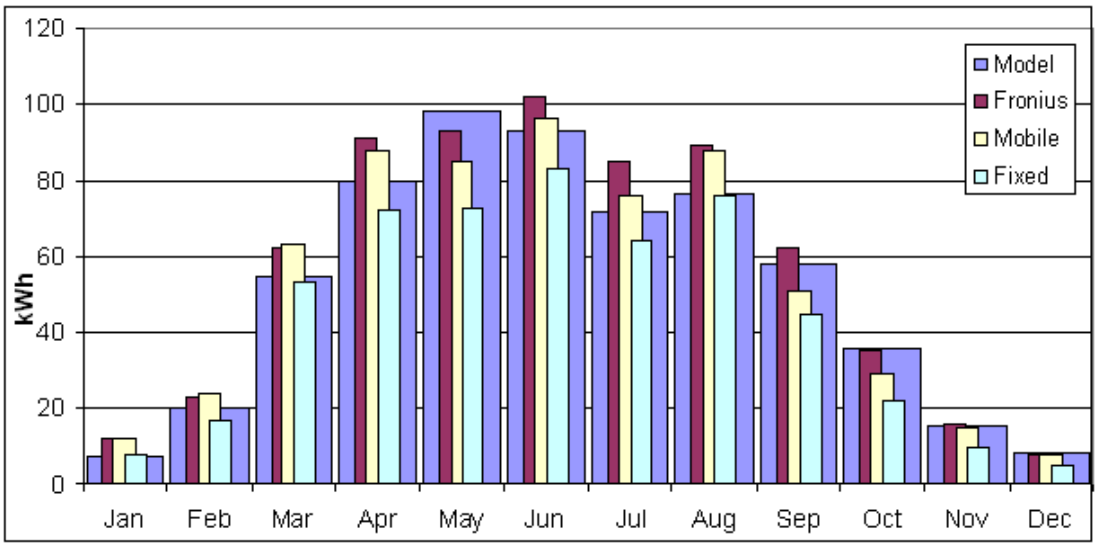

Figure 10.15: Monthly comparison of PV model with meter readings for Malvern

All three comparisons show that the model is able to provide a good estimate for PV generation. The best correlation is given for measurements recorded for Palmerston using the data logger. Weather data for June, July and August contains some gaps which were filled by interpolation, meaning the model is slightly skewed for these months. Generally it appears to be in line with the mobile meter readings, while the fixed meter readings give a considerably lower output. The total annual generation, shown in Figure 10.16, shows a similar picture.

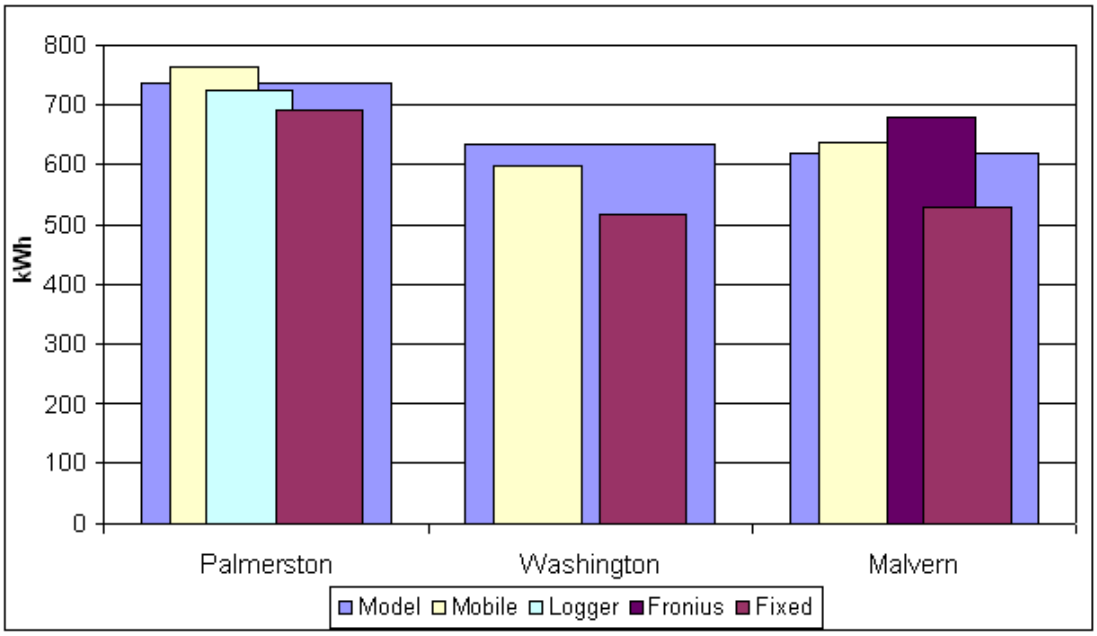

Figure 10.16: Annual comparison of PV model with meter readings from all test systems

In conclusion it can be said that the models' accuracy has been verified. On a daily basis the model correlates very well to the 5-minute interval measurements. It is able to provide monthly and annual estimates that fall well within the range of the measurements that were taken. However, this model does not account for inverter power consumption. While this could have been modelled, it was decided not to do so to avoid skewing the results for comparison with other meters.

10.8 Evaluation and Comparison of PV Estimation Tools

Despite previous attempts[185] it has been recognised that the lack of technical understanding of PV systems in particular, and the resulting inability to conclusively estimate the potential gains, presents a major barrier to the integration of PV technology in building design[186].

Now that the PV systems have been modelled to validate the measured results and explore the importance of correct temperature and inverter modelling, the tools that were used to gain an initial estimate can be critically evaluated. Based on this, it will be evaluated which tool would be most useful to architects and builders. Using this tool, a very simple method is subsequently derived to estimate the annual yield of a building-integrated PV system throughout the UK.

10.8.1 Quantitative Comparison

One of the most important factors in finding an adequate tool is the ability to accurately predict a site's yield. The estimated output from the various tools is compared to the measured results in Figure 10.17.

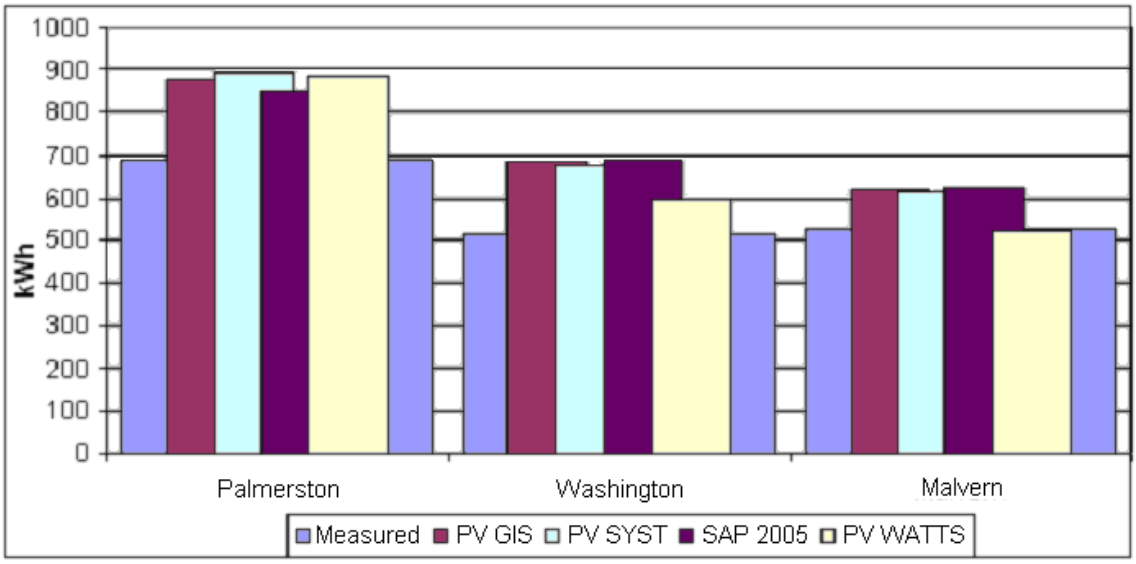

Figure 10.17: Annual yield estimated for the test site using various tools, compared with measured output

Figure 10.17 shows that with the exception of PV WATTS all estimation tools show a fairly good correlation with each other. PV WATTS shows an unexpectedly high drop-off for the east-facing systems. After a thorough examination of the tool, including further testing, it was concluded that the angle conversion algorithm is poorly designed and gives an excessive magnitude of error.

Interestingly the east-facing Washington system can be expected to perform slightly better than it actually did. There may have been some edge shading of one of the PV modules. If the designed overlap of the PV tiles is slightly exceeded during installation, the output can decrease significantly even if only a thin strip along the edge of a module is constantly shaded[187].

All estimation tools give values that are considerably higher than those shown by measurements. This can largely be explained by a difference in weather data and the lack of consideration for inverter energy consumption. The standard estimated loss factors suggested by the tools (14% for PV GIS) are also less than those derived from modelling (22%).

All tools except SAP 2005 allow some degree of loss factor adjustment, and this has been taken into account wherever possible. Table 10.K, Table 10.L and Table 10.M show a comparison to the measured data for PV GIS, PV WATTS and PV SYST respectively. The comparison includes percentage differences and the effect of any adjustments that can be made. The difference in weather data, in terms of annual in-plane irradiation, was also considered.

Table 10.K: Discrepancies of PV GIS results compared to measured data

Difference Case 1	14%
Difference Case 2	24%
Difference Case 3	20%
Average Difference	*19%*
Difference in Radiation	-8%
Adjusted System Losses	-8%
Overall Discrepancy	**3%**

Table 10.L: Discrepancies of PV WATTS results compared to measured data

Difference Case 1	3%
Difference Case 2	12%
Difference Case 3	20%
Average Difference	*12%*
Difference in Radiation	-7%
Overall Discrepancy	**5%**

Table 10.M: Discrepancies of PV SYST results compared to measured data

Difference Case 1	14%
Difference Case 2	22%
Difference Case 3	21%
Average Difference	*19%*
Difference in Radiation	-8%
Overall Discrepancy	**11%**
Discrepancy using EcoVillage weather data	**4%**

The above comparison shows that all tools provide estimates that are effectively within 5% of the measured value. After further considering of inverter consumption

of possibly 50kWh annually, the tools predict the output very accurately, to within 2-3% on average.

10.8.2 Qualitative Comparison

After the accuracy of all tools has been established, a detailed consideration of some other factors is provided in Appendix A, page 333.

Based on this comparison, Table 10.N provides a ranking of the compared tools according to a point system.

Table 10.N: Comparison of PV estimation tools

Category	Weighting	*PV GIS*	*PV WATTS*	*PV SYST*
Accuracy	10 points	8	7	9
Weather data	10 points	8	6	10
Output	10 points	10	7	9
Ease of use	10 points	10	8	5
Adjustability	10 points	7	5	10
Accessibility	5 points	5	5	3
Shading effects	5 points	5	1	3
Cost	5 points	5	5	1
TOTAL	65 points	**58**	**44**	**50**

After a thorough comparison it can be said that all three tools have their merits, but PV GIS appears to be the best choice for providing a quick, easy and accurate estimate for PV generation throughout Europe.

10.9 Considerations for the Integration of PV Systems

As specified previously, it is important for architects and designers with little technical knowledge to be aware of the capabilities of PV systems and their expected performance. At present there is no recognized independent method of designing PV systems for domestic properties in the UK apart from estimations stated by specialist suppliers, and there is no recommended benchmark data available from either the government or professional engineering institutions derived from real data from systems installed on dwellings and tested under real weather conditions. In many cases the Government's Standard Assessment Procedure (SAP) is used to estimate the PV output, which amongst other things

does not account for the latitude of the location, losses due to temperature effects, or any variations in local weather conditions. With PV being a relatively predictable source of renewable energy, some considerations are outlined in this section.

10.9.1 Minimum and Maximum Yields

Figure 10.18 shows the variation of weekly PV generation from the energy readings of the south-facing Palmerston system throughout one year. Minimum, maximum and average values are charted.

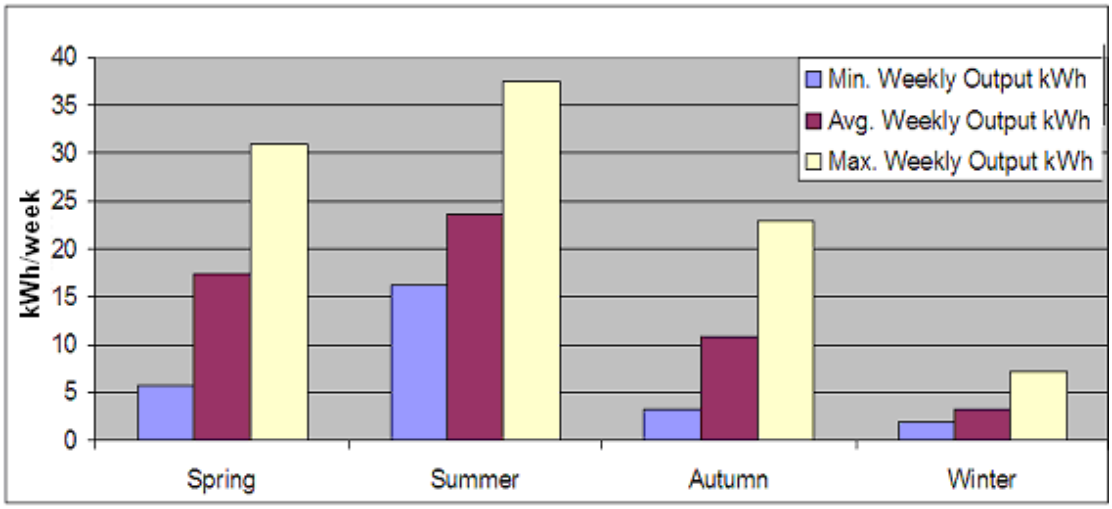

Figure 10.18: Weekly PV generation (maximum, minimum, & average weekly output)

Based on the seasonal weekly averages shown in Figure 10.18, Table 10.O shows the upper and lower bounds of expected annual PV generation:

Table 10.O: Estimated annual PV generation at extreme weather conditions

	East-facing kWh/yr	**South-facing** kWh/yr
Extremely Good Year	**1280**	**1570**
Extremely Poor Year	**350**	**429**
Measured Result	534	701

10.9.2 Effect of Varying Latitude

As explained previously, latitude of a PV system has a profound effect on the solar resources. Solar angles, thus solar intensity, reduce as distance from the equator increases. In the UK, moving north by as little as 1° latitude or a few hundred miles can already make a significant difference in PV generation. Just how significant the

effect is will be explored in the following section. Figure 10.19 shows a map of the UK with selected cities for latitude references.

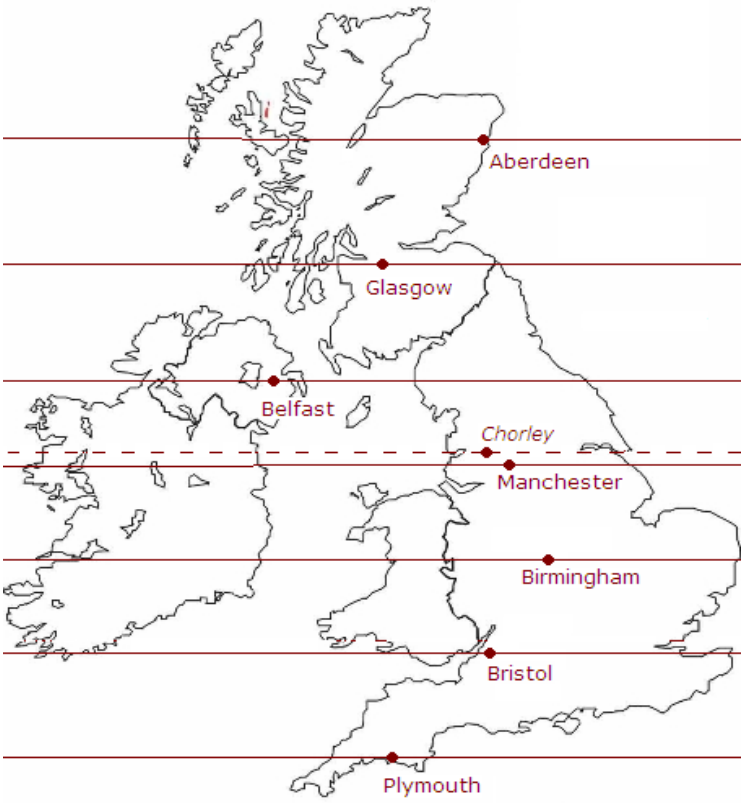

Figure 10.19: Distribution of Latitude references throughout the UK

The PV potential for the reference locations was assessed using PV GIS. The four most likely scenarios for roof-integrated PV systems are summarised in Table 10.P. The location of the test site, Chorley, is also included for reference.

Table 10.P: PV GIS estimates for reference locations throughout the UK

Location	Latitude	Longitude	45° / South (kWh)	60° / South (kWh)	45° / East (kWh)	60° / East (kWh)
Aberdeen	57.1	-2.1	741	712	569	522
Glasgow	55.9	-4.3	710	676	557	508
Belfast	54.6	-6	758	722	594	542
Chorley	*53.7*	*-2.6*	*763*	*725*	*595*	*539*
Manchester	53.5	-2.2	760	723	596	543
Birmingham	52.5	-1.9	769	729	605	549
Bristol	51.5	-2.6	816	773	639	580
Plymouth	50.3	-4.1	870	823	684	622

It can be seen that the annual PV generation decreases significantly with increasing latitude, with one exception. Glasgow receives less solar radiation and consequently has a lower PV output than Aberdeen, which is further north. This is also shown by other published data[188], and could be due to local weather conditions or differences in the geographical surroundings responsible for shading effects.

10.9.3 UK Benchmark – Look-up Chart for Estimating PV Output

As the results of PV generation shown in Table 10.P are fairly uniform, the mean average energy generation can be found to provide a UK national benchmark for 1kWp PV systems. Excluding the Chorley results to avoid distortion of the national average, this equates to 667.6kWh. This value has been rounded to **675kWh/yr** by an iteration process in constructing Figure 10.20. This benchmark value will be used as a baseline value for analyzing the effects of changing PV orientation and inclination in the following sections.

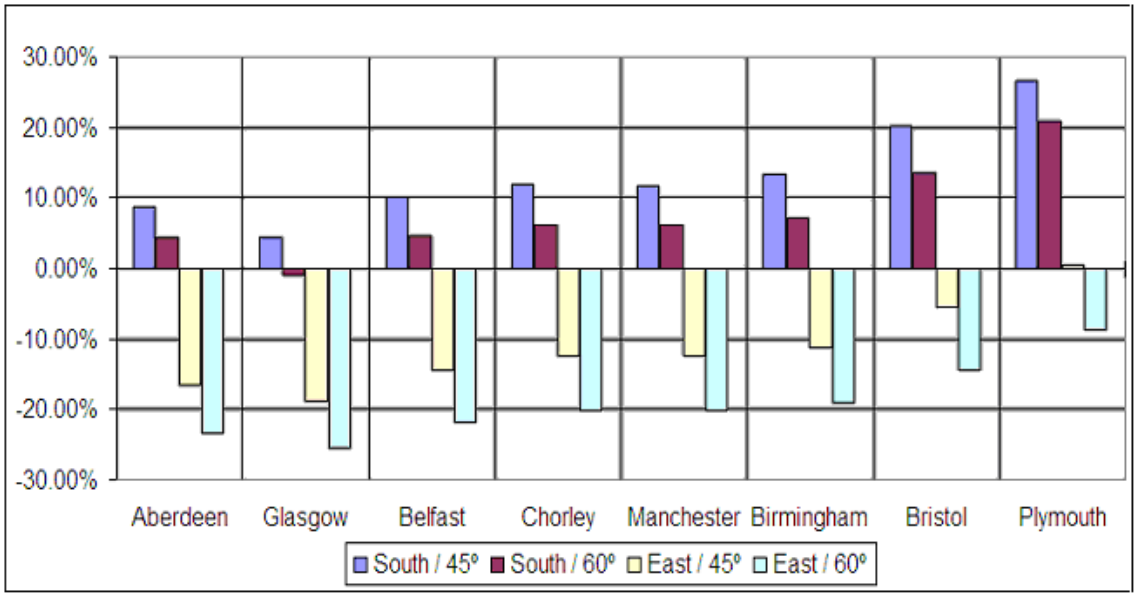

Figure 10.20: Percentage difference between PV GIS results and benchmark value

With reference to Figure 10.20, it can be expected that the average annual output estimate may differ by around ± 25% from the benchmark value, depending on latitude of the location, as well as orientation and roof inclination of the dwelling.

10.9.4 Effect of PV Inclination and Orientation

To take this analysis one step further and explore what changes have the most significant effect, the following orientation and inclination options are explored:

- A percentage comparison of the output with varying module *Inclination*
- A percentage comparison of the output with varying module *Orientation*

Results are summarized in Figure 10.21.

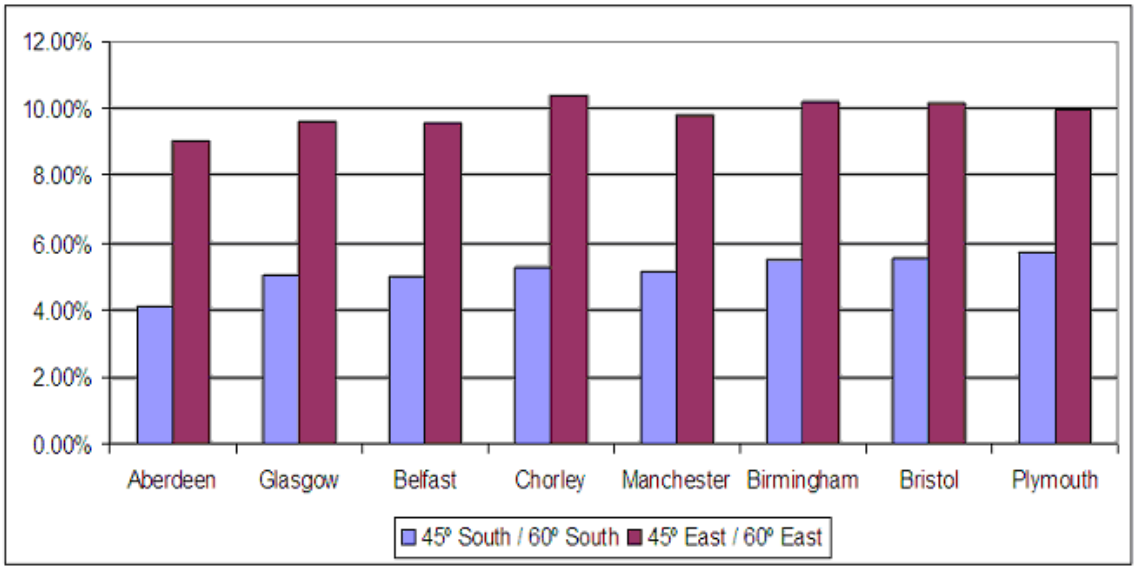

Figure 10.21: Showing percentage differences, focusing on module inclination

From Figure 10.21 it can be deduced that the difference in estimated annual output due to a change in module inclination is around 5% for south-facing systems, and around 10% for east facing systems. This indicates that the module inclination has a more significant effect on east-facing systems.

A similar comparison was carried out to investigate the performance variations with changing orientation of the PV module while keeping inclination fixed. Figure 10.22 shows the comparison between:

- South and South-West
- South and South-East
- South and East

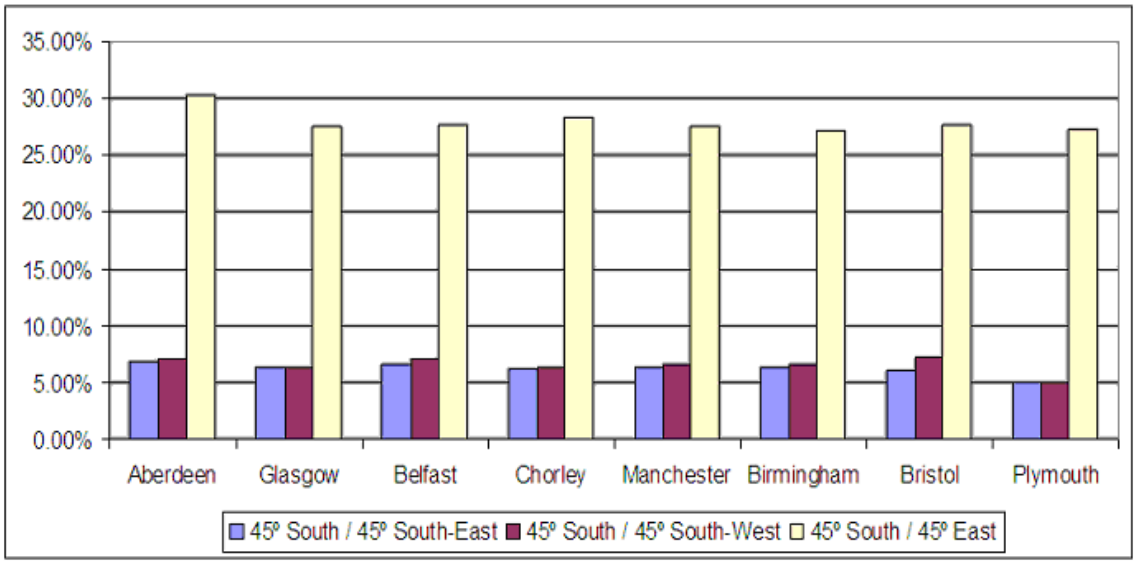

Figure 10.22: Percentage differences of annual output, focusing on module orientation

In terms of dwelling/module orientation as shown in Figure 10.22, the difference between SE and SW facing systems seems negligible. The differences in annual output between a directly south-facing and a SE- or SW-facing system are around 5-7%. However, the difference between directly south- and directly east-facing systems on the other hand is much more significant, between 25-30%.

10.9.5 Effect of Longitude

It was previously assumed that the Longitude of a location has no effect on the PV output. To confirm this, PV GIS has been used to establish the potential PV output at two different locations with equal latitude. Seaside locations near the west coast of England and the east coast of Ireland were used to minimize the shadowing effects of surrounding terrain. As expected, the results in Table 10.Q show only a negligible variation of PV output with longitude.

Table 10.Q: PV estimates for locations at different longitude

Latitude	**Longitude**	**Annual PV output** (kWh)
53.65º	-3.27º	717
53.65º	-5.48º	718

10.9.6 Summary

The previous sections on PV systems have outlined the expected PV generation in the UK and shown how the output will vary depending on different basic parameters. This should provide architects and builders with some practical background information when considering the integration of PV in modern UK homes. To summarize, the following has been established:

- Figure 10.20 can be used as a look-up chart together with the Benchmark value of 675kWh/yr to quickly and easily estimate the annual yield of a PV system in the UK
- PV output varies significantly depending on latitude
- Changes in inclination have a more significant effect on east-facing than on south-facing systems
- Output of SE/SW facing systems is close to that of directly south-facing systems, whereas differences between directly south- and directly east-facing systems are much more significant
- Differences between SE and SW facing systems are negligible
- Longitude of location has a negligible effects on PV performance

10.10 Financial, Energy and Carbon Savings

To provide a basis for savings calculations, generic values for capital cost, as well as embodied energy and carbon had been established in Table 10.A, Table 10.B and Table 10.C respectively. The values have been scaled to represent the PV systems at the EcoSmart village, with results summarised in Table 10.R.

Table 10.R: Capital cost and embodied carbon for roof-integrated 1kWp PV system

	EcoVillage 1kWp PV
Capital Cost	£4,500
Embodied Energy	11,856 kWh
Embodied Carbon	2,727 kgCO_2

Table 10.R presents values that are generic to roof-integrated mono-crystalline PV systems of size 1kWp, and as such can also be used as reference values for similar systems throughout the UK. Table 10.S provides a summary of the performance of all systems, as well as the previously established national benchmark value for UK systems.

Table 10.S: Performance of EcoSmart systems and UK PV Benchmark

	Measured (kWh) (inc. inverter consumption)	**Estimated** (kWh)
Palmerston (45º / South)	690	
Washington (45º / East)	515*	
Malvern (60º / East)	528	
UK Benchmark		**675**

*Underperformed by around 5-10%

Based on the methods outlined previously and using equation (6.8), the estimated financial payback periods are shown in Table 10.T. The maintenance cost[64] for PV systems is estimated to be £50 annually, based on the recommendation of an electrical inspection every 5 years and one inverter replacement throughout the life-time of the system. For calculation purposes the life-time is expected to be 30 years, although a typical PV system may well be usable far beyond that, albeit with degraded efficiency.

Table 10.T: Average financial savings assuming the systems are new-builds, installed before April 2012

System	Annual Savings	
	Electricity offset	2011 Feed-in tariff
Palmerston	£98.67	£249.10
Washington	£73.65	£185.92
Malvern	£75.50	£190.61
Benchmark	£96.53	£243.68

Table 10.T provides a good indication to the level of financial savings that can be expected from systems at the test site and throughout the UK. Table 10.U shows a summary of expected payback rates and life-time savings for the PV systems.

Table 10.U: Payback rates and lifetime savings; financial, energy and CO_2

System	Payback rate (years)			Net savings over system life (30 years)		
	Financial	Energy	Carbon	Financial	Energy (MWh)	CO_2 (t)
Palmerston	12.9	17.2	7.6	£4,688	8.8	8.0
Washington	17.3	23.0	10.2	£2,358	3.6	5.3
Malvern	16.9	22.5	10.0	£2,530	4.0	5.5
Benchmark	13.2	17.6	7.8	£4,488	8.4	7.7

Table 10.U shows that, due to feed-in tariffs, the PV systems have become a long-term financially viable option, being able to generate profits on invested capital of over 100% over its lifetime. The estimates of energy and carbon payback are in line with all the literature that was referred to previously. As PV displaces more carbon intensive electricity, life-time carbon savings are much greater than for solar thermal systems with a similar energy yield. However, the more carbon intensive manufacturing also means that in the short run (up to 10 years) the net carbon offset from PV systems will actually be negative as production rates increase to satisfy an increasing demand.

The UK Benchmark value can be scaled using Figure 10.20 to provide estimates for other systems throughout the UK. Throughout the country, variations of up to 25% can be expected.

10.11 Conclusion

During the literature review it was shown that PV systems experience a vastly growing popularity. They are perceived to be fairly simple and reliable systems with a long system life-time. This impression has been confirmed throughout this research. Furthermore, it was also found that, in general, architects and builders still tend to avoid the implementation of PV as they are not familiar with the systems and don't know what kind of performance can be expected. This issue has been addressed by providing an overview of the effect of varying installation parameters. A national benchmark value and look-up chart was derived to provide a simple method of estimating the output throughout the UK.

In detail, it was further shown that:

- PV Estimation tools such as PV GIS, PV WATTS and PV SYST can be very useful tools for architects and builders to determine the performance of a PV system at very early stages of a project, and without the need for extensive tests. PV GIS is the recommended choice.

- High operating temperatures of PV modules can have significant reduction on the system output and efficiency, and should be considered when integrating PV systems.

- Within the UK, the latitude of a location has a significant effect on PV generation (around 15% difference between Aberdeen and Plymouth), while longitude has no effect.

- Based on measurements from the EcoSmart Village, the average total PV generating hours would be around 3,000 hours per year out of a theoretical 4,480 hours. 'High power' generation (>40% of rated power) was only achieved rarely during summer months.

- Where it is not possible to install a south facing PV system, a performance reduction of 25-30% can be expected for directly west or east facing systems. Output of SE/SW facing systems is close to that of directly south-facing systems.

- Changes in inclination have a greater effect on east facing than on south facing systems.

- A method to estimate PV generation throughout the UK was derived using accurate models. This method is easier to use, more flexible and more accurate than SAP 2005. A Benchmark value for a 1kWp PV system in the UK was shown to be **675kWh** per annum. This value may vary by ± 25% depending on location, orientation and inclination of the PV system, and can be adjusted using the look-up chart in Figure 10.20.

- For 1kWp systems installed before April 2012 throughout the UK, the financial payback is expected to be 13.2 years ±25%. Net life-time financial savings are in the region of 200% of capital cost, and net carbon savings around 8 tonnes CO_2. However, carbon payback is fairly high, taking 8 years on average and up to 10 years for the 'worst-case' site and set-up.

11 Solar Thermal Systems

11.1 Introduction

Direct solar energy is considered the most abundant source of renewable energy on our planet. With selective materials having absorption efficiencies up to 95%[189], harnessing solar energy in the form of heat should be very effective. Since the 1980's solar thermal systems have become the most established type of micro renewable energy system in the UK, with approximately 100,000 systems installed nationwide[190] and annual installation rates of several thousand[191]. They are predicted to become even more popular in the future, with a forecast global growth of 15-17% by 2030[192], and 23% by 2050[193]. The following sections will assess several systems in practical as well as theoretical terms.

11.1.1 Background Theory

In its simplest form a solar thermal heater consists of pipes that are coated in a selective absorbing material. Transfer fluid is used to extract heat from the collector, typically consisting of a mixture of water and ethylene glycol (antifreeze), which is circulated through copper pipes that run along the absorber surface to ensure efficient heat conduction. Experimental research has previously suggested that other types of transfer fluid can be used, such as air[194] or supercritical CO_2[195]. While some performance improvements were noted, control and power issues mean these ideas are not currently applicable on a large scale.

Over the years these systems have evolved to become more efficient at heat absorption and to reduce losses. There are two common types of domestic Solar Thermal collectors used today, flat panel and evacuated tube.

Flat Panel Systems

Flat panel solar collectors are fairly simple systems consisting of an enclosed insulated volume that is covered by a flat sheet of glass. Copper pipes run through the enclosure, carrying transfer liquid to extract heat. A schematic diagram of the process is shown in Figure 11.1.

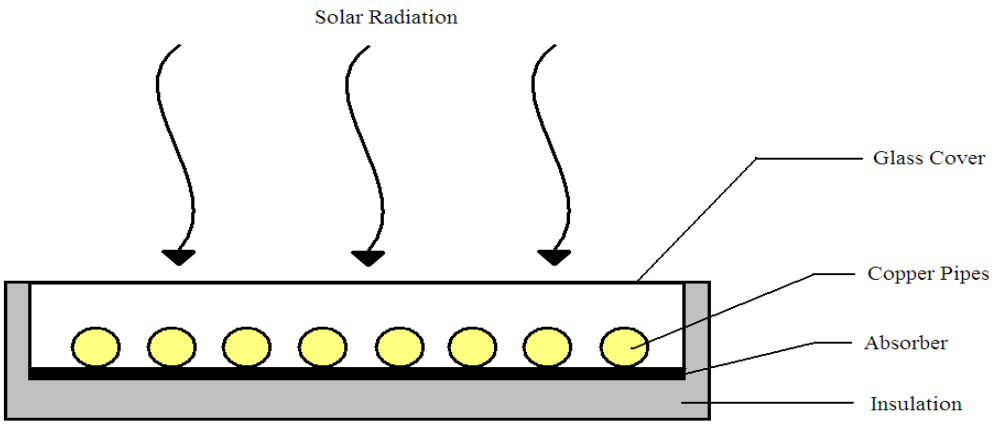

Figure 11.1: Simple schematic diagram of a typical flat panel solar thermal collector

Typical flat panel solar collectors can reach conversion efficiencies of around 75% under standard testing conditions.[196]

Evacuated Tube Systems

To further reduce heat losses and improve overall efficiency of the collector system, evacuated tube type solar collectors are designed to eliminate any losses from thermal convection. This type of collector consists of several glass tubes that contain a vacuum, or consist of double-glazed tubes that are separated by a vacuum. Each glass tube contains a copper tube that allows heat extraction using a transfer liquid. A simple schematic is shown in Figure 11.2.

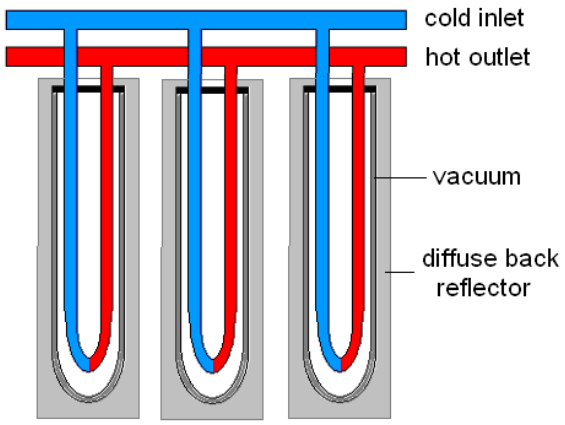

Figure 11.2: Simple schematic diagram of a typical evacuated tube solar thermal collector

While the copper tube can take different shapes and arrangements[197], it usually takes the form of a U-tube. The vacuum around each copper tube provides additional heat loss prevention, although not all losses can be avoided[198]. The vastly reduced heat loss makes the evacuated tube system particularly suitable for colder climates, such as in the UK. Zero-loss efficiencies of evacuated tube

systems, only accounting for optical losses, can reach values of up to around 80%[199]. This is slightly higher than for flat plate collectors due to the use of a diffuse reflector behind the evacuated tubes[200]. Evacuated tube systems also have the advantage of a more rapid start-up[201] and virtually no maintenance requirements.

After either flat panel or evacuated tube systems have been heated by the sun the hot transfer liquid is circulated to a storage cylinder, where a heat exchanger is used to transfer heat. After giving off heat to the colder storage cylinder, the cooled liquid is then circulated back to the solar collector.

Heat exchanger

To allow the solar panel to operate most effectively, the heat exchanger between the solar circuit and the storage cylinder must be as efficient as possible, ideally transferring all the heat and returning to the collector at lowest possible temperature. While experimental research[202] shows some alternatives such as mantle heat exchangers may provide improvements[203], the by far most common type used today comprises a horizontal coil inside the cylinder. This is often done using a counter-flow heat exchanger, which is more efficient than parallel flow, as shown schematically in Figure 11.3.

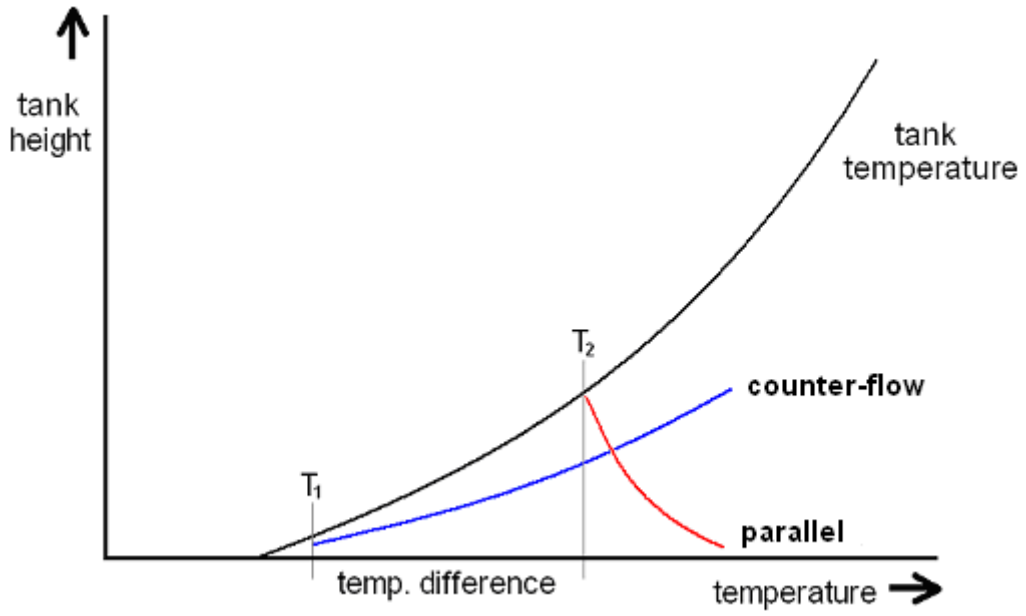

Figure 11.3: Variation of tank temperature and heat exchanger temperature for parallel and counter-flow

Figure 11.3 shows clearly that if the cylinder temperature varies with height, the heat exchanger will be able to give off more heat with the entrance (flow) in the top connection, and exit (return) in the bottom connection. Depending on the degree of stratification within the cylinder, this difference can be quite significant.

Control

A good control strategy is essential to ensure efficient heat transfer. Most Solar Thermal systems come with a control panel, which is equipped with several thermocouples to monitor system temperatures. If the panel sensor exceeds the bottom cylinder temperature by a certain control temperature difference (for example 7°C), the pump is switched on and heat is transferred from the collector to the storage cylinder. In general a low flow rate is desireable as this gives improved stratification within the storage cylinder[204], higher transfer temperatures through the heat exchanger which increases transfer efficiencies and slightly lower power consumption of the pump.

The control system is also used to prevent any overheating of the collector or the cylinder. Typically the control panel switches off the pump automatically when a certain safety temperature is reached at the bottom of the cylinder, or within the collector. When the safety temperature is detected, circulation is stopped and the transfer liquid left to expand. The fluid is forced into the expansion vessel attached to the solar circuit, where heat is dispersed until the temperature drops below a second threshold temperature, typically 70°C.

11.1.2 EcoVillage Set-up

Figure 11.4: Evacuated Tube System (left) and Flat Panel System (right)

Both types of Solar Thermal system, flat panel and evacuated tube, are tested at the EcoSmart village. Photos taken from both systems are shown in Figure 11.4, and the most important system parameters are summarised in Table 11.A. These values are taken from technical documents and building specifications.

Table 11.A: System parameters for flat panel and evacuated tube system

	Flat panel	**Evacuated tube**
Building	Windermere	Alderney
Orientation	south-facing	south-facing
Inclination	45°	45°
Panel area (m^2)	2.1	3
Water cylinder (L)	180	250
Warranty (yrs)	10	25

The flat panel system was supplied by SolarPanelSystems Ltd and was predicted to provide up to 70% of hot water to a typical household. For comparison, other research[205] suggests that a similar system is able to provide around 30% of hot water demand.

The evacuated tube system 'LaZer2' from the supplier Positive Planet Ltd. is predicted to provide 60-75% of hot water demand. While system efficiency is predicted to be around 50%, CO_2 emissions are expected to reduce by around 1000kg/year. The manufacturer-estimated financial payback rate is 31.5 years without RHI tariffs.

The schematic diagram of the flat panel system provided by the supplier is shown in Figure 11.5. In both cases an A-rated condensing gas boiler was used to provide auxiliary heat.

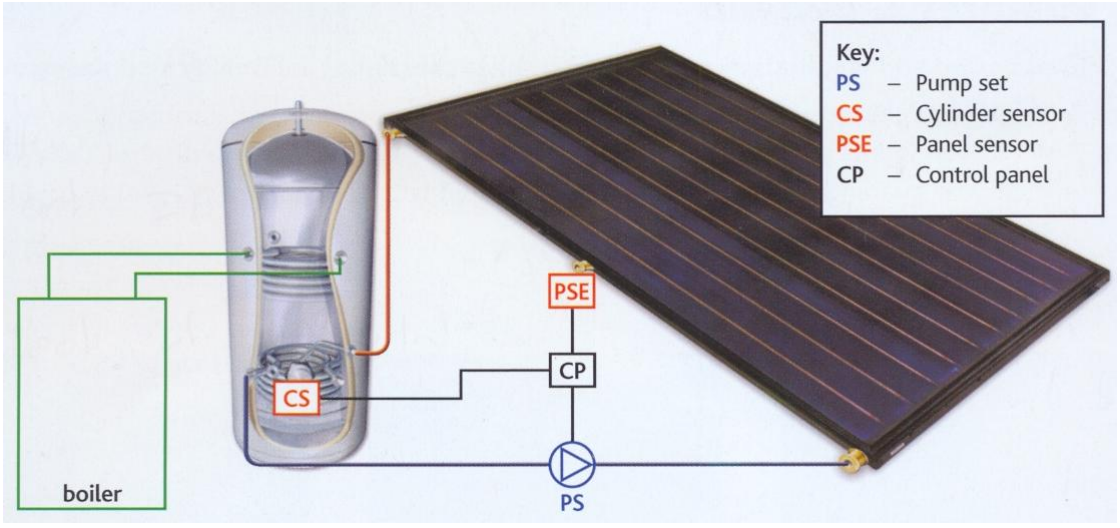

Figure 11.5: Solar thermal schematic diagram (source: SolarPanelSystems Ltd.)

11.1.3 Set-up Problems

During the 15-month investigation several problems were encountered. Both systems had problems with the heat meters that were installed by the manufacturers. They displayed error messages and were unable to produce any energy readings to evaluate system performance. Being able to monitor the performance of the system is not just important for this experimental set-up, but would also be important for home owners, allowing them to adapt to the system and use it more effectively.

Some time after the flat panel system was installed and connected to a water cylinder, it was found that the system that was installed included an incorrect panel. As a result of this, the complete system was replaced in February 2007.

The evacuated tube system was initially installed with water as a transfer liquid in the collector circuit. At the request of the research team, glycol (antifreeze) was eventually added to the system at a later stage in order to prepare for sub-zero temperatures. However, after this was done, the system was found to have air trapped in the collector circuit, which was rectified in October 2006.

After many efforts to rectify problems promptly it was possible to collect 12 months worth of meaningful data from the evacuated tube system, but only 4 months worth of limited data for the flat panel system.

11.1.4 Capital cost, Embodied Energy and Embodied CO_2

The Solar Trade Association[206] estimates general capital cost in the order of £4000, while other estimates are in the region of £3000-3500 for flat panel systems. The capital costs for the flat panel and evacuated tube systems at the EcoSmart village are shown in Table 11.B.

Table 11.B: Capital cost for EcoSmart village Solar Thermal systems

System	Capital Cost
Flat Panel (Windermere)	£2,600
Evacuated Tube (Alderney)	£3,500

The values for capital cost from the EcoSmart village are slightly below the general estimates, which is due to the fact that the cost of the heat store system is not included. Nonetheless, they will be used as baseline values as system capital costs can generally be expected to decrease with time.

Solar Thermal systems are made up of several materials that have a rather high energy and carbon content, such as aluminium, stainless steel and glass[122]. While no information about the embodied energy or carbon could be found for evacuated tube collectors, several sources were found that have previously evaluated the embodied energy and carbon for flat panel collectors.

Some of the reviewed literature suggests values for embodied energy in the region of 780kWh/m^2 (Canada[207]) to 890kWh/m^2 (Italy[208]), while the assessment[209] of a UK 2.1m^2 flat panel system estimated the embodied energy and carbon for different stages of the product life-cycle as shown in Table 11.C.

Table 11.C: Embodied Energy and CO_2 in solar thermal system life-cycle[209]

	Energy (kWh)	CO_2 (Kg)
Collector materials	844	240
Material transport to factory	63	5
External support (inc. pipe work)	553	143
System transport from Germany to UK	64	5
Installation	161	37
Total	1685	430

On average, the reviewed research agrees that the embodied energy for a 2.1m^2 flat panel solar thermal system is in the order of 1500-1870kWh, with a realistic UK estimate being around 1700kWh. The embodied carbon will be taken as 430kg.

Little data is available for embodied energy of evacuated tube collectors. The only energy estimate that was found[210] suggests embodied energy of 153kWh for an evacuated tube collector, but only considers the copper and glass content of individual tubes. Considering the materials that are involved the estimate for evacuated tube systems is not expected to change much from that of flat panel collectors. While considerably more glass is required, overall slightly less of the much more energy intensive metals are required for production. Energy resulting from transportation, installation and external support, making up around 50% of the embodied energy, can be expected to be very similar. Therefore the best available estimate for embodied energy is to assume a value equivalent to flat panel systems, of around 800kWh/m^2, with 205kg/m^2 embodied carbon.

11.2 Initial Energy Generation Estimate

There are two recognised methods that can be used in the design stages for estimating the contribution of solar thermal energy to hot water demand in dwellings:

1. The Utilisability method
2. The *f*-chart method

The utilisability method was developed by Whillier[211] and later redefined by Liu and Jordan[212]. While this method can be useful, many graphs are required for references, making it inadequate for analytical representation.

The f-chart method was developed by Klein et al[213], and is a more appropriate method for evaluating the performance of Solar Thermal systems. It is designed to calculate *f*, the solar fraction. This is defined as the fraction of the hot water load that is provided by the solar water heating system. The f-chart method which is summarised in this chapter is described in detail by Duffie & Beckman[131].

For liquid systems, the *f*-chart function is defined by equation (11.1):

$$f = 1.029Y - 0.065X - 0.245Y^2 + 0.0018X^2 + 0.0215Y^3 \qquad (11.1)$$

Detailed simulations of Solar Thermal systems have been used to develop the empirical correlations for the dimensionless variables (X) and (Y), which are required to calculate (*f*), the monthly fraction of loads carried by solar energy. The two dimension groups are:

$$X = \frac{A_C F_R' U_L (T_{ref} - \overline{T}_a)\Delta t}{L} \qquad (11.2)$$

$$Y = \frac{A_C F_R' (\overline{\tau\alpha}) \overline{H}_T N}{L} \qquad (11.3)$$

The relationships (11.2) and (11.3) can be re-written as:

$$X = F_R U_L \times \frac{F_R'}{F_R} \times (T_{ref} - \overline{T}_a) \times \Delta t \times \frac{A_C}{L} \qquad (11.4)$$

$$Y = F_R (\tau\alpha)_n \times \frac{F_R'}{F_R} \times \frac{(\overline{\tau\alpha})}{(\tau\alpha)_n} \times \overline{H}_T N \times \frac{A_C}{L} \qquad (11.5)$$

For the terms $F_R(\tau\alpha)_n$ and $F_R U_L$, generic values have been found for both the flat panel and the evacuated tube systems, as the manufacturer did not provide values at the time and has subsequently gone into receivership. These generic values are based on the RETScreen International 'Solar Water Heating Project Analysis (SWH3.2)' [214] and are shown in Table 11.D.

Table 11.D: Generic $F_R(\tau\alpha)_n$ and $F_R U_L$ values for solar thermal collectors

	$F_R(\tau\alpha)_n$	$F_R U_L$
Flat panel collector	0.68	4.9
Evacuated tube collector	0.58	0.7

Several other parameters needed for the *f*-chart method calculations can be deduced from the weather data, physical properties of the collector and energy requirements from the buildings. These values have been summarised on a monthly basis in Table 11.E.

The monthly hot water energy requirement (L) is based on the assumption that 200L will be drawn off every day, which will be about 40°C above the cold feed temperature. This results in a daily hot water energy requirement of 33.4MJ, or 3,390kWh per year. This is not far from the average measured hot water consumption from 60 single family homes in Denmark and Austria, which found an average annual consumption of around 3,600kWh[215].

Table 11.E: Monthly parameters required for *f*-chart calculations

	N	Δt (seconds)	$\overline{T}_a$ (°C)	$\overline{H}_T$ (MJ/m²)	L (MJ)	$T_{ref} - \overline{T}_a$ (°C)	$\overline{H}_T N$ (MJ/m²)
January	31	2.68E+06	7.4	1.5	1037	92.6	109.1
February	28	2.42E+06	6.0	3.3	936	94.0	196.8
March	31	2.68E+06	7.3	6.8	1037	92.7	355.7
April	30	2.59E+06	11.0	10.5	1003	89.0	516.6
May	31	2.68E+06	11.7	10.5	1037	88.3	363.0
June	30	2.59E+06	14.6	10.3	1003	85.4	465.6
July	31	2.68E+06	14.7	7.8	1037	85.3	332.6
August	31	2.68E+06	15.1	8.3	1037	84.9	359.6
September	30	2.59E+06	13.5	6.9	1003	86.5	299.7
October	31	2.68E+06	11.5	4.3	1037	88.5	204.3
November	30	2.59E+06	9.2	4.2	1003	90.8	125.8
December	31	2.68E+06	6.7	0.9	1037	93.3	73.5

However, determining the remaining two parameters, $\frac{F'_R}{F_R}$ and $\frac{(\overline{\tau\alpha})}{(\tau\alpha)_n}$, will require further calculations.

$$\frac{F'_R}{F_R} = \left[1+\left(\frac{A_C F_R U_L}{(\dot{m}C_P)_C}\right)\left(\frac{(\dot{m}C_P)_C}{\eta_H(\dot{m}C_P)_{\min}}-1\right)\right]^{-1} \qquad (11.6)$$

The mass flow rate for the flat panel system is given as 105litres/hr on a technical datasheet provided by the manufacturer. Assuming a water / glycol mixture in the collector side of the circuit with a density[216] of 1.1132 kg/l, this equates to a mass flow rate of 0.0325kg/s. The flow rate of the evacuated tube system is estimated to be 0.037kg/s, based on other comparable systems.

The values for specific heat capacity (C_P) can be assumed to be:

C_P = 4186 $JKg^{-1}°K^{-1}$ for water

C_P = 3350 $JKg^{-1}°K^{-1}$ for a 50%[217] glycol-water mixture[216]

Glycol is found to have the smaller capacitance, and the efficiency of the heat exchanger can generally be expected to take a generic value[131] of η_H = 0.7 .

The other parameter required for using the *f*-chart method is the term $\frac{(\overline{\tau\alpha})}{(\tau\alpha)_n}$, which gives a ratio of the average monthly transmittance-absorption losses compared to the transmittance-absorption losses under optimum conditions.

The optimum transmittance-absorption product can be found based on manufacturer specifications as 0.87 for the flat panel system and 0.93 for the evacuated tube system. The average monthly losses can be determined using equations (11.7) and (11.8), where $\overline{S}$ is the average absorbed solar radiation.

$$(\overline{\tau\alpha}) = \frac{\overline{S}}{\overline{H}_T} \qquad (11.7)$$

$$\overline{S} = \overline{H}_b \overline{R}_b (\overline{\tau\alpha})_b + \overline{H}_d (\overline{\tau\alpha})_d \left(\frac{1+\cos\beta}{2}\right) + \overline{H}\rho_g (\overline{\tau\alpha})_g \left(\frac{1-\cos\beta}{2}\right) \qquad (11.8)$$

The effects of ground reflection have been included in equation (11.8) for completeness, but will be neglected during the calculation due to their insignificant effect on the outcome. The following calculations will also make reference to two graphs, which are shown in Figure 11.6 and Figure 11.7 below.

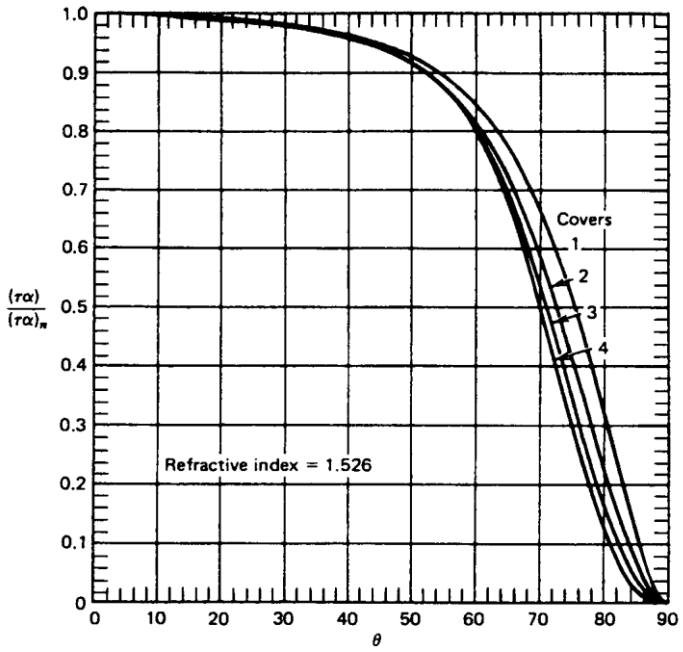

Figure 11.6: Reference graph for transmittance-absorption ratio calculations (source: Duffie and Beckman[131], 2006)

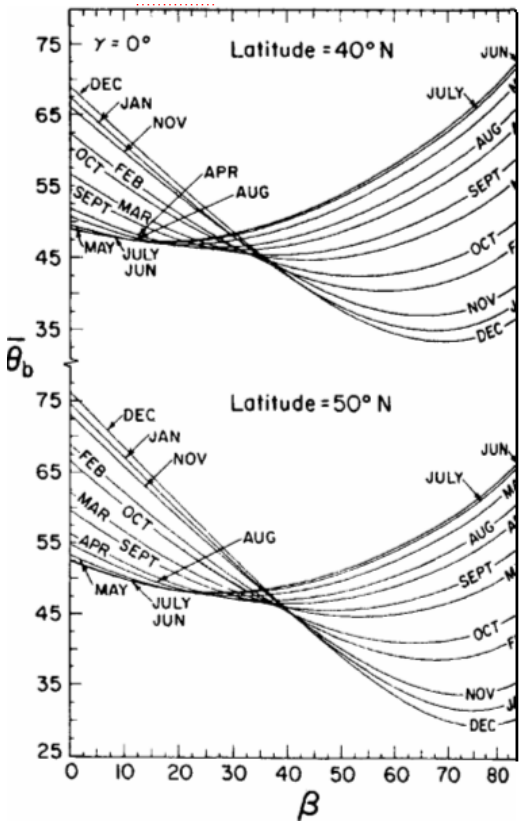

Figure 11.7: Reference graph for average angle of incidence ($\bar{\theta}_b$) calculations (source: Duffie and Beckman[131], 2006)

Using simple trigonometry, the effective angle for diffuse irradiation is 31.2° for the collector inclined at 45°. From Figure 11.6, the value for $\frac{(\overline{\tau\alpha})}{(\tau\alpha)_n}$ that corresponds to an inclination of 31° is 0.98.

The value for the diffuse transmittance-absorption losses is constant, whereas the value for the beam component varies throughout the year. A more accurate estimate can be calculated if specific values for each month are determined. Using Figure 11.7 it is possible to find monthly values of average beam inclination ($\overline{\theta}_b$) of the collector surface for given values of inclination, assuming a south facing orientation of the system. Using these values for average beam angles, Figure 11.6 can then be used to find the corresponding factor $\frac{(\overline{\tau\alpha})}{(\tau\alpha)_n}$, which allows the calculation of $(\overline{\tau\alpha})_d$ for each month. The results are shown in Table 11.F.

Table 11.F: Results from beam transmittance-absorption losses calculations

	$\overline{\theta}_b$	$\frac{(\overline{\tau\alpha})}{(\tau\alpha)_n}$	$(\overline{\tau\alpha})_b$
January	42°	0.95	0.822
February	42°	0.95	0.822
March	45°	0.94	0.813
April	47°	0.93	0.804
May	48°	0.92	0.796
June	49°	0.92	0.796
July	49°	0.92	0.796
August	46°	0.93	0.804
September	45°	0.94	0.813
October	44°	0.94	0.813
November	42°	0.95	0.822
December	42°	0.95	0.822

In order to complete the calculation for the effects of beam irradiation, the ratio between radiation on a horizontal plane and in-plane radiation for the collector surface ($\overline{R}_b$) must also be found. This can be done by using equation (11.9).

$$\overline{R}_b = \frac{\cos(\phi-\beta)\cos\delta\sin\varpi_s' + (\pi/180)\varpi_s'\sin(\phi-\beta)\sin\delta}{\cos\phi\cos\delta\sin\varpi_s' + (\pi/180)\varpi_s'\sin\phi\sin\delta} \qquad (11.9)$$

Where (ϕ) is the latitude, (β) the system inclination (δ) the solar declination angle. The term (ϖ_s') refers to the sunset hour angle for the tilted surface for the mean day of the month, which is given by equation (11.10):

$$\varpi_s' = \min\begin{bmatrix}\cos^{-1}(-\tan\phi\tan\delta)\\ \cos^{-1}(-\tan(\phi-\beta)\tan\delta)\end{bmatrix} \qquad (11.10)$$

Having found all variables, it is now possible to use the weather data in order to complete the calculations for ($\overline{S}$) and ($\overline{\tau\alpha}$) , shown in Table 11.G, hence allowing the determination of factors (X) and (Y). The results for each month are shown in Table 11.H for the flat panel, and Table 11.I for the evacuated tube system.

For Flat Panel System:

Table 11.G: Parameters required for *f*-chart calculation, based on flat panel system

	$\overline{H}_b$ (kJ/m²)	$\overline{R}_b$	$(\overline{\tau\alpha})_b$	$\overline{H}_d$ (kJ/m²)	$(\overline{\tau\alpha})_d$	$\overline{H}_T$ (kJ/m²)	$\overline{S}$ (kJ/m²)	$(\overline{\tau\alpha})$
Jan	2151	4.6	0.822	1370	0.848	3521	3349	0.78
Feb	4431	2.9	0.822	2597	0.848	7028	5863	0.79
Mar	6981	1.8	0.813	4493	0.848	11474	9271	0.78
Apr	10459	1.3	0.804	6759	0.848	17218	12112	0.77
May	5617	1.0	0.796	6077	0.848	11693	8320	0.76
Jun	5686	0.9	0.796	9716	0.848	15402	11338	0.75
Jul	3067	1.0	0.796	7585	0.848	10652	7947	0.74
Aug	3914	1.2	0.804	7680	0.848	11593	8691	0.75
Sep	3495	1.5	0.813	6493	0.848	9988	7838	0.76
Oct	2309	2.4	0.813	4281	0.848	6590	5517	0.76
Nov	2249	4.0	0.822	1943	0.848	4193	3852	0.78
Dec	1296	5.6	0.822	1075	0.848	2371	2240	0.78

Table 11.H: X and Y value calculations required for *f*-chart calculation, based on flat panel system

	$F_R U_L$	$F_R(\tau\alpha)_n$	$\frac{F'_R}{F_R}$	$\frac{(\overline{\tau\alpha})}{(\tau\alpha)_n}$	$T_{ref} - \overline{T}_a$	$\overline{H}_T N$	$\frac{A_C}{L}$	X	Y
Jan	4.9	0.68	0.961	0.91	92.6	109.2	2.01E-09	2.35	0.13
Feb	4.9	0.68	0.961	0.91	94.0	196.8	2.01E-09	2.15	0.24
Mar	4.9	0.68	0.961	0.90	92.7	355.7	2.01E-09	2.35	0.42
Apr	4.9	0.68	0.961	0.89	89.0	365.3	2.01E-09	2.18	0.60
May	4.9	0.68	0.961	0.88	88.3	292.4	2.01E-09	2.24	0.42
Jun	4.9	0.68	0.961	0.87	85.4	410.9	2.01E-09	2.09	0.53
Jul	4.9	0.68	0.961	0.86	85.3	298.7	2.01E-09	2.16	0.38
Aug	4.9	0.68	0.961	0.87	84.9	318.8	2.01E-09	2.15	0.41
Sep	4.9	0.68	0.961	0.87	86.5	258.1	2.01E-09	2.12	0.34
Oct	4.9	0.68	0.961	0.87	88.5	166.3	2.01E-09	2.24	0.23
Nov	4.9	0.68	0.961	0.90	90.8	125.8	2.01E-09	2.23	0.15
Dec	4.9	0.68	0.961	0.90	83.3	73.5	2.01E-09	2.37	0.09

Table 11.I: X and Y value calculations required for *f*-chart calculation, based on evacuated tube system

	$F_R U_L$	$F_R(\tau\alpha)_n$	$\frac{F'_R}{F_R}$	$\frac{(\overline{\tau\alpha})}{(\tau\alpha)_n}$	$T_{ref} - \overline{T}_a$	$\overline{H}_T N$	$\frac{A_C}{L}$	X	Y
Jan	0.7	0.58	0.961	0.91	92.6	109.2	2.87E-09	0.45	0.15
Feb	0.7	0.58	0.961	0.91	94.0	196.8	2.87E-09	0.42	0.27
Mar	0.7	0.58	0.961	0.90	92.7	355.7	2.87E-09	0.45	0.49
Apr	0.7	0.58	0.961	0.89	89.0	365.3	2.87E-09	0.42	0.70
May	0.7	0.58	0.961	0.88	88.3	292.4	2.87E-09	0.43	0.48
Jun	0.7	0.58	0.961	0.87	85.4	410.9	2.87E-09	0.41	0.61
Jul	0.7	0.58	0.961	0.86	85.3	298.7	2.87E-09	0.42	0.43
Aug	0.7	0.58	0.961	0.87	84.9	318.8	2.87E-09	0.42	0.47
Sep	0.7	0.58	0.961	0.87	86.5	258.1	2.87E-09	0.41	0.40
Oct	0.7	0.58	0.961	0.87	88.5	166.3	2.87E-09	0.43	0.27
Nov	0.7	0.58	0.961	0.90	90.8	125.8	2.87E-09	0.43	0.17
Dec	0.7	0.58	0.961	0.90	83.3	73.5	2.87E-09	0.46	0.10

Using the values for (X) and (Y) from Table 11.H and Table 11.I for the flat panel and evacuated tube systems respectively, the f-fraction and hence the contribution to hot water requirements can be found using equation (11.1). Table 11.J gives monthly and annual values of *f*-chart fraction, hot water requirement (L), potential energy generation of the system (Q_f) as well as system efficiency (η), which is calculated using equation (11.11):

$$\eta = \frac{Q_H}{H_T N} \qquad (11.11)$$

where ($H_T N$) is the total monthly in-plane irradiance.

Table 11.J: *f*-chart fraction, potential energy generation and efficiency of solar thermal systems at EcoSmart show village

	Windermere (Flat Panel)				**Alderney (Evacuated Tube)**			
	f	L (kWh)	Q_f (kWh)	η	f	L (kWh)	Q_f (kWh)	η
Jan	0.00	290	0.0	0.0%	0.12	290	34.7	38.2%
Feb	0.10	290	28.2	24.5%	0.23	290	68.0	41.5%
Mar	0.25	290	71.9	34.7%	0.41	290	120.3	40.6%
Apr	0.40	290	117.0	38.8%	0.58	290	168.3	39.1%
May	0.25	290	73.6	34.7%	0.41	290	120.1	39.7%
Jun	0.35	290	102.4	37.7%	0.52	290	150.1	38.7%
Jul	0.22	290	64.1	33.0%	0.38	290	108.9	39.3%
Aug	0.25	290	72.9	34.7%	0.41	290	118.3	39.5%
Sep	0.19	290	56.5	32.3%	0.34	290	99.9	40.0%
Oct	0.09	290	26.2	22.0%	0.23	290	67.6	39.7%
Nov	0.01	290	3.5	4.7%	0.14	290	41.0	39.1%
Dec	0.00	290	0.0	0.0%	0.07	290	20.7	33.7%
Annual	**0.18**	3480	**616.2**	**31.0%**	**0.32**	3480	**1118.0**	**39.7%**

Table 11.J shows system efficiencies that are considerably lower than the efficiencies stated by the manufacturer. The flat panel system shows an efficiency value of 31% compared to the claimed 44% throughout the year, while the annual efficiency of the evacuated tube system is around 40% compared to the claimed 50%. All values assume that there is an infinitely large storage capacity for the hot

water that is being generated. However, the *f*-chart calculations also account for the use of a heat exchanger, which results in overall higher system temperatures, meaning that energy absorption itself becomes less efficient. This is accounted for by the factor $\frac{F_R'}{F_R}$. If this factor would be neglected, the system efficiency would improve by around 4-5%, bringing the value closer to the manufacturer-stated efficiency value. Based on this observation it is expected that the efficiencies claimed by the manufacturer were derived from testing without solar cylinders, which is a widely accepted industry standard[218].

Based on the *f*-chart calculations, Figure 11.8 shows a comparison between the expected maximum hot water generation from the systems and the demand for hot water energy. For both cases the expected hot water demand throughout the year is around 12.5GJ, which equates to about 290kWh per month.

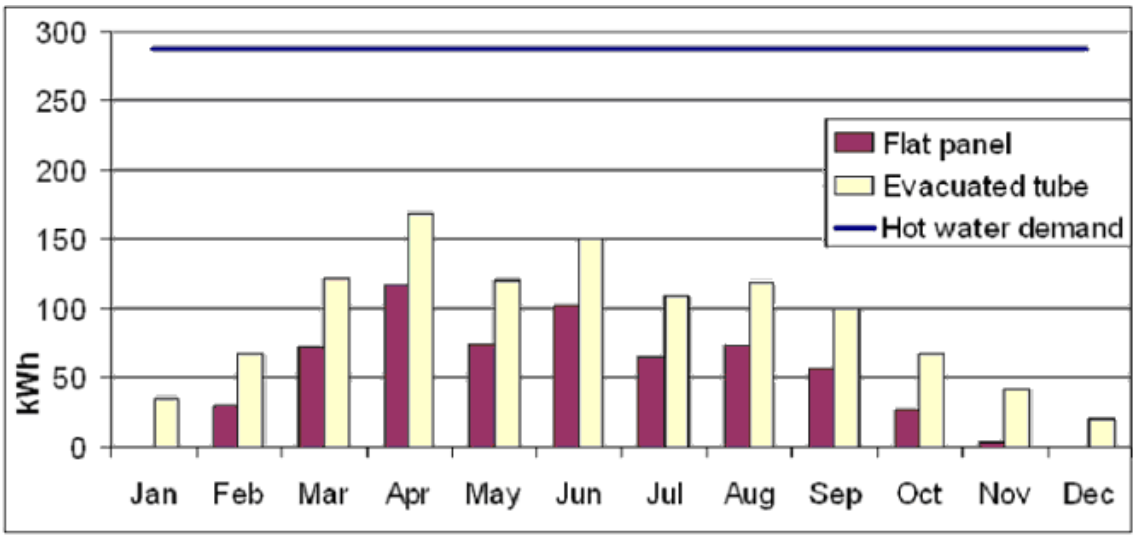

Figure 11.8: *f*-chart based output in relation to hot water demand

Figure 11.8 shows that both systems are unable to satisfy the monthly hot water demand, even during the summer months. The flat panel system in particular is expected to have practically zero energy output during winter months. The discrepancy between demand and generated output may be reduced by increasing the size of the system, but it will be virtually impossible to satisfy 100% of the hot water demand, as this would require consistent solar radiation throughout each month and an extremely large and well-insulated storage cylinder.

Figure 11.9 shows the average monthly efficiencies for both systems based on *f*-chart calculations, confirming that the evacuated tube system has much better performance during the colder winter months compared to the flat panel system.

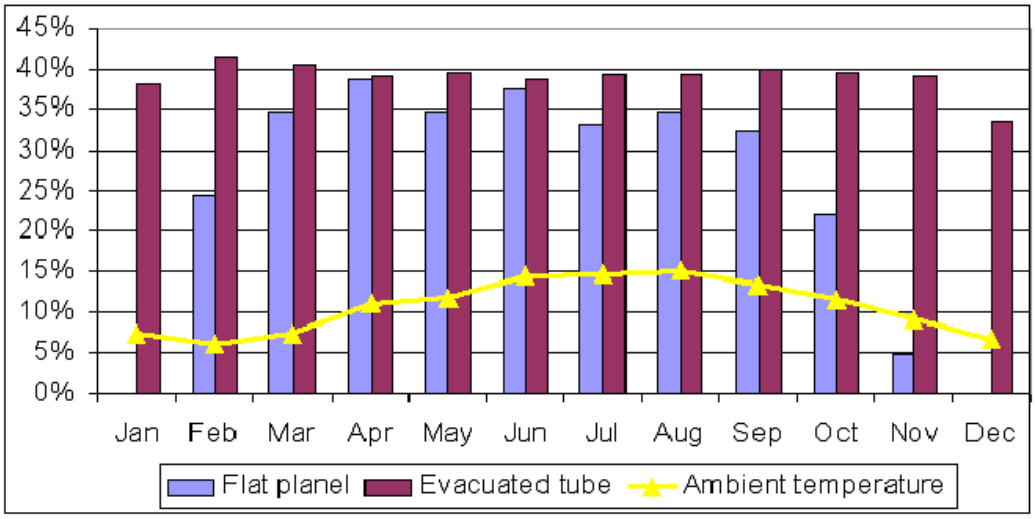

Figure 11.9: Comparison of system efficiency between flat panel and evacuated tube system

11.3 Measured Output from EcoSmart Systems

Both solar thermal systems at the EcoSmart village experienced problems with the heat meters as described previously. The energy that was measured by the evacuated tube control panel in the period from 28th October 2006 until 29th October 2007 is shown in Table 11.K. The resulting overall system efficiency was calculated using equation (11.11).

Table 11.K: Measured energy generation from evacuated tube system

Month	Energy output (kWh)	Efficiency
Nov-06	26	24.8%
Dec-06	15	24.5%
Jan-07	18	19.8%
Feb-07	44	26.8%
Mar-07	60	20.2%
Apr-07	97	22.5%
May-07	63	20.8%
Jun-07	72	18.6%
Jul-07	56	20.2%
Aug-07	63	21.0%
Sep-07	41	16.4%
Oct-07	33	19.4%
Annual	**588**	**21.3%**

IButton sensors were used to record temperature data from the flat panel system as the heat meter problems could not be resolved. In combination with the flow rate of the system, this allowed a calculation of the estimated energy that is being transferred to the water cylinder using equation (11.12). This data is available for the period between June and October 2007, and results are shown in Table 11.L.

$$Q_t = mC_p(T_e - T_{in}) \qquad (11.12)$$

Table 11.L: Comparison of *f*-chart estimate and measured generation from heat meter and IButtons

	Windermere (Flat Panel) (kWh)		**Alderney (Evacuated Tube)** (kWh)		
	f-chart	IButton	f-chart	IButton	Meter
Jun-07	102.4	**53.5**	150.1	**87.3**	72
Jul-07	64.1	**54.8**	108.9	**61.7**	56
Aug-07	72.9	**58.7**	118.3	**60.1**	63
Sep-07	56.5	**53.7**	99.9	**46.8**	41
Total	295.9	**220.7**	477.2	**255.9**	232

Table 11.L shows that the energy values which were calculated based on IButton temperature readings for the evacuated tube system are close to the measured values from the heat meter. The difference to the predicted f-chart estimates can be expected due to losses incurred by the interaction between solar panel, hot water storage and auxiliary heat control that is not accounted for by the f-chart method. The measured annual output of the evacuated tube system was 588 kWh. This suggests that the use of temperature data and equation (11.12) will give a reasonable estimate for the performance of the flat panel system.

The f-chart results can be used to scale the output up for the entire year. To do this, the percentage difference between f-chart and IButton results is found during the summer months, and then compared to the annual difference. This was found to be very similar at around 47%. The same method can now be applied to the flat panel system. The difference between f-chart estimate and the summer IButton values is 25%, suggesting that the annual output is also around 25% below the f-chart estimate. Based on this method, the annual yield of both systems is shown in Table 11.M.

Table 11.M: Annual yield of EcoSmart Village solar thermal systems

System	**Annual yield (kWh)**
Flat Panel (Windermere)	462*
Evacuated Tube (Alderney)	588

*based on 4 months of measured data

The results show that the flat panel system has performed much better than the evacuated tube system relative to its expected performance. However, it must be stressed that the results for the flat panel system can be expected to contain a high margin of error.

It is suspected that the main reason for this difference in performance can be related to the system control. In both cases additional heat energy was provided by a condensing gas boiler. Table 11.N provides an overview of the gas consumption for both dwellings, giving values independently recorded manually by the staff at the EcoSmart village and by the data logger.

Table 11.N: Gas consumption for Alderney and Windermere homes

	Alderney Evacuated Tube (kWh)		Windermere Flat Panel(kWh)	
	Logger	Manual	Logger	Manual
Nov-06	192	190	120	115
Dec-06	213	216	142	141
Jan-07	222	220	139	137
Feb-07	201	198	122	122
Mar-07	215	213	106	114
Apr-07	160	160	42	39
May-07	133	120	59	58
Jun-07	72	72	29	28
Jul-07	95	96	31	33
Aug-07	67	68	23	23
Sep-07	107	109	43	38
Oct-07	130	132	61	64
Annual	**1807**	**1794**	**917**	**912**

Table 11.N shows that the gas consumption of Alderney (evacuated tube) was approximately twice as high as the gas consumption of Windermere (flat panel). This seems to indicate that the boiler was running much more often in Alderney, which seems odd considering that the house contains a larger and more efficient solar thermal system. A possible reason for this is the temperature control of the water cylinder.

After examining the return temperatures and gas consumption in more detail this confirmed that the heating control system of Alderney was set to maintain the water temperature at the bottom of the water cylinder at a minimum of 30°C, using the boiler if required. This leads to a much higher base temperature which needs to be overcome by the solar thermal system, meaning that the temperature in the collector circuit would have to reach a minimum of 37°C before any heat exchange can take place. The higher base temperature also results in

lower transmission efficiencies through the heat exchanger. For the flat panel system this was not the case, base temperatures were generally much lower. As an indication, the average return temperatures for flat panel and evacuated tube systems over the same period were 23.1°C and 33.3°C respectively.

When analysing the gas consumption patterns from both houses, it also confirmed that both boilers were set to come on for 30 minutes in the morning and evening of each day, regardless of the temperature of the water cylinder. This means that it is unlikely that either system was able to generate energy before noon, when the hot water was usually drawn off.

Energy consumption

While the solar thermal systems are assumed to generate energy that is entirely carbon free, it must be considered that these active solar thermal systems rely on an electric pump to move the heat transmission fluid through the heat exchanger. The evacuated tube system was equipped with a 60W pump and the flat panel system used a 30W pump. The power demand was confirmed by independent electricity measurements. Table 8.B shows a summary of running time as well as overall electricity consumption of both solar thermal pumps.

Table 11.1.4.O: Energy consumption of solar thermal pumps

	Flat panel (Windermere)	**Evacuated tube** (Alderney)
Pump rating	30 W	60 W
Annual runtime	835 hrs	592 hrs
Runtime per kWh heat	1.81 hrs	1.01 hrs
Electricity consumption per kWh heat	54.3 Wh	60.6 Wh
Total annual electricity consumption	25.1 kWh	35.5 kWh

With 54-60Wh electricity required for every kWh heat, effectively giving a coefficient of performance of 17-19, it can be said that the energy required for the pump is relatively small, and based on this can be neglected for all further calculations.

11.4 Domestic Control Systems

As the heat meters of the solar thermal systems were not working properly, the data that was gathered for the two systems is not particularly robust. In order to verify this data, and to gain more experience from analysing other systems, two domestic control systems were found and monitored over extended periods of time. These will be referred to as 'Test System 1' and 'Test System 2'. In addition to this a third system, referred to as 'Control System', was set up in a controlled environment in an attempt to find out how exactly the solar thermal systems can be improved.

This section provides detailed information about these additional systems and the strategy which was used to analyse them. Initial conclusions will be drawn from the Solar Thermal set-up in a controlled environment.

11.4.1 Methodology

The two domestic control systems that were monitored are located in Manchester. These systems are installed in detached dwellings, each with a test family occupying the house and using hot water as they normally would throughout the test period. Both families have kindly volunteered to allow data to be collected at their homes. While this provides by no means a controlled laboratory set-up, it does provide a valuable insight into what happens during normal every-day use of the systems. This means that while data availability and accuracy is limited, the systems can be tested under real-life conditions. The most robust and comprehensive data was obtained from Test System 1, which will be used to validate the solar thermal model later on.

Another system was set up under controlled conditions at the University of Manchester. Based on this, conclusions about the practicalities of solar thermal installations will be drawn.

11.4.2 Test System 1

The home of test family 1 is located in south Manchester, near Manchester Airport. It is occupied by a family of 2, who can be described as energy conscious. They are generally careful not to waste hot water, and use most of their water in the morning, usually before any direct solar radiation reaches the west-facing solar collector. They are aware of the interaction between solar heat and supplementary

heat from the boiler, and try to keep central heating turned off for as long as is comfortable during the spring, summer and autumn seasons.

The solar thermal system, an evacuated tube model, has been in operation for about 2 years prior to monitoring, and required considerable effort to get working properly. Despite being supplied by an established company, Vaillant, the installers were reportedly inexperienced. Initially, a wrong solar cylinder was fitted which later had to be replaced. Also, temperature sensors were not fitted correctly, meaning that the energy output could not be determined using the appropriate function on the control panel. The control panel was later replaced by the supplier, and additional temperature sensors were installed to allow an energy display by the control panel. Some of the design parameters of the Vaillant vtk570 system are given in Table 11.P.

Table 11.P: Design parameters of Test System 1

Latitude	53.3°
Longitude	-2.3°
Collector type	Evacuated tube
Collector inclination	30°
Collector orientation	250° (W/SW)
Aperture area	3.0m^2
Zero-loss efficiency	64.2%

Due to the nature of this set-up, it was not possible to measure several important parameters independently and accurately, including:

- Direct solar energy generation
- Hot water consumption
- On-site weather data
- Exact flow rate of the solar system

Instead, the following measurements were taken:

- Temperatures at several points on the system pipe-work and cylinder at 10-minute intervals, available for 12 months with interruptions
- Cumulative energy reading from control panel
- Average hot water draw-off for a typical bath, etc
- Weather data from a weather station in close proximity (approximately 3 miles) to the test site
- Flow rate from a flow-meter included in the pipe-work, with estimated error of ±0.25L/min

Figure 11.10 shows a schematic diagram of the solar cylinder, including positions of temperature sensors. To measure and record the temperature conveniently,

IButtons were used. These were set to record at 10-minute intervals to provide a balance between data density and not disturbing the test family too much.

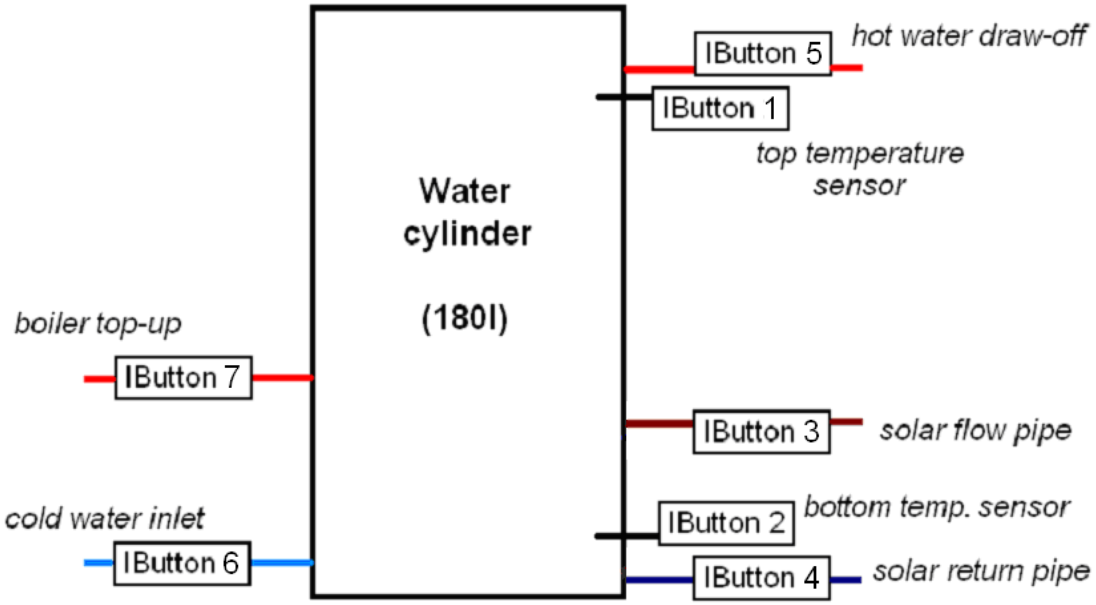

Figure 11.10: IButtons on domestic solar thermal system (test family 1)

As shown in Figure 11.10, IButtons were installed on every inlet and outlet point of the cylinder, as well as at the top and bottom of the cylinder, where cut-outs in the insulation had previously been made to attach sensors for the control panel. However, it proved later on that the 10-minute recording interval was too long for some of the readings. For example, the draw-off and cold water inlet sensors would not pick up a draw-off event that lasted, say, 5 minutes. The copper pipe with its very high thermal conductivity quickly resumed ambient (or cylinder) temperatures after the draw-off had been completed. Similarly, the solar flow and return sensors can only be considered accurate when energy transfer from the collector was uninterrupted and lasted longer than 10 minutes. The most useful and accurate temperature readings were found to be those giving top and bottom cylinder temperatures.

The boiler top-up temperature was measured to identify when heat was added by the boiler. Measuring the boiler return temperature was obsolete as the flow rate of this circuit was unknown.

Test System 1 Validation

The data from test system 1 will be used to validate the Solar Thermal model. However, before this can be done, the accuracy of this data must first be verified.

While there is little that can be done to validate the accuracy of the control panel figures, the use of the IButton sensors can be validated to some extent.

During a sunny day, the IButtons were set to record at 1-minute intervals. Measured amounts of hot water were drawn off, and temperature readings from the control panel were noted to compare with the IButton data. The control panel uses calibrated thermocouple sensors that are placed inside specially designed pockets that protrude into the cylinder, as well as similar sensors that are firmly attached to the pipe work of the solar circuit.

The IButton values at 1-minute intervals are shown in Figure 11.11, while Table 11.Q provides a comparison with the respective control values recorded from the control panel.

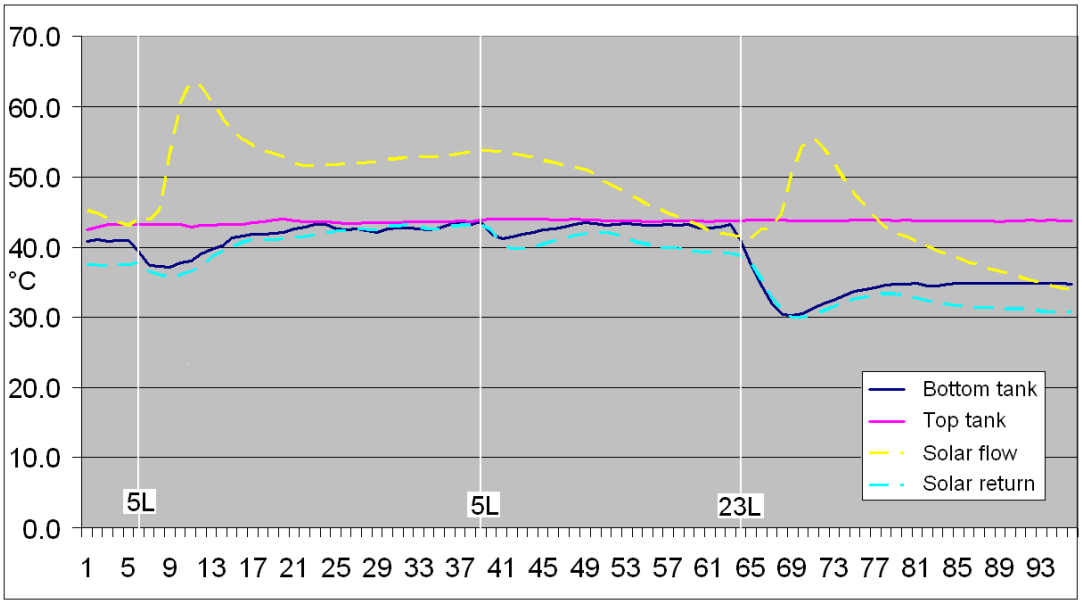

Figure 11.11: Temperature variations of 1-minute IButton sampling test, showing draw-off events

Table 11.Q: Control temperatures and respective IButton values, with reference to Figure 11.11

	Bottom cylinder		Top cylinder		Solar flow		Solar return		Special
Min.	IButton	control	IButton	control	IButton	control	IButton	control	Occurrence
6	38	41	43	45	60	61	36		5L draw-off
20	43	45	44	46	52	52	42	40	
39									5L draw-off
42	43	46	44	46	51	48	42		cloud (3 min.)
64	30	31	44	46	45	46	31	32	23L draw-off
70									cloud

From Figure 11.11 it can clearly be seen when hot water is drawn off, as the bottom cylinder temperature drops, which causes the pump of the solar circuit to come on. The relatively high rate of heat transfer means that the bottom temperature quickly resumes a temperature equivalent to the top of the cylinder,

before the solar pump is switched off again after a cloud begins to shield the direct beam radiation. After a further draw-off the temperature difference between the bottom of the cylinder and the collector becomes great enough to bring the pump on again, which transfers heat until another cloud comes in at 17:40 (after 70 minutes) and the sun is about to set.

Table 11.Q shows that the most of the IButton readings are very close to the control temperatures, although they generally appear to be slightly lower, which can be expected considering they are attached to the outside of the pipe using blu tack. The IButton values were adjusted to account for this error, based on methods outlined in section "6.3.2 - IButton sensors".

The comparison of IButton values to the thermocouples and their response to controlled events confirm that the data gathered from test system 1 is sufficiently accurate to validate the solar thermal model.

11.4.3 Test System 2

System 2 is located in a detached home in Wilmslow, south Manchester. Test family 2, a family of 2 persons, are often away from their home during the week. With this in mind they opted for a small system, with an aperture area of 2.3 m^2 and a storage cylinder of only 100L. When they are at home they use most of their hot water early in the morning, usually between 6:00-7:00, for 2 showers. It is reported that the storage capacity of the cylinder is barely sufficient to provide enough water for the showers. As a result of this, the boiler is set to supplement heat to the storage cylinder between 5:00 and 7:30 whenever the temperature half-way up the cylinder drops below 50°C. This means that the boiler typically has at least 30 minutes to heat the cylinder up to 50°C, only leaving an estimated volume of about 35L to be heated by the solar thermal system throughout the day. In the evening the boiler is set to come on again between 18:00 and 23:00. Figure 11.12 shows a schematic diagram of the hot water cylinder with attached IButton sensors.

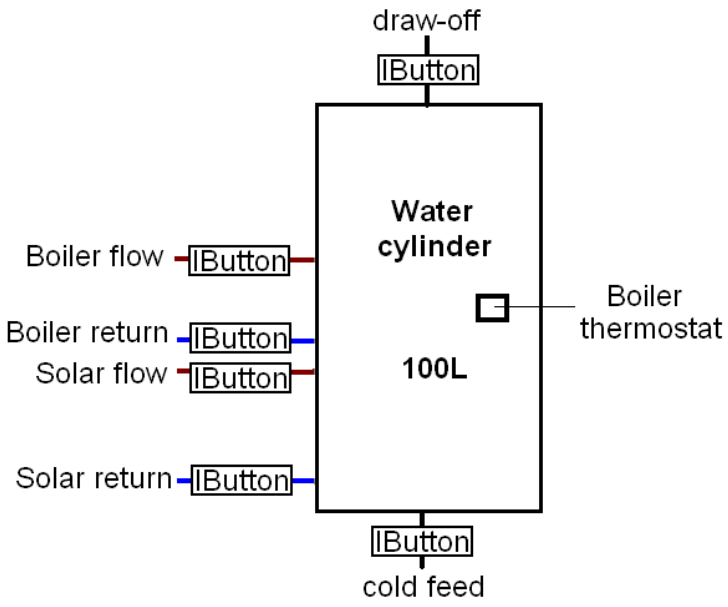

Figure 11.12: Test system 2 hot water cylinder and sensor arrangement

Details for the solar thermal system are given in Table 11.R. No complications during system installation were noticed by the test family.

Table 11.R: Design parameters of Test System 2

Latitude	53.3°
Longitude	-2.3°
Collector type	Evacuated tube
Collector inclination	45°
Collector orientation	225° (SW)
Aperture area	2.3m^2
Zero-loss efficiency	64.2%

The metering strategy adopted for this system is identical to that of test system 1, with temperature sensors (IButtons) installed in locations shown in Figure 11.10. Unfortunately no energy measurements were available from the control unit, as the control panel used by the system requires a flow meter to be connected in order to determine the energy output using the exact flow rate. The data that is available for analysis includes:

- Temperatures at several points on the system pipe-work at 10-minute intervals, as for test system 1, available for 4 months with interruptions
- Hot water draw-off for two morning showers, equal to cylinder capacity
- Weather data from a weather station approximately 4 miles from the test site
- Pump output power is known to be 50W

While the description of the family's hot water consumption is easily quantified and modelled, the irregular times of absence from the house are much more difficult to model. As an added complication, the system uses a variable speed pump. This makes any modelling of this system inherently inaccurate. The flow rate profile that is used by the control panel is shown in Table 11.S:

Table 11.S: Flow control profile based on temperature difference between cylinder and collector

Control temperature difference (°C)	Pump power
6	30%
10	40%
12	50%
14	60%
16	70%
18	80%
20	90%
22	100%

It was attempted to model this pump power variation based on temperature difference in order to accurately represent the flow rate variation. However, this attempt failed, as too many circular references were created. The flow rate is required to estimate the temperature output of the panel, while at the same time the flow rate depends on the temperature difference that is measured between the collector and the hot water cylinder. Instead of modelling the variation, a constant flow-rate of around 1L/min was assumed, which equates to operation at around 60-70% power.

The hot water usage profile of test family 2 is estimated to be:

- 100L draw-off in the morning, between 6:00-7:00
- approximately 20L draw-off in the evening, at around 22:00

The transfer liquid used in the solar circuit is not based on ethylene glycol as all other systems that were analysed, but on propylene glycol. The transfer liquid is called Tyfocor LS[219], has density of around 1.03Kg/m^3, and with 3700KJ/Kg°K a slightly higher specific heat capacity than ethylene glycol at 45°C.

11.4.4 Control System Set-up

After the experiences at the EcoSmart village it was decided to set up a solar thermal system in a controlled environment to provide more robust data for more flexible analysis.

It was also found that the solar irradiance on a vertical plane shows much less variation throughout a typical year than that seen on a 45° plane. Applying solar thermal systems to vertical surfaces would not only free up valuable roof space for potential PV application, but if the output is more consistent throughout the year it would make sizing of the panel much easier. Figure 11.13 shows the monthly variation of solar irradiance on a 45° plane compared to that on a vertical plane.

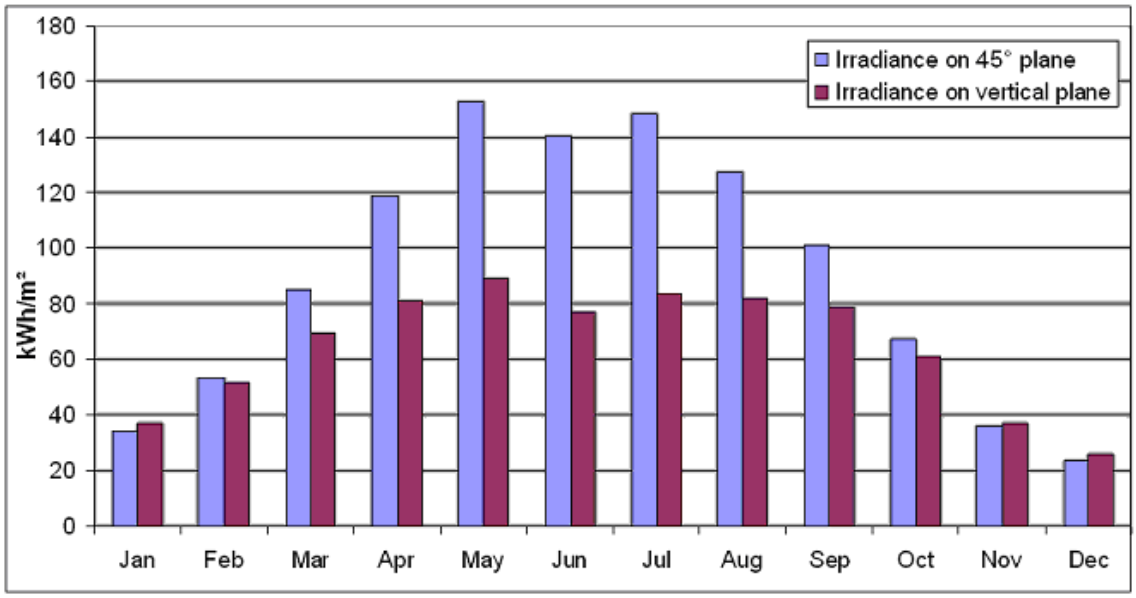

Figure 11.13: Comparison of Irradiance on a 45° inclined plane and vertical plane (source: PV GIS)

Hot water requirements of a typical household can be assumed to be slightly greater during winter than during summer months, with average seasonal variations of around 30%[220]. Figure 11.13 shows that the irradiance variation on a vertical plane is more closely matched to this distribution than that on an inclined plane.

Two identical flat panel systems were set up on the roof of a University of Manchester building to allow a more detailed and controlled study, and to assess the merits of a vertical system in detail. The flat panel systems had previously been used at the EcoSmart village and were sized 1m² each.

This set-up was planned and constructed in collaboration with another researcher, Rebecca Warren, who is investigating the potential risk of legionella bacteria forming within water cylinders that are used with solar thermal systems. The set-up plans were independently reviewed and approved by experts at SKM Consulting Ltd.

The controlled set-up was intended to replicate realistic conditions for domestic solar thermal systems, while also trying to create more favourable conditions to generate a higher energy output. To achieve this, an insulated shed was built on the flat roof of the building in order to replicate an insulated loft space. The panels are attached to the south facing wall (vertical) and roof (inclined at 45°) of this shed, and three water cylinders, each with a capacity of 200 litres, are installed inside. Each panel is connected to one of the water cylinders, while a third cylinder will be used to provide control reference readings. A simplified layout of this set-up is shown in Figure 11.14.

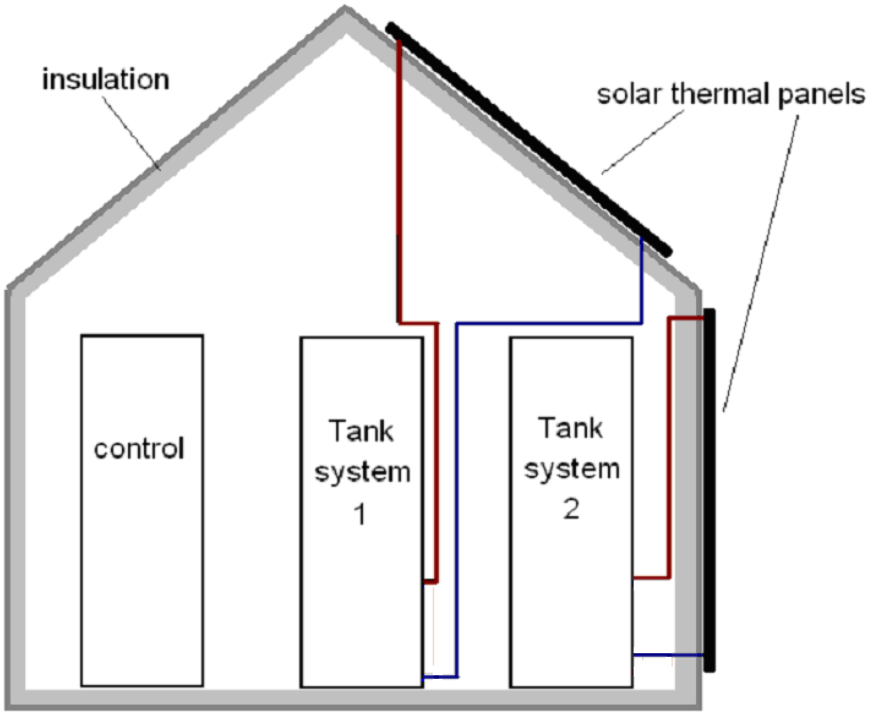

Figure 11.14: Simplified layout of solar thermal shed

Custom made cylinders were offered free of charge to the research team by a manufacturer of domestic water cylinders who was interested in supporting the research. These cylinders consisted of a standard stainless steel cylinder with 200L capacity, with an immersion heater inserted above the solar coil approximately one third of the way up the cylinder. On the control cylinder, the immersion heater is placed at the bottom of the cylinder. They are supplied with 8 sensor pockets that

protrude into the cylinder and provide space for thermocouples. Figure 11.15 shows the layout of the cylinders.

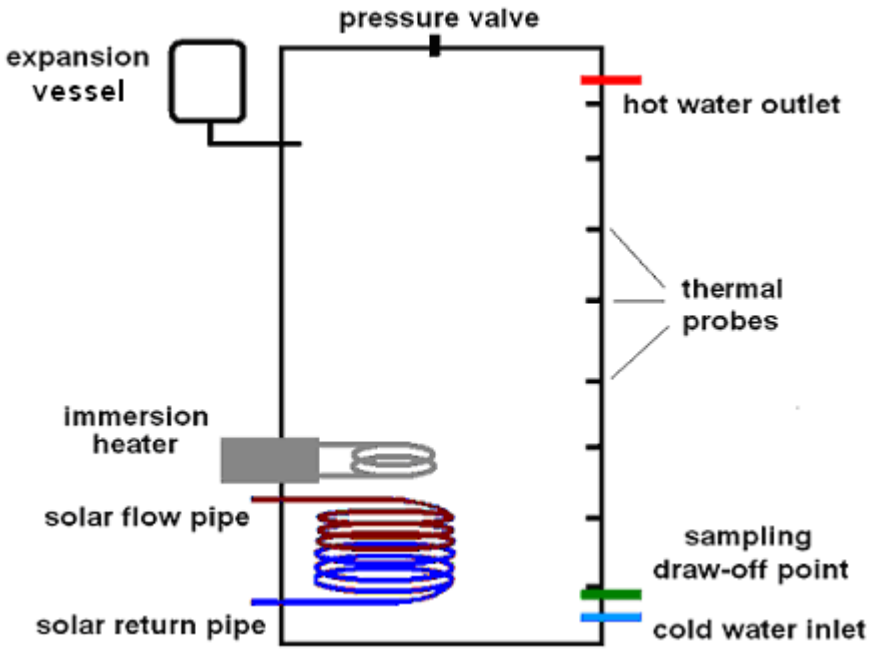

Figure 11.15: Layout of solar thermal cylinders

Hot water is automatically drawn off from the cylinders at regular intervals using motorised valves to simulate showers and baths. The immersion heater was placed above the solar heat exchanger to allow a certain amount of cold water to be available for solar heating, which is not affected by the immersion heater. The immersion heaters will be set to heat the cylinder temperature to 60°C once per day, which is a safety precaution to kill off any bacteria that may have accumulated in the cylinder.

Results

This set-up has proved to be much more difficult than initially anticipated. Work began in April 2009, with the shed scheduled to be completed by June, and plumbing by August 2009. While the construction of the insulated shed went well, it took slightly longer than scheduled and was completed by the end of July 2009. The plumbing side of the installation revealed many of the potential complications with setting up solar systems and continued well beyond the scheduled deadline.

When the custom made water cylinders arrived, all three had immersion heaters installed at the bottom, not as specified above the solar coil on the solar cylinders, and at the bottom of the control cylinder. The manufacturer attempted to solve this problem by on-site insertion of new immersion heaters, which proved to

be a difficult task for the stainless steel cylinders. After many unsuccessful attempts the cylinders continued to leak, and some thermocouple pockets were also found to be leaking under pressure. After spending 3 months trying to fix the cylinders they were abandoned, and new cylinders were ordered from a different manufacturer, incurring a further 6 week delay for delivery.

After further delays from adverse weather conditions the new cylinders were installed and connected by plumbers who are fully trained and certified to carry out solar system installations. After the systems were pressurised several leaks were discovered on the solar side. The original connections to the solar panels, which were left in-tact by the research team, had developed slow leaks. After taking the connections apart, it was found that these were fitted with non-solar rated rubber washers. The plumbers advised that only solar rated washers should be used, which are designed to cope with the high temperatures that can occur in the solar circuit.

After several days of operation, it was noticed that despite experiencing low elevation sun during March 2010 the vertical system was not performing as well as the inclined system. Eventually it was discovered that the system had been connected the wrong way around – with the return pipe from the cylinder leading into the top of the collector, and flow pipe to the cylinder coming out of the bottom end. As the control panel temperature sensor was attached to the top of the collector, this means that whenever the collector heated up enough for the pump to switch on, the cold temperature of the return liquid meant that it switched off again shortly thereafter. After several weeks the plumbers were able to rectify the mistake.

It was also found that the solar panels, in particular the vertical panel, had developed considerable amounts of condensation on the inside of the glass cover. On some days the area covered by condensation exceeds 50%.

Conclusions

Despite not producing data that is robust enough for analysis, this set-up was very successful in showing some of the many problems that can arise during Solar Thermal system installations.

- Even well trained and fully certified plumbers who specialise in solar system installations make mistakes that result in poor performance. When installing the system in a domestic home, the particular mistake made during this set-up (connecting the panel the wrong way around) would have been difficult to notice. Rigorous testing and commissioning of solar installations is essential.

- If (cheaper) non-solar rated washers are used to connect the solar panel, these may deteriorate after some time due to extreme temperatures and cause the system to leak and lose pressure. Again, this may not be easily noticed in a domestic situation.

- Receiving wrong specification cylinders was experienced during this set-up, and was also experienced by test family 1 as described previously. If a family with little or moderate technical understanding receives a cylinder with an immersion heater fitted at the bottom, instead of above the solar coil, they may not notice and experience poor performance from their solar system.

- Flat panel systems appear to be non-reusable. When uninstalling them, moisture can get into the insulated space, causing condensation on the inside of the glass cover. This may also occur on systems that are poorly designed and experience corrosion.

11.5 Solar Thermal Model

Considering some of the significant discrepancies between expected and measured performance encountered for the monitored Solar Thermal systems it is imperative that a robust model is used to reveal the reasons for this, and to show how the systems can be improved. This model will need to consider the interaction between the solar panel, the hot water cylinder and auxiliary heat systems to provide an accurate simulation of the Solar Thermal systems.

After reviewing existing literature, some models were found that dealt with solar thermal panels[221,222,223] and hot water cylinders[224] individually, while a recent model also considered the interaction in detail[225]. However, all models that were found are based on the TRNSYS platform, and no validated model was found that encompassed an interaction of all three subsystems identified previously.

11.5.1 Modelling Options

Several options were considered for solar thermal system modelling.

1. *f*-chart method: This method of solar thermal system modelling, used to provide initial estimates, is very generic and somewhat inflexible. It relies on average monthly or average daily values, making it difficult to create a dynamic model. While it is easily applied to systems for which very little data is available, its main weakness is that it does not account for the interaction with storage or control accurately.

2. Dynamic model based on BS EN 12975: The British Standard EN 12975 outlines testing procedures and energy calculations for solar thermal systems. Some of the methodology is similar to the *f*-chart method, but is much more flexible as 'real-time' data can be used. Using this method would provide a complex but flexible dynamic model.

3. RETScreen: This freely available tool was developed with contribution from many experts from academia, industry and government. It is based on the two methods introduced previously, the Utilisability method for cases without storage, and the f-chart method for cases with hot water storage. It was previously deduced that the f-chart method is prone to over-estimating the energy output due to various reasons. This is also reflected in the RETScreen analysis. In a validation exercise conducted by RETScreen, for

which the simulation was compared to measured results from 10 flat-panel systems in Canada, RETScreen was shown to overestimate the annual yield by 15-29%[226].

4. TRNSYS: This is a state-of-the-art modelling tool that has evolved over several decades. It is highly regarded by science and industry alike, with continuous development through many experts worldwide. Several existing models are available for the platform, some also including models for cylinders. However, the software was unavailable due to its price tag of $2250 for an educational license.

5. T*Sol: This is a solar estimation tool that has become highly regarded among European solar industry. It is able to calculate the solar fraction for solar systems using flexible parameters, by making use of its own weather data. However, with it being a commercial application, the methodology applied to generate the output estimates is not revealed to the general public. A demo version of T*Sol Express was obtained for trial purposes, but it was decided not to purchase the full version at £130.

After considering all options, it was decided to create a model for the solar collector based on BS EN 12975. This means the model can be flexibly designed to incorporate all aspects that are important to accurately simulate the solar thermal systems that were tested. This will be combined with a second model for a common hot water (dual coil) storage cylinder including stratification in 3 layers, with consideration for pipe losses and auxiliary heat. It was considered important to create a model of a stratified cylinder, as stratification combined with a relatively low collector flow rate can lead to significant improvements in transmission efficiencies, up to 38%[227].

The model will be created in MS Excel, which provides a flexible and powerful platform that allows viewing and editing on any system equipped with MS Office. To balance accuracy and practicality of the dynamic model, time intervals of 10 minutes were chosen.

11.5.2 Solar Collector Model

According to BS EN 12975, results that have been obtained from testing and equation (11.13) can be used to compute the collector output. The methodology that was adopted for Solar Thermal panel modelling shown by equations (11.13) to (11.20) is described in detail in the BS EN 12975 documentation[218].

$$\eta = \frac{Q}{A_C G''} \tag{11.13}$$

The term (G") is the net irradiance that also accounts for radiation losses, determined by equation (11.14).

$$G'' = G + (\varepsilon / \alpha)(E_L - \sigma T_a^4) \tag{11.14}$$

Terms (ε), the emittance of the collector, and (α), its absorptance, are given by the manufacturer as 0.06 and 0.935 respectively. The term (E_L) refers to the long-wave radiation in the collector plane.

The long-wave radiation on collectors inclined at 45º or less is given by equation (11.15).

$$E_S = \varepsilon_s \sigma T_a^4 \tag{11.15}$$

The term (ε_s), the emittance of the sky, can be found by considering the dew point temperature. This is shown in equation (11.16).

$$\varepsilon_S = 0.711 + 0.56\frac{T_{dp}}{100} + 0.73\left(\frac{T_{dp}}{100}\right)^2 \tag{11.16}$$

Having found G" for equation (11.13), equation (11.17) is used to determine (Q). Subscripts 'b' and 'd' refer to beam and diffuse components respectively.

$$\begin{aligned}\frac{Q_H}{A} &= F_R(\tau\alpha)_{en} K_{\theta b}(\theta) G_b + F_R(\tau\alpha)_{en} K_{\theta d} G_d - c_1(T_m - T_a) - c_2(T_m - T_a)^2 \\ &- c_3 u(T_m - T_a) - c_4(E_L - \sigma T_a^4) - c_5 \, {dT_m}/{dt} - c_6 u G^*\end{aligned} \tag{11.17}$$

Equation (11.17) is a generalised model that covers all types of solar thermal collectors. Evacuated tube type collectors experience close to zero convection losses and are not affected by wind, therefore terms including wind speed (such as coefficients c6 and c3) can be neglected. It is not mandatory for manufacturers to provide coefficients c4 and c5 in their technical data, so for general modelling purposes these terms will be neglected as well. Hence the simplified equation (11.18) is used for modelling purposes.

$$\frac{Q_H}{A} = F_R(\tau\alpha)_{en} K_{\theta b}(\theta) G_b + F_R(\tau\alpha)_{en} K_{\theta d} G_d - c_1(T_m - T_a) - c_2(T_m - T_a)^2 \quad (11.18)$$

When the mean collector temperature is equal to ambient temperature, the product of transmittance and absorptance at normal incidence, and the efficiency correction factor, is equal to the maximum efficiency.

$$\eta_0 = F_R(\tau\alpha)_{en} \quad \text{when} \quad T_a = T_m \quad (11.19)$$

To account for the situation where the solar irradiation is not normal (or within 2%) to the collector plane, an angle modifier is introduced to account for additional reflection losses at shallow angles, as shown in equation (11.20).

$$(\tau\alpha)_e = K_\theta (\tau\alpha)_{en} \quad (11.20)$$

The possibility of shading of the collector is also accounted for by the model. After specifying the boundary angles in a horizontal plane (azimuth) and vertical plane (elevation), these are compared to the solar azimuth and elevation angles for each time step. If the sun is within these specified boundaries, all direct beam values for the particular time interval are discarded. The diffuse component is assumed to remain unchanged.

A sky-view factor for the diffuse component is also introduced, shown by equation (11.21), where (β) refers to the inclination angle. This factor is then multiplied by the diffuse component for each time interval.

$$VF_{sky} = \frac{180 - \beta}{180} \quad (11.21)$$

Shading caused by adjacent vacuum tubes was neglected for this model, as other research[197] showed this only becomes significant at high angles of incidence of 70-80º. Performance reduction from dust accumulation was also neglected. Other research[228] concluded that regular precipitation results in negligible effects of dust accumulation.

11.5.3 Control System and Heat Transfer Model

An IF statement ("is temperature of collector greater than bottom cylinder temperature plus control temperature (for example 7°C)?") is used to determine whether heat transfer from collector to cylinder is taking place or not.

- If no heat transfer is taking place, the collector remains in a stagnant state and the absorbed energy is stored within the collector, raising its temperature.
- If the answer is yes, a second IF statement is used to determine whether the collector was previously in stagnant state or if heat transfer had taken place.

    - If heat transfer had taken place in the previous time interval, then the average temperature of the transfer liquid is calculated based on the solar energy that is absorbed during the current time interval.*
    - If the collector was in stagnant state previously, then the transfer temperature is calculated based on the heat stored in the collector up to this time, plus the solar energy absorbed during the current interval.

**Note: This makes the model sensitive to heat transfer rate. If the flow rate is high, the average temperature over the 10-minute time interval is reduced significantly. In real life the energy would still be transferred at a relatively high temperature, but the temperature would drop off rapidly, possibly causing it to return to the stagnant state before the 10-minute interval is over.*

A third IF statement is used to find out if the resulting temperature of heat transfer liquid exceeds the safety temperature that is specified in the solar thermal control panel (usually 75°C). Should this be the case, it is assumed that transfer is taking place at the specified safety temperature and any additional heat in the solar system is dispersed via the expansion vessel. The excess heat is still accounted for when finding the mean panel temperature so that the collector heat loss can be modelled accordingly.

If any heat transfer takes place from solar collector to the hot water cylinder, heat losses from the pipe-work are deducted. Energy losses in the 'flow' pipe are found using pipe dimensions and estimated U-value (U=2.5 W/m^2K), using equation (11.22).

$$Q_{loss} = UA_p(T_e - T_a) \tag{11.22}$$

The temperature drop over the length of the pipe can be determined using equation (11.23).

$$\delta T_e = \frac{Q_{loss}}{mC_P} \tag{11.23}$$

11.5.4 Cylinder Model

In order to account for stratification effects which take place within the cylinder, it is modelled as 3 different vertical sections, Layers 1, 2 and 3, shown in Figure 11.16.

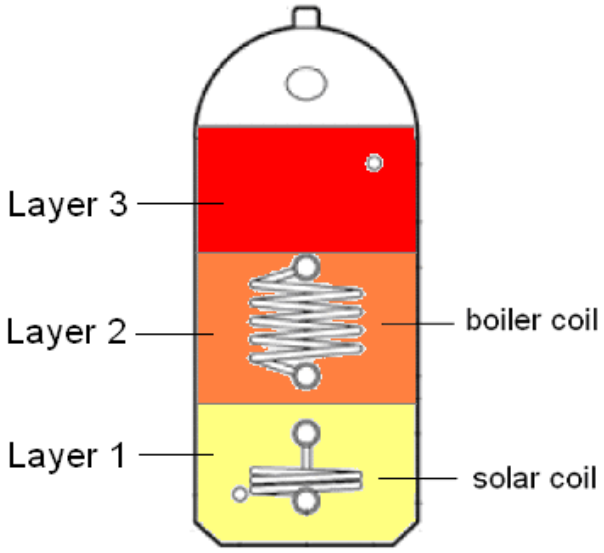

Figure 11.16: Schematic diagram of hot water cylinder showing 3 modelled layers

Heat from the solar system is added to layer 1. The temperature of layer 1 at the end of the time interval is found the energy balance shown in equation (11.24).

$$Q_{Layer1} = Q_{initial} + Q_{gain} - Q_{loss} - Q_{trans} - Q_{draw-off} \tag{11.24}$$

While the term (Q_{gain}) refers to the energy transferred from the solar system and ($Q_{initial}$) is the energy contained by layer 1 at the start of the time interval, (Q_{loss}) refers to thermal losses based on physical properties of the cylinder and its insulation. This is calculated using equation (11.22). Further energy losses are experienced when heat is transferred to the next layer, and when hot water is drawn off from the top and replaced by colder water entering the bottom. These two terms are referred to as (Q_{trans}) and ($Q_{draw-off}$) respectively.

The rate of temperature change of the particular layer is calculated using a differential equation where rate of energy out is subtracted from rate of energy in. This is done using equation (11.25), which determines the resulting temperature at the end of the time interval. The term (600s) refers to the number of seconds of the time interval. The rates of heat gain or loss are measured in Watts, multiplying by time will result in a value for energy, measured in Joules.

$$T_{Layer1} = T_{initial} + \frac{600s(\dot{Q}_{in} - \dot{Q}_{out})}{mC_P} \qquad (11.25)$$

Equation (11.25) is based on the differential equation shown below in equation (11.26). The method of breaking a differential equation down into small step changes has been developed and justified by Euler, describing the integration of ordinary differential equations[229].

$$mC_p \frac{\delta T}{\delta t} = \dot{Q}_{in} - \dot{Q}_{out} \qquad (11.26)$$

This temperature is then compared to the temperature of the next layer, layer 2. If the temperature is higher than the layer above, the energy difference is transferred to the next layer. In this case the energy difference is referred to as (Q_{gain}) for layer 2, and taken as (Q_{loss}) for layer 1. The same interaction occurs between layers 2 and 3. Using this method, the top layer is always the layer containing most energy, while the bottom layer contains the least energy.

As hot water is drawn off, the layers are used to simulate the effects of stratification within the cylinder by creating a layer of cold water at the bottom that does not mix with any warmer layers above.

11.6 Model validation

Results from Test System 1 are predominantly used to provide a comprehensive validation of the model. The annual results will also be compared to SAP and RETScreen estimates.

11.6.1 Finding U-value of the Storage Cylinder

To find a U-value for the cylinder allowing the calculation of the term (Q_{loss}), the model is based on the cylinder used by test family 1. The hot water cylinder from this particular system is a vented dual-coil Albion Superduty Eco AG 1350x450 with capacity of 180L. Figure 11.17 shows the schematic diagram supplied by the manufacturer Albion.

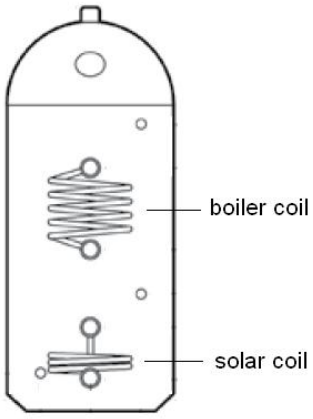

Figure 11.17: Schematic diagram of solar hot water cylinder (Source: Albion Superduty technical documentation)

After online research and contacting the manufacturer's sales team and technical support team, it was not possible to determine a U-value for the cylinder required to calculate the heat loss.

The U-value of the solar cylinder can be found using measured temperature data from the cylinder during holiday periods, while the central heating system was switched off. Figure 11.18 shows the variation of cylinder temperature over a 3-day holiday. The U-value that is found using this method will provide the average U-value, including losses that occur through pipe connections. These losses often make up a large proportion of the total losses from insulated cylinders.

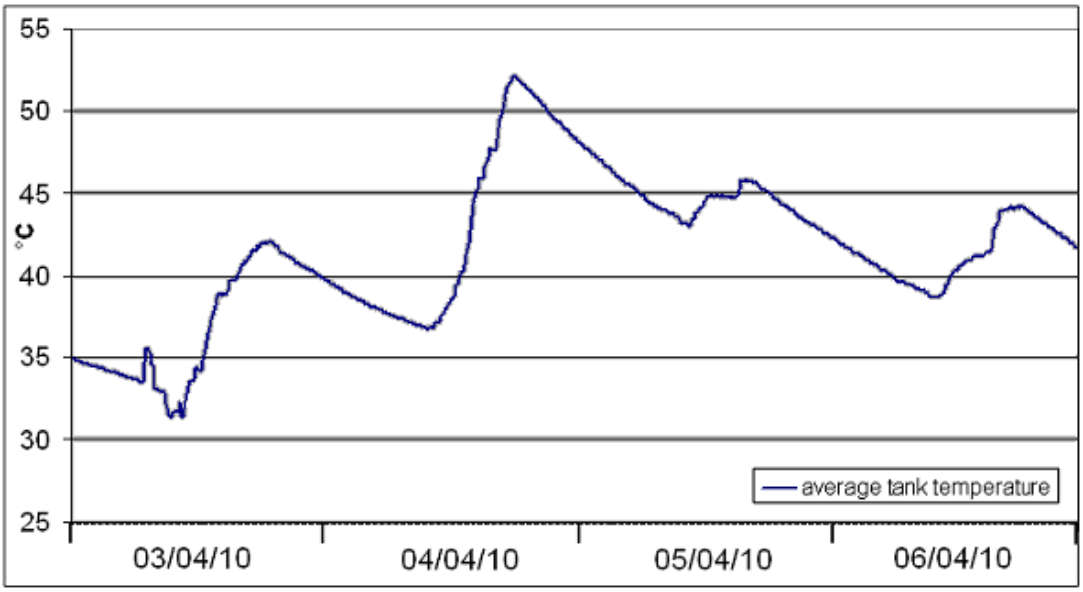

Figure 11.18: Variation of average temperature of solar cylinder during holiday period

The temperature change and rate of heat loss can be found from the data presented in Figure 11.18. Equations (11.27) and (11.28) are used to relate this to the U-value of the cylinder.

$$Q_T = mC_{P,w}(T_T - T_a) \tag{11.27}$$

$$U = \frac{\dot{Q}_{loss}}{A_T(T_{T,avg} - T_a)} \tag{11.28}$$

Using equations (11.27) and (11.28) with 25°C ambient temperature, cylinder area of 2.11m^2 and the measured over-night temperature losses, the U-values calculated for the 3 nights are:

3rd-4th April '10: U-value = 2.86 W/m²K
4th-5th April '10: U-value = 2.90 W/m²K
5th-6th April '10: U-value = 2.90 W/m²K

Mean U-value = 2.89 W/m²K

11.6.2 Steady-state Validation of Cylinder Model

Figure 11.19 shows the temperature variation of the cylinder model under steady-state conditions. The starting cylinder temperature is equal to the ambient temperature of 25°C. Heat is added at a steady input temperature of 40°C, assuming a flow rate of 1L/min, until the temperature of the cylinder levels out. The heat input is then removed and the cylinder is left to cool through conductive heat losses.

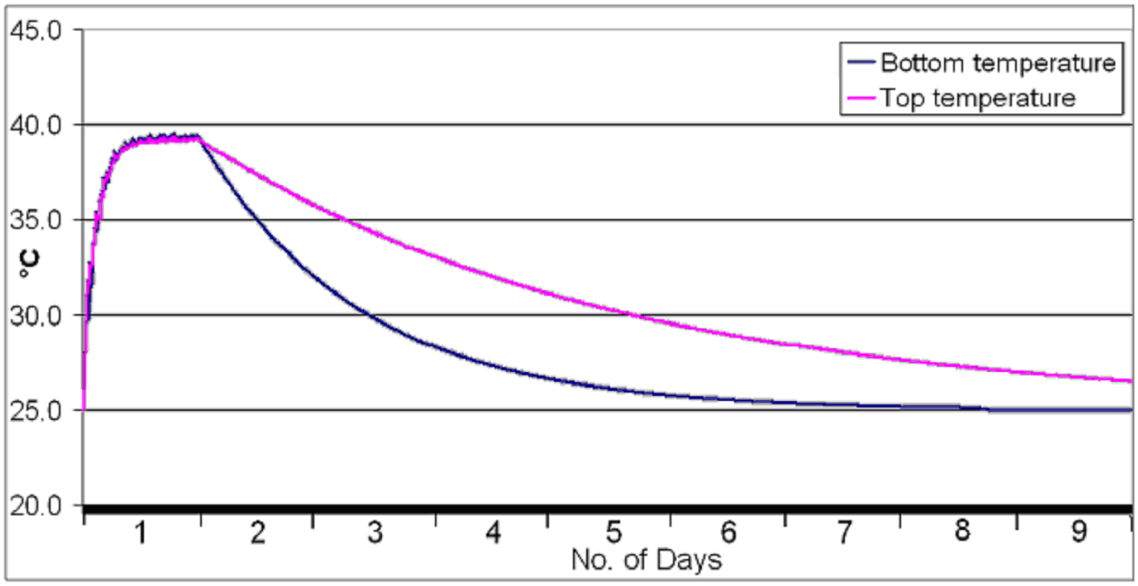

Figure 11.19: Temperature variation of cylinder model under steady-state conditions

As expected the temperature of the model shows an exponential increase with time. As heat is added, the energy is passed vertically up the cylinder through the 3 modelled layers. While there is little variation between top and bottom temperature, there are several step changes, which can be explained by the 10-minute modelling interval. Only allowing one heat exchange between layers per interval, heat getting into the bottom of the cylinder effectively takes 20 minutes to reach the top layer, while at the same time the cooler water from the top takes 20 minutes to reach the bottom layer by modelled convection. This also causes a slight time lag between layers if heat is added at high rates, and it means the cylinder can never quite get to 40°C.

As the cylinder cools, there is again an exponential temperature variation with time. The top layer takes considerably longer to cool down to ambient temperature (about 12 days after the heat source is removed, compared to only 7 days for the bottom layer). Again, this shows that the modelled convection between

the layers works well. The time constant[230] of the hot water cylinder can be determined using equation (11.29).

$$\tau_C = \frac{mC_P}{UA_T} \tag{11.29}$$

For the test system 1 cylinder, the time constant is equal to 48.1 hours. This means that, in theory, after 48.1 hours the cylinder should have given off 63.2% of its energy to its surroundings. After 2 days the model shows an average cylinder temperature of 30.5°C, which is a drop of 9°C assuming it started off at 39.5°C. Considering the initial 14.5°C difference between cylinder and surroundings, the cylinder has lost around 62.5% of its heat, confirming that the modelled heat loss is fairly accurate.

Figure 11.20 shows a validation for the modelled stratification effect within the cylinder. Temperature variations after draw-off events are shown over a 24-hour period for all 3 modelled layers of a 180L cylinder. The heat supply to layer 1 is kept constant at 40°C with flow rate of 1L/min. The simulated hot water draw-off is of 20L, followed by 80L, and finally 150L.

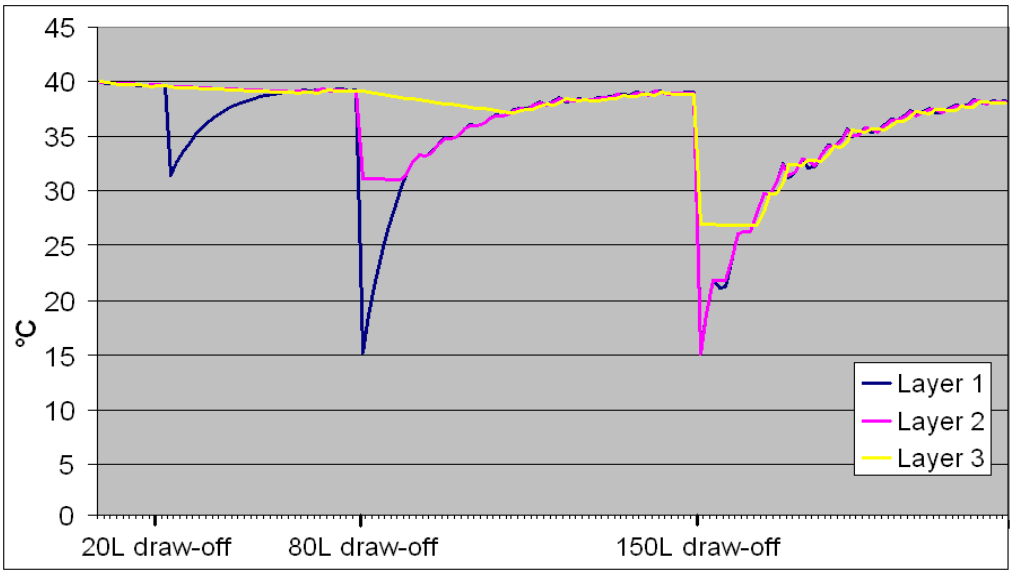

Figure 11.20: Stratification effect after various different draw-off events from the modelled cylinder

Figure 11.20 shows that the stratification model works well. Each layer has a capacity of 60L. The first draw-off of 20L means that 20L of cold water (at 15°C) enters the bottom layer, and the displaced volume is shifted upwards through the layers. Layer 1 takes a new temperature, comprising of the remaining hot water mixed with the 20L of cold water taken in. Layers 2 and 3 remain at their starting

temperature. Over the next few hours the temperature of layer 1 converges to near 40°C, the same temperature as the layers above.

The next draw-off is of 80L, which is 20L more than the capacity of layer 1. The entire volume in layer 1 is replaced by cold water. Layer 2 becomes a mixture of 20L cold water and 40L hot water at the previous temperature of layer 1, while layer 3 remains unchanged. After layers 1 and 2 have cooled down, it can be seen that layer 3 is now beginning to cool down (due to cylinder heat losses), as no additional heat is supplied from the layers below.

As 150L are drawn off, the entire volume of layers 1 and 2 is replaced by cold water, while layer 3 becomes a mixture of 30L cold water and 30L hot water at the previous temperature of layer 1. As layers 1 and 2 heat up again the step changes caused by the 10-minute interval in the model are particularly noticeable. On some occasions the temperature is even shown to decrease, which is a result of the overlap for a particular interval of more heat being taken away from a layer (as it is passed up to the next one) than is being supplied by either the solar circuit or the layer below. The 10-minute interval and resulting time lag is also responsible for the lower layers seemingly having a slightly greater temperature than the top layers on some occasions.

Apart from the unavoidable step changes which do not have any effect on the overall outcome, the stratification effect between 3 layers after hot water is drawn off is shown to be modelled correctly. This is important, as it will have a significant effect on the overall system performance.

11.6.3 Input Data for Model Validation

Test System 1 will be modelled for validation purposes. The relevant parameters for this system are summarised in detail in Table 11.T, based on technical data provided[231] or derived otherwise.

Table 11.T: Model input parameters for Test System 1

System	Latitude	53.3	°
	Longitude	-2.3	°
	Collector inclination	30	°
	Collector orientation	0	°
Collector	Aperture area	3	m^2
	Absorptance	0.935	
	Emittance	0.06	
	Area-related heat capacity	8.3	kJ/m^2K
	Zero-loss efficiency	0.642	
	Angle modifier transverse	1	
	Angle modifier longitudinal	0.9	
	Angle modifier	0.9	
	c1 coefficient	0.885	W/m^2K
	c2 coefficient	0.001	W/m^2K^2
Cylinder	Cylinder capacity	180	L
	Cylinder height	115	cm
	Cylinder diameter	45	cm
	Cylinder U-value	2	W/m^2K
	Distance collector to cylinder	5	m
	Pipe diameter	15	mm
	Typical ambient temperature	25	°C
Control	Transfer flow rate	1	L/min
	Control temperature difference	7	°C
	Boiler control		°C
	Safety (max temp) shut down	65	°C

In addition to the values shown in Table 11.T, weather data was used that was recorded at a distance of approximately 3 miles from the test site. The weather data consisted of 30-minute intervals which were linearly interpolated to give 10-minute values. Global and diffuse irradiance as well as dry bulb temperature are available.

When asked about their typical hot water consumption, test family 1 reported the following:

- A wash in the morning, around 6:30
- A shallow bath around 8:00
- Washing up later during the day, around 10:00
- Some hot water use throughout the day
- Little hot water use in the evening

With this in mind, the bottom cylinder temperature values throughout April 2010 were examined closely. As hot water is drawn off, there should be a sharp decrease in temperature as cold water (around 15°C) flows into the bottom of the cylinder. When draw off is stopped the temperature should level out again. Figure 11.21

shows the cold feed temperature variation throughout a sample day where several times of draw-off can be deduced.

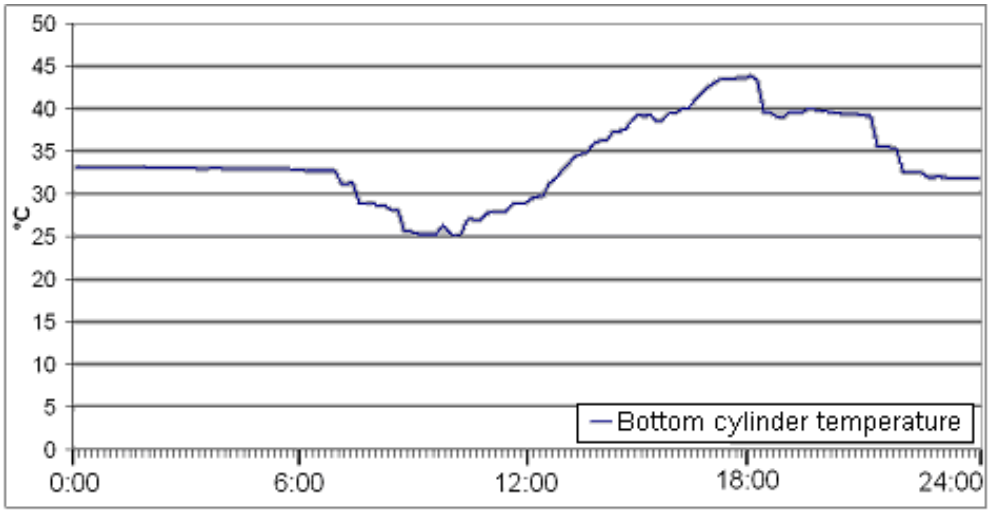

Figure 11.21: Bottom cylinder temperature variation on 14th April 2010

Several sharp temperature drop-offs can be seen in Figure 11.21. They indicate that hot water was drawn off mainly in the morning and the evening. The temperature decrease also provides an indication to the amount of water that was drawn off, while it must be kept in mind that while the solar system is transferring heat, the temperature drop will be less than for the same amount of water drawn off in the evening. For this particular sample day, the deduced hot water draw-off pattern is shown in Table 11.U.

Table 11.U: Draw-off pattern for 14th April 2010

Time	Draw-off (L)
07:10	5
07:40	5
08:50	20
09:20	5
10:20	5
11:30	5
15:30	5
18:10	15
21:20	10
22:00	5
Total	80

The data in Table 11.U coincides well with the description of typical consumption given by the test family for most of the day, except that quite a lot of hot water was used in the evening. This was not the case for most other days that were examined. The average daily hot water consumption during April 2010 (excluding holidays) was deduced to be 71L, using the method outlined above.

When considering draw-off, the temperature of the water that replaces the hot water must also be considered. This will be referred to as cold feed temperature. While average ground temperatures are around 10-12°C, some water will stagnate in the un-insulated copper pipe-work within the house and quickly reach internal ambient temperatures. This amount could easily be 5L or more before the cold feed temperature approaches soil temperature. It is therefore assumed that the average cold feed temperature throughout the modelling period is 15°C.

Based on evidence from April 2010 temperature data and from estimates made by the test family, the hot water draw-off pattern for a typical day is estimated as shown in Table 11.V.

Table 11.V: Typical draw-off pattern for Test System 1

Time	Draw-off (L)
07:00	10
08:30	30
11:00	10
16:00	5
21:30	10
Total	65

The pattern shown in Table 11.V will be used for all further analyses of test system 1 carried out using the model for months other than April 2010.

11.6.4 Detailed Model Validation - April 2010

As there were some gaps in all 3 data sets for Test System 1, the weather data, the logged temperature data and manually recorded values from the control panel, one month with sufficient sun and data of high quality in all 3 sets was chosen for validation purposes. This month is April 2010.

After recording energy generation data from the control panel it was found that this data contains errors. After the control panel was replaced by the manufacturer, the flow rate had been reset to 2L/min. However, the flow meter that is installed in the pipe-work consistently reads 1L/min. It was therefore decided that the temperature measurements from the cylinder would provide a more accurate set of reference data. Using equation (11.30), the energy change of the cylinder, based on average cylinder temperature, was calculated.

$$Q_{gain} = \frac{1}{2} mc_f [(T_{top} - T_{initial,top}) + (T_{bottom} - T_{initial,bottom})] \quad (11.30)$$

The results were summed to give daily totals and converted to kWh. The energy gain based on cylinder temperature is given in Table 11.W labelled 'Sensors (cylinder temp.)'.

A comparison between the manually recorded data and the model output is given in Table 11.W and Figure 11.22. For data gaps in the cumulative manual data, which result from periods of absence from the house, the 'Daily' value represents the cumulative value over the preceding gap. 'Manual data' refers to data recorded from the control panel.

Table 11.W: Comparison between measured and modelled generation of Test System 1

	Manual data (kWh)		Sensors (kWh)	Model (kWh)	
	Cumulative	Daily	(cylinder temp.)	Solar	Solar + boiler
01/04/2010	156	2		2.4	
02/04/2010	158	2	3.0	1.1	5.1
03/04/2010					
04/04/2010					
05/04/2010					
06/04/2010					
07/04/2010	174	16	12.4	8.8	11.0
08/04/2010	179	5	4.6	3.0	3.0
09/04/2010	184	5	3.6	2.8	3.2
10/04/2010	189	5	4.1	3.1	4.4
11/04/2010	193	4	4.1	4.4	4.4
12/04/2010	199	6	4.5	3.7	4.5
13/04/2010					
14/04/2010	205	6	6.0	4.2	6.3
15/04/2010					
16/04/2010					0.0
17/04/2010	223	18	14.3	10.2	11.3
18/04/2010	224	1	1.9	2.0	2.0
19/04/2010					
20/04/2010	229	5	4.5	3.7	4.1
21/04/2010	234	5	5.3	4.0	4.0
22/04/2010					
23/04/2010					
24/04/2010					
25/04/2010					
26/04/2010	253	19	16.9	13.5	13.5
27/04/2010	258	5	3.8	3.7	3.7
28/04/2010	260	2	2.4	2.8	2.8
29/04/2010	261	1	1.2	0.6	0.6
30/04/2010				2.3	2.3
Total*		**107.0**	**92.6**	**74.0**	**83.9**

*Total does not include 30th April as no comparative data is available

When comparing the manual readings taken from the control panel to the values calculated using cylinder temperatures, it becomes apparent that the error is far less than the 100% that might be expected from doubling the flow rate. The only other heat source to the cylinder is the boiler top-up when top cylinder temperature drops below 45°C, which is observed to rarely come on during April 2010. In fact, looking at the daily temperature distributions (Figure 11.23 to Figure 11.26), it doesn't appear to come on at all after the 21st of April.

To account for the added energy from the boiler, the boiler top-up has been added to the model. Figure 11.22 below shows a comparison for April 2010 between energy gains based on measured cylinder temperature, and modelled output including modelled boiler top-up.

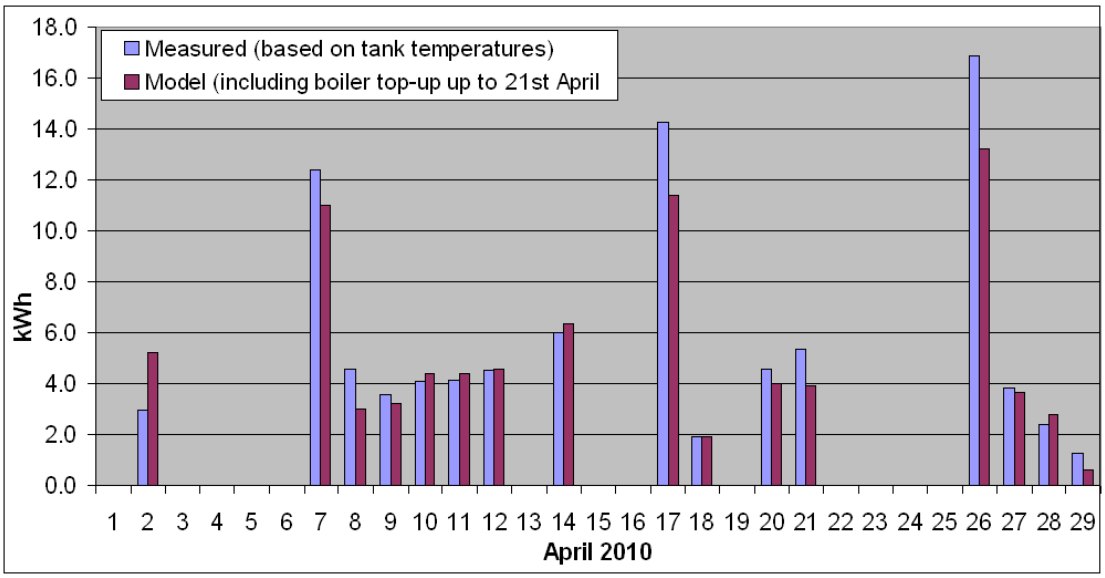

Figure 11.22: Measured energy input to cylinder (based on top and bottom temperatures) compared to modelled input including boiler top-up

The percentage errors between the two data sets are as follows:

- Average Daily error including holiday cumulative output = 19.1%
- Monthly total error = 9.6%

Using the t-test analysis, the t-value for the two sets was found to equal 0.69. The degree of freedom of the two data sets is assumed to be 28. Using the Student's t distribution table[232], the t-value of 0.69 at 28 degrees of freedom equates to a df/p value of less than 0.25 ($t_{(0.25,28)}$=0.683).

This means that when comparing the measured results to the model, less than 25% of values are expected to show a statistically significant difference. Given the uncertainties for hot water draw-off, flow rate and distance of 3 miles from the weather station, this is an acceptable accuracy.

To further compare the model to the measured data, temperature distributions for 4 weeks in April are shown in Figure 11.23 to Figure 11.26.

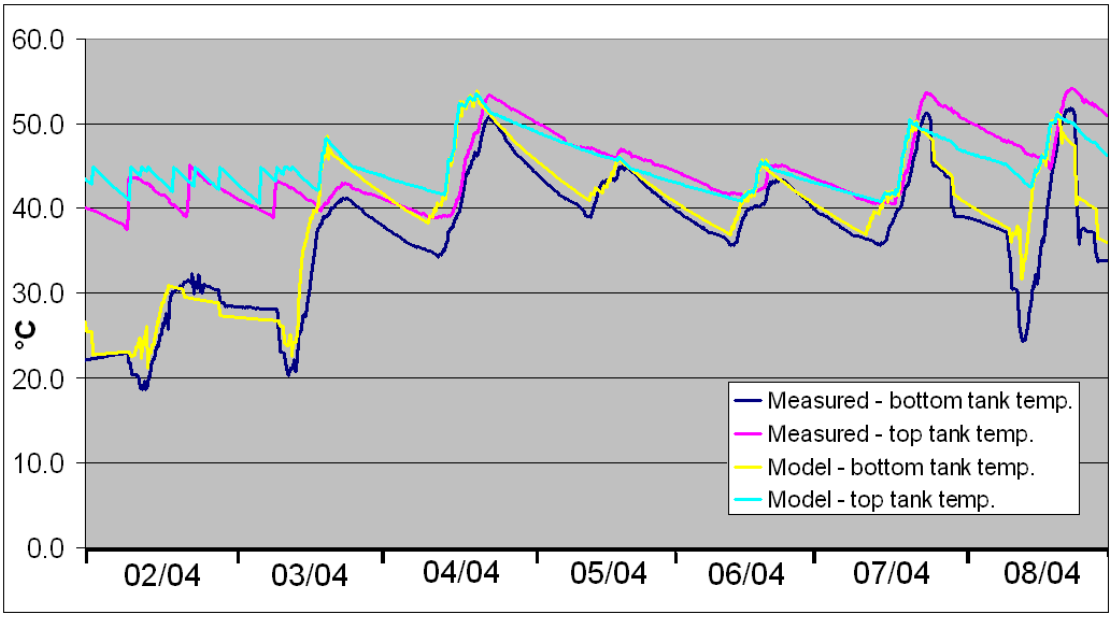

Figure 11.23: Comparison of measured cylinder temperatures and temperatures exported from model for week 1; 2nd to 8th April 2010

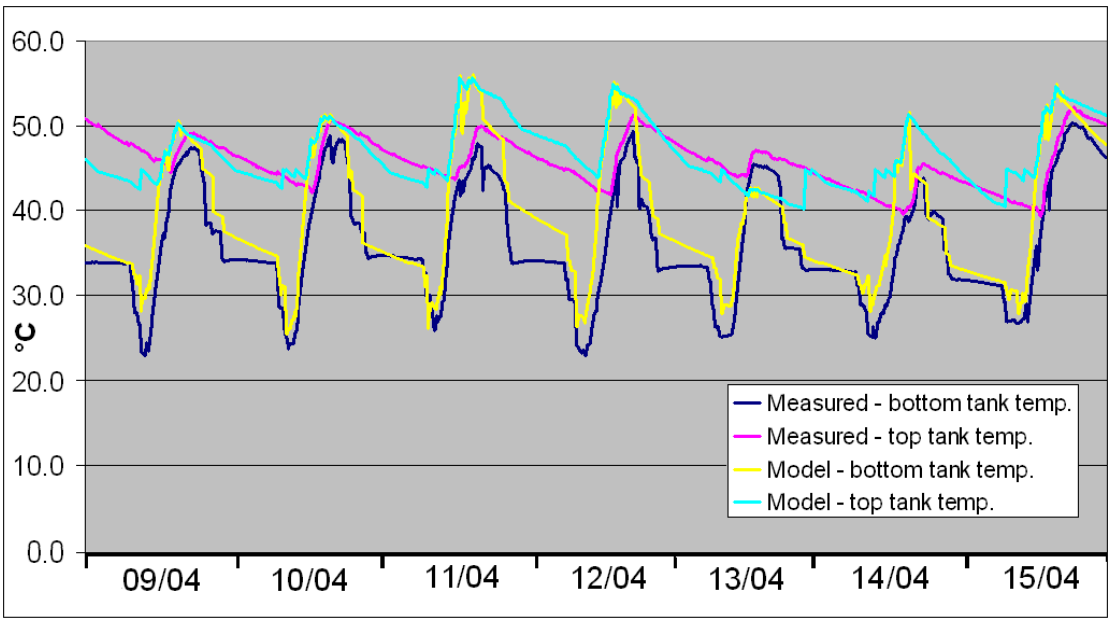

Figure 11.24: Comparison of measured cylinder temperatures and temperatures exported from model for week 2; 9th to 15th April 2010

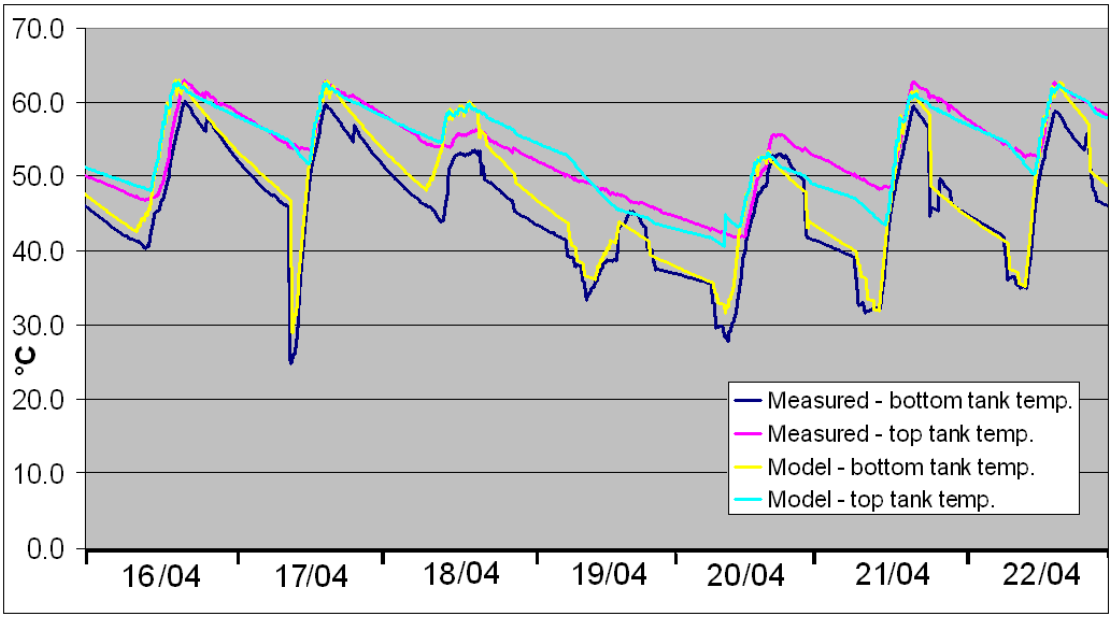

Figure 11.25: Comparison of measured cylinder temperatures and temperatures exported from model for week 3; 16th to 22nd April 2010

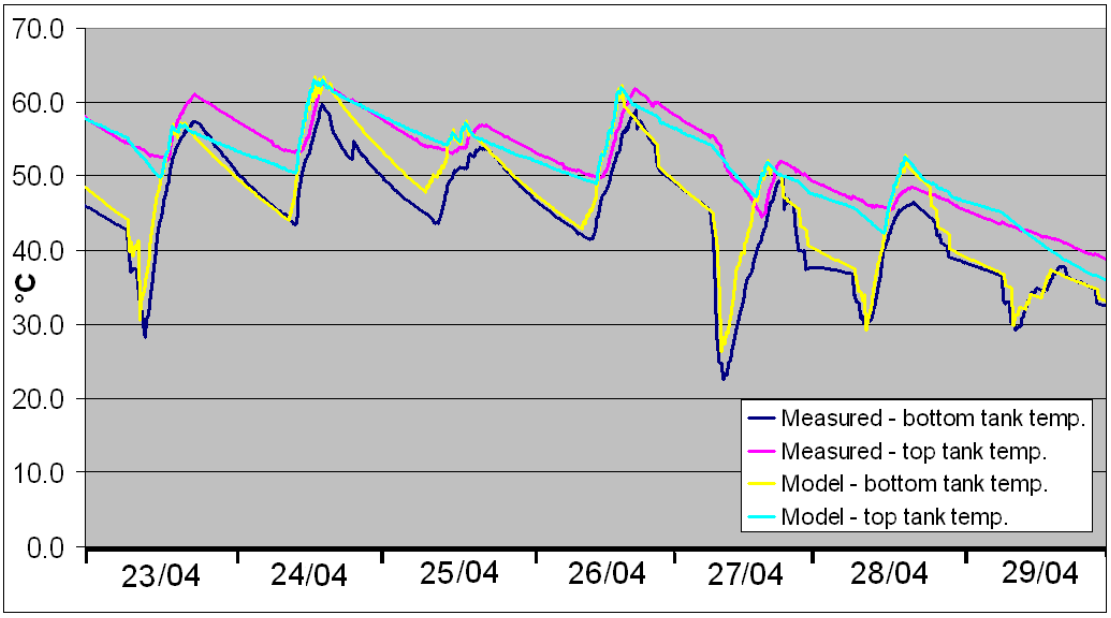

Figure 11.26: Comparison of measured cylinder temperatures and temperatures exported from model for week 4; 23rd to 29th April 2010

During most days in April the temperature variations are very close. Only on a few days, such as the 3rd, 8th, 11th and 13th, can significant differences be noticed. In particular some of the holiday periods (for example 4th to 7th April) without uncertain variables such as draw-off, show an excellent match between model and measured temperatures. To go into a bit more detail, Figure 11.27 provides an overview of the model and measured temperature variation for one sample day, in this case the 12th April, which shows an average correlation with respect to the other days.

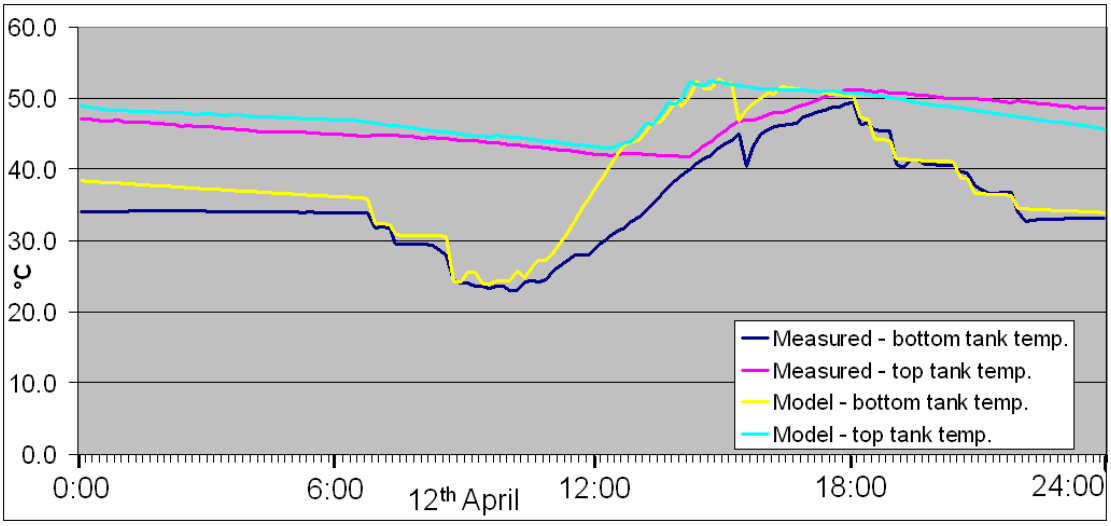

Figure 11.27: Temperature distributions for 12th April 2010, Test System 1

During the 12th of April the first hours of the day show little difference between model and measured temperatures. However, true ambient temperature at this time may have been close to or even above 30°C, whereas the model is based on an average 25°C. This is evident before 6am when modelled bottom cylinder temperature decreases at a faster rate than measured temperature, while top cylinder temperatures show a similar rate of heat loss.

The modelled temperature draw-offs for this day, which are very close to estimates made by the test family, seem to coincide very well with the measured draw-offs and resulting temperature drop at the bottom of the cylinder. For both model and measured distribution, heat from the solar circuit is only provided after 11am. This also occurs on every other day, which is a good validation for the shading calculations included in the model.

The rate of temperature increase of model bottom temperature is greater than the measured equivalent. As this is not the case for most other days (such as the holiday period of 4th-7th April), it may be assumed that inaccuracies in weather data, brought about by the distance of 3 miles between weather station and test site, are to blame. The maximum temperatures reached are similar for the model and measured values, the model only reaches maximum temperatures earlier during the day. The measured overall energy gain for this day is 4.1kWh, while the modelled gain is 4.5kWh.

For further comparison, Figure 11.28 shows the comparison of average cylinder temperature for the model and measured data sets.

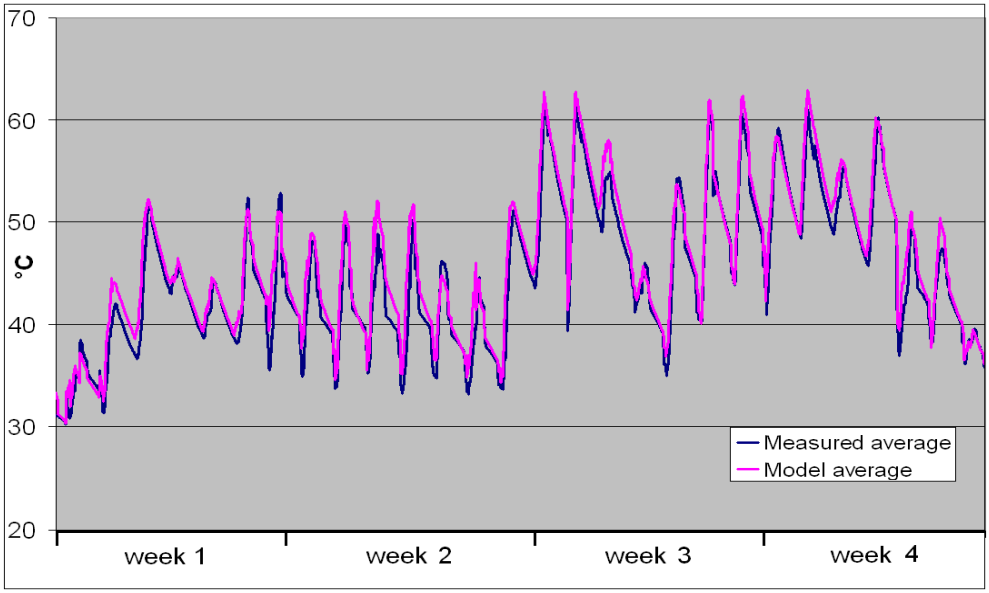

Figure 11.28: Comparison of average cylinder temperature in April 2010, measured vs. model

Again, the average cylinder temperatures shown in Figure 11.28 appear to show a very good correlation. This adds to the evidence that the model represents the performance of Test System 1 accurately, and is a validation of the correctness and accuracy of the model.

11.7 Modelling Domestic Solar Thermal Systems

Having verified the accuracy of the model, this can now be used to analyse the annual performance of all Solar Thermal systems in more detail. Test systems 1 and 2, for which accurate control data is available, will be analysed first to strengthen the robust verification of the model.

11.7.1 Analysing Test System 1

The model can now be used to fill gaps in the measured data for Test System 1, while at the same time using the available data for further verification of accuracy. Monthly totals of all values throughout the recording period are shown in table Table 11.X.

Table 11.X: Estimating annual yield of Test System 1, using model and measured results

	Model (kWh)	Measured (kWh)	
		Cylinder temperature	Control panel
Jun-09	103.2		
Jul-09	96.9	104.4	
Aug-09	96.5	93.4	
Sep-09	63.1	77.5	
Oct-09	30.8		
Nov-09	10.0		18.0
Dec-09	4.6		
Jan-10	6.2		
Feb-10	17.7		33.0
Mar-10	62.1		74.0
Apr-10	77.5	92.6	105.0
May-10	109.4		128.0
Jun-10	116.8	120.6	162.0

Table 11.X only provides values that are suitable for estimating the solar energy generation. While there are temperature measurements available for the cylinder between October 2009 and March 2010, these are not used as the central heating system was switched on during that period. Figure 11.29 shows a graphical comparison of all values presented in Table 11.X.

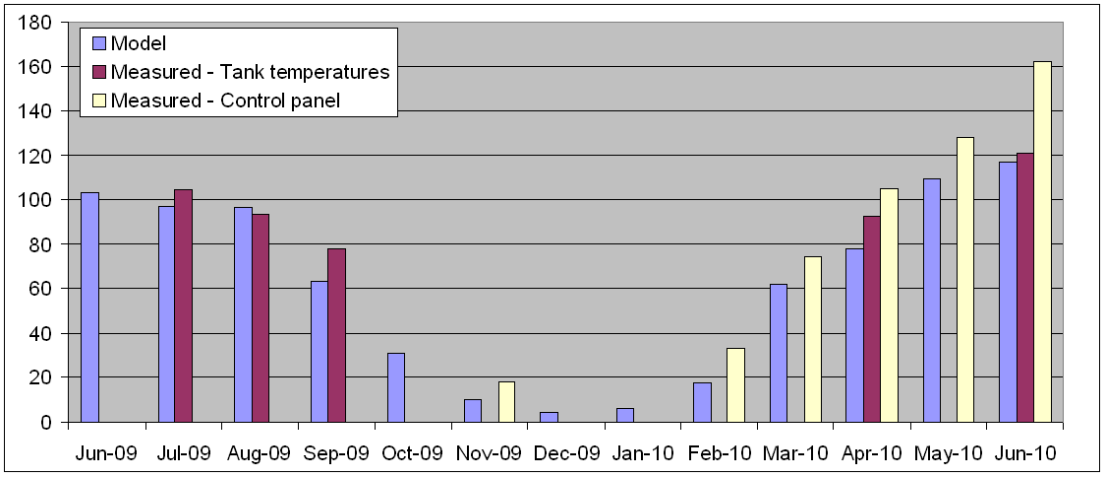

Figure 11.29: Monthly comparison of model and measured results, Test System 1

From Figure 11.29 it can be seen that there is a significant difference between energy output measured by the control panel and the model. Keeping in mind that the model was successfully validated and the flow rate setting of the control panel was found to be wrong, a significant difference was to be expected. Through a combination of wrong panel settings and the placement of temperature sensors that does not account for pipe losses, the control panel seems to consistently over-estimate the energy output. The average difference between monthly model and control panel totals is 29.2%, with standard deviation of 13.5%.

When comparing to monthly totals based on measured cylinder temperature, the model values show a good correlation, apart from the months of September 2009 and April 2010 where the model prediction is considerably lower. It has already been explained previously that the central heating was on for part of April 2010, the model validation month. To account for this, a boiler model was added and was able to account for the difference in energy input to the cylinder. As September is a seasonal transition month, similar to April, it is expected that the heating system being switched on part-way through the month is also the reason for the difference in energy added to the cylinder. A detailed examination of September results confirmed that this is the case, and the model can account for the difference if the simulated boiler is switched on after 17th September.

When neglecting September 2009 and April 2010, the average difference between the model and energy based on measured cylinder temperatures is 4.5%, with standard deviation of 2.3%. This confirms that the model has a very acceptable margin of error of less than 5% based on standard deviation. Using the model, the useful annual solar output can now be calculated for the test site and is presented in Table 11.Y.

Table 11.Y: Annual yield of Test System 1

Year	Useful Solar Energy
July 2009 - June 2010	692 kWh

Solar fraction

In order to calculate the solar fraction, the hot water demand must first be established. The previously estimated hot water demand was around 65L per day. Assuming that the cold feed temperature is approximately 15°C as justified previously, and hot water temperature varies between 50-60°C. This gives a temperature increase of approximately 40°C. Using equation (11.31) the daily hot water energy can now be calculated, where subscript 'cf' refers to cold feed temperature.

$$Q_{HW} = mc_f (T_{HW} - T_{cf}) \tag{11.31}$$

Using the parameters described above the energy required for daily hot water consumption is 10.9MJ, or 3.0kWh. Annually, this means that the test family consumes about 1100kWh for water heating. The solar fraction can now be estimated using equation (11.32) based on results from previous system modelling.

$$f = \frac{Q_{Sol}}{Q_{HW}} \tag{11.32}$$

$$f = 62.9\%$$

The calculated solar fraction is rather high, considering typical solar fractions of domestic solar thermal systems are estimated to be in the order of 40-50%[191] by the Energy Saving Trust. This is probably a result of the near optimum combination of system size, cylinder size and hot water consumption, as indicated during previous analysis.

11.7.2 Analysing Test System 2

As mentioned previously, modelling of test system 2 was rather difficult due to a lack of consistent quality data and a variable flow rate of the system. Nonetheless, the validated solar model should still provide a good indication of the energy generation of system 2 between July 2009 and June 2010. The temperature data of the solar flow and return pipes was available for 4 months, providing some control data for the model output.

It was previously identified that test system 2 uses unfavourable boiler settings, with the boiler being set to come on before, during, and just after peak hot water consumption. While the boiler is on it maintains approximately two thirds of the hot water cylinder at 50°C, leaving only the bottom third of the volume able to absorb heat efficiently. The model results for this are labelled 'current boiler settings'. Ideally test system 2 should be set to only receive heat top-up from the boiler before peak hot water draw-off, giving more cold water volume to absorb solar heat efficiently. The model results for this case are labelled 'optimised boiler settings'.

Figure 11.30 shows a comparison of modelled results for the current boiler settings and optimised boiler settings, as well as estimated generation based on available measured data.

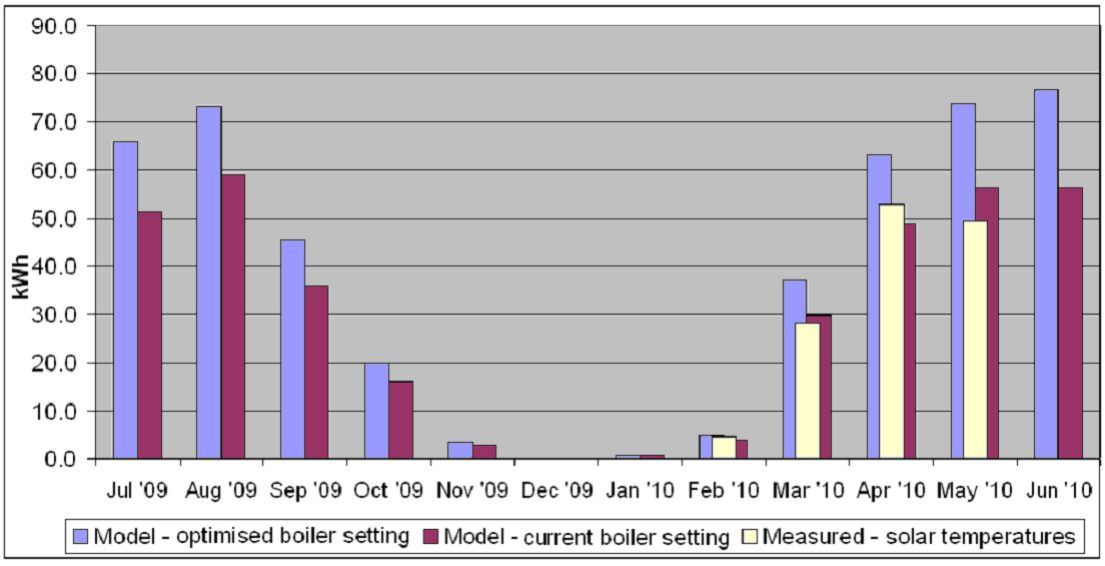

Figure 11.30: Comparison of modelled generation for different boiler settings and estimates based on measured data

Despite the uncertainties Figure 11.30 shows a good correlation between modelled results using current boiler settings and the estimates based on measurements.

Annual generation estimates between July 2009 and June 2010 for test system 2 are provided in Table 11.Z, comparing the two modelled boiler settings.

Table 11.Z: Modelled annual yield between July 2009 and June 2010

	Annual yield (kWh)
Current boiler settings	361
Optimised boiler settings	464

Table 11.Z shows an expected annual yield of 361kWh. This is 48% lower than Test System 1, which is a very similar system albeit slightly larger. This difference can be largely explained by the fact that the hot water cylinder for Test System 2 is much smaller than the cylinder for Test System 1, with 80% less capacity. This means that overall less volume is available to absorb heat, and this reduced volume will also heat up quicker, reducing the transmission efficiencies even further.

The unfavourable boiler settings also play a significant part, as explained previously. Modelling of optimised boiler settings shows an improvement in annual yield of 103kWh, which would provide 29% more energy than using current settings.

Based on the daily hot water draw-off profile of 120L, the daily hot water energy consumption is estimated to be around 5.6kWh/day, or 2030kWh annually. This provides the following solar fractions:

$$f_{current} = 17.7$$

$$f_{optimised} = 22.8$$

This means that currently around 18% of the annual hot water demand is satisfied by solar energy. The solar contribution could potentially increase to 23% if the boiler settings were optimised.

11.7.3 Analysing EcoSmart Alderney System

Having validated the solar thermal model thoroughly using data from both test systems, the model can now be used to provide a theoretical simulation for the evacuated tube system that was installed at the EcoSmart village. Table 11.AA shows the system parameters that were used for the modelled simulation.

Some of the parameters were not disclosed by the manufacturer. Values including the area-related heat capacity, the transmittance value, and the angle

modifiers were assumed to be the same as for Test System 1. The flow rate of the Alderney system is stated as 2.5L/min, which is considerably higher than the 1L/min used by Test System 1. As explained earlier, while an increased flow rate is not usually considered beneficial, the model is rather sensitive to any significant increases above 1L/min due to the 10-minute time steps. To avoid falsifying any results the flow rate in the model was left at 1L/min. The hot water draw-off was assumed to be 200L daily, drawn off at 12:00. The boiler model was used to simulate heating of two thirds of the storage volume to 55°C at 6am, and it was also used to constantly maintain the bottom cylinder temperature at a minimum of 30°C.

Table 11.AA: Input parameters for EcoSmart Village Alderney system modelling

System	Latitude	53.4	°
	Longitude	-2.4	°
	Collector inclination	45	°
	Collector orientation	0	°
Collector	Aperture area	3	m^2
	Absorptance	0.93	
	Emittance	0.06	
	Area-related heat capacity	8.3	kJ/Km^2
	Zero-loss efficiency	0.753	
	Angle modifier transverse	1	
	Angle modifier longitudinal	0.9	
	Angle modifier	0.9	
	c1 coefficient	1.54	W/Km^2
	c2 coefficient	0.01	W/K^2m^2
Cylinder	Cylinder capacity	250	L
	Cylinder height	120	cm
	Cylinder diameter	55	cm
	Cylinder U-value	2.5	W/Km^2
	Distance collector to cylinder	5	m
	Pipe diameter	15	mm
	Typical ambient temperature	25	°C
Control	Transfer flow rate	1	L/min
	Control temperature difference	7	°C
	Boiler control - on (temp.)	55	°C
	Boiler control - off (temp.)	55	°C
	Safety shut down (max temp)	70	°C

Figure 11.31 and Figure 11.32 show a comparison between the f-chart method that was previously used to obtain an initial estimate, the model, and the measured data that was recorded manually from the control panel of the solar thermal system.

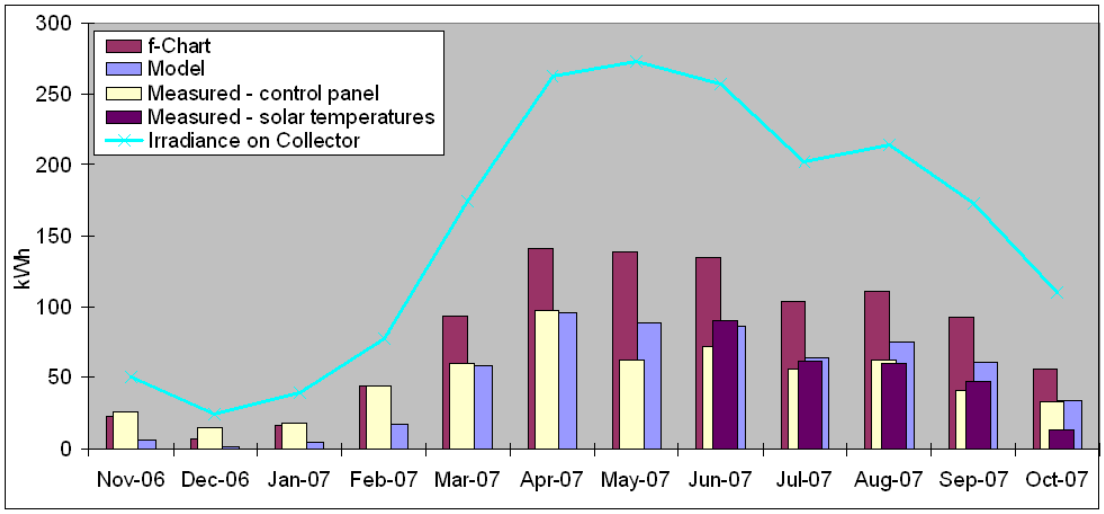

Figure 11.31: Comparison between f-chart method, solar thermal model and measured results over a 12 month period

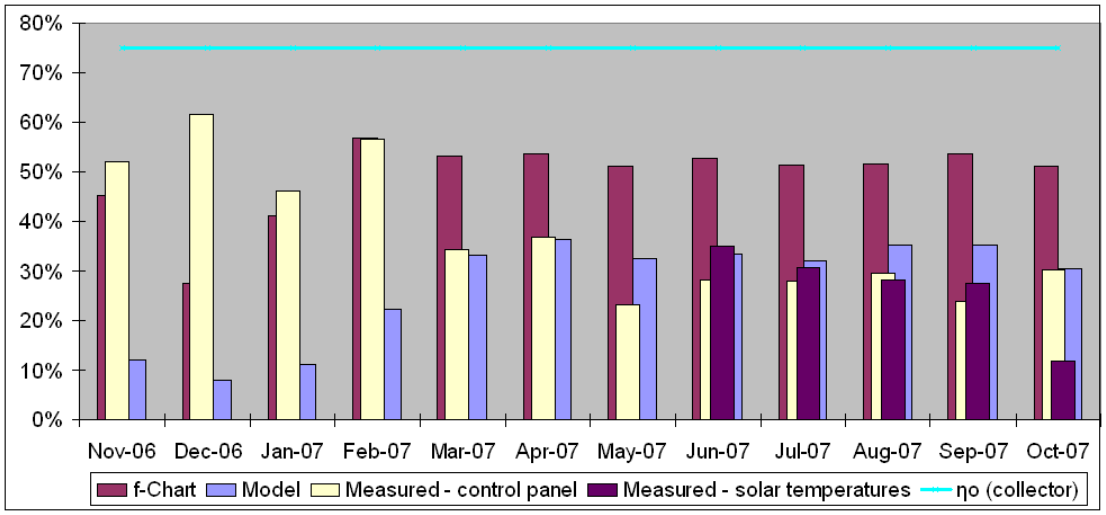

Figure 11.32: Comparison between monthly average efficiency of the Alderney evacuated tube system, using f-chart, model and measured results.

Figure 11.31, showing the monthly generation, indicates that while the model is proportional to the f-chart method, the f-chart consistently shows a significantly greater output, in the order of 50%. This percentage difference is further magnified during the winter months. While the model estimates a total output of 12.4kWh during November, December and January, the f-chart method estimates 45.4kWh for the same period. This over-estimation by the f-chart method, particularly during winter, can be explained by the fact that it does not consider interaction with the storage cylinder, nor does it consider any input from the boiler. While the f-chart method is able to estimate the amount of energy that is available to an infinite cold

storage volume, the model goes several steps further to consider constraints from storage size, stratification effects, draw-off patterns and boiler top-up.

Figure 11.32, showing the average monthly system efficiencies, confirms the observations. The f-chart method shows a significantly greater efficiency than the model for every month of the year, particularly during the winter. This is to be expected considering that only the model accounts for boiler interaction, as overcoming the temperature difference to the pre-heated storage cylinder becomes more difficult during the winter.

The measured results that were obtained from the control panel are inconsistent with both f-chart and model estimates. During summer months efficiencies are relatively low, while during winter efficiencies above 60% are presented, which is considerably greater than what is predicted by the inherently over-estimating f-chart method.

The collector has a fixed heat capacity, giving it a thermal inertia. When there is no direct solar radiation on the collector during the day, the material of the collector cools down to ambient temperature. This needs to be overcome first before any heat transfer can take place. During the winter, ambient temperatures are usually considerably lower, meaning more energy is required to bring the materials that make up the collector to a temperature that allows heat transfer. In addition to this, the proportion of energy required to overcome the thermal inertia with respect to the solar energy that is available is much greater during winter than it is during summer. On the other hand, due to its vacuum insulation the temperature dependence on the heat loss factor (given by c2 coefficient as described in BS EN 12795[218]) for any evacuated tube collector is very low, in the order of 0.01. With this in mind, it must be expected that the system efficiency, in other words the useful energy output to the storage cylinder with respect to available solar radiation as seen on the collector surface, is significantly greater during summer than it is during winter. This is confirmed by both model and f-chart simulations.

Considering the above, the values from the control panel do not appear to make much sense. When considering that the zero-loss efficiency (η_0) of the collector is given as 73.5%, this would mean that 84.4% of the solar energy that is absorbed by the collector during December ends up in the pre-heated storage cylinder. This is unlikely to be true, as most of the solar energy is already required to overcome the temperature difference between ambient temperature and water temperature in the cylinder. It appears that just as previously experienced with Test System 1, the energy output that is calculated by the control panel based on temperature and flow rate is rather inaccurate.

To summarise the comparison, it would appear that the solar thermal model which has been validated thoroughly gives the most accurate estimate of actual

energy generation for the EcoSmart Village system. The trend of monthly variation that can be observed from the control panel values, especially during the winter, suggests that these are inaccurate. Similarly, the generation values calculated based on flow and return temperatures have limited accuracy, particularly during winter months, due to the 10-minute logging interval in combination with a high flow rate of the system. The f-chart method can provide a good indication for the performance of optimised systems, but lacks the important consideration for interaction with a storage cylinder, and is therefore prone to significantly overestimating the output of most real life Solar Thermal installations.

11.7.4 Improving EcoSmart Alderney System

It was previously discussed that the Alderney evacuated tube system showed a significant under-performance compared to the Windermere flat-panel system. This was on first consideration a surprise, given that the superior performance of evacuated tube systems had already been established. This result was largely attributed to unfavourable boiler control. In order to evaluate the system performance under improved conditions, the model was used with the following changes:

- the bottom cylinder temperature is no longer maintained at minimum 30°C
- the boiler only comes on once in the evening at 19:00, heating layers 2 and 3 (67% of total capacity) up to 55°C

It is recognised that for convenience and to avoid the questionable[233] occurance of Legionella bacteria breeding, the boiler should come on at least once a day to ensure a comfortable and safe hot water temperature near 60°C is maintained. Results of a survey[234] among solar hot water users found that around 65% of users have their boilers set to come on regularly both in the morning and the evening. However, it is more beneficial for this to happen in the evening, rather than in the morning, or both. For this case, after the storage volume has absorbed all available energy from the sun, minimal amounts of heat must be added to reach 55°C. The water can then be used either in the evening or the following morning, effectively cooling the storage volume and thus allowing it to absorb a maximum amount of solar energy the following day. If the water is heated in the morning instead, it is likely that less hot water is used between boiler top-up and the next solar cycle. In addition to this, any heat that is lost from the cylinder over night would also need to be topped up again by the boiler, should it be set to come on in the morning. These over-night losses can be as much as 6°C over 12 hours, which can be 1.2kWh per day for a cylinder of 250L capacity, or 424kWh per year.

Figure 11.33 provides a comparison of model estimates for the EcoSmart Alderney (evacuated tube) system for the original boiler settings and the improved boiler settings outlined above.

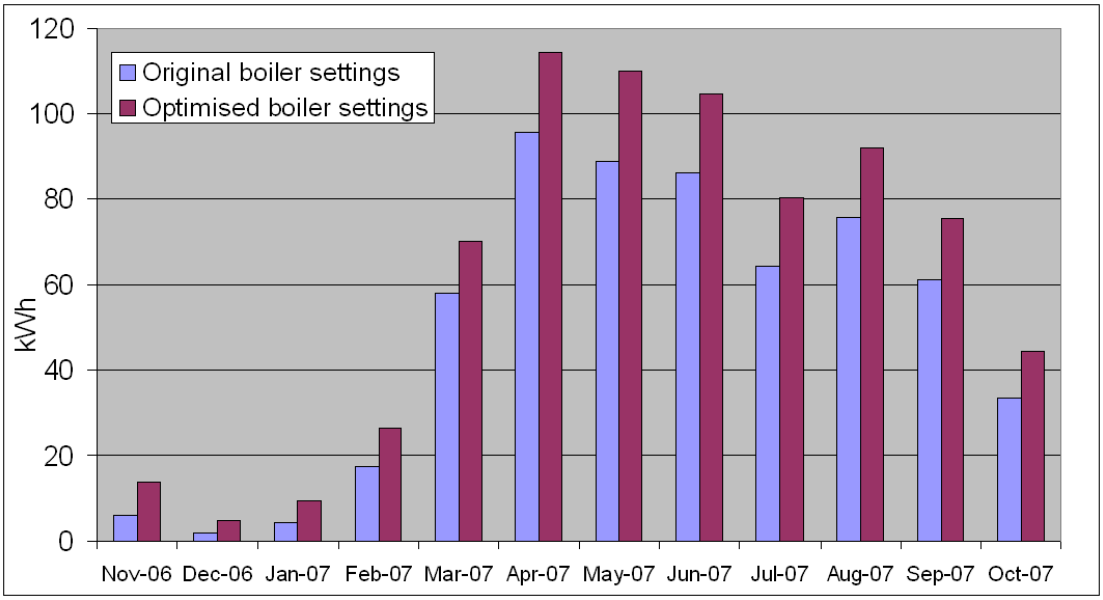

Figure 11.33: Comparison of effects of boiler setting on annual yield of EcoSmart Alderney solar system

Figure 11.33 shows a significantly increased output across the whole year if boiler settings are improved as described. In particular the winter months November, December and January show improvements of over 100%. Over the whole year, the optimised boiler settings are able to provide an increase in energy output of 25.9%. Table 11.BB compares the annual results for both scenarios.

Table 11.BB: Performance of Alderney evacuated tube system with optimised boiler

	Original boiler settings	Improved boiler settings
Annual yield (kWh)	592	746
Annual efficiency	32.5%	36.4%
Gas consumption (kWh)	1801	933

As already indicated by Figure 11.33, the improvements are significant. Not only are an additional 154kWh of energy generated, meaning the efficiency of the system is increased by 12%, but gas consumption is nearly halved. With less gas required to maintain a base temperature of 30°C and with additional heat generated by the solar system, the overall gas consumption is severely reduced. With other energy savings from avoided over-night storage losses and other avoided auxiliary losses (for example boiler efficiency or losses in pipe work from boiler to storage cylinder) which can be quite significant[235], the estimated annual

gas savings are 868kWh, or 48%. For comparison, the measured annual gas consumption of the overall colder Windermere, which has a smaller and less efficient flat-panel system, is around 915kWh.

11.7.5 Analysis Vertical Solar Thermal Panel

Previously it was discussed that a vertical collector may help to satisfy the hot water requirements throughout the year more consistently. For modelling purposes the same data was used as for the EcoSmart Village Alderney system, the only exceptions being that the inclination was set to 90° and the aperture area was doubled, now giving 6m^2. The results are shown in Figure 11.34, with results from Alderney system modelling at inclination of 45° for comparison.

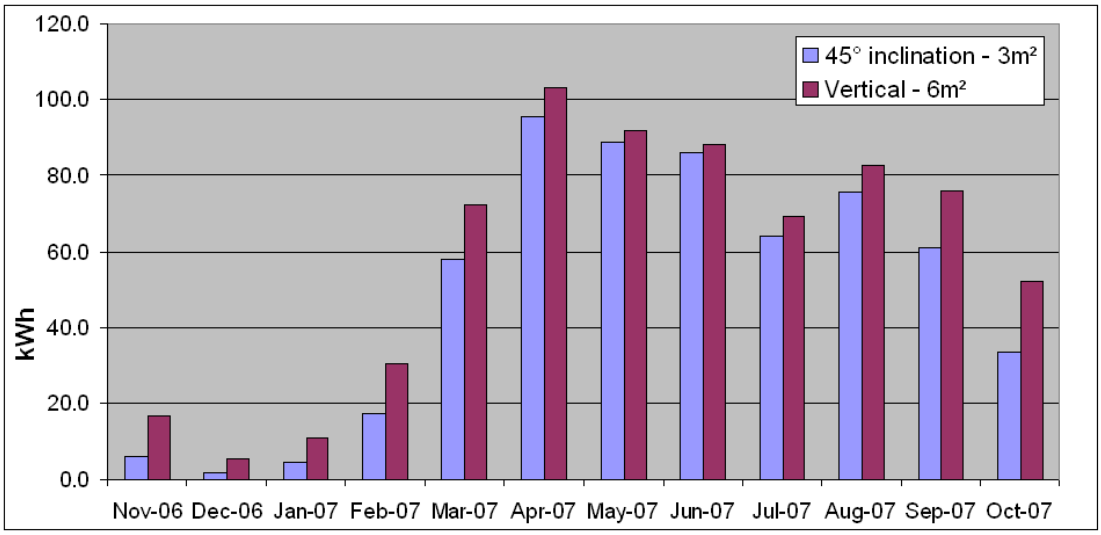

Figure 11.34: Comparison between solar thermal generation of collector inclined at 45° and vertical collector with twice the area

Figure 11.34 does indeed show a considerably higher output by the vertical system during the winter months, with 162% additional energy generated between November and January at 100% extra collector area. The summer months show a similar output between the two options, confirming that over-heating would not be any more likely.

However, throughout the whole year the improvement in energy generation is only 106.2kWh (17.9%), bringing the annual yield to 698kWh. Even considering that the extra energy can be considered more valuable to the household as it is generated during typical low-yield months, it comes at a high price considering the additional cost of doubling the collector area. Based on a preliminary financial anlysis, it must be concluded that from a financial point of view it is not worth installing a solar thermal system vertically and doubling the area. However, if a

cheap way is found to harness solar thermal energy, perhaps by using a simple flat panel system instead of evacuated tubes, then it may be considered as an option. The advantages are that a higher proportion of energy is generated during the winter, and roof space remains available for other alternatives such as PV.

11.8 Financial, Energy and Carbon Savings

The energy output of the system, and therefore annual savings and payback periods, are largely dependent on hot water requirements as well as user habits. Ideally the Solar Thermal system would constantly require a reservoir of cold water, to which the heat energy can be transferred at high transmission efficiencies.

The control system also plays a crucial role in Solar Thermal generation efficiencies. The example of the Alderney system showed, that if the system is set to maintain a certain minimum temperature, the energy output is significantly decreased. On the other hand gas consumption also increased for these settings, adding to the overall high energy consumption of the building.

Due to the uncertainties, payback and carbon savings should always be assessed for individual systems, taking into account as many aspects as possible such as variations in hot water demand and boiler settings.

To provide a comprehensive overview and comparison, payback periods will be estimated for the following cases:

1. EcoSmart Village Windermere (south-facing flat panel) system based on measured results
2. EcoSmart Village Alderney (south-facing evacuated tube) system based on modelled results
3. EcoSmart Village Alderney (south-facing evacuated tube) system with optimised boiler settings based on modelled results
4. Test System 1 (west-facing evacuated tube) based on modelled results
5. Test System 2 (southwest-facing evacuated tube) based on modelled results, using current boiler settings
6. Test System 2 based on modelled results, using optimised boiler settings
7. Vertical EcoSmart Village Alderney (south-facing evacuated tube) with double collector area based on modelled results

The lifetime of Solar Hot Water systems can be assumed to be around 25 years[236] with theoretically no requirement for maintenance[237].

Results of financial, energy and carbon payback calculations are shown in Table 11.CC, Table 11.DD and Table 11.EE.

Table 11.CC: Summary of system cost, energy and carbon

Case	Annual Yield (kWh)	Capital Cost (£)	Embodied Energy (kWh)	Embodied CO_2 (Kg)
1	462	£2600	1680	430
2	592	£3500	2400	615
3	746	£3500	2400	615
4	692	£5500	2400	615
5	361	£6300	1850	475
6	464	£6300	1850	475
7	698	£6500*	4800	1230

*Approximation based on doubling the collector area but maintaining similar installation cost

Table 11.DD: Financial annual savings

	Annual Savings	
Case	Gas offset	RHI tariff
1	£18.48	£83.16
2	£23.68	£106.56
3	£29.84	£134.28
4	£27.68	£124.56
5	£14.44	£64.98
6	£18.56	£83.52
7	£27.92	£125.64

Table 11.EE: Payback rates and lifetime savings; financial, energy and carbon

	Payback rate (years)			Net savings over system life (25 years)		
Case	Financial	Energy	Carbon	Financial	Energy (MWh)	CO_2 (t)
1	50.7	3.6	4.2	-£475	9.9	2.54
2	57.8	4.1	4.7	-£777	12.4	3.26
3	27.3	3.2	3.7	-£68	16.3	4.10
4	83.7	3.5	4.0	-£2,317	14.9	3.81
5	346.3	5.1	5.9	-£4,639	7.2	1.53
6	249.4	4.0	4.6	-£4,166	9.8	2.10
7	142.8	6.9	8.0	-£3,289	12.7	3.84

When comparing the cases that were analysed during this research, it is shown that assuming the systems work as they were modelled, none of them achieve financial payback over their lifetime. While the RHI tariff helps greatly to improve payback rates, the relatively low gas price means that after 20 years when the tariff is no longer available annual savings become very small compared to capital investment. For the four real-life cases (cases 1, 2, 4 and 5), financial payback rates are at least double the expected system life. The RHI contributes to reducing lifetime losses to £475-£4,639, where the flat panel system appears to provide the best value for money. If the boiler settings for the EcoSmart Village Alderney case would be improved, financial payback could be achieved after around 27 years, with only

about £70 lifetime losses. For test system 2 the optimised boiler settings would mean around £470 less is lost over system lifetime. The vertical option is rather poor, generating a financial loss close to £3,300 after 25 years of operation. However, if future capital cost predictions[237] prove to be correct, financial payback may become achievable in the medium to long term.

The estimated embodied energy of all Solar Thermal systems is offset fairly quickly, with payback ranging between 3.2-6.9 years. This allows net energy generation of 7.2-16.3MWh over system lifetime. Apart from Test System 2 which suffers from a small hot water cylinder, the Windermere flat panel system is able to generate least energy, while the Alderney system with optimised boiler settings would generate more than any other case presented.

A similar picture is presented for CO_2, with the embodied amount being offset after 3.7-8.0 years. This allows a total CO_2 offset during system lifetime of 1.5-3.8 tonnes. Again, the south-facing Alderney system with optimised boiler settings would prove to be most beneficial for the environment, while Test System 2 and the Windermere flat panel system are able to offset the least amount of carbon.

For comparison, Table 11.FF provides an overview of the energy and carbon payback estimates from other research.

Table 11.FF: Energy and CO_2 estimates from other research

System details	**Location**	**Energy payback** (years)	**CO_2 payback** (years)
FP, integ. storage, displacing gas	Australia	2.5[238]	-
Flat Panel, simple payback	Australia	2.5[238]	-
FP, integ. storage, no cylinder / pipes	Italy	0.5-1.6[239]	-
Flat Panel, integrated storage	Italy	2.5[208]	-
Flat Panel, simple payback	Canada	7.5[207]	<4
Flat Panel, simple payback	UK	2.6-6.1[209]	3.5-8.2
Flat Panel, simple payback	UK	3.0-5.2[235]	<2

The comparison with other research shows similar results, confirming the scalability of the analysis carried out for this project. Only the CO_2 payback shows some inconsistencies, which will likely be due to the variation in modelling parameters of the solar systems.

11.9 Visitor Feedback

The Buckshaw EcoSmart show village was open to any visitors, all of whom were asked to fill in a feedback questionnaire, asking for opinions of the set-up as well as individual systems.

As shown in Figure 11.35, the feedback on solar thermal systems was largely positive, with 91% of visitors stating they find solar thermal appealing, with 72% stating they found it extremely appealing. 21% of visitors definitely intend to buy a system, while a further 38% stated they would probably buy one. However, when asked for a maximum price at which they were willing to invest in a solar thermal system, assuming 2005 estimated payback rates, only 32% were willing to spend more than £1,500.

In the overall ranking of all systems tested at the EcoSmart show village the solar thermal system ranked first.

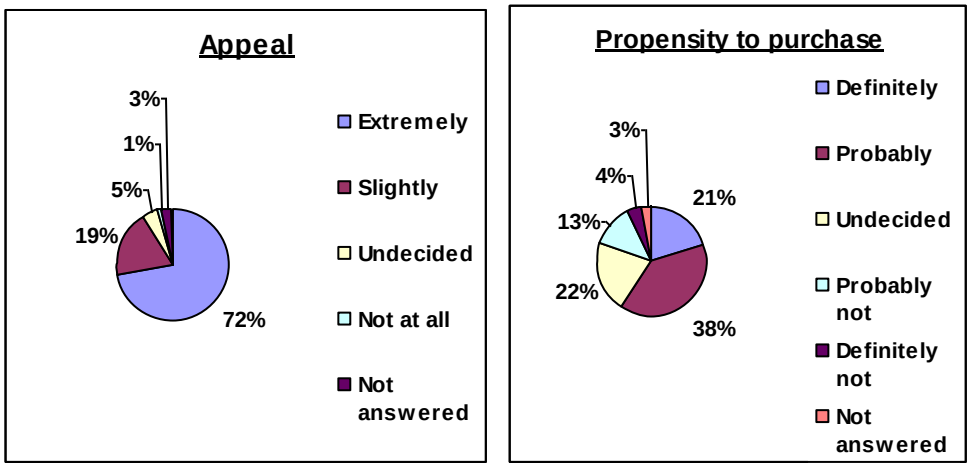

Figure 11.35: Statistics from feedback questionnaire. Source: SMS Market Research Summary Report

11.10 Conclusion

After analysing 4 different domestic Solar Thermal systems and attempting to set up an experimental test rig, the main conclusion to summarise the experiences is that Solar Thermal systems are very complex. In order to work well, many different aspects need to be considered, resulting in a high probability of mistakes that can severely impact energy generation. Specifically, this includes:

- Installation must be carried out by experienced professionals, and even then there is a chance of making mistakes that are very difficult to notice

but can cause severe underperformance of the solar system in the short and long term. Such mistakes were made during the installation of 4 out of the 5 test systems.

- Boiler control settings can make a significant difference to the efficiency of solar energy generation, hence solar energy output. Modelling has shown that this can make a difference in performance of over 25%. This was found to be a problem with 3 out of the 4 domestic test systems. A survey[234] of over 50 Solar Thermal households found that 65% use highly unfavourable boiler control settings, which can reduce the Solar Thermal generation by up to 75%.

- An efficient interaction between the solar system and the hot water storage cylinder must be ensured. If the storage size is too small, or doesn't contain a dedicated solar volume (as provided by a dual coil cylinder), the solar system will not be able to perform well. This was found to be a problem with 1 of the test systems.

- Energy readings provided by the control panel are sometimes not accurate. This means users can be misinformed about the performance of their solar system, and it further reduces the chance of noticing any mistakes made during installation. This was found to be the case with 2 of the 4 domestic test systems. For the other 2 domestic cases, energy estimates were not available at all due to missing sensors.

Further conclusions that can be derived from the analysis are:

- If a Solar Thermal system works well, it can be expected to reach average efficiency levels of 35-40% for evacuated tube systems, and around 25% for flat panel systems. This equates to an annual yield for typical south facing evacuated tube and flat panel systems of around 700kWh and 450kWh respectively.

- RETScreen can be considered a valuable tool for solar generation estimates during the design stage. Being predominantly based on f-chart methodology, it is prone to overestimate by around 15-30%, but requires relatively little information about the proposed system. T*Sol may also of value, although its exact methods are not disclosed and a license fee is charged.

- Visitors to the EcoSmart village found the solar thermal systems very appealing, ranking it first out of all systems that were tested. UK-wide research confirms this trend, showing there are more solar thermal systems installed nationwide than any other micro renewable system.

- The solar thermal systems that were evaluated during this research did not achieve financial payback after RHI tariffs. However, the carbon offset of a net amount of 2.5-3.8 tonnes of CO_2 over 25 years is substantial. Energy payback periods of the systems are in the order of 3.2-4.1 years.

12 Micro Wind Turbine Systems

In recent years urban micro wind applications have received much publicity, being an emerging technology that promises to be a very effective part of a solution to reducing carbon emissions. However, the lack of robust field data causes much speculation and debate among academia and government alike. The measurements taken from the EcoSmart test systems and the analyses set out below will help to provide a clarification over the real performance of building-integrated micro wind turbines, and what role they might play in achieving zero carbon homes.

12.1 Introduction

Large wind turbines are popular in many countries, and the achieved economies of scale have recently made them very worthwhile[240].

Applying wind generation at a small scale appears promising at first glance. In theory, the performance of small and micro scale wind turbines has been shown to be beneficial[241]. It also makes sense to move the energy source as close to the consumer as possible to avoid any transmission losses[242]. Clausen et al[243], for example, saw potential for micro wind, but also noted that technology had not reached the maturity of larger turbines.

However, it was also found in other research that manufacturers generally tend to over-estimate the projected output significantly, using average wind speed data from higher altitudes[244] or neglecting turbulence effects[245]. Some literature also suggests that horizontal axis turbines are inherently unsuitable for urban applications[246] due to the complex wind patterns generated by this environment[247]. Focusing on problems associated with wind generation in urban environments, Eliasson et al[248] measured counter-rotating vortices within the canyons, wind shear along canyon edges and high degrees of turbulence, even at low wind speeds. Wind tunnel simulations[249] showed strong evidence that sharp flow accelerations develop around roof tops, causing high fluctuations of horizontal velocities.

Despite some tentative warnings and concerns, in 2006 building-integrated micro wind energy was predicted to have a prosperous future[250].

12.1.1 Background Theory

Horizontal axis turbines are by far the most common type of micro wind turbine. Essentially, they consist of a number of blades rotating about a horizontal axis, driving a generator that uses this motion to generate electricity. Many blades are used when a high moment of inertia is desirable, while fewer blades are better for applications where a low starting torque and high end speed are required.

Aerodynamics

The blades attached to the rotor act as airfoils. The blades are designed such that when a certain wind speed is reached (typically about 3 m/s) the resultant lift force in the radial direction can overcome internal resistant forces and start to spin the rotor. As the blades begin to turn, another velocity vector is introduced, caused by the blades cutting through air in the direction of movement. The lift force then creates the resulting driving force of the system, as shown in Figure 12.1.

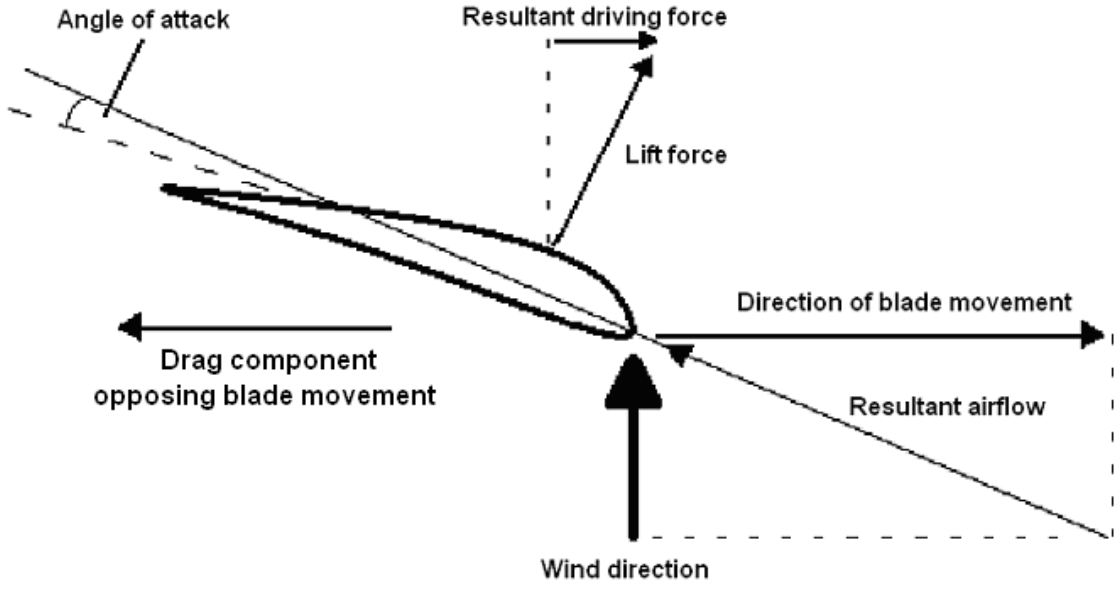

Figure 12.1: Forces acting on single turbine blade

Care must be taken to design the blades for a given optimal tip-speed ratio, referring to the ratio between wind speed and blade speed. For optimum performance the blades are usually twisted, such that the root of the blade is predominately orientated into the wind, whereas blade tips are orientated in the radial direction to account for the variation in relative radial velocity.

The Wind Power Equation

Derived from linear momentum theory[251], the power contained by the wind is given by equation (12.1).

$$P_0 = \frac{1}{2}\rho A\, u^3 \qquad (12.1)$$

However, as the air is still moving away from the rotor after it has passed through it, it is clear that not all power can be extracted from the wind. The maximum extraction efficiency, referred to as the power or performance coefficient (cp) is limited to 59% as defined by Betz's law[252]. The power generated by the turbine is therefore given by equation (12.2):

$$P_T = cpP_0 = cp\frac{1}{2}\rho A\, u^3 \qquad (12.2)$$

The actual value of (*cp*) largely depends on the tip-speed ratio of the blades, which is the ratio of rotational speed over wind speed. If the blades move too slowly in comparison to wind speed, a large part of the wind will pass through the turbine blades without losing any of its energy. If on the other hand blades move too fast, then the turbulent air from one blade will affect the next blade, reducing aerodynamic efficiency. The tip-speed ratio is mainly a function of the number of blades, but is also affected by the controller of the turbines as well as blade design[253].

A challenge for rotor design is to achieve this optimal tip-speed ratio at different wind speeds. In order to ensure a good efficiency the rotor must have a low moment of inertia about its horizontal axis. If the blades move faster than optimum, an electro-mechanical system can be used to monitor and adjust the tip-speed ratio to an optimal value. This system can also be used to restrict the rotor to a maximum radial velocity for safety reasons.

There are further losses other than the variation in tip-speed ratio, mainly resulting from the generation and conversion of electric power due to mechanical friction and unavoidable leakage of the electric field. Overall efficiencies of wind turbine generators are typically in the range of 30-40%.

12.1.2 EcoSmart Village Set-up

Figure 12.2: StealthGen wind turbine (left) and Windsave wind turbine (right)

Two different wind turbine models were tested at the EcoSmart village, the Windsave WS1000 and the StealthGen D400, both shown in Figure 12.2. The Windsave model was installed on the roofs of the Buckingham and Edinburgh, while the StealthGen was installed on the Alderney, Malvern and Windermere. The turbines were installed with around 1.5-2m clearance from the roof top, which is similar to any domestic micro wind turbine arrangement. The effective hub height is around 8m. The weather station used to record wind data was mounted in a similar position on the roof of the Edinburgh home. The specifications of both turbines, as provided by manufacturer technical documentation, are summarised in Table 12.A.

Table 12.A: Wind turbine specifications

	Windsave	**StealthGen**
Diameter (m)	1.75	1.1
Area (m^2)	2.4	0.95
Rated power (kWh)	1.0	0.4
cut-in speed (m/s)	3.0	2.5
cut-off speed (m/s)	12.5	16
Warranty (yrs)	10	1

While the StealthGen model has a smaller area, it has been optimised for high performance at low wind speeds, and has a greater wind speed range than the larger Windsave model. Power curves for both turbine models are also available, shown in Figure 12.3 and Figure 12.4, which were extracted from the technical manuals of the turbines.

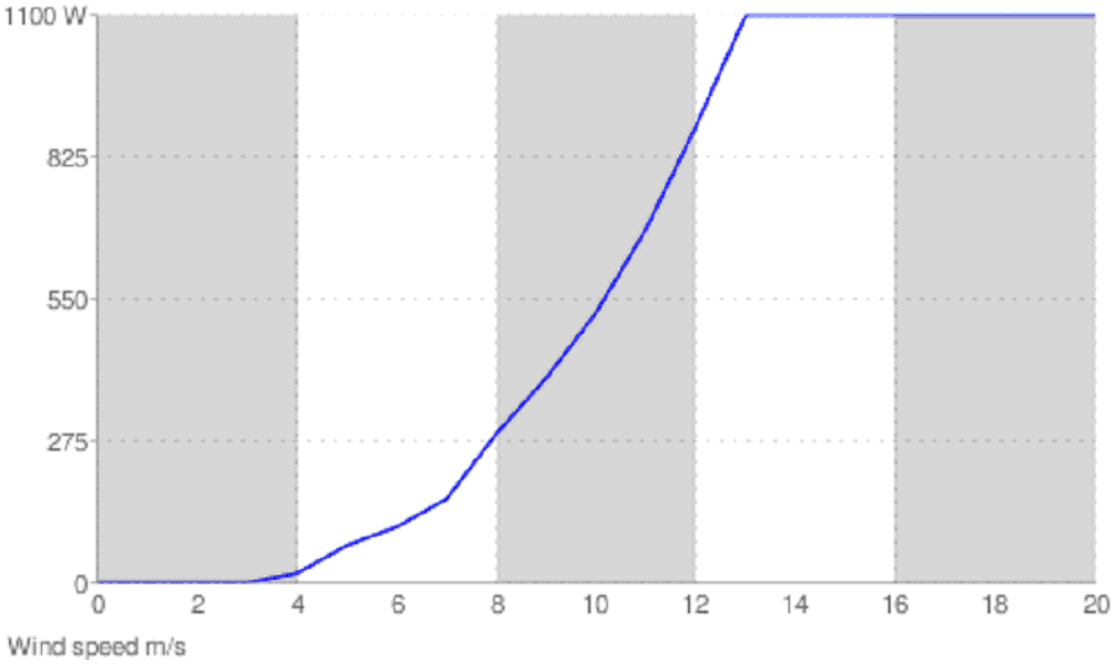

Figure 12.3: Power curve for Windsave WS1000 (Source: Windsave WS1000 datasheet)

Figure 12.4: Power curve for StealthGen D400 (Source: StealthGen D400 User's Manual)

The two wind turbine power curves indicate that the larger, 3-blade Windsave model has a reasonably constant coefficient of performance (cp), whereas the cp value for the 5-blade StealthGen model seems to vary significantly with wind speed.

Similar to the PV system, both turbine models are connected to an inverter and an import/export meter. Figure 12.5 shows a schematic diagram of the system layout, which also includes a picture of the inverter.

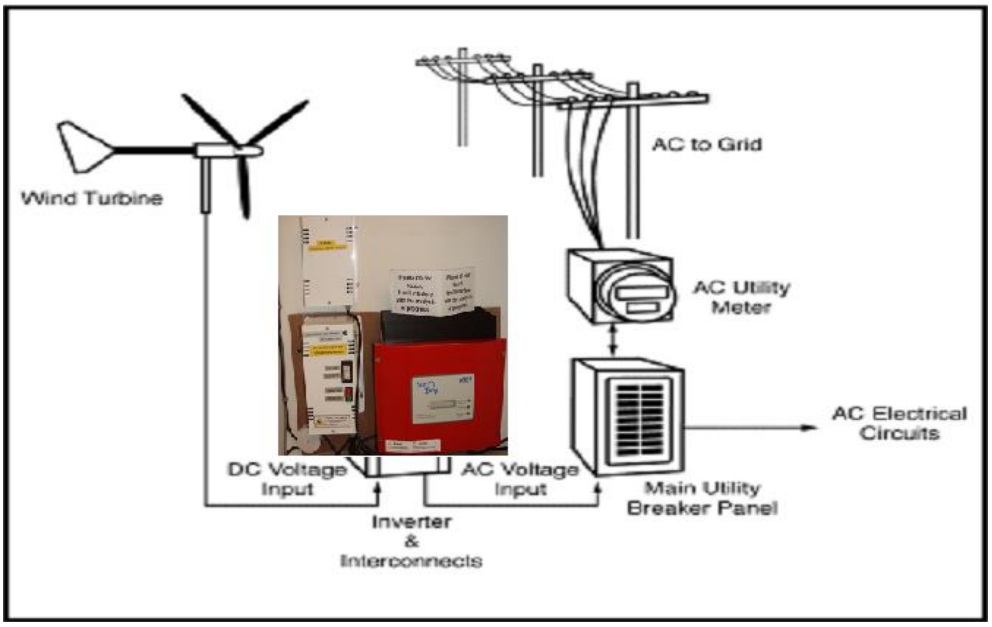

Figure 12.5: Schematic diagram of Wind Turbine system layout

12.1.3 Capital Cost, Embodied Energy and Embodied CO_2

This section will analyse the capital cost and embodied energy and carbon of the two micro wind turbines. As generic values for embodied energy and carbon are difficult to find for wind turbines, especially for small-scale models, they will be estimated based on components. Methods and ratios will be applied that are derived from other research.

Capital Cost

The capital cost of the micro wind turbine systems at the EcoSmart village is summarised in tab.

Table 12.B: Capital cost of the micro wind turbine systems

Windsave WS1000	StealthGen D400
£1,500	£2,250

Embodied Energy

Detailed analysis of embodied energy has previously been covered by other research. Lenzen and Munksgaard[254] for example released a very comprehensive study for a range of different sized wind turbine systems, covering over 50 case studies and an in-depth literature review. The relative mass and respective specific energy content of different components is summarised in Figure 12.6.

Component	Main material	Relative mass (%)	Energy content (MJ/kg)
Blades	Glass fibre, epoxy, PVC	2.7	61.8±35.7
Hub and mounting	Steel	3.5	36.8±18.5
Transmission	Steel	5.2	36.8±18.5
Generator	Copper	2.6	86.2±65.5
Nacelle cover	Glass fibre	0.3	61.8±35.7
Tower	Steel	23.3	36.8±18.5
Foundations	Concrete	60.3	3.2±1.9
Electrical	Copper	2.1	86.2±65.5

Figure 12.6: Typical ratios of component weight and specific energy content of their raw materials (Source: Lenzen & Munksgaard[254], 2002)

Due to the vast amount of data used to estimate these relationships they will be used as a basis for the energy and carbon analysis of the EcoSmart village systems. However, as no tower or foundation is required for the building-mounted micro wind turbines, these factors will be omitted. Instead of this a new factor will be introduced to represent the embodied energy of the mounting pole and brackets.

The mass of the Windsave turbine is 25kg, while the StealthGen turbine has a mass of 15kg. The embodied energy of the pole and mounting brackets was estimated based on a mass of 20kg and the properties of aluminium[255]. Table 12.C provides a breakdown of the estimated embodied energy of each component as well as transportation.

Table 12.C: Estimated embodied energy of EcoSmart turbines, by component

	Windsave (kWh)	StealthGen (kWh)
Blades	90	54
Transmission	103	62
Generator	120	72
Nacelle cover	10	6
Electrical	97	58
Mounting	872	872
Inverter	430	430
Transportation	410	410
Total	**2,132**	**1,964**

From Table 12.C the embodied energy of the Windsave and StealthGen turbines are about 2,130kWh and 1,960kWh respectively. The difference is smaller than might be expected at first glance, but most of the energy, such as from the mounting pole, inverter or transport will be similar. However it must be noted that this only accounts for energy in materials and transportation, but does not include energy used in turbine assembly. This factor would be required for a thorough life-cycle analysis[256].

An analysis of a 300W turbine[257] estimated an embodied energy of 1,815kWh, which is similar to 1,960kWh for the simliar 400W rated StealthGen turbine. Therefore it can be said that while the estimates may be on the low side, they can be seen as providing adequate results for this analysis.

Embodied Carbon

Based on the weight and material distribution of components, the embodied carbon content can also be found. Values for embodied carbon are largely based on the Inventory of Energy and Carbon (IEC) database[255] published by the University of Bath. Table 12.D provides the estimated embodied carbon of the two turbines.

Table 12.D: Estimated embodied energy of EcoSmart turbines, by component

	Windsave ($kgCO_2$)	StealthGen ($kgCO_2$)
Blades	29.8	17.9
Transmission	18.1	10.9
Generator	15.6	9.4
Nacelle cover	3.3	2.0
Electrical	12.6	7.6
Mounting	166.0	166.0
Inverter	98.9	98.9
Transportation	113.0	113.0
Total	**457**	**426**

The embodied carbon can be expected to have similar levels of accuracy as the values derived for embodied energy.

12.2 Urban Wind Potentials

In order to estimate the potential generation of the micro wind turbines it must first be established how much energy is actually available. To do this, the main factors affecting generation, such as wind speed and turbulence intensity must be quantified.

12.2.1 Average Wind Speed

With reference to equation (12.1), the power contained by the wind is highly dependent on wind speed. Hence this is the predominant value that needs to be determined to assess the wind energy potential.

Wind databases exist, such as the NOABL (Numerical Objective Analysis Boundary Layer) wind speed database, currently maintained by the Department of Energy and Climate Change. This database appears to be the main source used by wind turbine manufacturers to establish site-specific potential power generation[258]. However, detailed impartial assessment[259] of the database revealed the following limitations:

- There is no allowance for the effect of local winds, such as mountain or valley effects
- The model is based on a 1 km^2 grid and does not account for topography on a small scale or local surface roughness
- Each value is an estimated average over an area of 1 km^2

It is further explicitly recommended that this data should be used "as a guide only, and followed by on-site measurements for a proper assessment"[260].

For comparison, the average wind speed from the NOABL database is compared to the measured average speed at several urban, low-level locations. Measurements were taken at a hub height of approximately 8-10m for each location. For NOABL estimates the lowest possible height above ground level, 10m, was chosen. Results are shown in Table 12.E.

Table 12.E: Difference between measured Average Wind Speed and NOABL database (Data source: NOABL and Turan et al.[258])

	Average Wind Speed (m/s)		Difference
	Measured (8-10m)	NOABL (10m)	(percentage)
EcoSmart Village, Chorley	3.1	4.9	58%
Sports Centre, Scotland	2.7	4.3	59%
Primary School, Buckinghamshire	3.8	6.3	66%
Reading University	2.8	4.8	71%
Heriot Watt University, Edinburgh	2.8	5.1	82%

Table 12.E shows that the NOABL estimated average wind speed for every location is about 60-80% greater than the measured value for each location. The main reason for this is suspected to be the lack of consideration for surface roughness in the NOABL database. The following section will discuss this effect in more detail.

12.2.2 Turbulence Considerations

Turbulence caused by surface roughness can have a profound effect on the energy potential of a particular site. This section will show how increased surface roughness reduces the average wind speed, which is assumed to be one of the main factors explaining why the NOABL database consistently over-estimates average wind speeds, particularly for urban sites. It will also be shown how the turbulence intensity can be determined, and what implication this is expected to have on power generation using micro wind turbines.

Effects of Surface Roughness

As wind moves over the earth's surface, frictional forces are created when the air flow interacts with the ground, resulting in a layer of turbulent air. This layer is commonly referred to as the boundary layer. Wind shear within the boundary layer, and the related turbulence intensity, is greatest directly at the earths' surface and reduces as height above ground increases[261]. Mathematically, a simplified relationship for this variation is given by the logarithmic law. However, the logarithmic law causes some problems with negative numbers for any height below the reference plane, and is also difficult to integrate. For a more practical approach, the power law is often used by wind engineers[262]. Both relationships are outlined below.

Logarithmic Law

The logarithmic law was first derived by Prandtl[263] to describe the turbulent boundary layer on a flat plate. Based on this principle, the derived equation for wind shear (rate of change of mean wind speed) ($\overline{U}$) at height above ground (z) is given by equation (12.3). The term (z_0) refers to roughness length, while (k) refers to the von Karman constant, taking an empirically derived value of 0.4.

$$\overline{U}(z) = \frac{u_*}{k} \ln\left(\frac{z - z_h}{z_0}\right) \tag{12.3}$$

The term (u_*) is known as the friction velocity. Using a height of 10m as a reference plane, it is related to the surface drag coefficient (κ) and thereby effectively related to roughness length z_0 as shown by equation (12.4).

$$\kappa = \frac{u_*^2}{\overline{U}_{10}^2} = \left[\frac{k}{\ln\left(\frac{10}{z_0}\right)}\right]^2 \tag{12.4}$$

Power Law

This is essentially a simplified relationship which produces a similar result as the logarithmic law by matching the two laws at a reference height. This reference height (z_{ref}) is usually chosen as the average height over which matching is required. The power law that relates the wind shear at a height of 10m with any height (z) is given by equation (12.5), where equation (12.6) is used to match the power law to the logarithmic relationship.

$$\overline{U}(z) = \overline{U}_{10}\left(\frac{z}{10}\right)^x \tag{12.5}$$

$$x = \left(\frac{1}{\ln(z_{ref} / z_0)}\right) \tag{12.6}$$

The power law is able to give very similar results to the logarithmic law, hence can be seen as an adequate alternative to calculate wind shear for a given height within the turbulent boundary layer.

As shown by the logarithmic law and the related power law, the wind shear is highly dependent on roughness length (z_0) and surface drag coefficient (κ). Both values in turn are highly dependent on the type of terrain. Table 12.F gives a set of typical reference values which were adapted from the Australian Standard for Wind Loads[264], one of several reliable international standards[265].

Table 12.F: Roughness length and drag coefficient for different terrain types (Source: Australian Standard AS1170.2)

Terrain Type	Roughness length z_0 (m)	Drag coefficient κ
Very flat (snow, desert)	0.001-0.005	0.002-0.003
Open (grassland, few trees)	0.01-0.05	0.003-0.006
Suburban (buildings, height 3-5m)	0.1-0.5	0.0075-0.02
Dense urban (buildings, 10-30m)	1-5	0.03-0.3

Turbulence

The level of turbulence essentially describes the gustiness of air, and can be measured using the standard deviation of a set of wind speeds. Equation (6.2) for standard deviation can be re-written in terms of wind speed (*u(t)*), given by equation (12.7).

$$\sigma_u = \left\{ \frac{1}{n} \int_o^n \left[u(t) - \overline{U} \right]^2 dt \right\}^{\frac{1}{2}} \qquad (12.7)$$

Turbulence Intensity

The turbulence intensity[262] is given by the ratio of standard deviation of the fluctuating components to the mean value, or in other words the ratio of turbulence to average wind speed, as shown by equation (12.8).

$$\mathrm{I}_{Turb} = \frac{\sigma_u}{\overline{U}} \qquad (12.8)$$

With reference to equation (12.3) and using an empirically derived value for friction velocity, a good approximation for turbulence intensity in a longitudinal direction is given by equation[262] (12.9).

$$I_{Turb,longitudinal} = \frac{1}{\ln(z / z_0)} \qquad (12.9)$$

Turbulence and turbulence intensity exist in three different planes, the longitudinal, lateral and vertical plane. While it is much more difficult to obtain measured data in the lateral and vertical planes, empirically derived ratios are available to estimate these components. These are given by equations[262] (12.10) and (12.11).

$$I_{Turb,vertical} = \frac{0.88}{\ln(z / z_0)} \qquad (12.10)$$

$$I_{Turb,lateral} = \frac{0.55}{\ln(z / z_0)} \qquad (12.11)$$

As increased turbulence is associated with an increased change in wind direction and wind speed, it is widely accepted that, for horizontal axis turbines, an increase in turbulence results in reduced efficiency. It has been suggested that the longitudinal turbulence intensity can be used as a heuristic safety factor which effectively reduces the output by its percentage value[266].

For example, an initial approximation of the longitudinal turbulence at the EcoSmart village test site, given an 8m hub height and high suburban surface roughness of 0.5m, is estimated to be:

$$I_{Turb,longitudinal} = 0.36$$

This suggests that, as a result of turbulence, wind energy generation at the EcoSmart village can be expected to decrease by around 36% from the estimate purely based on wind speed.

12.3 Predicting Wind Generation

As discussed previously, the NOABL wind speed database appears to be inadequate for estimating wind potentials in urban areas as it does not consider any surface roughness or turbulence effects. Alternative sources for estimating wind potentials at a site with no measured data were sought, and are described in this section. This will subsequently be used to estimate the output of the micro wind turbines at the test site.

12.3.1 Estimating Average Wind Speed

As a result of the known limitations of the NOABL database, a wind speed prediction tool[267] was created by the Energy Saving Trust (EST). This tool accounts for local conditions and surface roughness, partly based on the user specification of the type of terrain. The available options include Urban, Suburban and Rural areas. While this tool was unavailable for the EcoSmart village project in 2006/2007, it can be a valuable tool to predict the potential generation for future projects. Table 12.G shows the Energy Saving Trust tool prediction for suburban terrain compared to measured average wind speed. The NOABL prediction, which was available in 2006/2007, is also shown for reference.

Table 12.G: Annual average wind speed predictions compared to measurements

Average wind speed at EcoSmart Village (m/s)		
Measured	EST tool	NOABL
3.07	3.29	5.4

Table 12.G clearly confirms that the NOABL estimate is much greater than the measured average wind speed, and that by considering surface roughness and local turbulence the Energy Saving Trust tool gives a value that is much more realistic. The EST value is only 7% greater than the measured value. The final recommendation by the EST tool is that this particular site is not suitable for micro wind generation, as the average wind speed is below 5m/s.

12.3.2 Weibull and Rayleigh Distribution

The Weibull distribution is a probability distribution which is often used to describe the probability of wind speeds occurring at a particular site[268]. Starting off with an even, bell-shaped distribution, the Weibull distribution introduces a shape parameter and a scale parameter to adjust its shape. The shape parameter is used to define the distribution of wind speeds while the scale parameter is related to average wind speed.

When little information is known about the actual wind distribution at a particular site, in the northern hemisphere it is often a good approximation to assume a shape parameter of 2. A Weibull distribution with shape parameter of 2 is referred to as a Rayleigh distribution, and often provides the basis for manufacturer estimated wind generation[269]. Equations (12.12) and (12.13) can be used to determine the Rayleigh distribution. Variable 'j' is the scale factor of the distribution, which is related to mean wind speed.

$$f(x) = \frac{2}{j^2} e\left[-\left(\frac{x}{j}\right)^2\right] \qquad (12.12)$$

$$j = \frac{2}{\sqrt{\pi}} \overline{U} \qquad (12.13)$$

Figure 12.7 shows the Rayleigh distribution for the EcoSmart village test site, based on the average wind speed provided by the EST tool.

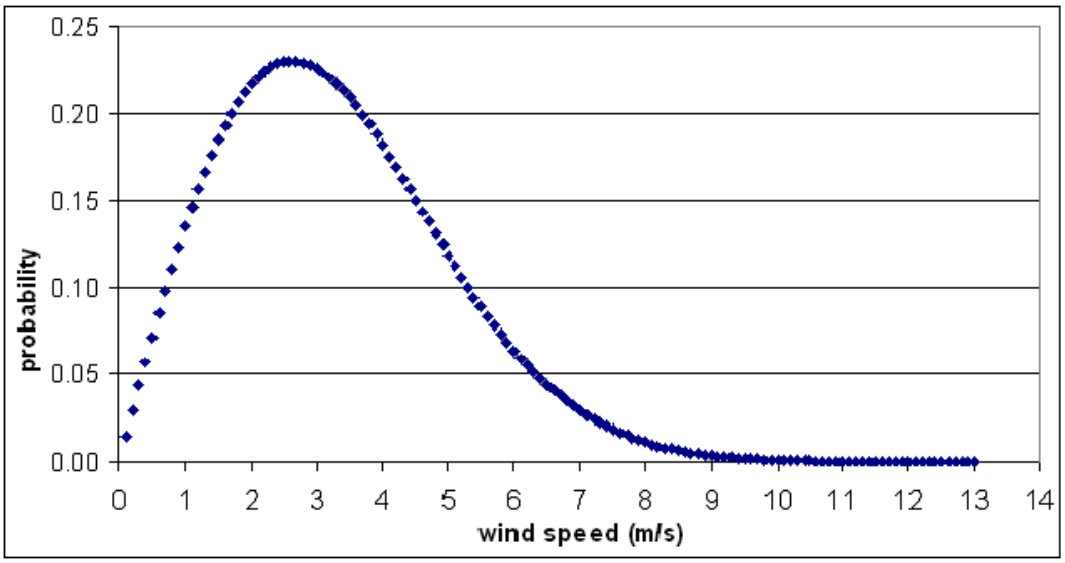

Figure 12.7: Rayleigh distribution of estimated wind speeds at EcoSmart village test site

12.3.3 Estimated Annual Yield

Based on the Rayleigh distribution, the annual energy output of the two micro wind turbines is estimated. Equation (12.14) is used for this purpose, where 8760 is the number of hours in a year and 0.36 is the percentage reduction factor based on estimated longitudinal turbulence. The function is integrated over a wind speed range (u_1) to (u_2), which is 3m/s to 12.5m/s for the Windsave turbine and 2.5m/s to 16m/s for the StealthGen turbine. The results for both the average windspeed estimated by the NOABL database and the EST tool are given in Table 12.H. The energy generation estimated by the manufacturer is also shown for comparison.

$$P_W = (1-0.36)*8760*\int_{u_1}^{u_2} p(U)*cp\frac{1}{2}\rho A U^3 dU \qquad (12.14)$$

Table 12.H: Initial estimates for micro wind generation at the EcoSmart test site

	Estimated Annual Yield (kWh)	
	Windsave	StealthGen
NOABL	907	394
EST tool	259	96
Manufacturer	1150	570

As shown by Table 12.H, the estimated output differs greatly, depending on the source of data. The estimate based on wind data from the EST tool, which was shown to be most realistic compared to the measured wind data, results in a very small energy yield estimate for the test site, only around 20-30% compared to the other estimates. The manufacturer estimate for energy generation is significantly greater than even the NOABL-based estimate, which was derived using data and methods that have been described as common industry practice. The difference can be accounted for if a different turbulence reduction factor is used. It was found that a commonly suggested average generic value[266] for turbulence intensity is 0.15. When using this value instead of the site specific value of 0.36, the difference between the NOABL estimate and manufacturer estimate becomes negligible.

12.4 Measured Data

This section will present the data that was recorded at the EcoSmart village during the test period. The recorded weather data is analysed in detail to establish the exact energy potentials at the site. This will be done using third party software[271]. The measured energy generation of all wind turbines will subsequently be presented.

To provide a better overview, Figure 12.8 shows the exact layout of the test site including marked locations of all wind turbines as well as the weather station. A legend for Figure 12.8 is given in Table 12.I.

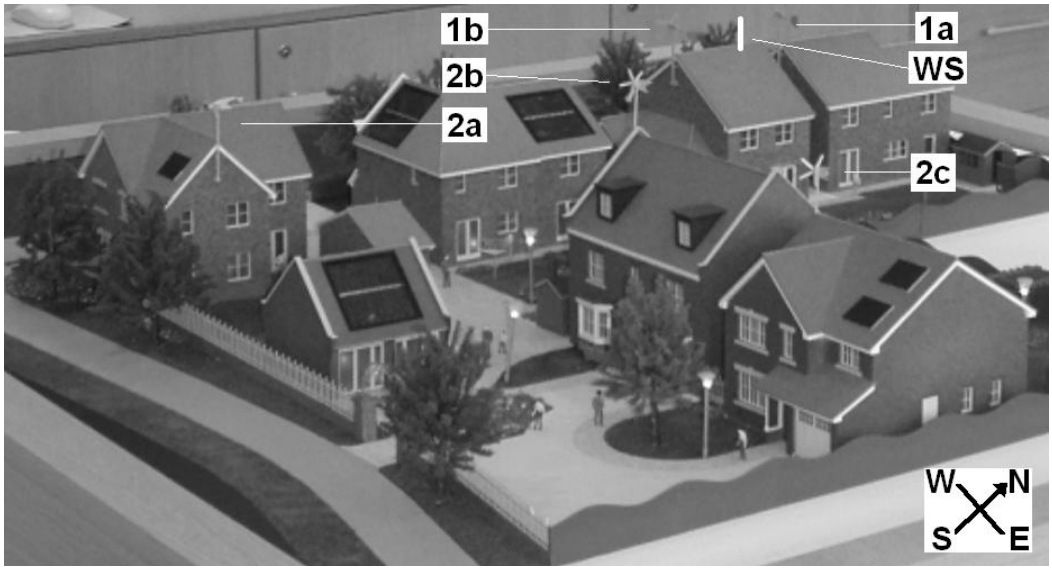

Figure 12.8: Model of the test site, showing Wind Turbines and Weather Station

Table 12.I: Key for Figure 12.8

Key	Building	Model
1a	Buckingham	Windsave
1b	Edinburgh	Windsave
2a	Alderney	StealthGen
2b	Malvern	StealthGen
2c	Windermere	StealthGen
WS	Edinburgh	Weather Station

12.4.1 Wind Data

Weather data, including wind speed, wind direction, atmospheric pressure and humidity have been recorded directly at the site at 10-minute intervals in accordance with BS EN 61400-21:2002. After testing was completed, the revised

BS 61400-21:2008[270] was released, which recommends using measurements at 1-minute intervals. While this would have vastly improved the analysis it could not be anticipated at the outset of the research in 2006. Data were acquired using the Davis Vantage Pro 2 Plus weather station, which is a combined package including an anemometer, wind vane, as well as other sensors. The accuracy of the anemometer and wind vane is given by the manufacturer as 2% for wind speed and ±7° for wind direction. However it must be noted that the rather compact mounting arrangement is likely to result in more significant inaccuracies due to wind distortions by other sensors or the mounting pole. Additionally, the weather station will experience different turbulence patters to those experienced by turbines 2a, 2b and 2c, which is a result of the different roof orientation.

For more detailed analysis of the raw wind data, a software program was used to provide statistics on the data including wind-rose diagrams and energy distributions. The software used for this purpose is Windographer, developed by Mistaya Engineering Inc[271]. The software is based on similar principles and methodology as the popular and validated HOMER software[272]. Table 12.J provides an overview of results from the Windographer analysis on wind data.

Table 12.J: Results from wind data analysis (Source: Windographer)

Variable	Value
Height above ground (m)	10
Mean wind speed (m/s)	3.069
Median wind speed (m/s)	2.682
Min wind speed (m/s)	0.000
Max wind speed (m/s)	18.327
Hour of peak wind speed	22
Mean power density (W/m²)	53
Mean energy content (kWh/m²/yr)	464

Table 12.J provides a summary of the wind data that was recorded from the test site. The mean energy content of the wind, under consideration of Betz's law, can provide a good indication to the maximum potential wind energy generation. Figure 12.9 provides a monthly breakdown of the recorded wind speeds, giving mean, daily high & low, as well as maximum and minimum wind speeds recorded for each particular month. As expected, both mean and maximum wind speeds are considerably higher during the winter period. Figure 12.10 provides frequency and Weibull distributions, which form the basis for Windographer energy generation estimates.

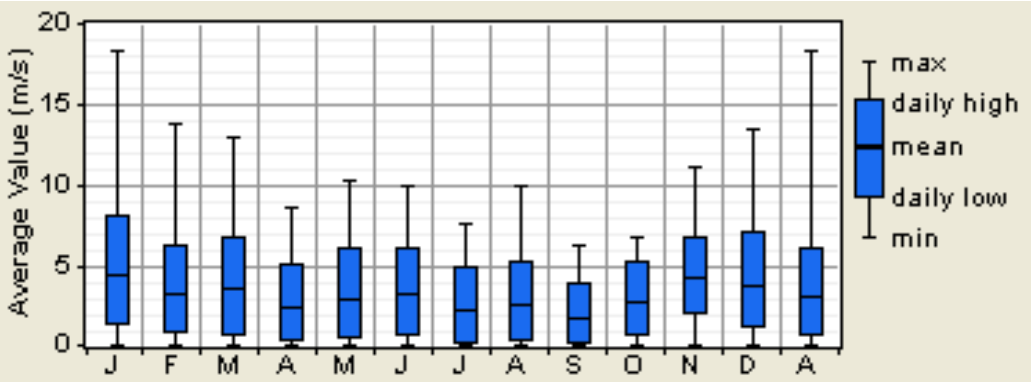

Figure 12.9: Monthly variation of wind speeds (source: Windographer)

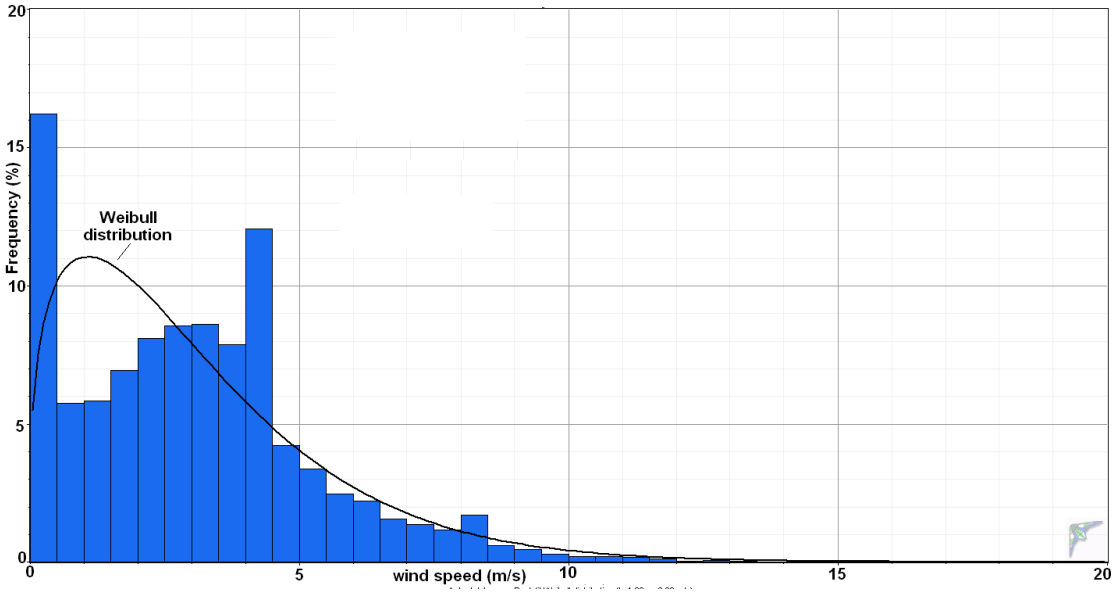

Figure 12.10: Frequency and Weibull distributions (source: Windographer)

Interestingly, Figure 12.10 shows that the most common wind speed that was recorded at the test site is 0m/s. This leads to suggest that the anemometer response is poor at very low wind speeds. While this has no effect on the modelled generation estimate given later on as the affected wind speeds are below the cut-in speed of the turbines, it does appear to skew the Weibull distribution slightly. This may have an affect on the estimate provided by Windographer, as this is based on the Weibull distribution.

Figure 12.11 and Figure 12.12 show wind rose plots. While Figure 12.11 shows the distribution of mean wind speeds, Figure 12.12 shows the distribution of energy contained by the wind. Both these plots show that the vast majority of wind energy is available from the west, with the second largest fraction being available from the south. This may well have been influenced by the more exposed western face of the weather station, as there are buildings to the north, south, and at some distance to the east of the mounting position. Although the weather station is mounted at a height that is slightly above those

buildings, it can be expected that small-scale turbulence effects over roof tops will have had a significant influence on the measured wind distribution.

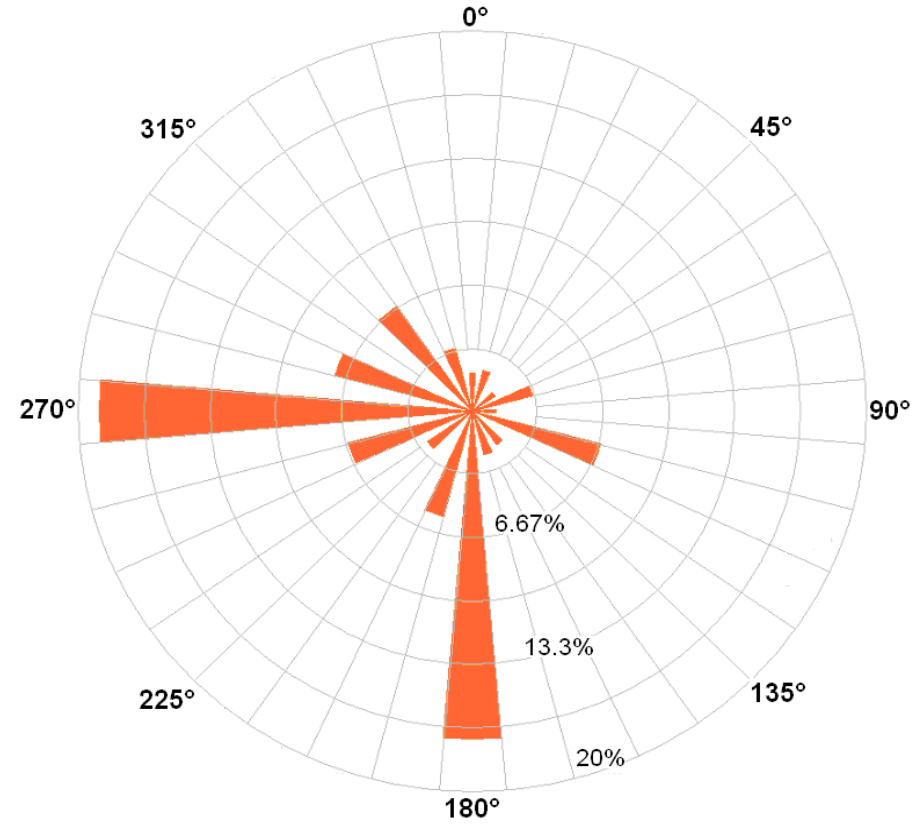

Figure 12.11: Wind rose plot showing wind speed distribution

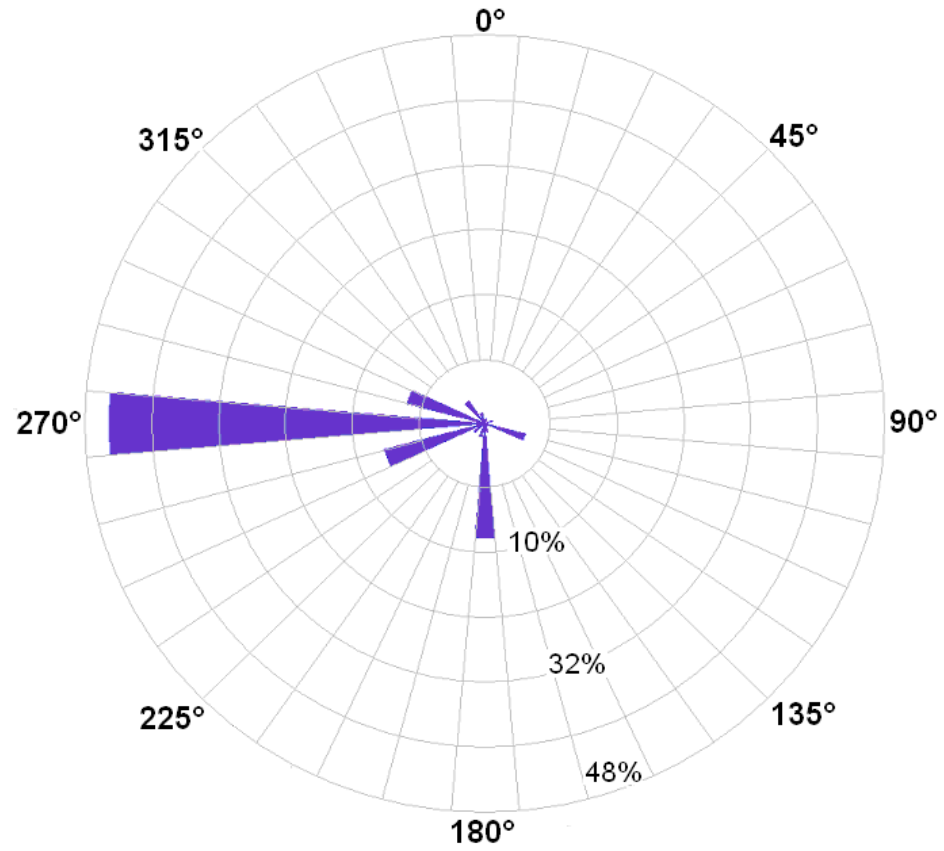

Figure 12.12: Wind rose plot showing energy distribution

The evident wind energy potentials at the EcoSmart village site suggest that while average wind speed is rather low, the highly predominant wind direction might lead to a higher generation than at similar sites with more frequently changing wind direction.

Before presenting the measured annual yield of the five micro wind turbines that were tested at the EcoSmart village, it must be noted that the electricity meters used to monitor the turbines were designed to measured electricity flowing both ways, hence recording both electricity consumption and generation as a positive output. While this did not create any complications for other systems, the meters for micro wind turbines also recorded power consumption of the inverters as a positive output.

12.4.2 Inverter Losses and Energy Consumption

The inverter losses have been previously described in section "7.2.1 – Efficiency losses". The measured daily inverter consumption from the wind turbine inverters is reiterated in Table 12.K.

Table 12.K: Average daily inverter energy consumption

		Daily Inverter consumption (Wh)			
Eco Home	**System**	**08/07/2007**	**19/07/2007**	**21/07/2007**	**Average**
Buckingham	Windsave	169.5	170.5	170.0	**170.0**
Edinburgh	Windsave	181.0	180.5	180.5	**180.7**
Alderney	StealthGen	159.5	159.5	159.5	**159.5**
Malvern	StealthGen	119.5	120.5	118.0	**119.3**
Windermere	StealthGen	122.5	130.0	130.0	**127.5**

12.4.3 Measured Energy Output

After having determined the energy consumption of the inverters the net energy generation was found. Table 12.L shows a summary of the actual energy output that was recorded in the period from 24/10/2006 until 27/10/2007 for all wind turbines installed at the EcoSmart village test site.

Table 12.L: Summary of annual wind turbine performance at EcoSmart village

Eco Home	System	Generation (kWh)	Inverter Consumption (kWh)	Net Output (kWh)	Downtime
Buckingham	Windsave	36.1	55.9	**-19.8**	36 days
Edinburgh	Windsave	3.9	64.1	**-60.2**	10 days
Alderney	StealthGen	1.8	47.7	**-45.9**	66 days
Malvern	StealthGen	38.0	41.5	**-3.5**	18 days
Windermere	StealthGen	5.6	41.1	**-35.5**	43 days

Table 12.L shows that the energy output of the wind turbines over the one year period was extremely poor. All systems showed severe underperformance compared to the estimations presented in Table 12.H. Only two systems showed a significant output, one Windsave turbine (turbine 1a in Figure 12.8) which generated 36.1 kWh and one StealthGen turbine (turbine 2b in Figure 12.8) which generated 38.0 kWh during the year. However, when considering the inverter energy consumption, all systems installed at the EcoSmart show village showed a negative net output, meaning in every case the inverter consumed more energy than the wind turbine was able to generate.

12.5 Reliability

System reliability is another area of concern. Table 6 has already provided an overview of system downtime, which was found to be in the range of 3%-18% over the one year period. These downtimes were largely caused by wind speeds that exceeded the rated 'cut-off' speeds of the turbines. While average wind speeds over 10 minutes that exceed the cut-off speed were rarely measured, gust speeds were likely to have been significantly higher on several occasions. It is also possible that the power curve supplied by the manufacturer is not 100% accurate, as was found in other research projects such as the Warwick wind trials[273]. The excessive wind speeds caused the turbines to shut down and, on many occasions, they failed to automatically start up again. The turbines had to be reset manually.

A major issue for concern is the systems' apparent lack of ability to deal with extreme wind speeds that far exceed the rated cut-off speeds. On one occasion during extreme winds in January 2007, where average wind speeds above 18m/s were measured, a blade from one of the turbines detached and was later recovered far from the installation site. Figure 12.13 shows a photograph of the blade as it was recovered.

Figure 12.13: Damaged turbine blade which had detached during the storm on 18th January 2007

While this is unlikely to have occurred during standard operation, it is possible that the furling mechanism was responsible for this. When the wind speeds exceed the rated cut-off speeds of the turbine, a braking mechanism is applied, which forces the blades to come to a standstill. However, at very high wind speeds the transient loads during turbine shut-down and the aerodynamic forces acting on a stationary blade apply an extreme amount of stress to the root of the blades. It is also possible that on this occasion the furling mechanism failed and the rotor continued to spin uncontrolled. As blades are designed to be light and thin to maximise turbine efficiency, safety margins in blade design may not have anticipated and accounted for the forces under such extreme wind speeds as experienced on the 18th January 2007.

A possible solution to this problem is to install the wind turbines using a tilting mechanism, which enables the home owner to manually retract the system in the event of a heavy storm. Such a system, shown in Figure 12.14, is suggested but not supplied by the manufacturer StealthGen.

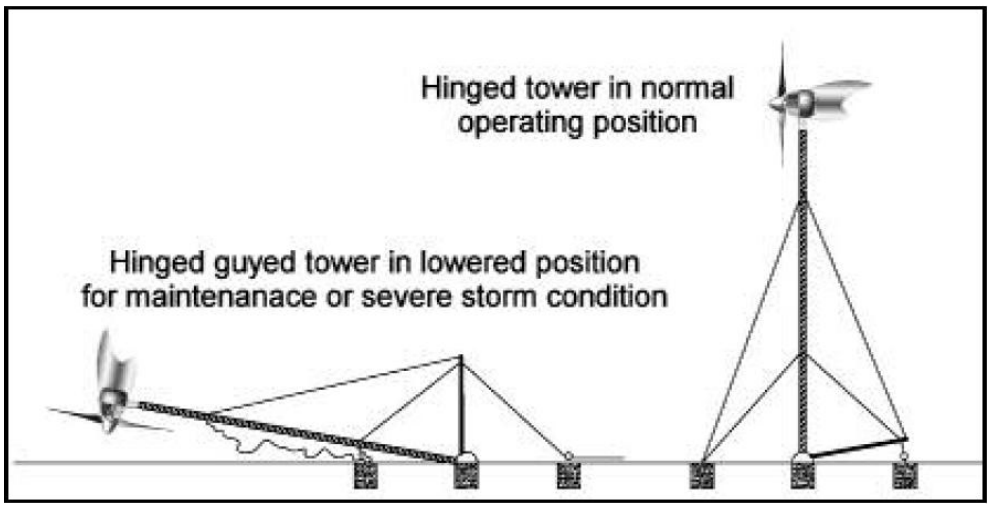

Figure 12.14: Retractable wind turbine (source: StealthGen D400 manual)

12.6 System Modelling

As shown by the preceding presentation of results, there is a significant difference between the expectations shown in Table 12.H, and the actual performance shown in Table 12.L. In order to explore what variables might account for this the micro wind turbine systems will be modelled. The following section will describe the methodology for this procedure.

12.6.1 Modelling Options

Two options have been identified to model the micro wind turbine systems in detail.

1. Using the wind data, a shape factor and scale factor for a Weibull distribution can be found. This probability distribution can then be used to find the energy output for binned wind speeds, using the power curve for each wind turbine.

2. A dynamic model can be created, that calculates the energy generated over each available interval of weather data.

Both options have their merits, but the dynamic model has the advantage of being more flexible and able to account for changing conditions during each interval. For example, the air density can be adjusted for each interval and accounted for when calculating the power output. The same is true for turbulence intensity. If the output is based on the Weibull distribution, the only way to account for density and turbulence variations is by using annual average values, which is not particularly accurate. With reference to Figure 12.10 showing frequency and Weibull distributions, the annual average turbulence intensity as well as the Weibull distribution itself would be skewed by the many zero readings for wind speed.

Based on the reasons explained above it was decided to use a dynamic model to represent the wind turbines. However, to provide control readings the model will be compared to results obtained from the Windographer software. Windographer uses the Weibull function as a basis for modelling.

12.6.2 Micro Wind Turbine Model

The dynamic model for wind turbine analysis will be based on the following steps:

- The air density is adjusted using methods outlined in section "8.3 – Estimating air density"
- The power curves of both turbines are modelled
- The turbulence intensity is calculated for each individual time interval
- A simple inverter model is used to account for inverter efficiency losses

Modelling the Power Curve

Figure 12.3 and Figure 12.4 show the relationship between wind speed and the conrresponding expected power output of the two wind turbines. These power curves do not follow the shape of a third order polynomial, which might be expected due to the term (U^3) in the wind power equation (12.2). This means that the coefficients of performance of the turbines are not constant, but vary with respect to wind speed. According to both manufacturers these power curves have been generated assuming an air density according to the international standard atmosphere (ISA), of 1.225kg/m^3.

By re-arranging the wind power equation (12.2), the coefficient of performance (cp) for different speed bands can now be determined using equation (12.15):

$$cp = \frac{2P_0}{\rho \times A \times U^3} \qquad (12.15)$$

Results for the (cp) variation with wind speed are shown in Figure 12.15.

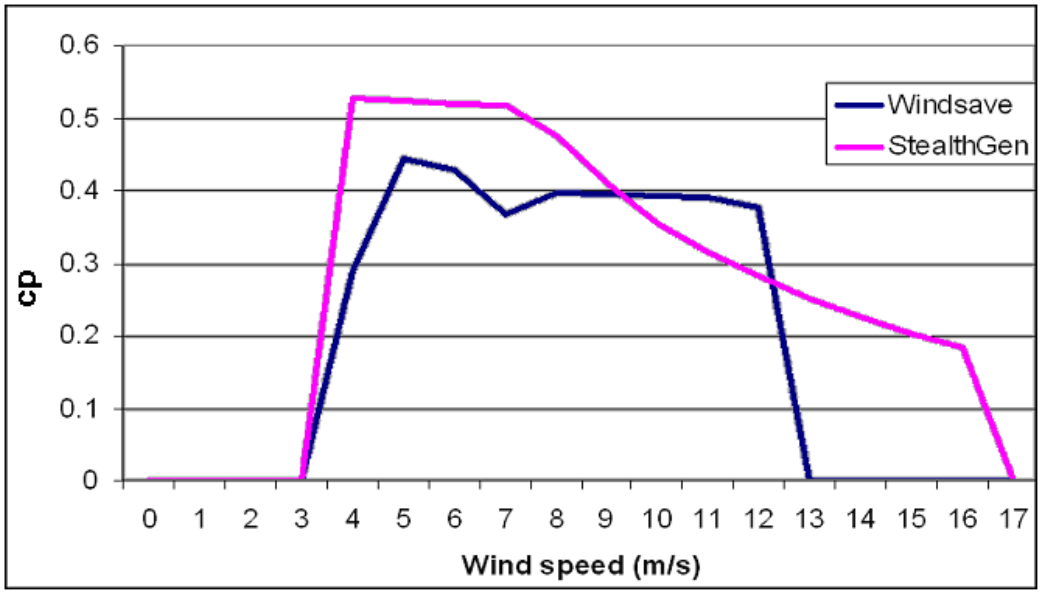

Figure 12.15: cp variation with wind speed

Figure 12.15 shows clearly that the StealthGen turbine was optimised for low wind speeds, whereas the Windsave model is designed to work at more consistent levels of efficiency.

Turbulence Intensity

It was decided to model the turbulence intensity for each individual time interval to obtain more accurate percentage reduction factors than for example a yearly average. To calculate individual values of turbulence intensity it was decided to find the standard deviation and mean wind speed over one hour, taking into account values up to 30 minutes before and 30 minutes after the particular time interval. While this should provide a great accuracy improvement over using a longer term (for example annual) average, the accuracy of this part of the model is still limited by the rather long time intervals of 10 minutes.

Inverter Model

The inverter model is based on the two models derived previously in section "7.1.4 – Inverter model". In addition to the efficiency, the inverter energy consumption will be included in the model. The average values that will be used for modelling purposes are given in Table 12.M.

Table 12.M: Inverter energy consumption used for inverter modelling

	Energy Consumption (kWh)	
	Daily	Annual
Windsave Inverter	0.176	**64.2**
StealthGen Inverter	0.136	**49.6**

12.6.3 Model Results and Discussion

The micro wind turbine systems at the EcoSmart village were modelled based on the methods outlined above. Table 12.N shows the results, split into winter and summer periods. The average wind speed recorded for each period is also given. For comparison, Table 12.O provides results from modelling using the Windographer software.

Table 12.N: Results from micro wind turbine model

	Average Wind Speed (m/s)	Energy Generation (kWh)	
		Windsave	StealthGen
Winter (Nov-Mar)	3.8	98.2	34.1
Summer (Apr-Oct)	2.5	-8.5	-11.2
Annual AC (DC)*	**3.1**	**90 (232)**	**23 (154)**

* DC generation given in brackets for comparison

Table 12.O: Results from Windographer simulation

	Windographer Estimate (kWh)	
	Windsave	StealthGen
Annual	**263**	**144**

With reference to Table 12.N, the model shows that in theory the maximum annual net energy that can be expected from the Windsave and StealthGen turbines is 90kWh and 23kWh respectively. With DC generation given as 232kWh and 154kWh, the inverter can be identified as the main source of losses.

When looking at the inverter efficiency curve in section "7.1.2 – Efficiency losses" it shows that the efficiency drops off dramatically, below 50% efficiency, when the inverter load is below 10%. For the case of the Windsave turbines for example, this would include all steady wind speeds below 5 m/s. During the one year trial period, 85% of all wind speeds that were measured at the EcoSmart village were below 5 m/s.

In addition to this, the energy consumption of the inverters is very high in proportion to the turbine output. For example, for the Windsave turbine the inverter consumes around 28% of the expected DC generation, for the StealthGen inverter the consumption is as high as 32% of expected DC output.

Unless DC storage becomes a useful option, reducing the inverter losses is a challenging task. The wind turbines have great range of power output, and the frequency of low power generation is far greater than the frequency of high power generation. A possible solution might be using multiple inverter stages, for example one small inverter that is efficient at low loads, and a second inverter that has a high power rating, being able to convert high DC loads efficiently. However, this only becomes a financially feasible option for much larger systems than a 1kW rated wind turbine.

The Windographer estimate is fairly close to the expected DC output, which at first glance may lead to believe that Windographer does not account for inverter losses. However, there are also other uncertainties. The method of using the Weibull probability distribution means that variations of parameters other than wind speed, such as air density, cannot be accounted for. The density model showed that due to high vapour content the air density was often around 10-20% lower than standard atmosphere density, which is directly related to the energy estimate. The same is true for turbulence. If accounted for at all by Windographer, a generic annual average would have to be used. On the other hand, the many zero wind speed readings have skewed the Weibull distribution somewhat, as shown by Figure 12.10. While lack of consideration for turbulence and density would lead to over-estimation, the skewed Weibull distribution results in the opposite. The errors for this case might cancel each other out to some extent, but this appears to be more reliant on chance than robust modelling methodology.

12.7 Detailed Analysis of Turbulence

Considering the model results and discussion above, there is still a significant difference between the modelled output and the measured wind generation. The only remaining variable that despite being modelled retains a high degree of uncertainty is turbulence intensity. It was previously discussed that, in hindsight, it would have been more useful to record wind data using the shortest possible interval to get a better feel for turbulence. Other research[274] confirms that the sampling period has a significant effect on measured wind speed, and using 1-minute intervals or less is advisable. Due to the lack of data the following discussion must take a more qualitative form, with limited mathematical analysis to confirm observed trends.

12.7.1 Micro Wind Turbine Response to Turbulence

Turbulence is inevitably created around the sharp edges of the roofs of the buildings. This disrupts the smooth airflow over the turbine blades by causing sharp and frequent changes in both wind speed and wind direction. It was observed during the operation of all wind turbines that they are apparently unable to adequately deal with this problem. To explain this in more detail, it must be remembered that turbulence can exist in three planes with respect to the turbine; longitudinal, lateral and vertical. Figure 12.16 shows an example of the wind profile over an isolated house, based on computational fluid dynamics analysis[275]. This presents the 'best case' scenario, with no obstructions of any kind in front of or near the building. Nonetheless this example already shows the extent of variation on a small scale even under optimum conditions.

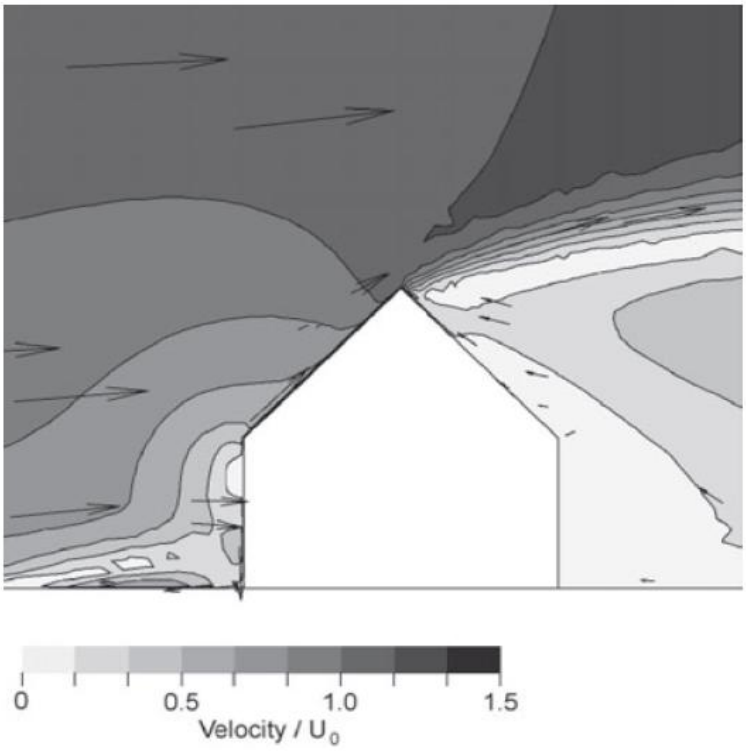

Figure 12.16: CFD diagram of wind velocity profile over a modelled isolated house (Source: Heath et al[275], 2007)

Longitudinal turbulence effectively refers to changes in wind speed, or more specifically the standard deviation of wind speed. The effect of this type of turbulence mainly depends on the mass of the blades, as well as their aerodynamic design. In many cases a sharp increase in wind speed will cause the blade, or at least part of it if the blade is twisted, to stall. Instead of

speeding up the rotor by creating extra lift due to increased wind speed, the stall condition will actually slow it down. However, if a blade is designed to be very light to give the rotor a low moment of inertia, and with adequate amount of twist, then the problem presented by longitudinal turbulence can be vastly reduced.

Problems caused by lateral turbulence (changes in wind direction) are more difficult to avoid for current horizontal turbine designs. At the EcoSmart village and another test site[276] it was observed that the turbines spend much of their time trying to turn into the wind, altering their direction very frequently. At the same time the blades often remained almost stationary, or spun up very briefly before coming to a standstill again while the turbine continues to adjust its direction. The turning mechanism of the wind turbines appears to be very effective, causing the turbines to react promptly to a change in wind direction. However, while the turbine changes its position, the airflow is disrupted for some time, which causes the blades to slow down dramatically even when there is seemingly an adequate amount of wind. Once slowed down, a significant amount of time can go by before the turbine starts up again. An investigation[277] into the start-up behaviour of micro wind turbines revealed that even under moderately high steady wind speeds of 6-7m/s the start-up time can be 20 seconds or more. Under turbulent conditions, it is very likely that the wind direction will change much more frequently than every 20 seconds. The start-up torque that defines this behaviour is largely influenced by blade design[278].

The effect of vertical turbulence is expected to be least significant, although being far from negligible. As the turbine is unable to react to changes in the vertical direction, the effective angle of attack on the blades can quite easily approach stall conditions. Also, blades on one side of the turbine will see the opposite effect as blades on the other side of the turbine. While being inherently inefficient, this can even result in lift being created in the same direction on both sides of the turbine, which is contrary to what is desirable for high rotational speeds.

12.7.2 Detailed Analysis of Turbulence at the Test Site

The turbulence intensity in each plane can be determined by standard deviation, of wind speed for longitudinal turbulence, and of wind direction for lateral turbulence. The changes in wind direction were found using the model described in section "8.4 – Finding wind direction difference". No measurements are available for vertical wind speeds.

The methodology of the dynamic wind turbine energy model was applied for this analysis, where the hourly standard deviation of measured wind speed or wind direction was found for each individual time interval. Turbines 1a and 2b, shown in Figure 12.8 have shown some energy output, so these turbines are used to analyse the effect of turbulence.

Interestingly, both turbines showed very similar generation patterns. Between April and June 2007 six time periods where identified independently where noticeable energy generation was measured. Five out of the six generating periods, ranging from 12 hours to approximately two days each, coincided exactly. The differences between theoretical and actual AC generation over these periods are shown in Table 12.P.

Table 12.P: Turbine generation and inverter losses during coinciding generating periods

Case	Duration (hours)	Turbine	Theoretical DC (kWh)	Total Inverter losses (kWh)	Theoretical AC (kWh)	Measured AC (kWh)	% of theoretical
1	28	1a	0.761	0.511	0.250	**0.214**	86%
		2b	1.475	0.571	0.904	**0.749**	83%
2	59	1a	1.591	1.368	0.223	**0.215**	96%
		2b	2.631	1.503	1.128	**0.431**	38%
3	42	1a	2.973	1.309	1.664	**1.058**	64%
		2b	6.132	1.446	4.687	**2.224**	47%
4	13	1a	0.932	0.325	0.607	**0.248**	41%
		2b	2.112	0.352	1.760	**1.296**	74%
5	38	1a	2.051	0.892	1.159	**0.673**	58%
		2b	4.586	0.989	3.597	**2.492**	69%

Having established that turbines 1a and 2b tend to generate energy at the same time, and having pin-pointed these times, the energy generation can now be correlated to turbulence estimates based on weather data.

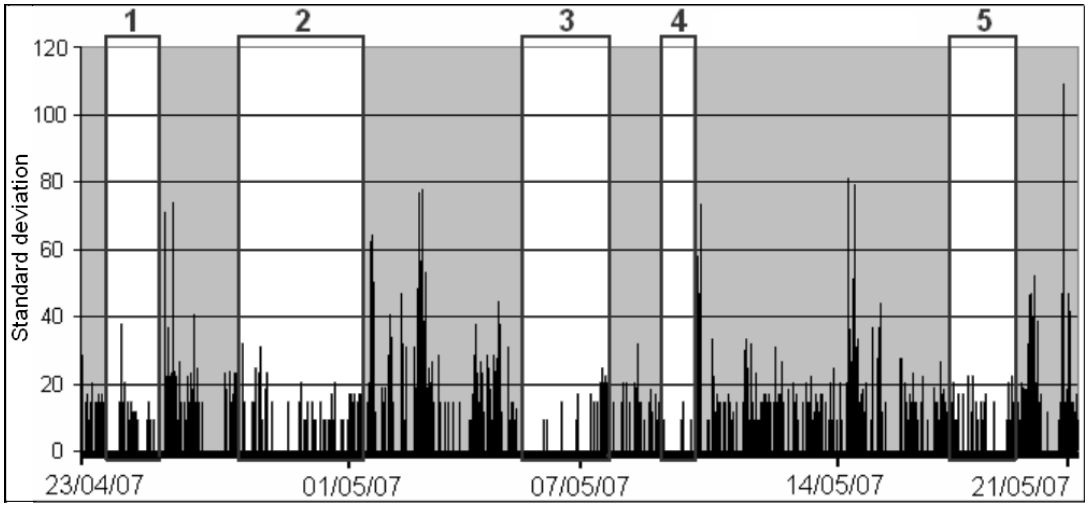

Figure 12.17: Lateral turbulence (hourly standard deviation of wind direction) during generating times of both turbines over a 4-week sample period in 2007

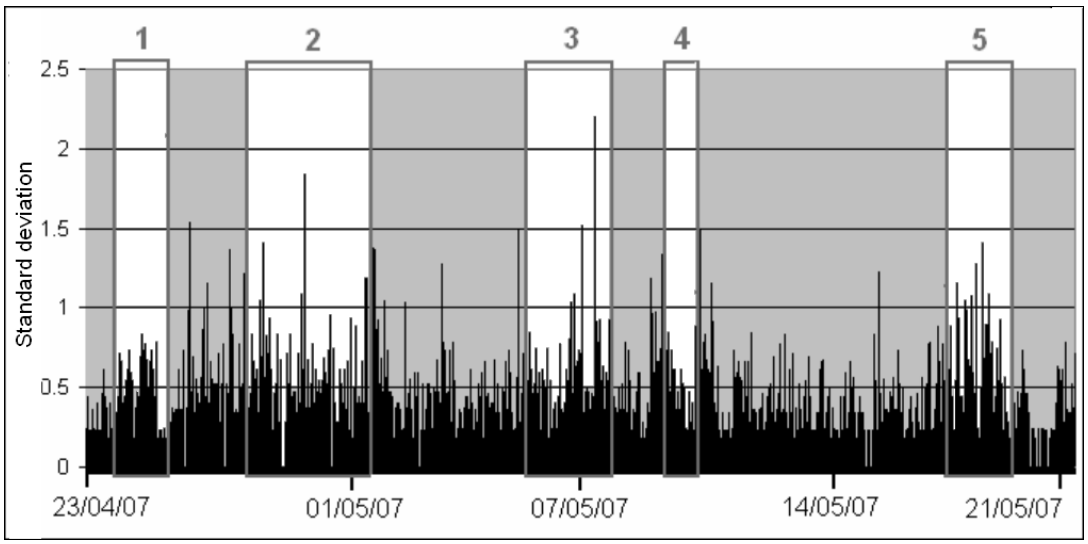

Figure 12.18: Longitudinal turbulence (hourly standard deviation of wind speed) during generating times of both turbines over a 4-week sample period in 2007

When looking at Figure 12.17 and Figure 12.18, showing lateral and longitudinal turbulence throughout the coinciding generating periods of turbines 1a and 2b, it becomes apparent that lateral turbulence seems to have a greater effect on energy generation. Lateral turbulence was found to be noticeably lower during periods of energy generation compared to periods where no generation was measured. Similarly, periods where no generation was measured but lateral turbulence was also low generally coincided with periods of low wind speeds.

Figure 12.18 on the other hand does not appear to show any direct correlation between low longitudinal turbulence and turbine generation. The average measured standard deviation of wind speed at the test site is 0.49m/s. Turbulence intensity has also been calculated for the entire data set where average longitudinal turbulence intensity over 12 months was found to be 0.52. For comparison, the initial estimate for longitudinal turbulence intensity at the test site was 0.36.

While the average standard deviation of non-generating periods is 0.44m/s, the average standard deviation during generating periods is actually higher, at 0.59m/s. It can be deduced that longitudinal turbulence does not appear to show a significant impact on turbine performance. To investigate this further, Figure 12.19 and Figure 12.20 show plots of lateral turbulence for periods of energy generation (cases 1 to 5 combined), and periods of no generation (combined 'gaps' between cases 1-5) respectively.

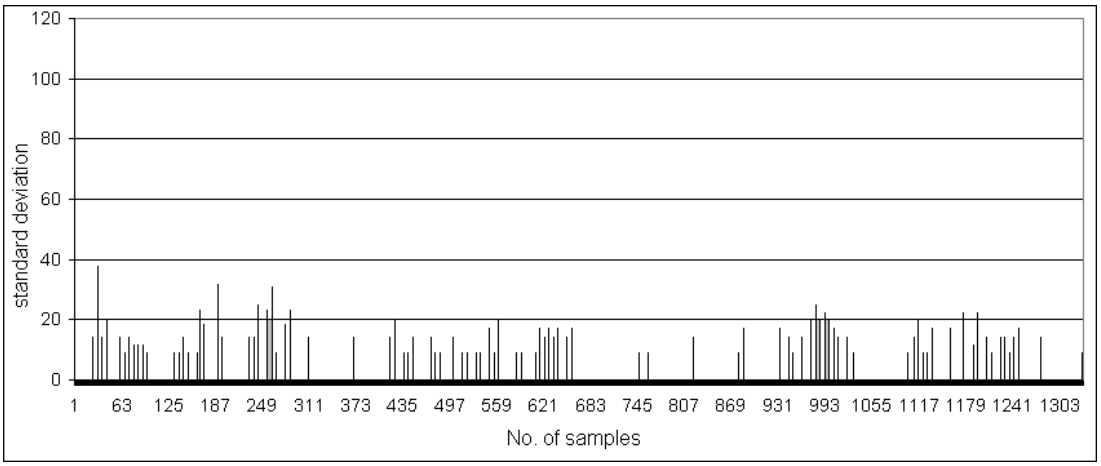

Figure 12.19: Lateral turbulence for combined periods of energy generation only, over a 4-week sample period in 2007

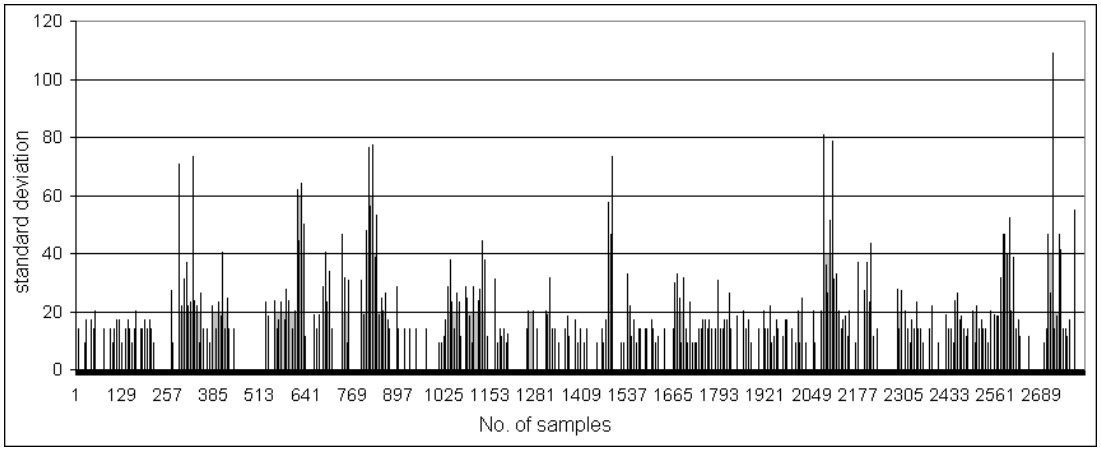

Figure 12.20: Lateral turbulence for combined periods of zero generation only, over a 4-week sample period in 2007

For this analysis all wind speeds below the cut-in speed of the turbine 2 (2.5m/s) have been neglected to avoid any skewing of the data, as the wind was found to change naturally more frequently at lower wind speeds. During periods of energy generation, the mean of the standard deviations of wind direction is 6.1° ± 8.1°. During non-generating periods on the other hand, the mean of the standard deviations of wind direction of is 10.9° ± 11.5°. The standard deviation is a measure for turbulence, indicating that lateral turbulence during non generating periods is about 80% greater than lateral turbulence for periods during which an

output was measured. To compare these values statistically, the t-test is used. This statistical function is able to compare two means in relation to the variation by finding the standard deviation of the difference.

For the two datasets shown in Figure 12.19 and Figure 12.20 the t-value is 5.36. This is a high t-value, meaning that the difference between the two means is statistically significant, beyond a 0.001 uncertainty. In relation to the wind turbines that were tested this indicates that energy generation is strongly related to the amount of lateral turbulence.

The actual turbulence experienced at the location of the turbines may even be enhanced by their mounting position relative to the building, and by the building geometry that surrounds them. The weather station is mounted in a similar position as both Windsave turbines, therefore this analysis can be seen as being representative for those two cases. For all of the StealthGen turbines however, the turbulence profile will be very different. Nonetheless it can still be expected to have a similarly significant effect. It appears that if micro wind turbines are to become a viable option for the urban environment in the future the technology must be improved dramatically to overcome this problem. Further testing and development by the manufacturer will be required.

Vertical axis turbines[279,280] could provide a potential solution if their efficiency can be improved. Alternatively, a better integration into building geometry might help to channel the airflow, increasing its velocity and also reducing lateral turbulence. Where this kind of building integration is not possible, a horizontally non-rotating, omni-directional ducted wind turbine could also be used. The duct would help to increase the speed of the airflow, increase aerodynamic efficiency of the blades, and if designed correctly eliminate most of the turbulence. This could be particularly useful if there is such a strong predominant wind direction as found at the EcoSmart village test site.

12.7.3 Corroboration with Other Research

The results from the micro wind turbine analysis were somewhat unexpected. As the five turbines only represent a very small sample it is important to validate these results as well as possible with reference to more comprehensive trials. While the EcoSmart Village project is one of the pilot projects investigating micro wind technology in detail, other large scale trials have also been carried out over recent years. The most noticeable investigations into micro wind turbine performance in the urban environment include the Warwick Wind Trials 2008, the WINEUR Project 2007 and the Energy Saving Trust (EST) Wind Trials 2009.

From these studies it was also concluded that urban wind turbines faced several problems. The Warwick Wind Trials for example concluded that turbulence reduces output by 15-30%[273]. It was further shown that the urban capacity factor was only around 4-6.4%, compared to around 10% for rural sites.

The WINEUR project specifically suggested[281] a set of minimum requirements to make urban wind generation viable, including average wind speeds above 5.5m/s, the turbine to be mounted at least 50% higher than its surroundings and at a hub height at least 30% greater than building height. This is also confirmed by a CFD (computational fluid dynamics) analysis conducted by Heath et al[275], showing that for a typical urban layout of buildings a hub height of at least 50% above building height is required to capture wind that is not significantly affected by surrounding buildings.

The EST Wind Trials[282] were the most recent and most comprehensive trials conducted in the UK, and concluded that micro wind turbines do work, but only if installed properly in a suitable location. Building mounted turbines generally showed poor output, and urban sites were consistently found to have inadequate wind resources. It was also found that power-curves provided by manufacturers were often inaccurate and sometimes incorrect.

Having reviewed recent reports on other research it can be concluded that the findings from the EcoSmart village are generally in line with more comprehensive large-scale trials. It appears that, at least using the current technology, horizontal axis micro wind turbines in built-up areas including urban and suburban terrain do not work well. The main reasons for this underperformance were identified as the lack of sufficiently high wind speeds as well as intense turbulence, in particular lateral turbulence, when mounted in close proximity to roof edges and other near-by obstacles further downstream.

12.8 Payback rate and carbon savings

As none of the micro wind turbine systems were able to generate a positive energy output, the actual payback periods and carbon offset were not calculated. Instead, the theoretical DC generation values will be considered for this analysis. It is also assumed that the turbines will be mounted in a way that reduces lateral turbulence, suspected to be the main cause for the abysmal measured performance. For comparison, payback rates for a second case will be estimated, which assumes the same optimum turbine placement but including the use of an inverter for a grid-tied solution. Table 12.Q is used to reiterate the estimated annual DC generation as well as cost and embodied carbon.

Table 12.Q: Capital cost and embodied energy and carbon, compared to estimated annual DC yield

	Windsave	**StealthGen**
Cost	£1,500	£2,250
Embodied Energy (kWh)	2132	1964
Embodied Carbon ($kgCO_2$)	457	426
Annual DC Yield (kWh)	232	154

Based on assumptions outlined in section "6.5.3 – Calculating simple financial payback" and on feed-in tariffs up to April 2011, the annual savings are shown in Table 12.R, and the resulting financial payback rates and life-time savings in Table 12.S. Based on other research[254] the expected life-time of the two turbines is estimated to be around 20 years.

Table 12.R: Annual savings expected at EcoSmart test site based on optimum conditions (No inverter, turbine located away from roof edges)

	Annual Savings	
System	Electricity offset	2011 Feed-in tariff
Windsave	£33.18	£80.04
StealthGen	£22.02	£53.13

Table 12.S: Payback rates from EcoSmart systems based on optimum conditions (No inverter, turbine located away from roof edges)

	Payback rate (years)			**Net savings over system life (20 years)**		
System	Financial	Energy	Carbon	Financial	Energy (MWh)	CO_2 (t)
Windsave	13.2	9.2	3.8	£770	2.5	1.9
StealthGen	29.9	12.8	5.4	-£747	1.1	1.2

Under optimum conditions Table 12.S shows reasonably good payback rates for the Windsave turbine, while the StealthGen turbine is simply too small to justify the financial and energy expense. It must be stressed that Table 12.R and Table 12.S show results for the case of no inverter being used, and the turbines being mounted at a significant distance from roof edges or any other nearby obstacles. Wind speeds are assumed to be as measured by the EcoSmart village weather station, but it is assumed that lateral turbulence which caused great problems for the test systems is largely avoided.

Table 12.T presents a case for which turbines have been mounted in an optimum location to avoid most of the lateral turbulence, but are grid-tied, using an inverter.

Table 12.T: Estimated payback rates for optimum placement but using an inverter

	Payback rate (years)		
System	Financial	Energy	Carbon
Windsave	34	24	10
StealthGen	200	85	36

Table 12.T shows that if an inverter is used, then the best possible payback rates to be expected from the test site are 34 and 200 years for the Windsave and StealthGen turbines respectively. This exceeds the expected lifetime of the systems. While the Windsave model can at least offset some carbon in the second half of its life, the smaller StealthGen turbine is shown to generate a positive net amount of carbon rather than offsetting any.

Under the actual testing conditions, all systems showed a negative net output. This means that all systems would generate significant amounts of carbon over their lifetime, and the capital investment is lost entirely.

Other studies have been conducted to show the viability of urban micro wind turbines. Financial payback estimates range from 170-240 years[283] for a range of wind data from Turkey, to 30-90 years[284] in the UK using a model that accounts for wind shear and terrain correction. A different approach to life-cycle analysis was taken by Allen et al[285], who calculated the energy payback to be 9 years using a micro wind turbine model based on a Weibull distribution, including inverter.

12.9 Visitor Feedback

Extracts of the feedback questionnaire results regarding micro wind turbines are shown in Figure 12.21. The feedback on micro wind turbines showed a relatively high appeal, with 59% of visitors stating they find micro wind turbines extremely appealing, and a further 24% stating a slight appeal. 18% of visitors said they definitely intend to buy a system, while a further 33% said they would probably buy one. The most frequently (27%) stated maximum price visitors were willing to pay was £1,000, while only 18% of visitors were willing to invest more than £1,000 in a micro wind turbine, assuming 2005 estimated payback rates.

In the overall ranking of all energy systems tested at the EcoSmart village the micro wind turbines ranked a close third, behind solar thermal and micro CHP systems.

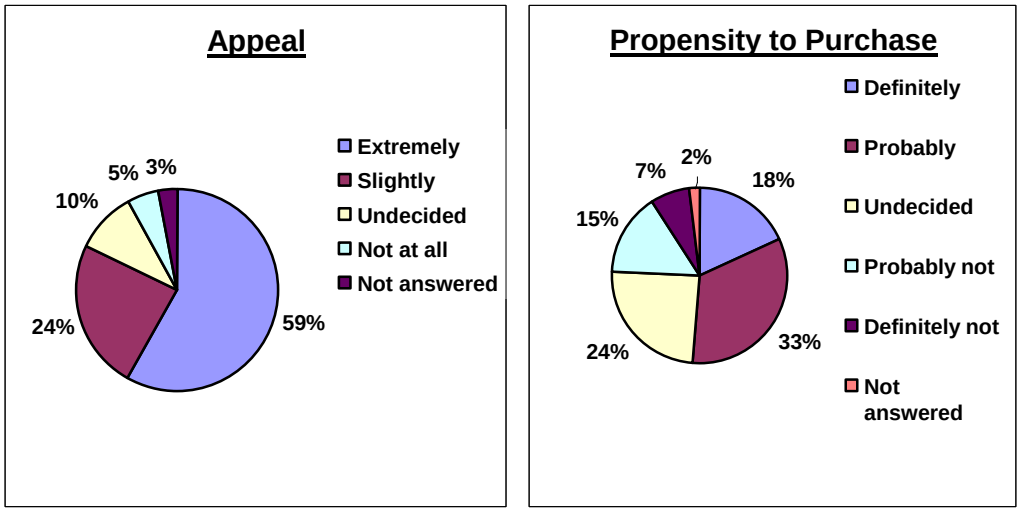

Figure 12.21: Statistics from feedback questionnaire (source: SMS Market Research Summary Report)

12.10 Conclusion

Based on the analyses of the five micro wind turbines that were tested at the EcoSmart village it must be concluded that under the given conditions they do not work. The average wind speed was found to be 3.1m/s, which is much lower than the commonly suggested minimum average of 5m/s before wind turbines become a viable option. As well as low wind speeds, two other factors were found to have a major impact on system performance: Turbulence and Inverters.

Turbulence is created around sharp edges, such as roof edges, and exists in a longitudinal, lateral and vertical plane. The amount of lateral turbulence in particular was found to have a profound effect on generation potential, and the common horizontal axis turbine design appears to be inadequate to deal with this.

Inverters have poor efficiencies at low loads, which are very common when considering the physics behind wind generation and the typical available resources (U^3 factor, Rayleigh wind distribution). At the test site it was found that for 85% of all wind speeds the inverter efficiency was below 50%. On top of this, the inverters consume energy when in standby, up to 60kWh annually. What little energy was generated by the turbines at the EcoSmart village was offset by inverter consumption.

Modelling showed that significant improvements are possible if the systems are used to supply DC electricity, thereby avoiding all inverter losses, and if the turbines are mounted in a location some distance away from the roof and other downstream obstacles to avoid the worst of the lateral turbulence. When comparing both turbines, the smaller StealthGen turbine is much less viable, not by design but because of its size.

Summary of conclusions:

- All turbines showed net negative output

- With average wind speed of 3.1m/s the test site has inadequate wind resources

- Under optimum conditions that are rarely found in any urban area, DC generation at the test site is estimated to be 232kWh and 154kWh for Windsave and StealthGen turbines respectively, resulting in financial payback after 13-30 years.

- Even under optimum conditions and given much greater wind speeds than those measured at the test site it seems unlikely that the output predicted by the manufacturer can be achieved

- Inverters consumed a considerable amount of energy, ranging between 41kWh to 64kWh annually. At low loads inverter efficiency is very poor.

- Turbulence, in particular lateral turbulence, is a major concern for urban and suburban sites. This needs to be overcome by improved technology or building integration

- At present, some micro wind turbines can pose severe safety risks due to detaching blades at extreme wind speeds

- In 2006/2007, visitors to the EcoSmart village generally found micro wind turbines very appealing. This may have changed however, as these systems have received increasingly bad press after many systems were found not to work well

13 Ground Source Heat Pump Systems

Ground Source Heat Pumps (GSHPs) are not strictly renewable energy systems, but help to use energy most effectively by effectively providing energy efficiencies far greater than 100%. This is achieved by absorbing heat energy from the ground, increasing it through the heat pump, and transferring it to the inside of the dwelling, thus providing energy for space heating.

While being proven technology using electricity, it has not yet established itself as a common space heating solution compared to gas boiler systems in the UK. However, with the impending requirements of achieving zero-carbon rating in domestic homes, and considering that space heating typically accounts for over half of the energy used, GSHP systems need to be considered as an option. The following section will assess the performance of the three GSHP systems that were installed at the EcoSmart village site and their potential applications in future zero-carbon homes.

13.1 Introduction

Ground Source Heat Pumps are well evolved systems. The concept was first published in 1852 by Lord Kelvin, and after some further development they have gained commercial popularity in Europe[286] and North America[287].

In the UK, the take-up of GSHP technology has been very slow. In 2001 the reasons for this were explored[288], and they were found to be a combination of the relatively mild climate, generally poor insulation levels of the UK housing stock and the competition presented by the extensive national gas grid. Other barriers included a lingering public perception of poor design and reliability issues from earlier days[289].

Since then however technology was adapted and GSHP systems were officially recognised as having a role to play by the Affordable Warmth and the Clear Skies programmes[287]. Research from the USA[290], Netherlands[291] and Switzerland[292] all come to the conclusion that GSHP systems can provide cost-effective means of reducing the carbon footprint of a domestic home.

13.1.1 Theoretical Background

The term heat pump refers to any device that takes up heat at a certain temperature and releases it at a higher temperature. Ground source heat pumps use the earth as a heat source, or a heat sink for reverse cycle models. The theory behind heat pump operation is set out in BS EN 15450:2007[293].

The Ground as an Energy Source

Energy is transferred to the earth's crust mainly by solar radiation. The ground absorbs this energy, and whatever remains after some initial long-wave radiation losses to the sky, is conducted deeper into the ground. It is difficult to estimate the exact amount of energy that is available for extraction, as this will not just change with soil density and composition, but also with weather conditions and moisture content. Nonetheless it is the soil temperature that is the most important factor to consider for ground source heat pump applications, as this is directly related to the extraction efficiency. A heat exchanger is used to extract heat from the ground, usually consisting of pipe-work that can be several hundred meters long.

Different Types of GSHP Systems

There are two types of GSHPs; vertical and horizontal systems. Vertical borehole systems are typically applied in domestic scenarios, where the borehole depth can be anything up to 180m, depending on system size and the anticipated load.

It was found by several studies[293, 294] that soil temperature shows little seasonal variation below a depth of around 5m and horizontal heat exchanges may be applied to alleviate some of the capital cost of the system. While being more cost effective they are only viable for relatively small systems, as a larger horizontal area is required and the ground needs to be free of large rocks and boulders.

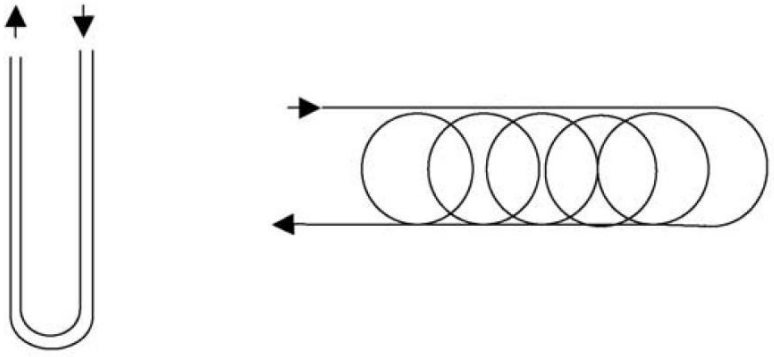

Figure 13.1: Vertical U system (left) and horizontal slinky-type system (right) (source: Curtis[288], 2001)

The Compression / Expansion Cycle

The compression / expansion cycle forms the heart of the GSHP system. An electric pump is used to circulate the transfer liquid through the earth loop at a low base temperature of approximately 0°C. As the ground is considerably warmer, the transfer liquid will absorb heat directly through the pipe system. When the warm transfer liquid re-surfaces, it goes through a heat exchanger (the evaporator), giving off heat to the compression circuit. In this circuit, shown in Figure 13.2, a refrigerant is compressed, thus increasing the temperature in accordance with the gas law, shown in equation (13.1), where terms (n) and (R) are constants for the specific refrigerant.

$$PV = nRT \tag{13.1}$$

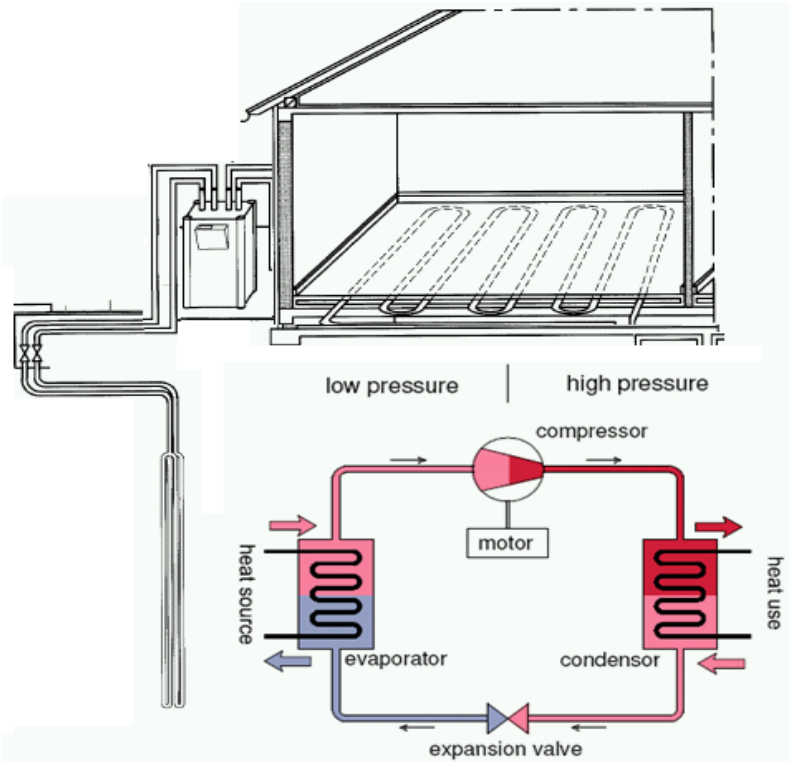

Figure 13.2: Compression / expansion circuit of GSHP system (source: Calorex GSHP user manual)

After the refrigerant has been compressed enough to reach temperatures of around 40°C, it then flows through a second heat exchanger, the condenser. There the heat energy is transferred to a third circuit which circulates water between the heat pump and the storage tank. After the heat has been transferred to the internal distribution circuit, the refrigerant then passes through an expansion valve, where it is expanded and cooled back down to temperatures of around 0°C, ready to absorb more heat from the ground loop circuit.

13.1.2 EcoSmart Village Set-up

Figure 13.3: GSHP unit (left) and borehole/piling operations (right)

Three ground source heat pump (GSHP) systems, shown in Figure 13.3, were installed and tested at the EcoSmart village. Two of the systems were vertical borehole systems installed at the Palmerston and Washington homes, with pipes laid down to a depth of approximately 70m under ground. The third system, installed in the Malvern home, was intended to have a combination of pipes laid in a vertical borehole as well as pipes laid in a horizontal trench. Unfortunately, the horizontal part of the system was damaged beyond repair during the installation process. As a result of this the horizontal section was abandoned, and the Malvern home was forced to rely only on the vertical borehole system to satisfy its space heating requirements. The increased rate of heat extraction of this system is likely to result in reduced performance and lower efficiency[294].

The two systems installed at the Palmerston and Washington homes have rated power input levels of 4.8kW, whereas the rated input power of the remaining functional part of the Malvern system was 3.6kWh. The heat pumps were supplied by Geothermal Ltd. The heat pump systems were used in conjunction with the Gledhill smart storage system, which acted as a buffer for the space heating demand. As in every other house, the heat is distributed using an under-floor distribution system. This is vital to ensure good efficiency of the heat pump systems, as compression ratios and therefore power consumption would have to be much higher to reach the 55-60°C required for conventional radiators, as opposed to the 35-40°C that are sufficient for under-floor heat distribution. Figure 1.18 shows a schematic diagram of the ground source heat pump systems.

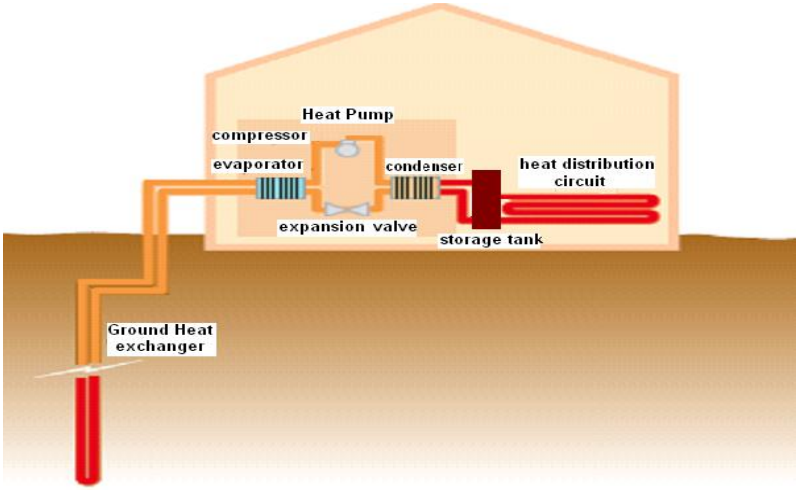

Fig. 1.18: typical GSHP schematic diagram (Source: Energy Saving Trust[295], 2004)

The GSHP systems are expected to have a coefficient of performance (CP) of 3 or above according to the manufacturer, which means that in theory, for every 1kWh of electricity consumed by the system it is expected to generate at least 3kWh of heat energy. System properties and specifications have been summarised in Table 13.A.

Table 13.A: EcoSmart village GSHP system specifications

	Palmerston	**Washington**	**Malvern**
GSHP type	vertical	vertical	vertical
Model number	HCW.048-4B	HCW.048-4B	HCW.036-4B
Power rating (electric)	4.8kWh	4.8kWh	3.6kWh
CP	>3	>3	>3
Flow rate (internal circuit)	21.0 L/min	21.0 L/min	14.7 L/min
Transfer liquid 1 (ground circuit)	brine	brine	brine
Transfer liquid 2 (internal circuit)	water	water	water

To measure the performance of the GSHP devices, the input and output of the systems had to be monitored. Electricity meters were used to record the energy input to the system. Heat meters that were attached to the pipe work of the internal heat distribution circuit, as seen in figure 1.17, were intended to provide data for heat output of the system. However, it was found that all GSHP heat meters were not functioning correctly. This is a similar problem as was encountered for the solar thermal heat meters. The faulty meters could not be replaced as this would have involved opening up the GSHP circuit. Instead, IButton temperature sensors were fixed to the flow and return pipes of the internal circuit to measure and record temperatures.

13.1.3 Set-up Problems

Some problems were encountered with the GSHP systems at the EcoSmart village. As mentioned, all heat meters failed shortly after installation and could not be replaced, as they were integrated into the heat exchanger circuit. This severely impacted on the quality of the available data.

While the heat meters presented a purely testing-related problem, the Malvern system also experienced a more significant problem that would affect the potential customer. After the pipes had been laid in trenches in the ground, part of the heat exchanger broke as the trenches were filled. It is suspected that this may have been caused by a sharp rock, or heavy machinery that operated directly over the pipes. A decision was made from a commercial point of view to abandon this horizontal system, as replacing the heat exchanger pipe would have been too expensive. While no literature was found that reports a similar problem, it is likely that this could happen if horizontal GSHP systems were to be regularly installed in new homes by Barratt or any other builder.

13.1.4 Capital Cost and Embodied CO_2

Capital Cost

The cost of a GSHP system can generally be divided into two parts; the cost of the heat pump and the cost of installing the heat exchanger. The effort and time involved with installing the heat exchanger largely depends on the type of heat exchanger, horizontal or vertical, and the consistency of the soil that needs to be penetrated. In general it can be assumed that installing the heat exchanger will account for 30-50% of total cost[296]. The capital costs of the three GSHP systems at the EcoSmart village are given in Table 13.B.

Table 13.B: Capital cost of GSHP systems at the EcoSmart village

System	Type	Capital Cost
Palmerston	Vertical	£7,800
Washington	Vertical	£7,800
Malvern	Vertical + Horizontal	£12,250

When considering capital cost for the Malvern system it must be kept in mind that this is for a combined horizontal and vertical system, for which the horizontal part had to be abandoned due to irreparable damage.

No literature was found that had established the embodied energy or carbon content of a typical GSHP system in detail. The only research in this area had been conducted on a very large GSHP scheme in Tokyo in 2002, involving 43,200 vertical boreholes[297]. This provided valuable information about the CO_2 footprint of the drilling process required to install the vertical ground heat exchanger. Other values for embodied carbon were derived based on simplified assumptions and principles. Results of this analysis are given in Table 13.C.

Table 13.C: Estimated embodied CO_2 of GSHP units at EcoSmart village

Process / Part	Embodied CO_2 ($kgCO_2$)
Drilling	370
Transport	353
Ground Heat Exchanger	82
Heat Pump Unit	393
Total	**1,198**

The value for the drilling process is adopted from Genchi et al[297], the value for transport is based on the assumption that drilling machinery is transported 100km using a heavy transport vehicle, while the pump unit is transported 200km using a light vehicle. It is assumed that the excavated soil is used for landfill nearby. Due to the lack of information it was further assumed that the pump unit, with mass of 132kg, consists of 80% Steel for the pump, 15% Copper for pipes and fittings and 5% Aluminium for casing. The values for average embodied CO_2 of these materials were taken from the ICE database, and a factor of 30% was used to account for transport of primary material and pump assembly.

13.2 Available Energy from the Ground

For closed loop ground source heat pumps the ground provides a reservoir of renewable thermal energy, which is mainly replenished by the sun. However, the question must be asked, how much energy can the ground provide?

As indicated previously this is not easily answered and depends on many factors including soil composition, moisture levels and density. The rate at which heat is added by the sun is also impotant as the ground only acts as a heat store.

Various different models[298, 299, 300] exist to estimate the variation of soil temperature, that have largely been verified using measured results. The results from a verified model[294] estimating ground temperatured for an area near Nottingham are reproduced in Figure 13.4. Figure 13.5 shows the temperature

distribution to be expected across Britain according to the standard BS EN 15450:2007[293], which deals with the design of heat pump systems.

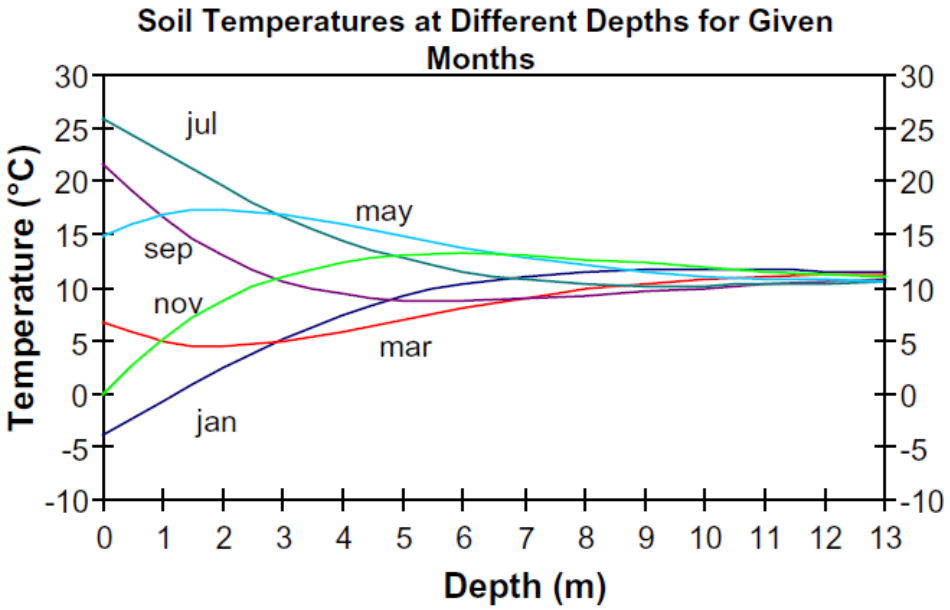

Figure 13.4: Modelled soil temperature variation in UK (Source: Doherty et al[294], 2004)

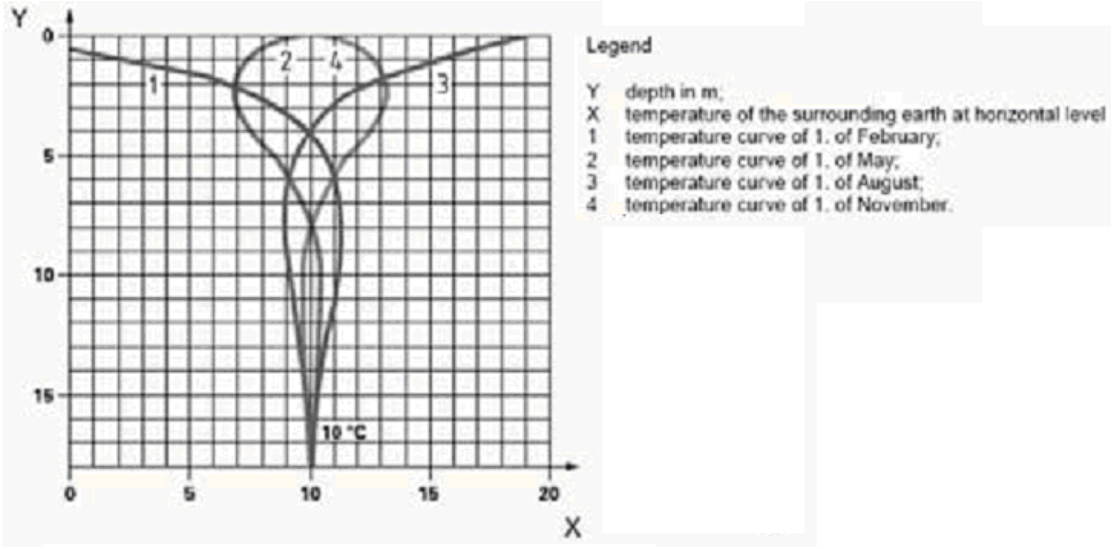

Figure 13.5: Soil temperature variations in Britain (Source: BS EN15450[293])

Figure 13.4 and Figure 13.5, taken from two independent sources, both show that soil temperatures only vary significantly at depths less than about 3-5m. Beyond 10m it can be assumed that the soil temperatures are constant at around 10°C, with maximum variations of around ± 1°C.

After assessing the temperature variation with depth of typical soil, it must also be considered that the use of a GSHP means heat is extracted from the soil, and the

distribution can change over time. This has been investigated previously, and measurements have shown the change in temperature profile due to use of a vertical GSHP system. Figure 13.6 shows soil heat distribution after 3 months of GSHP operation during the winter in Germany[286].

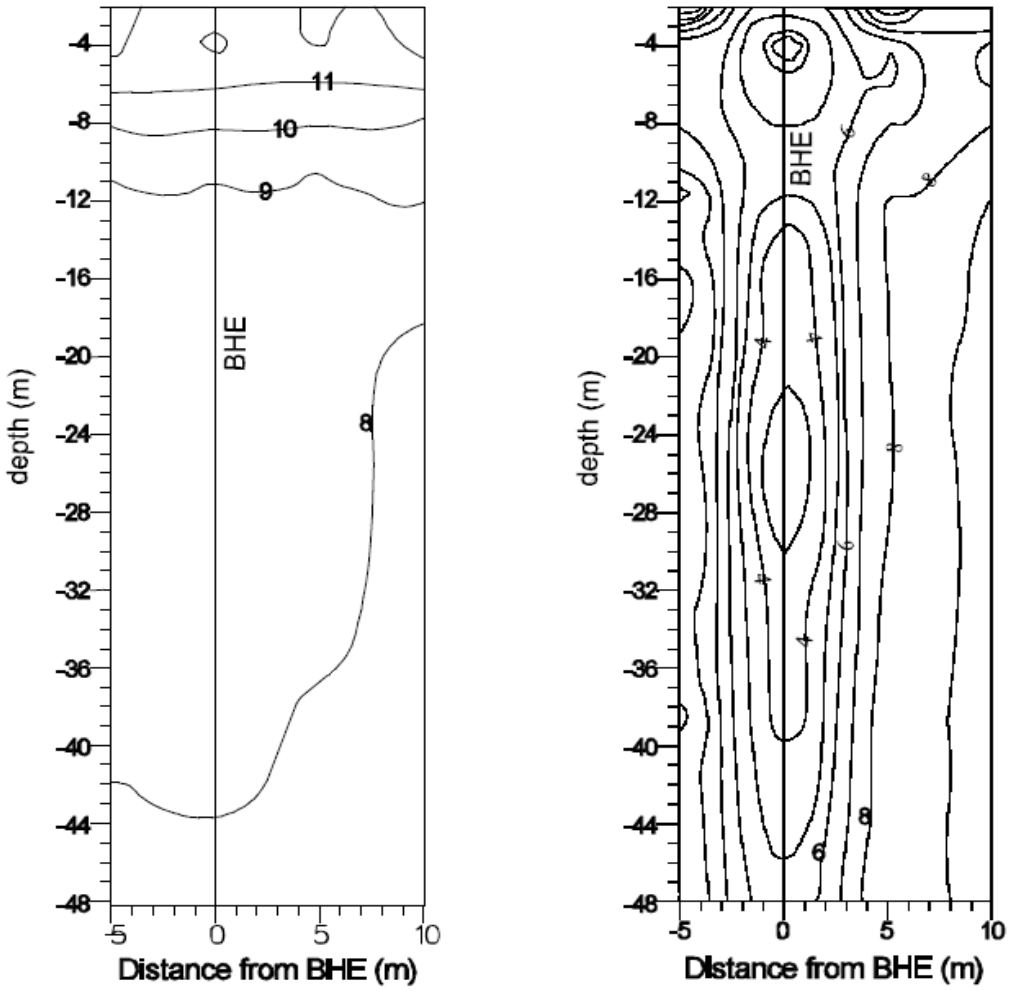

Figure 13.6: Temperature profile in °C near borehole (BHE) at beginning [left] and after 3 months operation during winter in Germany [right] (Source: Raybach & Sanner[286], 2000)

Figure 13.6 shows that the temperature decreases significantly in immediate proximity to the borehole, particularly within a 5m range around it. Other research[298] confirms this, where modelling of the ground temperature using a reverse-cycle heat pump in Hong-Kong resulted in significant temperature variations predominantly within a 5m range around the borehole. After conducting a detailed investigation, Hopkirk & Kaelin[301] suggested that if several vertical heat-exchangers are placed in close proximity they should at least be 5m apart, ideally 15m, to avoid any thermal interference.

13.3 Theoretical Output

Determining the theoretical performance of the heat pumps, which will be useful for system sizing for example, is relatively simple. The coefficient of performance (CP) of the GSHP systems determines how much electrical energy is required to satisfy the space heating demand of a building. According to the manufacturer, at least 3kWh heat energy can be expected from an input of 1kWh of electrical energy. Using this CP value together with the estimated space heating requirements for the homes, the theoretical amount of required electrical energy can be established. This involves a simple calculation using equation (13.2).

$$Q_E = \frac{1}{CP} Q_H \qquad (13.2)$$

Table 13.D is used to reiterate the space heating energy demand of the three dwellings previously found in section "9.2.4 – Model comparison", while Table 13.E shows the estimated electrical energy required to satisfy this demand using the GSHP systems. CASAnova was previously shown to give the most accurate prediction, but SAP estimates are required for compliance and are therefore also included. A moderate Coefficient of Performance (CP) value equal to 3 is assumed.

Table 13.D: Estimated space heating requirements

Q_H	SAP (adjusted) (kWh)	**CASAnova (kWh)**
Palmerston	4,576	**7,638**
Washington	3,628	**6,066**
Malvern	10,821	**14,936**

Table 13.E: Electrical energy required for space heating using GSHP, assuming CP=3

Q_E	SAP (adjusted) (kWh)	**CASAnova (kWh)**
Palmerston	1,525	**2,546**
Washington	1,209	**2,022**
Malvern	3,607	**4,987**

13.4 Measured Results and Discussion

As the heat output of the pumps could not be measured directly because the integrated heat meters were not working, the heat demand of the buildings must be determined as accurately as possible. To improve accuracy the ventilation losses must be adjusted to account for frequent opening of doors. Based on the adjusted energy demand and on the electricity consumption of the heat pumps the Coefficient of Performance (CP) can be calculated.

13.4.1 Adjusting Ventilation Losses

The energy demand for space heating was already assessed previously using the software CASAnova, which was validated and shown to be accurate using two of the EcoSmart buildings. However, it was also noted that one of the major unknown factors was ventilation losses of the dwellings.

Apart from building construction, other factors also have an affect on ventilation in practice. Opening doors for example, would allow for an air change of the building within minutes or even seconds. As the EcoSmart village homes were used as show homes, they had frequent visitors, who on the whole behaved very unpredictably. On some occasions it was observed that front doors were left open while people were inside, and even after they had left the building, in summer as in winter. This is a factor that becomes important when evaluating the performance of a space heating system based on estimated heat demand. For the purpose of determining the GSHP efficiency basd on heat demand the ventilation rate will need to be adjusted to account for the relatively frequent opening of doors. This, however, is inherently inaccurate as it was impossible to obtain any measured values other than the number of visitors.

In order to estimate the additional heat losses due to the frequent opening of front doors, several assumptions have to be made. These are as follows:

- the area of the front door is taken as 2m² with reference to the building specifications
- while the door is open, it is assumed that there is a wind speed of 3m/s, with reference to the average annual wind speed of 3.1m/s. The Palmerston front door faces west and the Malvern door faces south, which are the two most predominant wind directions
- the average daily time period during which the door is open is estimated to be 5 minutes per day, which appears reasonable for an average recorded 7 visitors per day

- the door is fully opened for relatively short periods at a time, thus allowing for a volume flow rate equal to the wind speed with relation to door area, and individual air changes less than 100% of building volume

The volume flow rate ($\dot{V}$) of air through the fully open door is given by equation (13.3):

$$\dot{V} = AU_w \qquad (13.3)$$

For the case of the EcoSmart village the volume flow rate is 6 m^3/s. The effective change in air change rate (Δ_{ach}) is given by equation (13.4), where (t_{door}) is the estimated time the door is open per day, V_t is the total building volume and 24 the number of hours per day.

$$\Delta_{ach} = \left(\frac{\dot{V} t_{door}}{V_t} \right) \div 24 \qquad (13.4)$$

The air change correction (Δ_{ach}) can then be added to the previously stated rate of air change due to ventilation losses by design (*N*), which does not account for open doors. The adjusted air change rates (N_a) for all three GSHP systems are given in Table 13.F.

Table 13.F: Adjusted air change rates

	N	Δ_{ach}	N_a
Palmerston	0.79	0.43	**1.22**
Washington	0.74	0.53	**1.27**
Malvern	0.83	0.18	**1.01**

13.4.2 Electricity Consumption

The GSHP systems for the Palmerston and Washington dwellings are identical, and both buildings have a similar heat demand. It has been established that ventilation losses have a significant effect on the space heating demand of a building, which will be used to assess the performance of the GSHP systems. The ventilation losses of the Palmerston building were determined using a pressurisation test. Given the similarity between the Palmerston and Washington and the fact that Palmerston

heat demand will be more accurate, only the Palmerston system will be analysed in detail. The Washington system will be used to provide control readings. The Malvern system, being different in design, will also be analysed in detail.

To reiterate, the available measurements to assess the GSHP performance consist of electricity consumption of the GSHP systems, electricity consumption of the Gledhill heat store systems, as well as temperatures of the flow and return pipes of the internal heat distribution circuit that connects the heat pump with the storage tank. Both the data logger readings and 'manual' readings from the import/export meters are available for the electricity consumption. Table 13.G provides a monthly breakdown of the results that have been recorded for the Palmerston and for the Malvern system, where the subscripts 'man', 'log' and 'store' refer to readings from the import/export meters (taken manually), the data logger and the Gledhill heat-store respectively.

Table 13.G: Monthly summary of GSHP related data for Palmerston and Malvern

	Palmerston (kWh)			Malvern (kWh)		
	$Q_{E,man}$	$Q_{E,\log}$	$Q_{E,store}$	$Q_{E,man}$	$Q_{E,\log}$	$Q_{E,store}$
Nov-06	*346*	346	178	*1477*	1477	230
Dec-06	*435*	435	161	*1131*	1131	274
Jan-07	*492*	492	170	*1315*	1315	233
Feb-07	376	339	78	988	1019	176
Mar-07	29	0	92	770	778	162
Apr-07	246	230	71	435	441	99
May-07	180	176	71	394	426	102
Jun-07	120	110	69	159	177	75
Jul-07	133	121	83	248	240	81
Aug-07	223	18	124	112	106	84
Sep-07	204	32	138	171	209	135
Oct-07	232	167	99	391	451	102
Annual	**3,016**	2,466	1,334	**7,591**	7,770	1,753

As for all other systems, the readings taken manually from the import/export meters will be used to analyse the performance of the GSHP system, as these meters are typically used by energy service companies. The 'manual' readings are only available after January 2007, prior to this the data logger readings will be used. The remaining 9 months generally show a close correlation between manual and data logger readings, indicating that this is a valid approach. From Table 13.G the resulting annual total electricity consumption for the Palmerston and Malvern systems are 3016kWh and 7591kWh respectively. The difference is a result of the different size of homes where Malvern, having a building volume that is 240% of the Palermerston volume, will invevitably have a much greater space heating demand.

13.4.3 Coefficient of Performance

After correcting the ventilation loss factor and finding the electricity consumption of the heat pumps the coefficient of performance can be calculated. Table 13.H shows the annual values for corrected heat demand, electricity consumption and resulting Coeffiecient of Performance (CP).

Table 13.H: Adjusted annual heat demand and resulting annual CP values

	Q_H (kWh)	Q_E (kWh)	CP
Palmerston	9,210	3,016	**3.05**
Washington	7,942	2,818	**2.82**
Malvern	17,409	7,591	**2.29**

Table 8.F shows that the CP values for Palmerston and Washington appear to be reasonably close to the manufacturer expectations, predicting a CP value 'of at least 3'[302]. The Malvern CP value on the other hand is considerably lower, seemingly showing an underperformance of the system. At this point it must be noted that the Palmerston system has the most accurate and reliable data due to the fact that a pressurisation test was carried out on the dwelling. It must also be remembered that the Malvern system was effectively undersized after the horizontal part of the heat exchanger had to be abandoned, and a smaller heat pump used as a result.

Validation

The temperature data from the pipe work of the distribution circuit can be used together with the flow rate to find an approximation of the heat energy that is transferred to the storage tank. According to manufacturer specification, the flow rate value has an accuracy of 10%[303], which will directly relate to the accuracy of the heat energy calculations. The specific heat capacity and density of pure water is used for these calculations.

Table 13.I shows the results for these calculations for the Palmerston and Malvern dwellings. As the temperature data only appears to be reliable for the period between July and October 2007, the analysis will be based on these months only.

Table 13.I: Results from manual heat energy calculations based on temperature

	Palmerston			Malvern		
	Q_E (kWh)	Q_H (kWh)	CP	Q_E (kWh)	Q_H (kWh)	CP
Jul-07	133	**492**	**3.7**	248	**651**	**2.63**
Aug-07	223	**607**	**2.72**	112	**358**	**3.19**
Sep-07	204	**631**	**3.09**	171	**465**	**2.72**
Oct-07	232	**786**	**3.39**	391	**1058**	**2.7**
Average			***3.2***			***2.8***

Table 13.I shows the calculated heat output based on temperature calculations alongside the measured electricity consumption of the systems, and the resulting coefficients of performance (CP) over the corresponding month. An average CP value was determined, based on the data available for the 4-month period. The resultant average values of CP are 3.2 for Palmerston and 2.8 for Malvern. While the Malvern CP value is relatively consistent, the Palmerston value does show significant variations, ranging between 2.7 and 3.7. There is a range of possible reasons for this, including variation in ground water and ground temperature which cannot be determined, as well as metering errors. Particularly the pipe temperatures, taken at 20-minute intervals, leave much room for error. For the Palmerston system in August for example, an error of 10% in the temperature readings would directly relate to the CP and result in a difference of 0.27, giving a value of 2.99.

When comparing the results from Table 13.I to the previously calculated CP shown in Table 13.H, there is little difference. The annual Cp value for Palmerston shows a difference of only 5%, while the Malvern system shows a difference of 22%. In general it can be expected that the CP during summer months is greater than the annual average, and given the relatively high error margins these temperature calculations appear to confirm that the previously calculated CP values are reasonably accurate.

13.4.4 Temperature and Humidity Control

The GSHP systems in all homes, including the Malvern, were found to be very good at consistently maintaining comfortable temperature as well as humidity levels. Table 13.J shows the average measured internal temperatures throughout the test year compared to the thermostat settings.

Table 13.J: Annual average internal temperatures

	Thermostat setting (°C)	Measured (°C)
Palmerston	21.0	21.1
Washington	21.0	21.3
Malvern	21.0	20.9

Table 13.J confirms the impression of the good temperature control. No other building at the EcoSmart village had internal temperatures as well controlled as those equipped with GSHP systems. This will also, to a large part, be down to the smart heat store.

To provide a more detailed overview, Figure 13.7 and Figure 13.8 show examples of the temperature and humidity variations for the Palmerston lounge during the coldest period of the test year, January to February 2007.

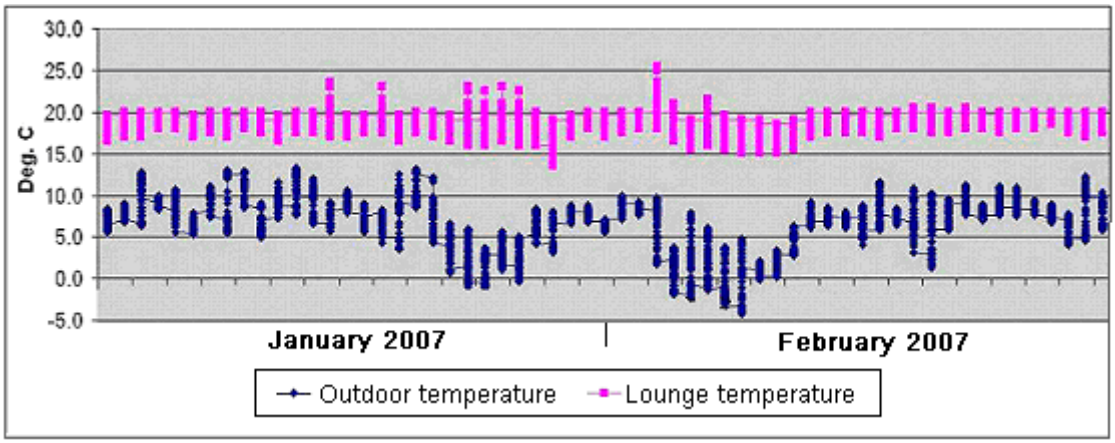

Figure 13.7: Palmerston internal temperature variations during winter period

Figure 13.7 confirms that while external temperatures reach sub-zero levels, the GSHP system is able to maintain internal temperatures at comfortable 16-21°C.

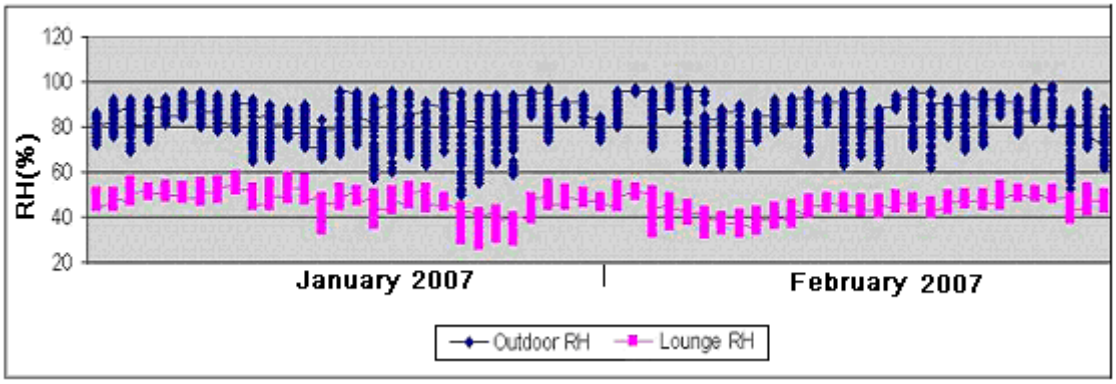

Figure 13.8: Palmerston internal humidity variations during winter period

As shown by Figure 13.8, the internal humidity levels measured in the Palmerston lounge were found to be at very comfortable levels, around 40-60% RH, while external values vary and are usually much greater. This is achieved without any active humidity control, and is suspected to be a result of the low temperature heat distribution system. Conventional radiators provide a much hotter surface that can dry out air that passes over it more than the cooler under-floor heating would. The under-floor heating may also be able to provide a comfortable atmosphere at lower air temperatures due to the increased room surface temperature, further reducing the 'dry air' effect caused by space heating.

13.5 System Reliability

While all systems worked well most of the time, some reliability issues were encountered during the test period.

Metering problems, which would not affect the system under real-life performance, have already been discussed. The Palmerston under-floor heating system was found to have a slow leak. This only became noticeable several months after construction was completed, and it was eventually discovered that the leak resulted from a nail being struck through one of the delicate pipes while the system was installed in the building. Finding the exact location of this leak was a costly and time-consuming process, which involved the removal of large areas of floor including bathroom tiles. Construction work was on-going for several weeks and would have caused severe disruptions for any family living in the home.

As for the GSHP system itself, it was functioning well most of the time. The only exception is a 3-week 'down-time' of the Malvern system, where the system was operating at extremely low temperatures. During this time the system was not able to fully satisfy the relatively low heat demand. Figure 13.9 shows heat pump electricity consumption, internal and external temperatures for this period.

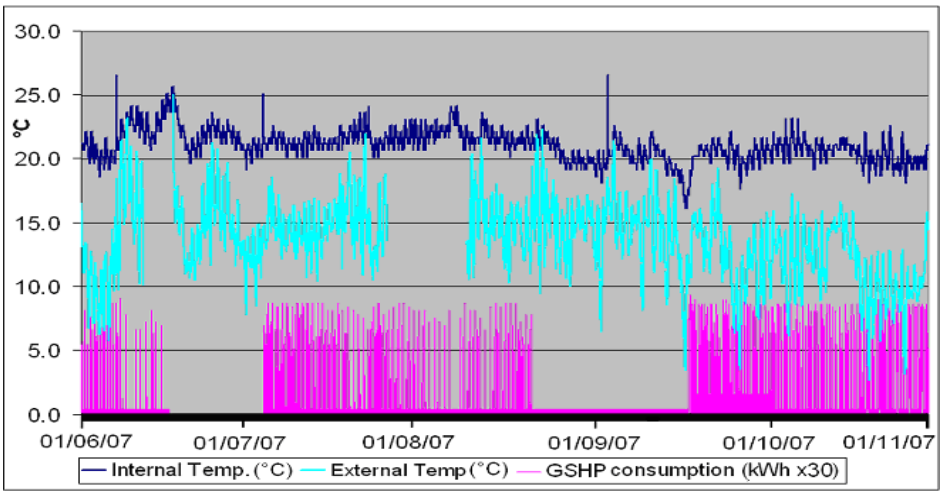

Figure 13.9: Malvern heat pump power consumption and temperature variations

Figure 13.9 shows two gaps in the GSHP power consumption. The two-week gap towards the end of June is caused by a power failure of the data logger. However, the 3-week gap towards the end of August and beginning of September shows a partial failure of the GSHP system. While the system still consumed some power it is evident that the high-power compressor could not have been running. This is also reflected in internal temperature variations, which show that a sharp drop in external temperature to around 3°C in mid September in particular cannot be compensated. The system was repaired on 18th September.

13.6 Performance Assessment

This section will discuss the performance and any reasons for discrepancies in more detail. Before doing so it must be stressed that the available data, in particular for Washington and Malvern systems, has a relatively high error margin for reasons outlined previously. Given additional accurate data, including ground temperature measurements, the GSHP systems could be modelled and the sensitivity to all variables explored in more detail. Several comprehensive GSHP models[304, 305, 306] already exist that could be used for this purpose.

During this 12-month test the Washington system and Malvern system showed CP values of 2.8 and 2.3. This is below 3, which is the minimum expected Coefficient of Performance. The Palmerston system achieved a CP of 3.1.

One factor that will have negatively affected the performance of all three systems is the fact that the pump units and some of the pipe-work of the internal distribution circuit was located outside. With reference to Figure 13.3, the pipes were somewhat poorly insulated and the pumps were encased in a thin wooden box to keep out the worst of wind and rain. There will have been substantial thermal losses, both inside the actual pump unit as well as from the pipe work. Also, any heat generated by the actual operation of the pump and compressor is lost to the atmosphere, whereas it could have generated internal gains to the home if located inside. The location was chosen to save space inside the home and avoid any problems from noise and vibrations.

Another common problem may have been the spacing between the ground heat exchangers. Being spaced approximately 5m apart, this is merely the minimum space recommended by other research[301], and given the fact that the area was surrounded by buildings that provide significant solar shading this may not have been enough for optimum performance. Based on other research[287, 291] it

should be possible to achieve a CP of at least 3.5, provided that the losses described above can be avoided.

For the Washington system, data accuracy could be responsible for the apparent underperformance of the system. The main source of error is assumed to be the rate of ventilation losses from the building. No pressurisation test was carried out, and the significant effect of visitors opening doors is only a crude estimate. It can therefore be said that when analysing the system performance, the nearly identical Palmerston set-up has far greater data accuracy and should therefore be used as a main reference for the performance benchmark for the 4.8kW heat pump model. The Washington system should be seen as verification of the Palmerston values. Given that the difference between Palmerston and Washington is less than 10%, it serves the purpose of confirming that the Palmerston value appears to be correct and relatively accurate.

The Malvern system shows the largest difference between measured and expected CP values, with the measured value being 23% below expectations. The main reason is expected to be the fact that the system was partially damaged during installation. The remaining part of the system consisted of a 3.6kW heat pump which had to satisfy a much greater space heating demand than the other two 4.8kW systems, which were installed in smaller homes. As a result of this the system was running and transferring heat at much longer intervals than the other two systems. This drained more heat from a smaller volume of soil. Also, greatest heat transfer efficiencies appear to be achieved when the heat pump system is switched on and the temperature in the storage tank is considerably lower than the output temperature of the heat pump system. When the systems are active and transferring heat for a long time, flow and return temperatures tend to converge, effectively reducing the efficiency of heat exchange. Figure 13.10 shows a typical variation of temperature difference between the flow and return pipes of the internal heat distribution circuit from the Malvern GSHP system.

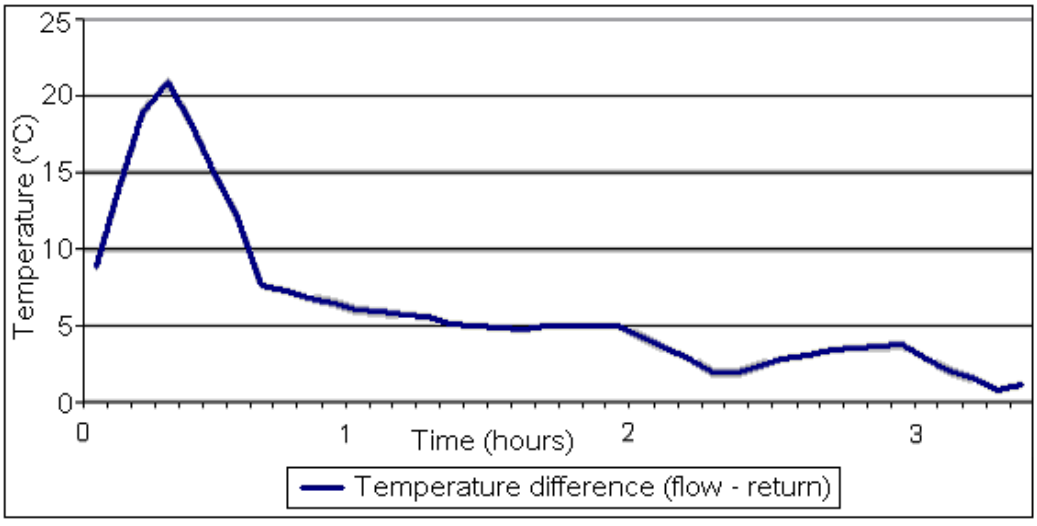

Figure 13.10: Temperature difference between Malvern GSHP flow and return pipes

Another reason for the discrepancy between expected and measured performance is again the ambiguity over ventilation losses. The Malvern represents the luxury line of Barratt homes, and could be perceived as the most 'exciting' building for visitors to take a look at. It is quite possible that the Malvern was viewed more frequently than any other home in the EcoSmart village, thus experiencing higher ventilation losses from open doors than any other building at the show village.

13.7 Visitor Feedback

A summary of the feedback questionnaire results for GSHP systems are shown in Figure 13.11. The feedback showed that 51% of visitors found the systems have extremely high appeal, and a further 25% of visitors said they had slight appeal. These values are lower than for all other systems tested. Only 12% of visitors stated they definitely intend to buy a system, while another 22% said they would probably buy one. Again, the values for propensity to purchase are lower than for any other system. With the £7800 capital cost in mind, only 16% said they were prepared to pay more than £3000 for the system assuming 2005 estimated payback rates, while 30% of visitors did not answer this question.

In the overall ranking of all energy systems tested at the EcoSmart show village the GSHP system was ranked last.

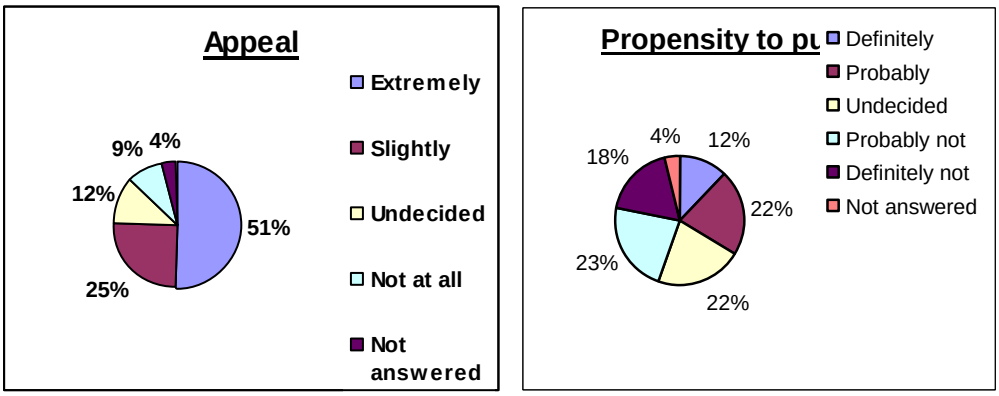

Figure 13.11: Statistics from feedback questionnaire (Source: SMS Market Research Summary Report)

13.8 Financial and Carbon Savings

The annual savings as well as financial and carbon payback periods shown in Table 13.K and Table 13.L are based on results from Table 13.H. As no reliable information could be found for the expected life-time of the system, the length of the RHI tariff (23 years) was assumed. In reality the GSHP systems should last longer than that, depending on the quality of the pump and the ground heat exchanger. It is also assumed that no maintenance will be required. The energy consumption of the smart heat store is also considered. Even though a different type of heat store may be available with considerably lower energy consumption, it is a requirement of the GSHP systems to be interfaced with such a buffer system to ensure smooth and efficient operation.

Table 13.K: Annual savings of the three GSHP systems, based on 2011 RHI tariffs

	Annual Savings			
System	Electricity offset	Heat store	2011 RHI tariffs	**Total**
Palmerston	**-£62.89**	**-£190.76**	**£644.70**	**£391.05**
Washington	-£85.29	-£180.32	£555.94	£290.32
Malvern	-£389.15	-£250.68	£1,218.63	£578.80

Table 13.L: Financial and carbon payback periods and life-time savings

	Payback rate (years)		**Net savings over system life (23 years)**	
System	Financial	CO_2	Financial	CO_2 (t)
Palmerston	**19.9**	**4.6**	**£1,194**	**4.8**
Washington	26.9	10.3	-£1,123	1.5
Malvern	21.2	-	£1,062	-11.1

Table 13.L shows a relatively poor performance of the GSHP systems. The Washington system would not achieve financial payback, and the Malvern system would generate 11.1 tonnes of CO_2 emissions over its expected life-time. However, these figures are slightly misleading, as several factors are not accounted for. As explained previously the Washington estimate is subjected to many uncertainties, and the Malvern system suffered from poor performance after the horizontal ground heat exchanger had to be abandoned.

The only one of the three systems that produced reliable data and had no problems was the Palmerston system, which has an estimated financial payback period of around 20 years, and would offset at least 4.8 tonnes of CO_2 during the first 23 years of its operation. It is believed that this could be significantly improved if the heat pump was installed inside the building, rather than subjecting it to outside temperatures. Another potential improvement to performance might be

spacing the vertical heat exchangers further apart. However, it is difficult to quantify these improvements without further testing.

Regardless of any uncertainties in performance however, a comparison of the annual savings of the three systems shows an important trend. The larger the house, and the higher the overall heat demand, the more financially viable a GSHP system would become. Although exact methods of the RHI tariff have not yet been clarified, it is most likely that the tariff will be paid based on estimated heat demand. From this research it can be deduced that the 4.8kW rated systems used in Palmerston and Washington dwellings would probably have been of sufficient size for the Malvern home.

Carbon offset would also improve over time, as more renewable energy sources are integrated into the national grid. Alternatively, highly effective zero-carbon space heating could be possible if the GSHP system is combined with a suitably sized PV system.

13.9 Conclusion

Firstly it must be mentioned that the data and resulting analyses of the GSHP systems has a high margin of error, with the most reliable analysis being that of the Palmerston system. The following points would have been required to provide robust data for the analysis:

- The temperature of the ground along the length of at least one of the ground heat exchangers, and half way between at least two of the heat exchangers would have had to be measured

- The homes should not have been used as show homes, and a pressurisation test carried out on all three dwellings to accurately determine the heat loss

- In hindsight the heat meters should have been tested prior to integrating them into the heat pump circuits. However, constructing a suitable test rig would have been relatively expensive and time-consuming and at the time could not have been justified commercially.

Nonetheless, the data that was obtained still provided some valuable indications, which are summarised below:

- All systems were able to consistently maintain comfortable temperature and humidity, which is reflected by the measured annual average internal temperatures of 21.1°C, 20.9°C and 21.3°C

- The CP values were estimated to be around 3.1 for Palmerston, 2.8 for Washington and 2.3 for Malvern

- Horizontal heat exchangers are more fragile than vertical ones and can sustain irreparable damage

- The Malvern system showed that frequent long and continuous periods of system run-time can lead to inefficiencies. It is therefore important to size the systems appropriately, although a smaller system can still provide sufficient heating

- The ability to offset carbon emissions is highly dependent on Coefficient of Performance. The threshold value is currently 2.61, although this may reduce if more 'green' energy sources are integrated into the power grid in the near future

- Thanks to the RHI scheme annual savings in the order of £300-600 can be expected, where savings are proportional to the heat demand of the dwelling. For an annual heat demand below 10MWh, financial payback takes at least 20 years. GSHP systems can become financially viable for heat demand above 20MWh, for which payback reduces to 10 years and an annual return on investment of over 10% is received.

- If a 'green' source of electricity is used and the system is sized appropriately then the GSHP could provide a 70% energy reduction and 100% carbon emission reduction for space heating

- During the testing period, the general public found the GSHP systems unappealing, which may be related to the high capital investment. However, 2011 RHI tariffs may help to change public appeal in the future

14 Micro Combined Heat and Power Systems

Combined Heat and Power (CHP) generators have been around for some time, typically consisting of a steam turbine that drives an electric generator, while producing useful heat in the process. The idea of micro CHP (μCHP) is to scale the CHP concept down to become applicable to individual households. This was achieved in the late 1990's, when the first μCHP emerged on the market. Being able to run on solid fuels such as wood-chips, the μCHP unit could be a highly efficient solution to provide net zero carbon auxiliary heat for future zero carbon homes.

14.1 Introduction

Several different technologies are available for μCHP units[307], including Internal Combustion, Steam Engines and Turbines, Gas Turbines, Fuel Cells, Organic Rankine Cycle (ORC), and the Stirling Engine.

In a 2002 report[308] to the Energy Saving Trust it was suggested that around 13.5 million UK households were suitable for small μCHP units, and around 3.2 million specifically for Stirling engine based μCHP units. However, it was recommended that more extensive independent product testing and field trials would be required. In a 2007 study from the Netherlands[309] it was also concluded that the predominant barrier to successful μCHP implementation on a large scale was perceived to be technological uncertainty, further emphasising the need for robust field trials.

14.1.1 Theoretical Background

The μCHP unit can be compared to a conventional boiler, where the main difference is that there is a focus on generating electricity, and using the 'waste heat' in the primary circuit of the central heating system. The μCHP unit that is tested at the EcoSmart village uses an external combustion Stirling engine to drive the electric generator. The Stirling engine, found to be more efficient, less noisy and having less vibration than internal combustion[310], is able to burn many different types of fuel, provided the heat exchanger is specifically designed for this type of fuel. The operating temperature of the Stirling engine is around 700-1000 °C. The working

gas, in the case of the test unit (WhisperGen) Nitrogen, is repeatedly heated and cooled, causing a change in pressure which moves pistons back and forth. The pistons then drive an alternator to generate electricity.

The Stirling engine can also be described by idealised thermodynamic analysis[311]. In phase 1, the isothermal expansion, the gas absorbs heat from the heat source as it expands, causing it to maintain a near constant temperature. Phase 2 is the isovolumetric heat removal phase, where the gas cools while remaining at a near constant volume. In the third phase, the isothermal compression, the volume is reduced while the gas remains at an almost constant low temperature by giving heat off to the heat sink. Phase four is the isovolumetric heat addition phase. This is where the gas is exposed to the heat source while it is compressed, so heat is added and pressure increases while the volume remains almost constant.

As the pistons create a cyclic movement, they are able to turn a wheel which is used to drive an electric AC generator. When the heat from the external combustion is captured and transferred to a heat transfer liquid, the system is able to provide heat energy as well as an electrical output. As this cyclic piston motion takes some time to reach a constant rhythm, the Stirling engine operates best when allowed to run for long continuous time periods.

14.1.2 EcoSmart Village Set-up

Figure 14.1: WhisperGen μCHP system at EcoSmart show village

The micro combined heat and power (μCHP) system tested at the EcoSmart village is the model 'WhisperGen Mk5' from the manufacturer WhisperTech, shown in Figure 14.1. The system is gas-fired and uses an external-combustion 4-cylinder Sterling engine. Two similar systems are tested independently, both controlled on heat demand. While being compact, at the size of a small dishwasher, the system is also reasonably quiet with low levels of vibrations.

The μCHP systems are connected to a Gledhill heat store system, which acts as a buffer for heat demand. This setup should allow the systems to run more smoothly and efficiently by decreasing the cycling periods of the systems. Table 14.A provides more detailed system specifications.

Table 14.A: Manufacturer specifications of WhisperGen μCHP system

Model	Mk5 AC Gas fired
Engine	4 Cylinder double acting Stirling engine
Fuel	Natural Gas
Electrical output	1kW rated
Thermal output	7.5-13 kW
Dimensions	480 x 560 x 840 (w x d x h)
Dry weight	150 kg

Figure 14.2, an extract of the technical specifications sheet, provides a more detailed overview of the WhisperGen Mk5 μCHP system. It shows the internal layout of the unit and provides a brief overview on how it works. At the EcoSmart village the electricity that was generated by the systems was exported to the grid using an import/export meter.

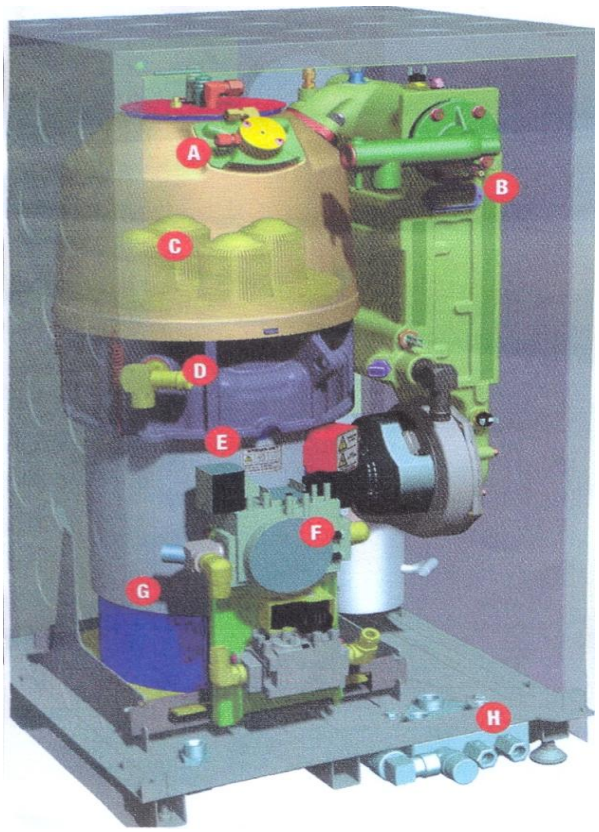

Figure 14.2: WhisperGen μCHP system (source: WhisperGen technical specification brochure)

Figure 14.2 shows the internal arrangement of the WhisperGen μCHP unit. This works as follows:

A) The gas burner heats the four cylinder heads of the Stirling engine
B) The exhaust heat recovery unit uses the heat energy from exhaust gasses to heat the water
C) The Stirling engine uses the heat from the gas burner to push the pistons back and forth
D) The water is further heated as it passes through the engine
E) The 'wobble yoke' converts the straight line motion of the pistons into a rotating motion for the alternator
F) The gas valve supplies and regulates the gas to the burner
G) The rotary alternator generates AC electricity
H) The water pipe connections deliver the hot water to the home's hot water cylinder, for the case of the EcoSmart village the heat is delivered to the smart heat store

14.1.3 Capital Cost and Embodied Carbon

Capital Cost

The capital cost of the WhisperGen systems in 2006 is given in Table 14.B. However, it is expected that the capital cost of μCHP systems in general will increase significantly as new technology begins to replace inferior existing models. In 2011/2012 the projected capital cost[64] is around £5,000, based on 1kWe rated fuel-cell systems.

Table 14.B: Capital cost of μCHP system at EcoSmart village

System	Cost
WhisperGen 1kWe	£2,700

Embodied CO_2

Similar to GSHP systems, there appears to be no estimates for embodied energy or carbon for the μCHP systems. The embodied carbon of the system will be estimated based on mass and presumed composition of materials. The system mass is specified as 150kg, and as a crude estimate it may be expected that 75% of the weight is Steel for the engine, 20% Copper for the generator and 5% Aluminium for casing and some internal parts. From previous experience for the somewhat similar GSHP system a factor of 30% should be suitable to account for primary transport and assembly. For secondary transportation, including delivery to the customer and

a factor for on-site installation, the value used for Micro Wind Turbine analysis is adopted. This is based on an average 400km round trip of one medium-sized commercial vehicle. Results are summarised in Table 14.C.

Table 14.C: Estimated embodied CO_2 of the WhisperGen μCHP units

Process / Part	Embodied CO_2 ($kgCO_2$)
μCHP materials	357
Primary transport / Assembly	107
Secondary transport	410
Total	**874**

14.2 Results from Other Research

Being relatively new technology, the Stirling engine μCHP systems, and in particular the WhisperGen (Whispertech) units, were subjected to some field trials and simulations. These are summarised below to provide a comparative overview of the practical research that was going on outside the EcoSmart show village.

In 2003, a Whispertech μCHP unit with a rated 0.75kWe output was tested for three months in a controlled domestic dwelling set up in Ottawa, Canada[312]. This unit performed well, satisfying all heat demand including hot water, and reaching efficiencies of 82%, where 76% was heat and 6% electricity. It was also found that the unit required a 'warm-up' period of 30 minutes before it was able to generate any electricity[313]. After the assessment it was recommended that more robust, long-term testing is carried out to fully establish reliability and to verify performance.

In a simulation[314] of 6 gas-powered μCHP units in Belgium in 2006, the units were able to reduce carbon emissions 9-27% compared to using an A-rated boiler and grid electricity. The WhisperGen unit specifically was able to provide 9% CO_2 savings. The simulated space heating demand was 32.4MWh, and it was concluded that Stirling engines show the greatest potentials in offsetting CO_2.

Also in 2006, results from the Carbon Trust micro-CHP Field Trials were released[315]. During these trials, 8 WhisperGen 1kWe systems, the same model that was tested at the EcoSmart village, were installed in customer homes and used under real-life conditions. The annual heat demand of the trial homes covered a wide range of 8-41MWh, and average overall efficiency of the 8 systems was 79.6% over one year. Based on the data that is presented the electric generation efficiency was 7.8% on average, resulting in an average CO_2 saving of 2% compared to an A-rated boiler. Two of the 8 systems failed to generate any CO_2 savings for that particular scenario.

14.3 Theoretical Output

The μCHP system has a rated electrical output of 1kW AC, and the manufacturer suggests that a simultaneous thermal energy output of around 7.5-13kW is achievable. This would indicate that when the system is designed to satisfy the heating requirement of a home, it is able to generate around 77-133Wh of electricity for every 1kWh of heat energy generated. In other words, around 8-13% electricity generation efficiency can be expected. The overall expected efficiency of the system is given as 90%.

The estimated heat energy demand for the two μCHP test buildings, the Buckingham and Edinburgh, are shown in table Table 14.D. The previously validated CASAnova results will be used, SAP results are shown for comparison.

Table 14.D: Estimated heating requirements

	SAP (adjusted) (kWh)	**CASAnova (kWh)**
Edinburgh	7,800	**10,207**
Buckingham	7,070	**8,753**

Equations (14.1) and (14.2) are used to calculate the primary energy (in this case Natural Gas) required to satisfy the space heating demands, as well as the theoretical electricity generation of the two systems. The term η_{total} refers to the overall efficiency of the systems including thermal and electricity output, whereas η_E is used for electrical efficiency only, based on the thermal output. The subscript 'Gas' refers to the total primary energy requirement.

$$Q_{Gas} = \frac{1}{\eta_{total}} Q_H \qquad (14.1)$$

$$Q_E = \eta_E Q_H \qquad (14.2)$$

Based on the above equations the estimated gas consumption and electricity generation was evaluated, as shown in Table 14.E.

Table 14.E: Estimated gas consumption and electricity generation of μCHP systems

	Edinburgh (kWh)		**Buckingham (kWh)**	
	Q_{Gas}	Q_E	Q_{Gas}	Q_E
CasaNova (kWh)	**11,341**	**910 – 1,470**	**9,725**	**780 – 1,260**
SAP (kWh)	8,667	590 – 1,050	7,856	530 – 950

14.4 Measured Output

The μCHP systems were interfaced with heat and electricity meters, and a gas meter was used to measure the gas consumption of the dwellings. Therefore it was possible to measure the performance of the systems directly, without the need to do any further calculations involving other measurements or estimates.

The following section will provide monthly generation and efficiencies, as well as annual values. The results will be discussed and any reasons for discrepancies to the expected performance will be explored.

14.4.1 Buckingham System

Table 14.F provides an overview of the recorded monthly values from the data logger as well as from the 'manual' readings for the Buckingham system. The manual readings were read off on a daily basis from import / export and gas meters by EcoSmart show village staff. The subscript 'store' refers to energy consumption of the smart heat store system used in conjunction with the μCHP system.

Table 14.F: Monthly breakdown of measured results for Buckingham μCHP system

	Data logger readings				Manual meter readings			
	Gas (m^3)	$Q_{E,store}$ (kWh)	Q_H (kWh)	Q_E (kWh)	Gas (m^3)	$Q_{E,store}$ (kWh)	Q_H (kWh)	Q_E (kWh)
Nov-06	188.4	72.4	1432	82.1	187.8		1400	24.6
Dec-06	219.8	77.2	1757	66.5	226.5		1818	11.4
Jan-07	218.0	75.9	1712	93.4	222.1		1731	32.1
Feb-07	116.9	38.3	982	54.4	121.4	38.6	1012	9.0
Mar-07	106.2	39.1	752	91.8	120.4	41.5	852	66.5
Apr-07	79.4	16.4	533	69.1	92.0	18.8	614	45.6
May-07	88.5	18.5	67	72.0	85.1	17.9	71	43.8
Jun-07	48.1	10.7	1	38.4	49.1	10.7	0	23.4
Jul-07	57.6	12.9	61	46.3	58.7	13.2	59	26.9
Aug-07	45.7	10.6	96	36.8	46.3	10.8	95	22.1
Sep-07	73.8	16.2	257	63.1	65.9	14.5	228	35.8
Oct-07	93.4	18.9	356	79.3	99.9	20.6	376	53.6
Annual	**1335.7**	**407.1**	**8006**	**793.2**	**1375.2**	**186.6**	**8256**	**394.8**

Table 14.F shows very little difference between the values recorded by the data logger and the control readings taken manually. With the exception of electricity generation, total values show discrepancies of less than 5%, which might be

expected given some degree of rounding error for manual readings and some losses in data logger transmission.

However, the readings for electricity output from the μCHP system shows some significant differences between data logger and manual control readings. To further highlight this discrepancy, Figure 14.3 shows a comparison between the two electricity output readings. The gas consumption and scaled heat generation are shown for reference. Gas consumption has been converted to energy based on the assumption that $1m^3$ of natural gas in the UK contains 10.8kWh of energy[316].

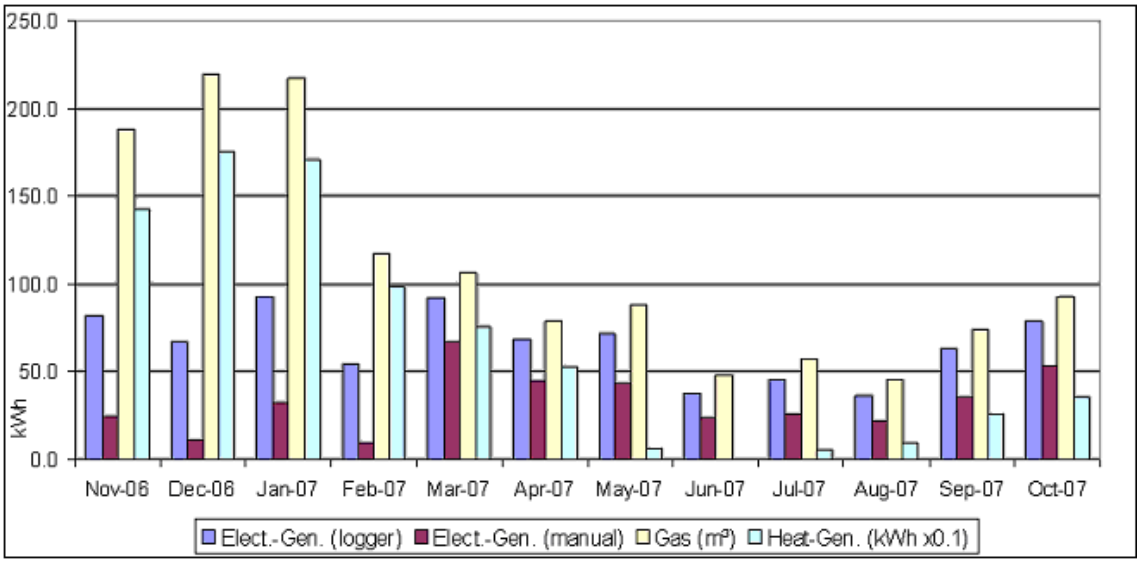

Figure 14.3: Comparison of Buckingham data

As evident from Figure 14.3, the manual readings taken from the import / export meter do not agree with the data logger readings. In particular before February 2007 the difference is very significant. This problem was not encountered for the Edinburgh system, and the data logger readings appear to be much closer to the expected output than the manual readings, in particular during the period from November 2006 until February 2007. This suggests there may have been a problem with the import/export meter used for this system.

In general the values from the manual readings would be used to assess the performance of the system, as these are taken from meters that would otherwise be used by Energy Service Companies for energy consumption charges. In this case however, based on the evidence that suggests metering errors, the data logger readings for generated electrical energy will be used for the assessment of the Buckingham μCHP system.

Figure 14.4 provides a comparison between the heat output and the electricity output for the Buckingham system. The primary energy consumption from gas is also shown to provide a first impression of the kind of efficiencies that were achieved.

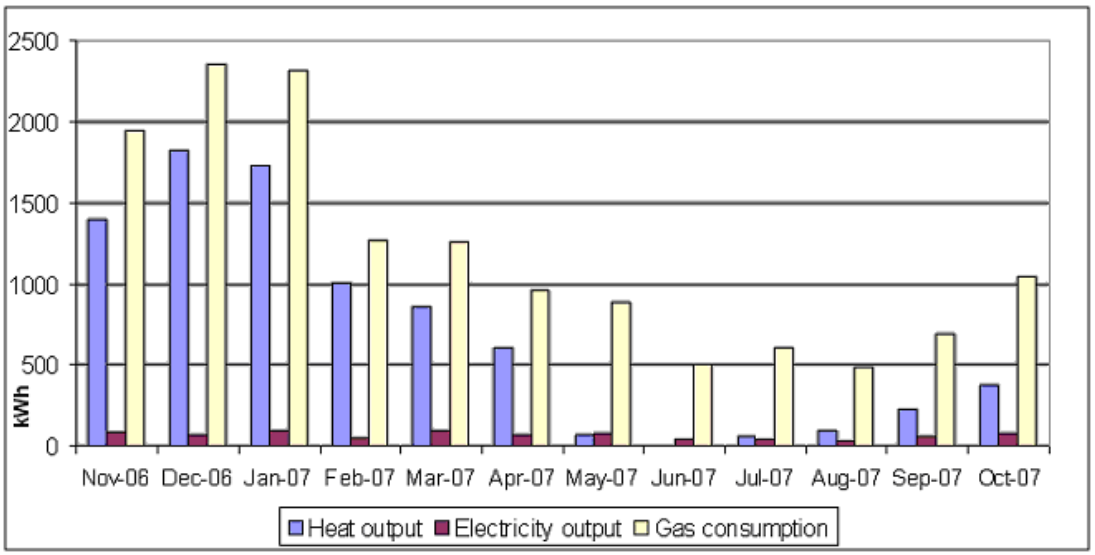

Figure 14.4: Buckingham heat and electricity output compared to gas consumption

Figure 14.4 shows some variation in μCHP performance throughout the test year. During most months the heat generation is proportional to the gas consumption. However, during the summer months May-August 2007, heat generation drops off dramatically while gas consumption of the unit remains reasonably high. This is highlighted when comparing the months of April and May 2007 directly. While the gas consumption is at comparable levels, the heat output during April is much higher than the heat output during May. Interestingly the electricity output, which is a result of the heating process, also remains at comparable levels. However, the internal temperatures of the dwelling, as seen in Figure 14.5 below, show that the heating system must have been functioning during this period. Considering that electricity generation is a direct result of heat generation, the most likely conclusion is that the Buckingham μCHP heat meter was not functioning properly during the summer periods. Given the many problems experienced with the heat meters in other applications this is entirely feasible.

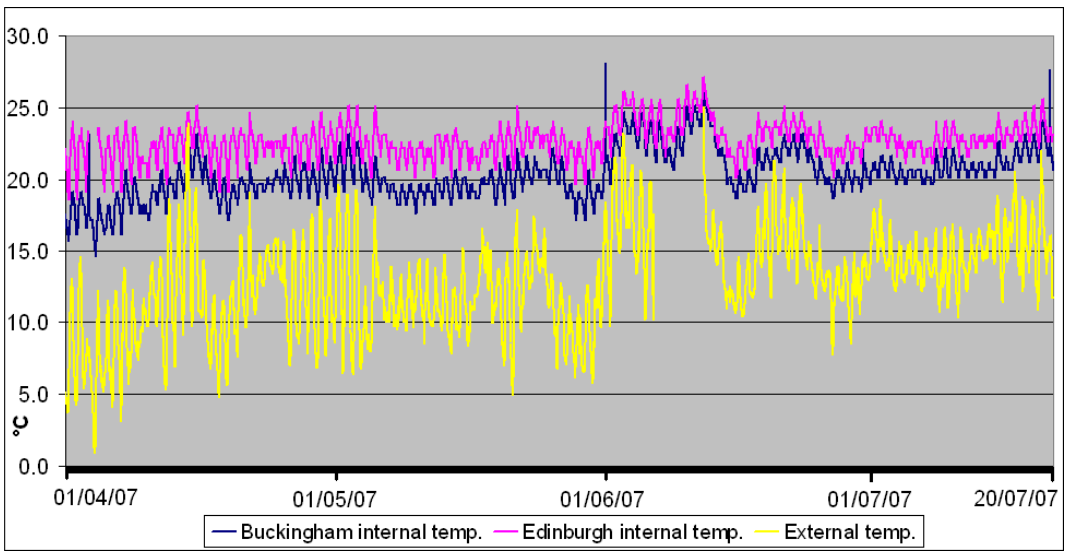

Figure 14.5: Internal temperature of μCHP-controlled homes, April-July 2007

Another discrepancy can be observed in Figure 14.4 during the period between January and April 2007. While external temperatures and solar irradiation do not change much from January to February, both gas consumption and heat output drop off quite significantly by around 40%. Figure 14.6 shows the temperature comparison for this period.

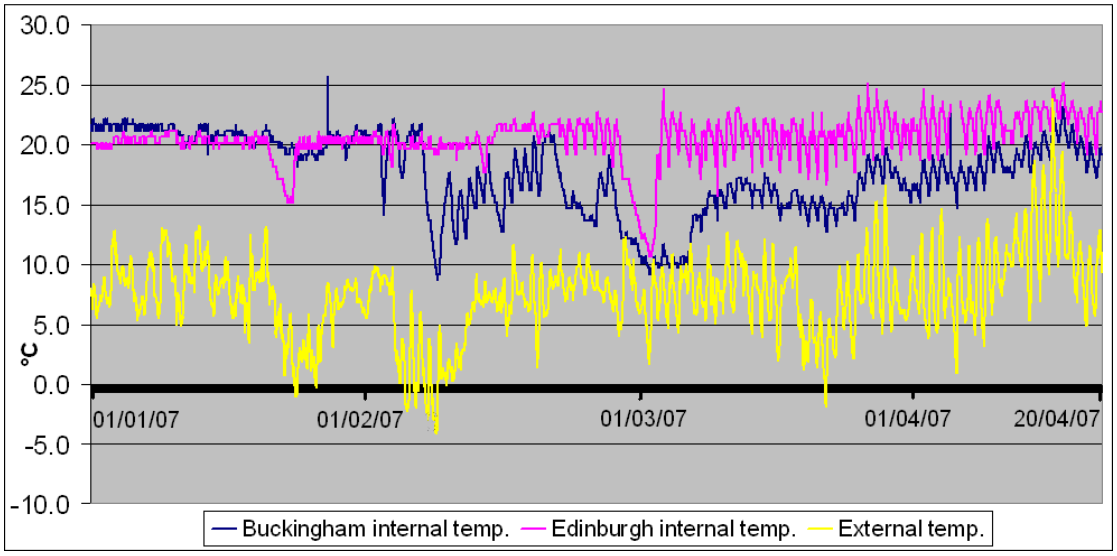

Figure 14.6: Internal temperature of μCHP-controlled homes, January-April 2007

Figure 14.6 provides confirmation for the unexpected variation seen in terms of Buckingham gas consumption for the period of February-March 2007. While both homes are very well controlled during January, performance of the Buckingham system drops off temporarily during February and early March. The system suddenly appears to be unable to control the internal temperature adequately, leading to large temperature variations and minimum internal temperatures as low as 9°C. The performance seems to recover throughout March, but temperatures are not as well controlled as before. It almost seems that a problem was triggered when the system was pushed to its limit by high heat demand. The manufacturer withdrew the unit from the market in 2007 as inhouse testing had revealed problems[317]. However, the nature of these problems was not disclosed.

Efficiency

To assess the performance of the Buckingham μCHP system in more detail, the efficiency of electricity generation was calculated on a monthly basis. The expected efficiency based on heat output should be 8-13%, and based on primary energy consumption the efficiency should be 7-11%. Table 14.G and Figure 14.7 provide a monthly comparison of electrical efficiency with respect to heat generation and to

primary energy. The monthly overall system efficiency is also found and shown for comparison.

Table 14.G: Electrical efficiency and overall system efficiency for Buckingham

	Electrical efficiency (%)		System efficiency
	of heat generation	of primary energy	
Nov-06	5.5%	4.2%	75.9%
Dec-06	3.5%	2.8%	80.0%
Jan-07	5.1%	4.0%	79.0%
Feb-07	5.1%	4.3%	84.5%
Mar-07	9.7%	7.3%	75.4%
Apr-07	10.1%	7.2%	71.4%
May-07	50.4%	8.1%	16.2%
Jun-07	100.0%	7.5%	7.5%
Jul-07	43.9%	7.6%	17.2%
Aug-07	27.9%	7.6%	27.4%
Sep-07	21.7%	9.2%	42.5%
Oct-07	17.4%	7.6%	43.8%
Annual	**8.8%**	5.5%	**63.3%**

Table 14.G shows fairly consistent values until February, giving around 5% electrical efficiency based on heat output and close to 80% overall efficiency. This is very close to what was measured during previous trials in Canada (2003) and by the Carbon Saving Trust in the UK (2003-2006). However, after February 2007 performance apparently dropped off dramatically. Based on internal temperature measurements this is true during March and April, while results for the rest of the year are inconclusive due to suspected metering errors. Figure 14.7 shows the efficiency variation in graphical form.

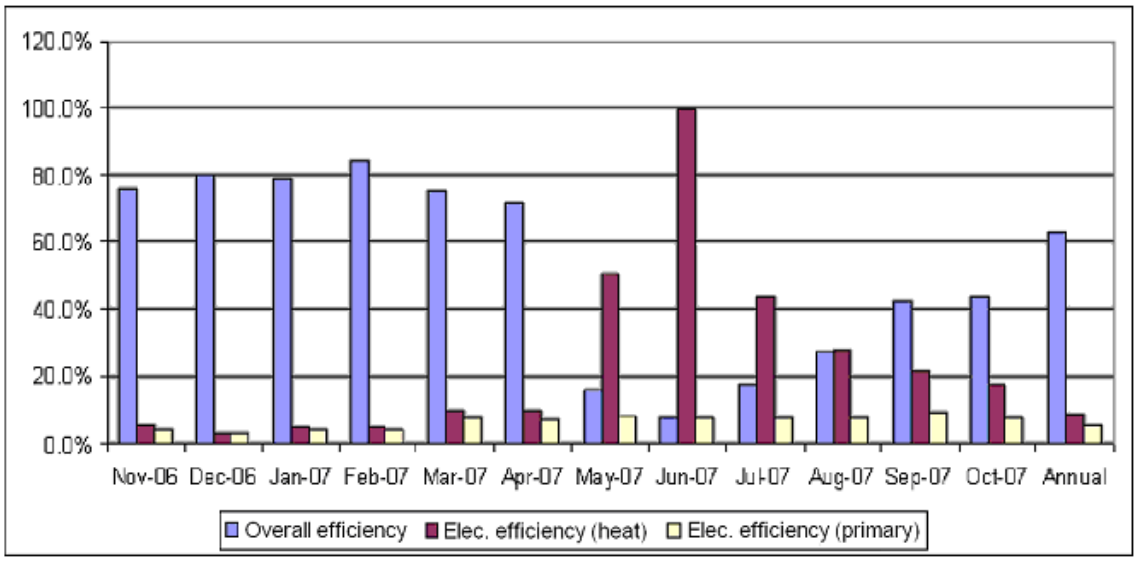

Figure 14.7: Electrical efficiency and overall efficiency of Buckingham system

To summarise it can be said that throughout the 12-month period the Buckingham μCHP system showed variable performance. Until February 2007 performance was in line with other field trials, giving overall efficiency of 80% and electrical efficiency of around 5%. During February however the system appears to have developed a problem. While electricity generation surprisingly remained high, heat generation was somehow reduced during the winter months, as evident by the internal temperature measurement which dropped to a low value of 9°C in February and March. After April 2007 the heat meter appears to have developed a problem, meaning results for the summer period are inconclusive. Nonetheless, an annual overall efficiency was recorded as 63.3%, which is significantly lower than the expected 90%. In terms of electricity generation the system performed just within the lower range of expectation, achieving an average electrical efficiency of 8.8%.

14.4.2 Edinburgh System

Table 14.H shows a monthly breakdown of the measured parameters for the Edinburgh μCHP system. While no manual control readings were obtained for the electricity consumption of the heat-store system, the data consistency of all other measurements suggest that the data logger readings can be considered to be sufficiently accurate.

Table 14.H: Monthly breakdown of measured results for Edinburgh μCHP system

	Data logger readings				**Manual meter readings**		
	Gas (m³)	$Q_{E,store}$ (kWh)	Q_H (kWh)	Q_E (kWh)	Gas (m³)	Q_H (kWh)	Q_E (kWh)
Nov-06	189.4	80.8	1553	83.2	189.3	1531	52.5
Dec-06	200.5	186.2	1369	113.2	204.5	1408	104.3
Jan-07	227.0	50.4	1032	150.9	236.6	1069	145.4
Feb-07	198.2	49.8	1375	105.6	202.9	1389	97.1
Mar-07	170.2	42.0	1255	97.5	180.9	1291	106.0
Apr-07	104.8	18.8	697	66.6	118.3	798	70.2
May-07	113.2	19.8	709	70.1	110.4	693	66.7
Jun-07	64.2	11.3	378	41.1	64.8	382	40.5
Jul-07	79.5	13.5	464	52.6	81.1	473	52.8
Aug-07	66.9	11.2	392	44.9	67.7	396	47.7
Sep-07	96.4	16.5	606	66.3	87.2	548	60.0
Oct-07	117.4	21.2	771	76.6	125.6	812	84.2
Annual	**1627.4**	**521.7**	**10601**	**968.6**	**1669.3**	**10790**	**927.4**

For Edinburgh, all readings show good consistency apart from the electricity generation for November 2006. For consistency with the Buckingham system, the data logger reading will be used for subsequent analysis. When comparing annual values, all logger and control readings are within 5% of each other, providing a verification of accuracy. Figure 14.8 shows a monthly performance comparison in terms of heat output, electricity output and gas consumption.

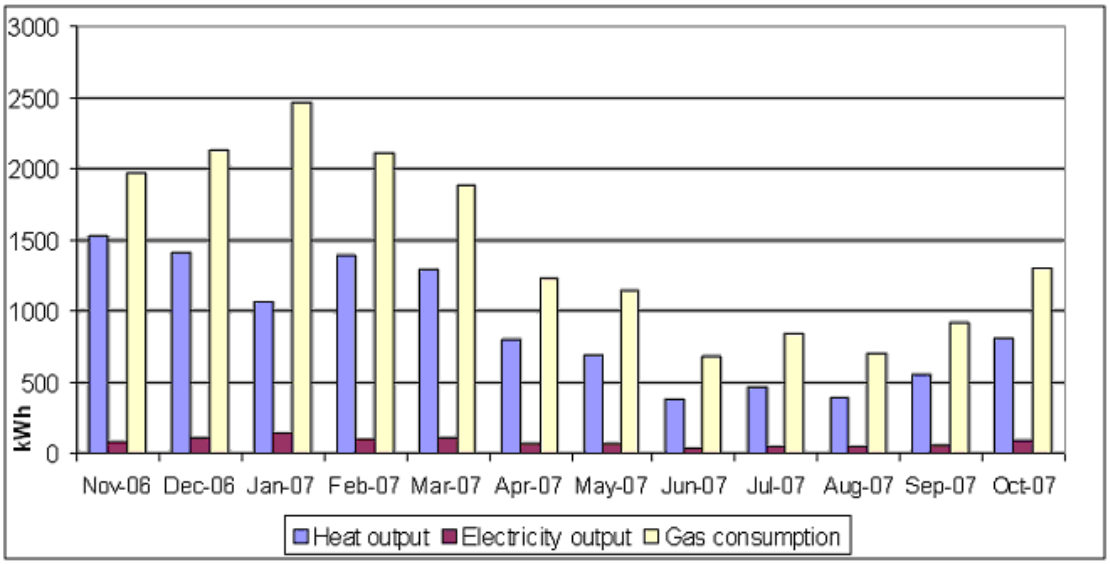

Figure 14.8: Heat and electricity output compared to gas consumption of Edinburgh system

With reference to Figure 14.8 the heat generation and gas consumption are generally in proportion to each other, with the exception of January 2007. This month shows the highest gas consumption, but lowest heat generation during the period November 2006 – March 2007. Apart from January 2007 there appears to be very little unexpected behaviour of this system, and performance seems good throughout. This is confirmed when looking at the temperature variations shown in Figure 14.5 and Figure 14.6, which show that the Edinburgh internal temperature seems to be much more stable than the Buckingham internal temperature. Having said this, when looking at Figure 14.6 there are several days in January and towards the end of March 2007, where the Edinburgh system appears to have temporary problems for several days.

Efficiency

Table 14.I provides an overview of the monthly efficiencies of electrical generation as well as overall system efficiencies.

Table 14.I: Electrical efficiency and overall efficiency for Edinburgh system

	Electrical efficiency (%)		**System efficiency**
	of heat generation	of primary energy	
Nov-06	5.2%	4.2%	82.0%
Dec-06	6.9%	4.9%	71.1%
Jan-07	12.0%	5.9%	49.4%
Feb-07	6.5%	4.6%	70.4%
Mar-07	7.6%	5.6%	74.3%
Apr-07	8.1%	5.7%	70.6%
May-07	8.8%	5.8%	66.2%
Jun-07	9.6%	6.0%	62.7%
Jul-07	10.0%	6.3%	62.3%
Aug-07	10.8%	6.8%	63.0%
Sep-07	9.9%	6.6%	67.0%
Oct-07	9.4%	6.4%	68.6%
Annual	**8.2%**	5.5%	**67.7%**

Table 14.I confirms the consistent performance of the system, with January being the only month where performance drops off. Efficiency of electricity generation is similar to that of the Buckingham systems, although these measurements can be seen as being more reliable. Again, the annual electrical efficiency is at the bottom end of what was expected. Overall efficiency however is rather disappointing. Even though the system generally worked well, except for a few days in January, the overall annual efficiency is only 68%. This is less than the expected 90%, and is poor compared to an A-rated condensing gas boiler. Figure 14.9 shows a graphical representation of efficiency variation throughout the test year.

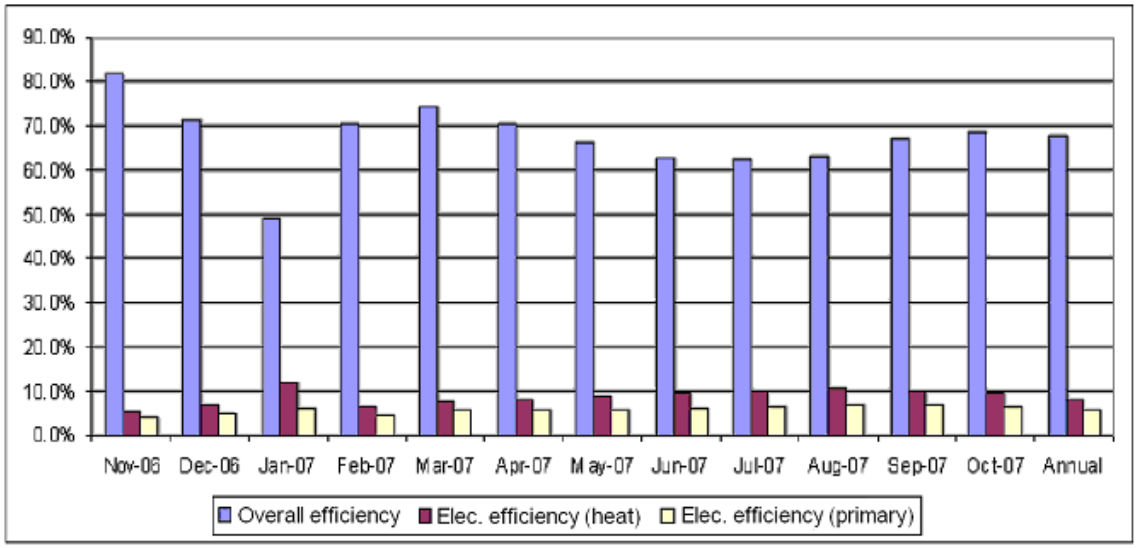

Figure 14.9: Electrical efficiency and overall efficiency of Edinburgh system

As emphasised by Figure 14.9, the overall efficiency of the Edinburgh system ranges between 62% - 82% when neglecting the January value, which is much more consistent than the Buckingham system. Apart from a few days the system appeared to work without any problems. However, despite having much fewer problems, the annual system efficiency of 67.7% is only slightly higher than the Buckingham system and much lower than that of an efficient condensing gas boiler.

14.4.3 Summary and Discussion

Both systems have shown relatively poor efficiencies. While an overall efficiency of 90% was predicted by the manufacturer, other previous field trials found efficiencies to be in the region of 75-80%. At the EcoSmart village however, the reliable data of the Buckingham system shows an annual efficiency of 68%.

The main advantage of the µCHP over conventional boilers lies in the ability to generate electricity as well as heat. Both systems have shown that the electricity generation is not quite as good as expected by the manufacturer. It was previously found in other trials[312] that there was a certain start-up time before electricity generation reached peak efficiencies. Figure 14.10 shows an extract of the typical gas consumption and electricity generation over one cycle for the Edinburgh system.

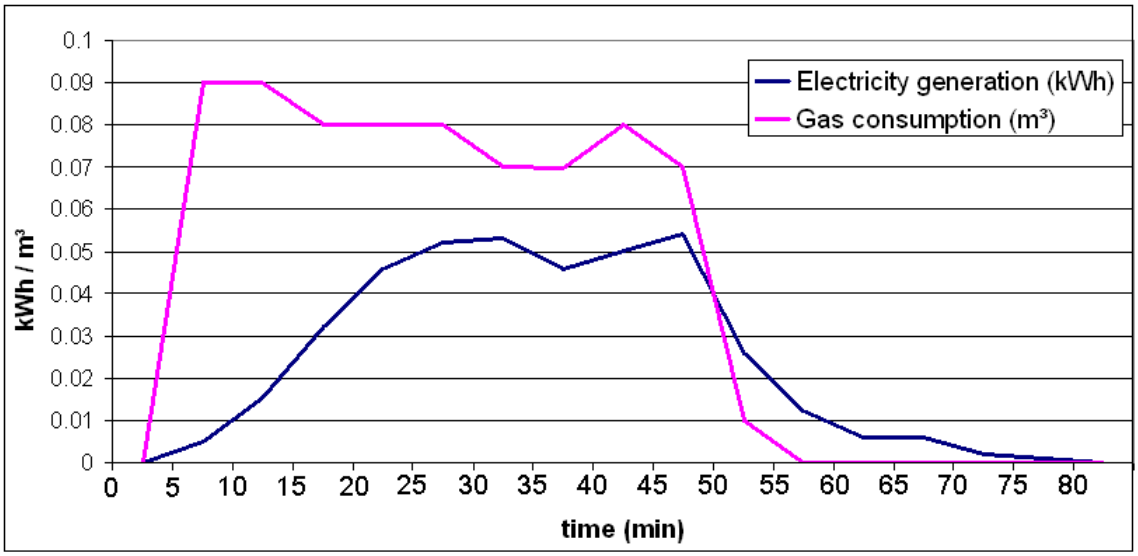

Figure 14.10: Gas consumption and electricity generation over one cycle

Figure 14.10 confirms that after the gas comes on, the μCHP system takes some time to start generating electricity at peak levels. This time period is around 30 minutes in this case, overall start-up times were found to vary between 25-40 minutes. During this time electricity generation is of rather poor efficiency. As the μCHP system runs for periods of less than 30 minutes at a time on several occasions this can be seen as a key reason for the poor overall electricity generation. The system does continue to generate some electricity from latent heat after the gas is switched off, but at much lower levels than peak performance, and only for 10-15 minutes.

A reason for this behaviour lies in the nature of the Stirling engine. The temperature difference between the two pistons needs to build up first, before the piston interaction can become a rhythmic motion, overcome all resistances and eventually drive the generator at high speeds. This is a result of the Stirling engine having a low power density. After the heat source is switched off, there is still some momentum in the system, as well as a temperature difference between the two pistons, hence some additional energy can be generated without a direct heat source.

Based on this analysis it can be concluded that the Stirling engine μCHP can only work efficiently when allowed to run for long periods of time, making them somewhat unsuitable for the demand profiles found in modern UK homes. This is also confirmed by other research[318], suggesting that for this reason this technology will be even less viable in the future.

14.5 System Reliability

Both systems showed several reliability problems throughout the test period. In particular the Buckingham system was unable to control the internal temperatures of the test home during an extensive period of around two months. While the Edinburgh system performed better throughout the test year, it also experienced problems during a total period of around 10 days. These problems occurred despite the use of a heat-store, which was expected to reduce reliability issues by extending the run-time period of the systems. Extensive testing by the manufacturer Whispertech revealed similar problems, which resulted in the unit being withdrawn from the market to allow further testing and development to take place. The manufacturer Whispertech expects to be able to release an improved and updated version of the WhisperGen unit some time in 2011.

14.6 Visitor Feedback

Results from the feedback questionnaire with regard to µCHP systems are shown in Figure 14.11. The feedback on µCHP systems shows high levels of appeal of 86%, where 63% of visitors stated they find micro µCHP systems extremely appealing. 20% of visitors stated they definitely intend to buy a system, while a further 41% would probably buy one. 20% of visitors said they were prepared to pay between £1750 and £2000 for a system, but only 11% were prepared to pay more than £2000 based on 2005 estimated annual savings of £108.

In the overall ranking of all energy systems tested at the EcoSmart village the µCHP system ranked second, behind solar thermal systems.

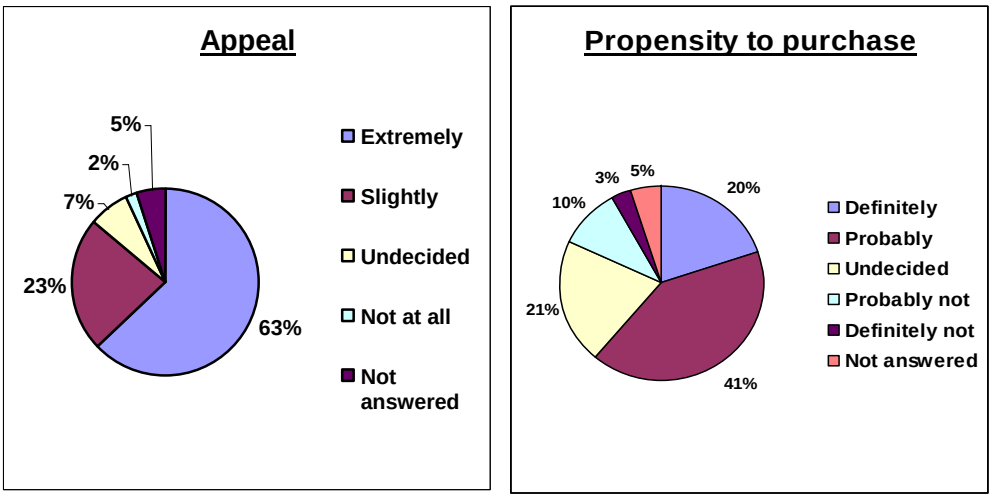

Figure 14.11: Statistics from feedback questionnaire (Source: SMS Market Research Summary Report)

14.7 Financial and Carbon Savings

By nature, the gas-fired μCHP unit is a non-renewable energy system with efficiency below 100%. However, grid electricity is considerably more expensive than natural gas, and also has much higher carbon implications. Therefore due to the onsite electricity generation the systems should, in theory, be able to generate some carbon savings and hopefully financial savings compared to a condensing gas boiler and imported grid electricity.

Table 14.J shows the annual savings for the two μCHP systems. It can be expected that typically 50% of the electricity generated by μCHP systems is exported to the grid[319]. Based on the Feed-in tariff, it is therefore assumed that an additional 5p/kWh will be paid for 50% of the electricity generation. The carbon offset is calculated in comparison to a 90% efficient condensing gas boiler. Similar to GSHPs, the μCHP payback calculations also consider energy consumption by the heat store, as such a heat store unit would presumably have to be used to allow smooth and efficient operation. As the data for the Edinburgh system is more reliable, this system should be seen as the benchmark system.

Table 14.J: Annual savings for the μCHP systems at the EcoSmart village

System	Annual Savings				
	Electricity offset	Gas offset	Heat store	2011 FIT tariffs	**Total**
Buckingham	£113.40	-£139.30	-£58.20	£115.01	£30.91
Edinburgh	**£138.57**	**-£142.17**	**-£74.60**	**£140.45**	**£62.25**

Based on the annual savings, the payback period is calculated. Carbon payback is also calculated based on the estimated embodied CO_2 shown in Table 14.C. The results are presented in Table 14.K, which also shows net life-time financial and CO_2 savings. The lifetime of a Stirling engine CHP is estimated to be 15 years[320].

Table 14.K: Payback rates and life-time savings of the μCHP systems

System	Payback rate (years)		Net savings over system life (15 years)	
	Financial	CO_2	Financial	CO_2 (t)
Buckingham	87.4	-	-£2,237	-4.2
Edinburgh	**43.4**	**-**	**-£1,766**	**-3.0**

The results of this analysis show clearly that these particular μCHP units would have been out-performed by a modern A-rated condensing gas boiler. While the Edinburgh system shows a better performance, the additional electricity consumption from both systems is not sufficient to overcome the losses due to poor

overall system efficiency. The only reason why the systems could eventually achieve payback is given by the FITs, which help to overcome any financial losses and even generate a small income.

No carbon offset is achieved in comparison to a 90% efficient condensing boiler, meaning that these systems, as tested at the EcoSmart village, would not provide a particularly good option to reduce the domestic carbon footprint. However, it must be stressed that these problems were recognised by the manufacturer and are currently being resolved.

14.8 Conclusion

Based on their ability to offset carbon emissions, which is the primary objective of systems that were being tested at the EcoSmart village, the µCHP systems have both failed. While one system had serious problems, even the system with minor problems had such poor efficiency that it could not provide any carbon savings compared to a modern A-rated condensing gas boiler. In detail, the following conculsions have been drawn:

- Both systems were able to control internal temperatures very well for some time, before experiencing problems after a few months of operation which seems to have been caused by high heat demand during winter

- One system failed for around 10 days, the second system experienced continuous problems over a period of approximately 2 months

- Both systems showed low ratios of electricity generation, of 5-10%. A probable cause for this was identified as the long start-up time for electricity generation, which severely reduced efficiency during intermittent operation

- System efficiencies for system one varied greatly and showed an annual average of 63.3%, while system two was more stable with annual average efficiency of 67.7%. Both values are far below the 90% estimated by the manufacturer.

- The Feed-in tariffs are able to make up for financial losses, but the carbon footprint of the systems is significantly higher than that of a modern A-rated condensing gas boiler

- Due to reliability issues and underperformance the model has been withdrawn from the market by the manufacturer for further development

- In 2006, the μCHP systems had high public appeal of 86%, with 20% of visitors of the EcoSmart village intending to buy one

15 EcoSmart Village Performance and Recommendations

The performances of the building-integrated energy systems at the EcoSmart village have been assessed in detail. Based on modelling and literature research, advice was given on how these systems can be improved and what gains might be expected from the improvements. The results of the analyses are summarised in this chapter to facilitate a comparison.

15.1 Performance of Renewable Energy Systems

The performances of the energy systems in terms of their financial life-time savings and their ability to offset carbon emissions are summarised in Table 15.A. The result from the Malvern GSHP system is not included as it was felt that the lack of performance caused by the failure of the horizontal heat exchanger would skew the results. Methods and assumptions for these calculations are outlined in section "6.5.3 – Calculating simple financial payback".

Table 15.A: Estimated life-time financial and carbon savings based on EcoSmart village measurements

System	Net Life-time Savings			Specific cost per tCO_2
	No. years	Financial	Carbon (tCO_2)	
PV (1kWp)	30	£2,360 to £4,690	5.3 to 8.0	-£445 to -£586
Solar Thermal (FP)	25	-£475	2.5	£187
Solar Thermal (ET)	25	-£777	3.3	£238
MWT (Windsave)	20	-£1,614	-0.4	-
MWT (StealthGen)	20	-£2,316	-0.2	-
GSHP (vertical)	23	-£1,123 to £1,194	1.5 to 4.8	£749 to -£249
microCHP	15	-£2,237 to -£1,766	-3.0 to -4.2	-

Table 15.A clearly shows that the best performing system was the PV system. Even for the 'worst-case' generation substancial carbon offset and financial savings can be expected over its expected life time of 30 years. Carbon savings were also achieved by the solar thermal systems, albeit at rather high cost of £187-238 per tonne. The GSHP system performance varied considerably for reasons previously discussed, while micro wind turbines and micro CHP systems failed to achieve any carbon savings.

15.2 Recommendations of EcoSmart Village systems and possible improvements

Throughout the analyses of test data, detailed system modelling and further research, it became apparent that there is significant room for improvement for all systems in the EcoSmart village test homes. It is expected that all the improvements suggested below could in future easily be carried out by a builder before, during, or shortly after the construction phase.

- Micro wind turbines and micro CHP systems did not work well at the EcoSmart village and failed to generate any carbon savings. This was mainly due to design flaws, and substantial effort from the manufacturers would be required to achieve any positive output. Until these problems are resolved it is recommended that these systems are omitted.

- The efficiency of the GSHP systems can be improved significantly if the pump units and all exposed pipe work is installed inside the building, and the ground heat exchangers are placed at least 10-15 meters apart. It is estimated that given these improvements a Coefficient of Performance of 3.5 is achievable. The horizontal heat exchanger proved to be rather fragile and it can be assumed that a GSHP with slightly larger size than the Palmerston and Washington systems, at around 20% extra cost, would be sufficient for the Malvern home.

- The smart heat stores used for GSHP systems consumed excessive amounts of energy. It should be possible to run a similar system using around 10% of the energy, based on the requirement for a small distribution pump and a very basic microprocessor control circuit.

- If the boiler control for the solar thermal systems would be optimised, the performance of the systems could improve by an estimated 16-27%.

- The comparison of the PV systems showed that as expected, the south-facing system inclined at 45° shows the best performance. Based on modelling using the tool PV GIS this can be taken as the optimum set-up for PV systems across the UK.

If the above mentioned improvements would be carried out at a site that is similar to the EcoSmart village, financial and carbon savings could be vastly improved. The expected savings, based on previous modelling and literature research, are summarised in Table 15.B. Methods for calculation are consistent with the methods

used for each of the previous payback analyses. For this comparison the Malvern GSHP system has now been considered, provided it is improved as described above.

Table 15.B: Expected life-time savings of improved EcoSmart village systems

System	Net Life-time Savings			Specific cost per tCO_2
	No. years	Financial	Carbon (tCO_2)	
PV	30	£4,690	8.0	-£586
Solar Thermal	25	-£68	4.1	£17
GSHP (vertical)	23	£2.479 to £12,804	12.2 to 22.2	-£203 to -£577

The expected effects of system improvements presented in Table 15.B confirm that the GSHP systems show a vast potential for improvement. The greatest benefit can be achieved by the Malvern home, which has a relatively high space heating demand. For the Malvern system, the financial savings for each tonne of carbon offset is comparable to that of the PV system.

Overall, the PV system remains the most beneficial system in terms of life-time performance. It is able to provide the greatest financial return on CO_2 emission offsetting, and also has the potential to provide greatest overall life-time carbon savings if the size of the system is increased.

16 Conclusion

The EcoSmart village was designed and built to test a range of renewable energy systems, to establish how they can contribute to reducing carbon emissions in domestic homes, how reliable they are and how they can be improved. Another important aspect for the successful integration is the ability to accurately predict the performance of these systems. The analysis of the test site was able to provide answers to all these points, which are summarised below.

16.1 Availability of Resources

The availability of adequate resources forms the basis for renewable energy systems to work well in the urban environment. These natural energy resources include direct solar radiation, wind and heat from the ground.

Even in UK climate the availability of direct solar radiation is sufficient for solar systems to generate a substantial amount of energy. The relatively cold ambient temperatures mean solar thermal systems can become less efficient unless well insulated using a vacuum, but they can also increase the efficiency of PV systems.

Wind resources in urban environments generally appear to be insufficient for wind energy generation. Average wind speeds of 3.1m/s were measured at the test site. A widely recognised minimum average wind speed for efficient wind generation is 5m/s.

Although ground temperatures were not measured, other UK research and the performance of the EcoSmart GSHP systems throughout the winter months suggest that resources are adequate. However, as ground energy is mainly supplied by the sun, it can be expected that ground shading will have a significant effect on the available resources. This should be investigated further if the application of GSHP systems is considered.

16.2 Predicting Realistic Performance

During this research it was identified that there is a significant gap between the accuracy of methods used to predict system performance by academia and by industry. In an attempt to close this gap several methods were presented that can be used to accurately predict the performance of renewable energy systems. The methodology of these tools was critically reviewed and validated using data from the EcoSmart village. The following methods can also be used to validate the accuracy of future standard industry methods, such as SAP 2009.

PV: Several freely available and accurate tools were found and validated. For the UK, the recommended tool is PV GIS, developed by the European Commission Joint Research Centre. To provide an even simpler alternative, a prediction method was developed during this research that uses a UK benchmark value and a look-up chart to account for variables.

Solar Thermal: Due to the complexity and many variables it is very difficult to accurately predict the performance of these systems. A complex model was created and validated using results from this research. A less accurate but more user-friendly tool is provided by RETScreen, developed by many experts from government, academia and industry in Canada.

Micro Wind Turbines: Accurately assessing the available resources is essential for predicting wind turbine performance. The annual average wind speed can provide a good indication. A tool created by the Energy Saving Trust uses methodology that appears to provide accurate estimates. The use of the NOABL database is not recommended for urban or suburban sites. Apart from using average wind speeds each individual site must also be analysed for sources of turbulence, which can be caused by any nearby obstacle, including the roof on which the turbine may be mounted. It is recommended by other research to mount turbines at least at a height 50% above obstacle height.

GSHP: In order to accurately predict the performance and carbon or financial savings from these systems the heat demand must be known. The most accurate tool or method that was reviewed during this research is given by the tool CASAnova, although in general some errors can be expected from variations in ventilation losses. Developed as an educational tool, it is freely available and does not require any licensing. SAP 2005 was found to underestimate the space heating demand. After establishing the heat demand, the coefficient of performance can be used to find the electric energy demand of the heat pump. It was found that a

realistic CP estimate is 3-3.5, although this can vary significantly based on heat pump model, installation method, and the composition and shading factor of the ground.

MicroCHP: Similar to GSHP systems, it is essential to predict the energy performance of the building to predict system performance. When this is known the efficiency factors provided by the manufacturer or system field trials must be relied upon.

16.3 Actual System Performance at the EcoSmart Test Site

After thoroughly testing the integrated systems over a period of 12 months under real weather conditions and analysing the data in detail, a final verdict on the performance can be drawn.

PV: The PV systems worked consistently and reliably. With the exception of one system, which showed underperformance of around 5%, it was found that all systems performed as expected. Based on 2006/2007 weather conditions the systems would save 5.3-8.0 tonnes of CO_2 emissions throughout their expected life-time (30 years). With 2011 Feed-in Tariffs the annual return on investment would be 5.9-7.7%.

Solar Thermal: Both Solar Thermal systems had some reliability issues resulting from incorrect installation and set-up, as well as mismatching components. Due to unfavourable boiler settings both systems were found to under-perform by an estimated 17-26%. The measured annual generation was found to be 462kWh (flat panel) and 588kWh (evacuated tube). This results in carbon emission savings of 2.5-3.3 tonnes over the expected system life-time of 25 years. With 2011 RHI Tariffs the annual returns on investment would be 4.1% for the flat panel and 3.6% for the evacuated tube system, meaning no payback is achieved within the expected system lifetime.

Micro Wind Turbines: These systems had several reliability issues. Manual start-up was required after turbine furling during high wind speeds, leading to significant down-time. On one occasion a blade detached during extreme wind speeds, posing a high safety risk. The turbines also failed to perform well, which is a result of inadequate wind resources, lack of consideration for turbulence and inverter inefficiencies. The systems did not generate any carbon emission or financial savings.

GSHP: The only horizontal ground heat exchanger to be tested was damaged beyond repair during installation. As a smaller vertical heat exchanger remained in tact, this heat pump system effectively became undersized. Despite this it was able to maintain comfortable internal temperatures, albeit at significantly reduced efficiency. All systems using vertical ground heat exchangers worked consistently and reliably. However, the under-floor heat distribution circuit in one of the homes was found to have a slow leak, resulting in tedious and expensive repairs. All three systems underperformed slightly. This is suspected to be a result of the pump as well as some pipe work being exposed to cold ambient temperatures, and of the vertical heat exchangers not being placed far enough apart. Given the installation problems and general lack of performance, one system was found to effectively emit 11.1 tonnes of CO_2 over the expected lifetime of 23 years, while the other two achieved emission savings of 1.5-4.8 tonnes of CO_2. The estimate of 4.8 tonnes CO_2 savings is based on the most reliable set of data. This system would also achieve financial payback after 19.6 years, while across all three systems the annual return on investment is in the range of 3.7-4.7%. This includes the energy consumption of the smart heat sore.

MicroCHP: Neither of the two systems worked reliably. While one experienced down-time of around 10 days, the second showed severely reduced performance throughout 2 winter months. Overall efficiencies were 63% and 68%, with approximately 5-6% electricity generation. Both systems failed to outperform a grade A condensing gas boiler.

16.4 Lessons Learnt

While on the whole the energy generation from the systems tested at the EcoSmart village may be seen as disappointing, very valuable lessons have been learnt from many of the problems that were encountered. The detailed analysis of the test site has revealed that many of the problems can easily be avoided, while others are inherent to technology that has not yet fully matured. To summarise, the main problems include:

- Solar Thermal systems are very complex systems. A finely tuned interaction of correct installation, sizing of components and control settings is required for these systems to work efficiently.

- Current designs of horizontal axis Micro Wind Turbines appear to be unable to adequately deal with turbulence, in particular the lateral turbulence caused by downstream obstacles and roof edges in urban environments.

- GSHP systems should ideally be placed in a warm environment, such as the inside of the house, and the ground heat exchangers must be placed far enough apart (at least 10-15m) to work efficiently.

- The gas-fired μCHP systems did not achieve the predicted efficiencies, and were found to have a higher carbon footprint than modern condensing gas boilers. The problems were recognised by the manufacturer and the unit was subsequently withdrawn from the market for further development.

- The support systems, inverters for electrical and smart heat stores for space heating systems, can severely reduce the performance of the renewable energy systems. Both consume significant amounts of energy and, in the case of the inverters, are likely to lead to vastly reduced generation efficiencies.

16.5 Recommendation

Based on the analysis carried out as well as some experiences from other research, a final recommendation can be made.

Solar thermal systems are able to provide significant hot water savings of up to 40% if the system performance is improved. However, this is a challenging task. Due to the complexity and many variables, 4 out of 5 systems experienced problems as a result of inadequate installation, mismatch of components, and unfavourable control settings. Metering inaccuracies make it difficult to detect some of these problems. If solar thermal systems are used, it is essential that these are installed by experienced suppliers with good track record, and customers must be informed about how they can get the best performance from these systems. The actual savings will heavily depend on the hot water requirements of individual households.

PV systems have proven to be reliable and have consistently performed as expected. As grid electricity has higher carbon content than natural gas they can be very effective at reducing domestic carbon emissions, offsetting around 10% of the annual carbon footprint per 1kWp. With 2011 Feed-in Tariffs, average 1kWp PV systems throughout the UK are expected to generate a return on investment of 7.6%, achieving payback after 13.2 years. Based on the reliability and the ability to

offset carbon emissions while generating considerable long-term financial savings, the integration of PV systems in every new home is recommended.

The horizontal axis micro wind turbine systems appear to be inherently inefficient in turbulent conditions, which are inevitable in urban environments. In addition to this, it can be expected that in most urban environments there is insufficient wind energy potential to see any significant output from these systems. It is therefore not recommended that these systems are installed on typical urban or suburban low or zero carbon homes.

GSHP systems are generally reliable and have the potential to perform well. However, care must be taken when installing the systems and the suggested improvements should be considered. It is recommended that only vertical ground heat exchangers are used, as horizontal heat exchangers appear to be fragile and can be damaged beyond repair. The under-floor heating system used with GSHPs can also lead to problems if they develop leaks after installation. The ability of the GSHP systems to generate carbon emission and financial savings generally increases with heat demand of the building. If the annual heat demand is relatively high (15-20MWh), the total carbon footprint of the home can be reduced by around 15%, and an annual return on investment up to 12% can be achieved. It is recommended that GSHP systems are considered for large homes with high space heating demand. However, the main priority should be to reduce space heating demand as much as possible, meaning this should not be considered as a standard heating solution for typical low or zero carbon homes, unless applied to a communal scheme. The application of Air Source Heat Pumps (ASHP) might also be considered as a more mainstream solution, although it was outside the scope of this project to review and analyse these systems.

MicroCHP systems could potentially have some benefits, in particular if they are using bio fuel. However, they have not performed well at the EcoSmart village. It is therefore recommended that the improved systems are subjected to rigorous long-term (at least 12 months) independent testing before they are considered for large-scale application in new homes.

17 Further Work

Due to the limited time and resources that were available for this research project, it was not possible to examine all aspects in the same amount of detail. This section will present a recommendation for some of the areas that will need to be explored further to provide a more complete picture.

It was already discussed that the available data for GSHP systems in particular was insufficient for an accurate assessment. It is recommended that in further field trials of these systems ground temperatures are measured to provide an overview of the effects of heat removal and in particular heat addition by the sun, as well as the effects of ground shading.

It was also mentioned that Air Source Heat Pumps (ASHPs) might provide a more practical alternative. These systems should be reviewed, tested, and compared to GSHPs.

During this research it was shown that support systems, such as the smart heat store, can have a significant effect on system performance. It is recommended that the control strategy and also the energy consumption of these stores are investigated in more detail.

Many of the heat meters used at the EcoSmart village were not functioning properly. To avoid these problems in future it would be a useful exercise to test these meters and develop a better understanding of why exactly they failed.

References

[1] Tyndall J, "On the absorption and radiation of heat by gases and vapours, and on the physical connection", Philosophical Magazine Vol. 22, pg. 277-302, 1861

[2] Revelle R, Broecker W, Craig H, Kneeling C, Smagorinsky J, "Restoring the Quality of our Environment: Report of the Environmental Pollution Panel", Presidents Science Advisory Committee, The White House, 1965

[3] Pales J, Keeling C, "The concentration of atmospheric carbon dioxide in Hawaii", Journal of Geophysical Research Vol. 70, pg. 6053-6076, 1965

[4] Mitchel J, "On the world-wide pattern of secular temperature change", Changes of climate: Proceedings of the Rome Symposium organised by UNESCO and the World Meteorological Organisation, 1963

[5] Balling R, "The Heated Debate: Greenhouse Predictions versus Climate Reality", Pacific Institute for Public Policy, 1992

[6] Shanahan J, "A Guide to the Global Warming Theory", The Heritage Foundation, Backgrounder: Energy and Environment, 1992

[7] Michaels P, "Meltdown: The Predictable Distortion of Global Warming by Scientists, Politicians and the Media", Cato Institute, ISBN 1930865597, 2004

[8] Singer S, Avery D, "Unstoppable Global Warming Every 1,500 Years", Rowman & Littlefield, ISBN 0742551172, 2007

[9] Will G, "March of the polar bears", Washington Post press article, 22/05/2008

[10] Peterson T, Connolley W, Fleck J, "The Myth of the late 1970s Global Cooling Scientific Consensus", American Meteorological Society, DOI:10.1175/2008BAMS2370.1, 2008

[11] Hansen J, Wang W, Lacis A, "Mount Agung eruption provides test of a global climatic perturbation", Science Vol. 199, 1065-1068, 1978

[12] Sommerville R, Le Treut H, Cubasch U, Ding Y, Mauritzen C, Mokssit A, Peterson T, Prather M, "Climate Change 2007 – Chapter 1: Historical Overview of Climate Change", IPCC Fourth Assessment Report, Working Group I: The Physical Science Basis, 2007

[13] Levermore G, "A review of the IPCC Assessment Report Four, Part 1. The IPCC process and greenhouse gas emission trends for buildings worldwide", BSERT Vol. 29-4, 349-361, 2008

[14] IPCC, "Climate Change 2007: Synthesis Report – Summary for Policy Makers", Fourth Assessment Report, 2007

[15] A list of all EIT countries is given at http://www.oecd.org/document/53/0,3746,en_2649_34361_2346101_1_1_1_1,00.html, viewed 01/01/2011

[16] A list of all OECD member countries is given at http://www.oecd.org/document/58/0,2340,en_2649_201185_1889402_1_1_1_1,00.html, viewed 01/02/1011

[17] HM Treasury, "Background to Stern Review on the Economics of Climate Change", Cabinet Office, 2006

[18] Stern N, "Stern Review: The Economics of Climate Change – Summary of Conclusions", HM Treasury London, 2006

[19] Adam D, "I underestimated the threat, says Stern", The Guardian press article, 18/04/2008, available at http://www.guardian.co.uk/environment/2008/apr/18/climatechange.carbonemissions, viewed 20/10/2010

[20] Hubbert M, "Nuclear Energy and the Fossil Fuels", American Petroleum Institute, 1956

[21] De Almeida P, Silva P, "The peak of oil production – Timings and market recognition", Energy Policy Vol. 37, pg. 1267-1276, 2009

[22] Hirsch R, Bezdek R, Wendling W, "Peaking of World Oil Production – Impacts, Mitigation, & Risk Management", Report prepared for United States Department of Energy, February 2005

[23] Hirsch R, "Mitigation of maximum world oil production: schortage scenarios" Energy Policy Vol. 36-2, pg 881-889, 2008

[24] "The Kyoto Protocol", British Energy Informational Report, 2008

[25] DECC, "UK Climate Change Sustainable Development Indicator: 2008 Greenhouse Gas Emissions, Final Figures", Department of Energy and Climate Change, Statistical Release, 2010

[26] "Delivering carbon savings in the domestic sector", Business Council for Sustainable Energy UK, Publication, 2010

[27] DECC, "The UK Low Carbon Transition Plan" Department of Energy and Climate Change, 2009

[28] DCLG "Code for Sustainable Homes: A step-change in sustainable home building practice", Department of Communities and Local Government Publication, 2006

[29] DCLG "What Standards may be in 2013 & 2016", Department of Communities and Local Government Publication, 2007

[31] DCLG "Code for Sustainable Homes: Technical Guide", Department of Communities and Local Government Publication, 2008

[32] DCLG, "Grant Shapps sets out grand design for the future of green housing", Department of Communities and Local Government press release, available at http://www.communities.gov.uk/newsstories/newsroom/1602634, viewed 10/10/2010

[33] Shorrock L, Henderson J, Utley J, "Reducing carbon emissions from UK housing stock", Housing Centre, BRE Environment, BR 480, ISBN 1 86081 752 1, 2005

[34] Boardman B, Darby S, Killip G, Hinnels M, Jardine C, Palmer J, Sinden G, "40% House", Environmental Change Institute, ISBN 1874370397, 2005

[35] RCEP, "Energy-The changing climate", The Royal Commission on Environmental Pollution, Stationery Office, 2000

[36] Boardman, "Examining the carbon agenda via the 40% House scenario", Building Research and Information Vol. 35-4, pg. 363-378, 2007

[37] Thomson, "High density micro-generation in UK distribution networks", International Conference and Workshop on Micro-Cogeneration technologies and Applications, Ottawa, Canada, 2008

[38] EST, "Potential for Microgeneration Study and Analysis", Energy Saving Trust, commissioned by Department of Trade and Industry, 2005

[39] Maunsell F, Capener P, "Supporting and Delivering Zero Carbon Developments in the South West", Final Technical Report for SWRA, SWERDA and GOSW, 2007

[40] DTI, "Our Energy Future – Creating a low carbon economy", Department of Trade and Industry, Energy White Paper, 2003

[41] DTI, "The Energy Challenge – Energy Review Report", Department of Trade and Industry, 2006

[42] Fay R, Treloar G, Iyer-Raniga U, "Life cycle energy analysis of buildings: A case study", School of Architecture and Building, Deakin University Australia, 2000

[43] RAB, "The role of onsite energy generation in delivering zero-carbon homes", Renewables Advisory Board, URN Number: 07/1555, 2007

[44] Moloney S, Maller C, Horne R, "Housing and sustainability: Bridging the gap between technical solutions and householder behaviour", 3rd AHRC Conference, Housing Research for a Sustainable Affordable Future, RMIT University Melbourne Australia, 2008

[45] Shipworth D, "Synergies and conflicts on the landscape of domestic energy consumption: beyond metaphor", ECEEE Summer Study – What works and who delivers?, Panel 6 – Dynamics of consumption, pg. 1381-1391, 2005

[46] Chen B, Pitts A, Ward I, "Indicator for Sustainable Housing Design: from EcoHomes to the Code for Sustainable Homes", Paper 131 at Conference on Passive and Low Energy Architecture, Dublin, 2008

[47] BRE, "EcoHomes 2006 – the the environmental rating for homes: The Guidance / Pre-assessment eliminator", Issue 1.2, 2006

[48] Theobald K, Walker S, "Meeting the challenge of zero cabon homes: A multi-disciplinary review of the literature and assessment of key barriers and enablers", School of the Built Environment, Northumbria University, 2008

[49] WWF-UK, "How low. Achieving optimal carbon savings from the UK's existing housing stock", Centre for sustainable Energy and Association for the Conservation of Energy, 2008

[50] DEFRA, "Attitudes and Behaviour Study", Department of the Environment, Farming and Rural Affairs, London, 2008

[51] Sale O, "Public attitudes to climate change, motivators and barriers to action: Newcastle and the North East", CarbonNeutral Newcastle, 2005

[52] Dodds L, Dobson G, "Tackling barriers to take-up of fuel poverty alleviation measures", Sustainable Cities Research Institute, Northumbria University, 2008

[53] Policy Studies Institute, "A synthesis review of the public understanding research projects", DEFRA, London, 2007

[54] Dresner S, Enkins P, "Economic instruments to improve UK home energy efficiency without negative social impacts", Fiscal Studies 27-1, pg. 47-74, 2006

[55] Tzortzopoulos P, Cooper R, Chan P, Kagioglou M, "Clients' activities at the design front-end", Design Studies Vol. 27-6, pg. 657-683, 2006

[56] Shaw R, "Eco-towns and the next 60 years of planning", Town and country planning: tomorrow series, paper 9, 2007

[57] Banfill P, Peacock A, "Energy-efficient new housing: the UK reaches for sustainability", Building Research and Information Vol. 35-4, pg. 426-436, 2007

[58] Lowe, "Assessing the challenges of climate change for the built environment", Building Research and Information Vol. 35-4, pg. 343-350

[59] Kuznik F, Virgone J, Noel J, "Optimisation of a phase changing material wallboard for building use", Applied Thermal Engineering Vol. 28, pg. 1291-1298, 2008

[60] Holford J, Woods A, "On the thermal buffering of naturally ventilated buildings through internal thermal mass", Journal of Fluid Mechanics Vol. 580, pg. 3-29, 2007

[61] UK-GBC, "Zero Carbon Task Group", UK Green Energy Council, 2008

[62] Calcutt, "The Calcutt review of housebuilding delivery", Department for Communities and Local Government, London, 2007

[63] DCLG, "Cost Analysis of The Code for Sustainable Homes", Final Report, Department for Communities and Local Government Publications, London, 2008

[64] DCLG, "Code for Sustainable Homes: A Cost Review", Department for Communities and Local Government, ISBN 978-1-4098-2236-3, 2010

[65] Gupta R, Chandiwala S, "Achieving low carbon buildings using Code for Sustainable Homes in the UK", International Journal of Low-Carbon Technologies Vol. 4, pg. 187-196, 2009

[66] Passiv Haus Institute, "What is a Passiv Haus", Publication, 2008

[67] AECB, "The Energy Performance Standards", Carbon Lite Programme Vol. 3, 2008

[68] Sweett C, "A cost review of the Code for Sustainable Homes", English partnerships, Housing Corporation, 2007

[69] Chow Y, "Utilizing district energy system as a cost-effective measure in meeting UK domestic 'zero-carbon' targets", International Journal of Low-Carbon Technologies Vol. 0, pg. 1-6

[70] Mortal A, Chow Y, "A comprehensive assessment of low carbon energy systems for the domestic sector", European Meeting Point: Energy for Development Conference, 2007

[71] London Energy Partnership, "Towards Zero Carbon Development: Supportive Information for Boroughs", The Crown and Greater London Authority, 2006

[72] http://www.greenhouseleeds.co.uk/intro, viewed 10/10/2010

[73] http://zerocarbonhousebirmingham.org.uk/, viewed 10/10/2010

[74] http://www.zerocarbonhouse.com/Home.aspx, viewed 10/10/2010

[75] Kingspan "Climate for change", Presentation, Project Sentinel, 2008

[76], "Green House by Barratt – A home for the future", National Centre for Excellence in Housing Publication, 2008, available at http://dcfw.org/media/publications/25/en/green_house_by_barratt_nc_brochure3_a4_v5_print.pdf, viewed 28/01/2011

[77] Twinn C, "BedZED", The ARUP Journal 1, 2003

[78] Willimas A, "Friends of the Earth?", The Architects Journal Vol. 221-14, pg. 39-40, 2005

[79] Sommerhoff E, "Carbon-neutral neighbourhood: ZED factory – BedZED", Sutton Architecture Vol. 92-4, pg. 87-89, 2003

[80] Jennings I, Newman P, "Cities as Sustainable Ecosystems: Principles and practices", Island Press, ISBN 9781597261883, 2008

[81] Lazarus N, "Beddongton Zero (fossil) Energy Development: Toolkit for Carbon Neutral Developments –Part II", Bioregional Development Group, 2003

[82] "Case Study: Hanham Hall, South Gloucestershire – Rising to the Carbon Challenge", Homes & Communities Agency, 2010

[83] http://www.breeam.org/newsdetails.jsp?id=692, viewed 10/10/2010

[84] PRP Architects Press release regarding Greenwatt Way zero-carbon development, available at http://www.prparchitects.co.uk/news/news-releases/438/innovative-development-in-slough.html, viewed 10/10/2010

[85] Meikle J, "Family builder moves into millionaire's row", The Guardian Article, 21/09/1999, available at http://www.guardian.co.uk/uk/1999/aug/21/jamesmeikle, viewed 26/09/2010

[86] 'Greensitt & Barratt' Company prospectus from 1968

[87] Wellings F, "Dictionary of British Housebuilders: A Twentieth Century History", Wellings publishing, ISBN 9780955296505, 2006

[88] Office for National Statistics, "Age Structure of United Kingdom", available at http://www.statistics.gov.uk/populationestimates/flash_pyramid/UK-pyramid/pyramid6_30.html, viewed 27/09/2010

[89] Barratt Develpoments, "History", Promotional and Informational website content, available at http://www.barrattdevelopments.co.uk/barratt/en/aboutus/history, viewed 24/09/2010

[90] Twigger R, "Inflation: The Value of the Pound 1750-1998", House of Commons Library, Economic Policy and Statistic Section, 1999

[91] "British Homebuilder Buys Developer in Record Deal", The New York Times press article, 05/02/2007, available at http://dealbook.blogs.nytimes.com/2007/02/05/uk-homebuilder-buys-developer-in-record-deal/, viewed 28/09/2010

[92] "Annual Report and Accounts 2009", Barratt Developments PLC, 2009

[93] DCLG, "Homes for the future: more affordable, more sustainable", Department for Communities and Local Government, London, 2007

[94] RAB, "The role of onsite energy generation in delivering zero-carbon homes", Renewables Advisory Board, URN Number: 07/1555, 2007

[95] DCLG, "Housing and Planning Statistics 2009", Department for Communities and Local Government, ISBN 9781409819769, 2009

[96] NHBC, "Flats Continue To Rise", Press Release, 29/11/07

[97] DCLG, "House Price Index – August 2010", Department for Communities and Local Government, 2010

[98] Drucker P, "The Practice of Management", Elsevier Ltd., ISBN 9780750685047 (Revised version), 1955

[99] McInnes W, "A conceptual approach to marketing", Theory in Marketing, Homewood, 1964

[100] Dickson P, "Toward a General Theory of Competitive Rationality", Journal of Marketing, Vol. 56, pg. 69-83, 1992

[101] Wind, "Mastering Management Part 15: Big Questions for the 21st Century", Financial Times, 1996

[102] Greyser S, "Janus and Marketing: The Past, Present, and Prospective Future of Marketing." In Reflections on the Futures of Marketing: Practice and Education, Marketing Science Institute, 1997

[103] Landis GYR, "Single Phase BS Standard Credit Meter 5235", Technical data, http://www.alternativeenergystore.co.uk/pdfs/LandisGyr5235B.pdf, viewed 13/10/2010

[104] http://www.microcustom.co.uk/metermaid_tech.html, viewed 13/10/2010

[105] http://www.maxim-ic.com.cn/products/ibutton/ibuttons/thermochron.cfm, viewed 13/10/2010

[106] Hawkes A, Leach M, "Impacts of temporal precision in optimisation modelling of micro-Combined Heat and Power", Energy Vol. 30, pg. 1759-1779, 2005

[107] Ghahramani S, "Fundamentals of probability", 3rd Edition, Prentice Hall, ISBN 0131453408, 2004

[108] Wolberg J, "Data Analysis using the Method of Least Squares: Extracting the most Information from your Experiments", 1st Edition, Springer, ISBN 3540256741, 2005

[109] Fadem B, "High-Yield Behavioural Science (High-Yield Series)", 3rd Edition, Lippincott Williams & Wilkins, ISBN 0781782589, 2008

[110] Personal correspondence with Professor PJ Laycock, School of Mathematics, University of Manchester

[111] http://www.statsoft.com/textbook/distribution-tables/#t, viewed 21/09/2010

[112] "Planning and Energy Act 2008", *Office of Public Sector Information*, 11/2008 414211 19585, 2008

[113] "Consultation on supply license conditions", *Dpt. of Energy & Climate Change*, 2009

[114] DECC, "Feed-in Tariffs – Government's Response to 2009 Consultation", *Department of Energy & Climate Change,* 2010

[115] DECC, "Renewable Heat Incentive – Consultation on the proposed RHI financial support scheme", *Department of Energy & Climate Change,* 2010

[116] DECC, "Updated energy and carbon emissions projections 2008", Department of Energy and Climate Change, London, 2008

[117] UK Photovoltaic Manufacturers Association (http://www.uk-pv.org), viewed 26/06/2010

[118] British Gas Report, "Domestic Carbon Emission Levels for selcted Cities", *Centrica*, 2006

[119] Anderson B, "SAP 2009", BRE Presentation given April 2010, available at http://www.sesg.strath.ac.uk/Presentations/2010%20Regs%20SAP%202009%20BA_2010-04-20.pdf viewed 29/09/2010

[120] POSTnote, "Carbon Footprint Of Electricity Generation", Parliamentary Office of Science and Technology, Number 268, October 2006

[121] Hammond G, Jones C, "Embodied energy and carbon in construction materials", Proceedings of the ICE – Energy Vol. 161-2, pg. 87-98, 2008

[122] Hammond G, Jones C, "Inventory of Carbon and Energy (ICE) Version 1.6a", Sustainable Energy Research Team, University of Bath, 2008 available at www.basth.ac.uk/mech-eng/sert/embodied, viewed 02/11/2010

[123] Ishikawa T, "Grid-connected photovoltaic power systems: survey of inverters and related protection equipments", Central Research Institute of Electric Power Industry Japan, IEA-PVPS T5-05: 2002, 2002

[124] Grauers A, "Synchronous generator and frequency converter in wind turbine applications: system design and efficiency", Chalmers University of Technology, Technical Report no. 175 L, ISBN 91-7032-968-0, 1994

[125] Cace J, et al. "Urban Wind Turbines: Guidelines for Small Wind Turbines in the Built Environment", WINEUR Project Report, Intelligent Europe, 2007

[126] Personal Communication with Dr Alan Williamson, Senior Research Fellow at the University of Manchester

[127] Mondol J, "Sizing of grid-connected photovoltaic systems", *International Society for Optical Engineering, SPIE Newsroom*, 2007

[128] Orgill J, Hollands K, "Correlation Equation for Hourly Diffuse Radiation on a Horizontal Surface", Solar Energy Vol. 19, pg. 357-362, 1977

[129] Erbs D, Klein S, Duffie J, "Estimation of the diffuse radiation fraction, for hourly, daily and monthly-average global radiation", Solar Energy Vol. 28, pg. 293-307, 1982

[130] Reindl D, Beckmann W, Duffie J, "Diffuse Fraction Correlations", Solar Energy Vol. 45, pg. 1-8, 1990

[131] Duffie J, Beckman W, "Solar Engineering of thermal processes", 3rd Edition, *Wiley & Sons*, ISBN-13 978-0-471-69867-8, 2006

[132] Levermore G., Parkinson J., "Analysis and algorithms for new test reference years and design summer years for the UK", *BSERT Vol. 27-4, pg. 311-325*, 2006

[133] Roberts J, "Dew Point Temperature", Encyclopaedia for Agricultural, Food and Biological Engineering, ISBN 0824709381, 2003

[134] Lawrence M, "The Relationship between Relative Humidity and the Dewpoint Temperature in Moist Air: A Simple Conversion and Applications" American Meteorological Society Vol. 86, pg. 225-233, 2005

[135] Shelquist R, "An Introduction to Air Density and Density Altitude Calculations", Shelquist Engineering Publication, 2010

[136] Jones F, "Techniques and Topics in Flow Measurement", CRC Press, ISBN 0849324750, 1995

[137] Lide D, "CRC handbook of chemistry and physics", 87th Edition, CRC Press, ISSN 0147-6262, 2006

[138] Schlatter T, Baker D, "Thermodynamic subroutines", *National Oceanic and Atmospheric Administration*, 1991

[139] Shorrock L, Utley J, "Domestic Energy Fact File 2003", BRE Housing Centre, ISBN 1860816231, 2003

[140] CIBSE, "Guide B - 2. Ventilation and air conditioning", ISBN 1903287588, 2002

[141] Jaakkola J, Miettinen, "Ventilation rate in office buildings and sick building syndrome", Occupational Environmental Medicine Vol. 52, pg. 709-714, 1995

[142] Personal communication with Dr. Rodger Edwards, University of Manchester

[143] Sherman M, "Tracer-gas techniques for measuring ventilation in a single zone", Building and Environment Vol. 25-4, pg. 365-374, 1990

[144] Sherman M, "Estimation of infiltration from leakage and climate indicators" Energy and Buildings Vol. 10-1, pg. 81-86, 1987

[145] Sherman M, Grimsrud D, "Infiltration - pressurization correlation: Simplified physical modelling", ASHRAE Transactions, OSTI ID: 5443198, 1980

[146] SAP "The Governments Standard Assessment Procedure for Energy Rating of Dwellings", 2005

[147] Clemens J., Benkert S., Heidt F. D., "CASAnova - An educational software for energy and heating demand, solar heat gains and overheating risks in buildings", Sixth European Conference on Energy in Architecture and Urban Planning, Bonn, September 2000

[148] Born F, et al "On the integration of renewable energy systems within the built environment", Building Serv. Eng. Res. Technol. Vol. 22-1, pg. 3–13, 2001

[149] Schoen T, "Building-integrated PV installations in the Netherlands; Examples and operational experiences", *Solar Energy* Vol. 70-6, pg. 467–477, 2001

[150] Erge T, Hoffmann V, Kiefer K, " The German experience with grid-connected PV systems", *Solar Energy* Vol. 70-6, pg. 479–487, 2001

[151] Masters G, "Renewable and Efficient Electric Power Systems", Wiley Interscience, ISBN 0471280607, 2004

[152] Messenger R, Ventre J, "Photovoltaic Systems Engineering", CRC Press, ISBN 0849317932, 2004

[153] Southgate L, "Sustainable Electrical Building Services Masters Programme - Module 5", *University of Manchester*, 2006

[154] DCLG, "Code for Sustainable Homes: A Cost Review", Department of Communities and Local Government Report, ISBN 978-1-4098-2236-3, 2010

[155] Alsema E, Frankl P, Kato K, "Energy Payback time of photovoltaic energy systems: Present status and future prospects", 2nd World Conference on Photovoltaic Solar Energy Conversion, Vienna, 1998

[156] Phylipsen G, Alsem E, "Environmental life-cycle assessment of multi-crystalline silicon solar cell modules", Department of Science, Technology and Society Report 95057, Utrecht, 1995

[157] Alsema E, Nieuwlaar E, "Energy viability of photovoltaic systems" Energy Policy Vol. 28, pg. 999-1010, 2000

[158] Nawaz I, Tiwari G, "Embodied energy analysis of photovoltaic (PV) system based on macro and micro level", Energy Policy Vol. 34, pg. 3144-3152, 2006

[159] Wilson R, Young A, "The embodied energy payback period of photovoltaic installations applied to buildings in the UK", Building and Environment Vol. 31-4, pg. 299-305, 1996

[160] DTI, "Photovoltaics in Buildings: Safety and the CDM regulations", 2000

[161] http://www.jgiesen.de/daylight/

[162] Braun J., Mitchell J., "Solar geometry for fixed and tracking surfaces", *Solar Energy* Vol. 31-5, pg. 439-444, 1983

[163] http://solardat.uoregon.edu/SunChartProgram.html

[164] Murphy G, Kummert M, Anderson B, Counsell J, "A comparison of the UK Standard Assessment Procedure and detailed simulation of solar energy systems for dwellings", Building Performance Simulation, **DOI:** 10.1080/19401493.2010.494734, 2010

[165] Suri M, Huld T, Dunlop E, "PV GIS: A web-based solar radiation database for the calculation of PV potential in Europe", Int. J. Sustainable Energy Vol. 24-2, pg. 55-67, 2005

[166] Scharmer K, Greif J, "Database and Exploitation software", ESRA vol.2, 2000

[167] Wald L, "SoDa: A project for the integration and exploitation of networked solar radiation databases", 2000 – http://www.soda-is.com

[168] http://edcdaac.usgs.gov/gtopo30/gtopo30.html

[169] Suri M, Hofierka J, "A new GIS based solar radiation model and its application to PV assessment", Transactions in GIS Vol. 8-2, pg. 175-190, 2004

[170] Rigollier C, Bauer O, Wald L, "On the clear sky model of ESRA with respect to the Heliosat method", Solar Energy Vol. 68-1, pg. 33-48, 2000

[171] Neteler M, Mitasova H, "Open Source GIS: A GRASS GIS approach", Springer, ISBN 978-0-387-35767-6, 2008

[172] http://re.jrc.ec.europa.eu/pvgis/solres/solmod3.htm

[173] Source: http://rredc.nrel.gov/solar/codes_algs/PVWATTS/

[174] Boyle G, "Renewable Energy", 2nd Edition, Oxford University Press, ISBN 0199261784, 2004

[175] Eicker U, "Solar Technologies for Buildings", Wiley, ISBN 0-471-48637-X, 2003

[176] Jones A, Underwood C, "A Thermal Model for Photovoltaic Systems", Solar Energy Vol. 70-4, pg 349-359, 2001

[177] Merrigan U, "Sunlight to Electricity", MIT Press, ISBN 0262131749, 1982

[178] Schott T, "Operational temperatures of PV modules", 6th PV Solar Energy Conference, pg 392-396, 1985

[179] Holman J, "Heat Transfer", McGraw Hill Higher Education, ISBN 007003002, 1994

[180] ASHRAE, "Handbook: Fundamentals", ASHRAE Publication, 1989

[181] Pratt A, "Heat Transmission in Buildings", Wiley, ISBN 0471279714, 1981

[182] Nishioka K, Hatayama T, Uraoka Y, Fuyuki T, Hagihara R, Watanabe M, "Field-test analysis of PV system output characteristics focusing on module temperature", Solar Energy Materials and Solar Cells Vol. 75, pg. 665-671, 2003

[183] Solarcentury, "C21 Solar Tiles & Slates – Datasheet", 2009

[184] Davis M, Dougherty B, Fanney A, "Prediction of Building Integrated Photvoltaic Cell Temperatures", US National Institute of Standards and Technology, DOI: 10.1115/1.1385825, 2001

[185] JONES, PATTERSON, "The Development of a Practical Evaluation Tool for Urban Sustainability", Indoor Built Environ 2007 Vol. 16 Issue 3 pg. 255–272, 2007

[186] Attia S, De Herde A, "Sizing Photovoltaic Systems during Early Design - A Decision Tool for Architects", American Solar Energy Society, SOLAR 2010 Conference Proceedings, 2010

[187] Sabry M, Ghitas A, "Effect of edge shading on the performance of silicone solar cell", Vacuum Vol. 80, pg 444-450, 2006

[188] CIBSE Guide J: Weather, Solar and Illuminance Data, CIBSE publication, 2002

[189] Tretheway R, "Residential building solar thermal analysis: A case study on Sophia Gordon Hall", MSc thesis, Tufts University, 2009

[190] Element Energy Ltd., "Numbers of micro-generation units installed in England, Scotland and Northern Ireland", Cambridge, 2008

[191] Energy Saving Trust, "CE131: Solar water heating systems – Guidance for professionals, conventional indirect methods", London, 2006

[192] OECD, "World energy lookout 2006", International Energy Agency, Paris, 2006

[193] EST, E-connect, Element Energy, "Potential for micro-generation: study and analysis", Energy Saving Trust, London, 2005

[194] Ward D, Ward S, "Design considerations for residential solar heating and cooling systems utilizing evacuated tube solar collectors", Solar Energy Vol. 22, pg 113-118, 1979

[195] Zhang, Yamaguchi, "An experimental study on evacuated tube solar collector using supercritical CO_2", Applied Thermal Engineering Vol. 28, pg. 1225-1233, 2008

[196] Turner L, Dale A, McKenzie B, "Solar heating for Home, Farm and small Business: Basic Facts about Collection, Storage and Utilisation", Purdue Extension Publications, WorldCat ID: 16788457, 2007

[197] Kim Y, Seo T, "Thermal performances comparisons of the glass evacuated tube solar collectors with shapes of absorber tube", Renewable Energy Vol. 32, pg. 772–795, 2007

[198] Harding G, Zhiqiang, D MacKey, "Heat extraction efficiency of a concentric glass tubular evacuated collector", Solar Energy Vol. 35-1, pg. 71-79, 1985

[199] Deutsche Gesellschaft fuer Sonnenenergie e.V. (German Society for Solar Energy), http://www.dgs-solar.org/, viewed 02/10/2010

[200] Theunissen P, Beckmann W, "Solar transmittance characteristics of evacuated tubular collectors with diffuse back reflectors", Solar Energy Vol. 35-4, pg. 311-320, 1985

[201] Zinian H, Hongchuan G, Jiang F, Wei L, "A comparison of optical performance between evacuated collector tubes with flat and semicylindric absorbers", Solar Energy Vol. 60-2, pg. 109-117, 1997

[202] Dehghan A, Barzegar A, "Thermal performance behaviour of a domestic hot water solar storage during consumption operation", Energy Conversion and Management Vol. 52-1, pg. 468-476, 2010

[203] Knudsen S, Furbo, "Thermal stratification in vertical mantle heat-exchangers with application to solar domestic hot-water systems", Applied Energy Vol. 78, pg. 257-272, 2004

[204] Fanney A, Klein S, "Thermal performance comparisons for solar hot water systems subjected to various collector and heat exchanger flow rates", Solar Energy Vol. 40-1, pg. 1-11, 1988

[205] Thuer et al, "Energy savings for solar heating systems", Solar Energy Vol. 80, pg 1463-1474, 2006

[206] The Solar Trade Association, http://www.solar-trade.org.uk/solarHeating/efficiency.cfm, viewed 04/11/2010

[207] Leckner M, Zmeureanu R, "Life cycle cost and energy analysis of a Net Zero Energy House with solar combisystem", Applied Energy Vol. 88, pg. 232-241, 2010

[208] Ardente F, Beccali G, Cellura M, Lo Bran V, "Life cycle assemssment of a solar thermal collector: sensitivity analysis, energy and environmental balances", Renewable Energy Vol. 30, pg. 109-130, 2005

[209] Menzies G, Roderick Y, "Energy and carbon impact analysis of solar thermal collector system", International Journal of Sustainable Engineering Vol. 3-1, pg. 9-16, 2009

[210] Hough T, "Trends in Solar Energy Research", pg. 152, Nova Science Publishers, ISBN 1-59454-866-8, 2006

[211] Whillier A., "Solar energy collection and its utilisation for house heating" ScD Thesis, MIT, 1953

[212] Liu B, Jordan R, "Availability of solar energy for flat-plate solar heat collectors", ASHREA GRP 170, 1977

[213] Klein S, Beckman W, Duffie J, "A design procedure for solar heating systems", *Solar Energy Vol. 8-2, pg. 113-127*, 1977

[214] RETscreen International can be accessed via http://www.retscreen.net/ang/home.php, viewed 10/10/2010

[215] Ellehauge K, "Solar Combisystems", Final Report of ALTENER Project, Denmark, 2003

[216] Kingman N, Rosenberg A, Bastos M, Wadso I, "Heat capacity of poly (ethylene glycol) – water mixtures: Poly (ethylene glycol) – water interactions", Thermochimica Acta Vol. 169, pg. 339-346, 1990

[217] Personal communication with Mr. Andy Beasley (solar certified plumber) confirmed 50% water-glycol mixture is typically used in solar thermal systems

[218] British Standard EN 12975: 2006, "Thermal Solar Systems and Components. Solar Collectors. Test Methods", BSI, 2006

[219] TYFOROP Chemie GMBH, "Tyfocor LS Technical Information", 1999, available at http://www.solaressence.co.uk/downloads/03%20TYFOCOR.pdf, viewed 10/10/2010

[220] Krapmeier H, "CEPHEUS Austria – Final Report", Energieinstut Vorarlberg, Austria, 2004

[221] Perers B, Bales C, "A Solar Collector Model for TRNSYS Simulation and System Testing", Solar Energy Research Centre SERC, 2002

[222] Budihardjo I, Morrison G, "Performance of water-in-glass evacuated tube solar water heaters", Solar Energy Vol. 83, pg. 49-56, 2009

[223] Pillai I, Banerjee R, "Methodology for estimation of potential for solar water heating in a target area", Solar Energy Vol. 81, pg. 162-172, 2007

[224] Kleinbach E, Beckman W, Klein S, "Performance Study of One-dimensional Models for Stratified Thermal Storage Tanks", Solar Energy Vol. 50-2, pg. 155-166, 1993

[225] Rad et al, "Combined solar thermal and ground source heat pump system", IBPS International conference, Glasgow, Scotland, 2009

[226] RETScreen International, "Solar Water Heating Project Analysis", 2004, available at www.retscreen.net

[227] Hollands K, Lightstone M, "A Review of Low-Flow, Stratified-Tank Solar Water Heating Systems", Solar Energy Vol. 43-2, pg 97-105, 1989

[228] El-Nashar, "The effects of dust accumulation on the performance of evacuated tube collectors", Solar Energy Vol. 53-1, pg. 105-115, 1994

[229] Press W, Flannery B, Teukolsky S, Vetterling W, "Numerical Resipes – The Art of Scientific Computing (Fortran Version)", Cambridge University Press, ISBN 0521383307, 1989

[230] North G, "Lessons from Energy Balance Models", Physically-based Modelling and Simulation of Climate and Climatic Change, Springer, pg. 627, ISBN 9027727899, 1988

[231] Manual Vaillant VTK540, Chapter 'Technical Information', pg. 39

[232] http://www.statsoft.com/textbook/distribution-tables/#t, viewed 21/09/2010

[233] Kemna R, van Elburg M, Li W, van Holsteijn R, "Eco-Design of water heaters", for European Commission, 2007

[234] Hill F, Lynch H, Levermore G, "Consumer impacts on dividends from solar water heating", Energy Efficiency, DOI: 10.1007/s12053-010-9086-2, 2010

[235] Allen S, "Micro-generation for UK households: thermodynamic and related analyses", PhD thesis, University of Bath, 2009

[236] BERR, "Energy consumption in the United Kingdom", Department for Business, Enterprise and Regulatory Reform, London, 2008

[237] Allen et al, "Integrated appraisal of micro-generators: methods and applications", Energy, Vol. 161-2, pg. 73-86, 2008

[238] Crawford R, Treloar G, Ilozor B, Love P, "Comparative greenhouse emissions of domestic solar hot water systems", Building Research and Information Vol. 31-1, pg. 34-47, 2003

[239] Battisti, Crawford R, "Environmental assessment of solar thermal collectors with integrated water storage", Journal of Cleaner Production Vol. 13, pg. 1295-1300, 2005

[240] Mathew S, "Wind Energy: Fundamentals, Resource Analysis and Economics", Springer, ISBN: 3-540-30905-5, 2006

[241] Celik A, Muneer T, Clarke P, "An investigation into micro wind energy systems for their utilization in urban areas and their life cycle assessment", Power and Energy Vol. 221, pg 1107-1117, 2007

[242] Bialek J, "Attempts to introduce locational marginal loss charging in the UK", 6th International Conference Advances in Power System Control, Operation and Management, pg. 108-116, Hong-Kong, 2003

[243] Clausen P, Wood D, "Recent advances in small wind turbine technology small wind turbines", Wind Engineering Vol. 24-3, pg. 189–201, 2000

[244] Rankine R, Chick J, Harrison J, "Energy and carbon audit of a rooftop wind turbine", Power and Energy Vol. 220, pg. 643-654, 2006

[245] Robinson P, "Small wind turbines for the urban environment: State of the art, case studies & economic analysis", Reading University, Energy Group, 2005

[246] Bussel G, Mertens S, "Small wind turbines for the built environment", 4th European and Asian Wind Engineering Conference, Prague, 2005

[247] Bahaj A, Meyers L, James P, "Urban energy generation: Influence of micro-wind turbine output on electricity consumption in buildings", Energy Buildings Vol.39-2, pg. 154-165, 2007

[248] Eliasson I, Offerle B, Grimmond C, Lindqvist S, "Wind fields and turbulence statistics in an urban street canyon", 2006, Elsevier, Atmospheric Environment Vol. 40, pg. 1–16, 2006

[249] Kastner-Klein P, Fedorovich E, Rotach M, "A wind tunnel study of organised and turbulent air motions in urban street canyons", Journal of Wind Engineering and Industrial Aerodynamics Vol. 89, pg. 849–861, 2001

[250] Akpinar E, "A statistical investigation of wind energy potential", Energy Sources Part A Vol. 28, pg. 807-820, 2006

[251] Boyle G, "Renewable Energy" , 2nd Edition, Oxford University Press, ISBN: 0199586519, 2004

[252] Hansen M, "Aerodynamics of Wind Turbines", 2nd Edition, James & James Ltd., ISBN 978-1-84407-438-9, 2007

[253] Wood D, "Dual Purpose Design of Small Wind Turbine Blades", Wind Engineering Vol. 28-5, pg. 511-527, 2004

[254] Lenzen M, Munksgaard J, "Energy and CO2 life-cycle analyses of wind turbines – review and applications", Renewable Energy Vol. 26, pg. 339-362, 2002

[255] IEC, "Inventory of Energy and Carbon", Version 1.6a, University of Bath, 2008

[256] International Standards Organisation, "ISO 14040: 1997 environmental management, life cycle assessment, principles and framework", ISO Geneva, 1997

[257] Domros R, "Energetische Amorsisationszeit von Windkraftanlagen auf Basis der Prozesskettenanalyse", Diploma Thesis, Technische Unversitaet Berlin, 1992

[258] Turan S, Peacock A, Newborough M, "Micro and Small Wind Turbine Applications in the Built Environment", ISESCO Science and Technology Vision Vol. 3-3, pg. 106-110, 2007

[259] Hillary J, Anderson M, Palutikof J, Watson S, Dunbabin P, Bunn J, Dukes M, Surguy I, "Assessment of the accuracy of BERR's database of UK wind speeds", ETSU W/11/00401/REP, 1995

[260] Department of Energy & Climate Change, NOABL Wind Speed Database, available at http://www.decc.gov.uk/en/content/cms/what_we_do/uk_supply/energy_mix/renewable/explained/wind/windsp_databas/windsp_databas.aspx, viewed 27/10/10

[261] Roth M, "Review of atmospheric turbulence over cities", Quarterly Journal of Royal Meteorological Society Vol. 126, pg. 941-990, 2000

[262] Holmes J, "Wind Loading of Structures", Spon Press, ISBN: 041924610, 2001

[263] Prandtl L, "The mechanics of viscous fluid" Aerodynamics Theory Vol. 3, pg. 34-208, 1935

[264] Australian Standard for Wind Loads, AS1170.2, 1989

[265] Zhou Y, Kijewski T, Kareem A, "Along-Wind Load Effects on Tall Buildings: Comparative Study of Major International Codes and Standards", Structural Engineering Vol. 128-6, pg. 788-796, 2002

[266] Allen S, "Micro-Generation in UK Households – Thermodynamic and related analyses", PhD Thesis, University of Bath, Department of Mechanical Engineering, 2009

[267] Domestic Wind Speed Prediction Tool, Energy Saving Trust, available at http://www.energysavingtrust.org.uk/Generate-your-own-energy/Can-I-generate-electricity-from-the-wind-at-my-home, viewed 26/10/10

[268] Wizelius T, "Developing wind power projects: theory and practice", Earthscan, ISBN: 978-1-84407-262-0, 2007

[269] Manwell J, McGowan J, Rogers A, "Wind energy explained: theory, design and application", Wiley & Sons, ISBN 9780471499725, 2002

[270] British Standard BS EN 61400-21, "Wind Turbines. Measurement and assessment of power quality characteristics of grid connected wind turbines", BSI, ISBN 9780580567506, 2008

[271] Windographer, wind data analysis and modelling software, http://www.mistaya.ca/index.htm, viewed 28/10/10

[272] Lilienthal P, "HOMER micropower optimization model", DOE Solar Energy Technologies Program Review Meeting, Denver, 2004

[273] Encraft, Warwick Wind Trials Final Report, available at: http://www.warwickwindtrials.org.uk, accessed on 08-07-2010

[274] Makkawi A, Celik A, Muneer T, "Evaluation of micro-wind turbine aerodynamics, wind speed sampling interval and its spatial variation" Building Serv. Eng. Res. Technol Vol. 30-1, pg. 7-14, 2009

[275] Heath M, Walshe J, Watson S, "Estimating the potential yield of small building-mounted wind turbines", Wind Energy Vol. 10, pg 271-287, 2007

[276] Micro Wind Turbines were observed that are mounted on the roof of Portland Tower, Portland St., M13HA, Manchester

[277] Wright A, Wood D, "The starting and low wind speed behaviour of a small horizontal axis wind turbine", Wind Engineering and Industrial Aerodynamics Vol. 92, pg. 1265-1279, 2004

[278] Wood D, "A Blade Element Estimation of the Cut-in Wind Speed of a Small Turbine", Wind Engineering Vol. 25, pg 249-255, 2001

[279] Liu S, Bian Z, Li D, Zhao W, "A Magnetic Self-pitch Vertical Axis Wind Turbine", Power and Energy Engineering Conference (APPEEC), 2010

[280] Muller G, Jentsch M, Stoddart E, "Vertical axis resistance type wind turbines for use in buildings", Renewable Energy Vol. 34, pg. 1407-1412, 2009

[281] Cace´ J, et al., "Urban Wind Turbines: Guidelines for Small Wind Turbines in the Built Environment", available at www.urbanwind.org, viewed 08-07-2010

[282] EST, "Location, Location, Location – Domestic small-scale wind field trial report", Energy Saving Trust, London, 2009

[283] Celik A, Muneer T, Clarke P, "An investigation into micro wind energy systems for their Utilization in urban areas and their life cycle assessment" Journal of Power and Energy Vol. 221-8, pg. 1107–1117, 2007

[284] Bahaj A, Myers L, James P, "Urban energy generation: Influence of micro-wind turbine output on electricity consumption in buildings", Energy and Buildings Vol. 39, pg. 154–165, 2007

[285] Allen S, Hammond G, McManus M, "Energy analysis and environmental life cycle assessment of a micro-wind turbine", Journal of Power and Energy Vol. 222, pg. 669-684, 2007

[286] Rybach L, Sanner B, "Ground-Source Heat Pump Systems – The European Experience", Geo-Heat Centre Bulletin, Institute of Geophysics ETH Zurich Switzerland, 2000

[287] Lund J, Sanner B, Rybach L, Curtis R, Hellstrom G, "Geothermal (Ground-Source) Heat Pumps – A World Overview", Geo-Heat Centre Bulletin, Oregon Institute of Technology USA, 2004

[288] Curtis R, "Earth Energy in the UK", Geo-Heat Centre Quarterly Bulletin Vol. 22-4, 2001

[289] Sanner B, Karytsas C, Mendrinos D, Rybach L, "Current status of ground source heat pumps and underground thermal energy storage in Europe", Geothermics Vol. 32, pg. 579-588, 2003

[290] L'Ecuyer M, Zoi C, Hoffman J, "Space Conditioning: The next frontier", US Environmental Protection Agency, Washington DC USA, 1993

[291] Okkan P, "Reducing CO2 emissions – How do heat pumps compete with other options?", IEA Heat Pump Centre Newsletter Vol. 11-3, pg. 24-26, 1993

[292] Rognon F, "Heat pumps and ecological balances" IEA Heat Pump Centre Newsletter Vol. 15-2, pg. 26-28, 1997

[293] British Standard, "BS EN15450:2007 – Heating systems in buildings. Design of heat pump heating systems", BSI, ISBN 9780580563850, 2007

[294] Doherty P, Al-Huthalili S, Riffat S, Abodahab N, "Ground source heat pump – description and preliminary results of the Eco House system", Applied Thermal Engineering Vol. 24, pg. 2627-2641, 2004

[295] EST, "CE82 Energy Efficiency Best Practice in Housing - Domestic Ground Source Heat Pumps", Energy Saving Trust publication, 2004

[296] Rawlings R, Sykulski J, "Ground Source Heat Pumps: A Technology Overview", BSERT Vol. 20-3, pg. 119-129, 1999

[297] Genchi Y, Kikegawa Y, Inaba A, "CO2 payback-time assessment of a regional-scale heating and cooling system using a ground-source heat-pump in a high energy-consumption area of Tokyo", Applied Energy Vol. 71, pg. 147-160, 2002

[298] Lee C, Lam H, "Computer simulation of borehole ground heat exchangers for geothermal heat pump systems", Renewable Energy Vol. 33, pg. 1286-1296, 2008

[299] Nagano K, Katsura T, Takeda S, "Development of a design and performance prediction tool for the ground source heat pump system" Applied Thermal Engineering Vol. 26, pg. 1578-1592, 2006

[300] Nam Y, Ooka R, Hwang S, "Development of a numerical model to predict heat exchange rates from a ground-source heat pump system", Energy and Buildings Vol. 40, pg. 2133-2140, 2008

[301] Hopkirk R, Kaelin B, "Analysis of vertical tube heat exchangers for design optimisation" IEA Heat Pump Centre, Proceedings of Workshop on Ground Source Heat Pumps Montreal, pg. 149-168, 1991

[302] Barratt Development PLC, Buckshaw EcoSmart Show Village Promotional Material, 2006

[303] Geothermal Ltd., Technical information brochure for GSHP system, 2006

[304] Yavuzturk C, "Modeling of vertical ground loop heat exchangers for ground source heat pump systems", PhD Thesis, Technische Universitaet Berlin, 1999

[305] Lamarche L, "A fast algorithm for the hourly simulations of ground-source heat pumps using arbitrary response factors", Renewable Energy Vol. 34, pg. 2252-2258

[306] Hepbasil A, "Thermodynamic analysis of a ground-source heat pump system for district heating", Energy Research Vol. 29, pg. 671-687, 2005

[307] Dong L, Liu H, Riffat S, "Development of small-scale and micro-scale biomass-fuelled CHP systems – A Literature review", Applied Thermal Engineering Vol. 29, 2119-2126, 2009

[308] Crozier-Cole T, Jones G, "The potential market for micro CHP in the UK", Report to Energy Saving Trust, P00548, 2002

[309] Meijer I, Hekkert M, Koppenjan J, "How perceived uncertainties influence transitions; the case of micro-CHP in the Netherlands", Technological Forecasting & Social Change Vol. 74, pg. 519-537, 2007

[310] d'Accadia M, Sasso M, Sibilio S, Vanoli L, "Micro-combined heat and power in residential and light commercial applications", Applied Thermal Engineering Vol. 23, pg. 1247-1259, 2009

[311] Finkelstein T, Organ A, "Air Engines: The history, science and reality of the perfect engine", ASME Press, ISBN 0791801713, 2001

[312] Bell M, Swinton M, Entchev E, Gusdorf J, Kalbfleisch W, Marchand R, Szadkowski F, "Development of micro combined heat and power technology assessment capability at the Canadian Centre for Housing Technology", Final Report B-6010, Ottawa Canada, 2003

[313] Entchev E, Gusdorf J, Swinton M, Bell M, Szadkowski F, Kalbfleisch W, Marchand R, "Micro-generation technology assessment for housing technology", Energy and Buildings Vol. 36, pg. 925-931, 2004

[314] De Paepe, D'Hert P, Mertens D, "Micro-CHP systems for residential applications", Energy Conversion and Management Vol. 47, pg. 3435-3446, 2006

[315] E.ON UK Report "Performance of Whispergen micro CHP in UK homes", Based on data from Carbon Trust micro CHP Field Trial, 2006

[316] ORNL, "List of conversion factors", Bioenergy Feedstock Development Program, available at http://bioenergy.ornl.gov/papers/misc/energy_conv.html, viewed 28/10/10

[317] Personal correspondence between Dr. Tony Sung (former project supervisor) and Barratt Development PLC.

[318] Cockroft J, Kelly N, "A comparative assessment of future heat and power sources of the UK domestic sector", Energy Conversion and Management Vol. 47, pg. 2349-2360, 2006

[319] Peacock A, Newborough M, "Impact of micro-CHP systems on domestic sector CO_2 emissions", Applied Thermal Engineering Vol. 25, pg. 2653-2676, 2005

[320] Ben Maalla E, Kunsch P, "Simulation of micro-CHP diffusion by means of System Dynamics", Energy Policy Vol. 36, pg. 2308-2319, 2008

Appendices

A. PV Watts and PV SYST Comparison

PV WATTS

PV Watts[321], developed by the RReDC[322], is also a freely available web-based tool. It requires the following user input:

- Location, where 9 different locations can be selected from for the UK
- PV System DC Rating
- DC to AC Derate Factor to calculate losses, comprising:
    - Inverter / Transformer efficiency
    - Diodes, connections and mismatch losses
    - Wiring losses
    - Soiling losses
    - Shading losses
    - Age
- Array Type, including options for fixed tilt or sun tracking
- Array tilt & azimuth
- Energy supply data, should the user wish to estimate energy bill savings

As for PV GIS, typical values have been suggested for each of the losses to improve user-friendliness, but can be adjusted individually if known. A separate help file is also available, providing explanations of parameters that may be unclear.

PV WATTS Method

The PV WATTS calculator uses actual representative samples of historic weather data, rather than averages based on historic weather data. These were chosen from several historic decades and comprise hourly values.

To calculate the output PV WATTS determines the solar radiation incident to the selected PV plane, as well as the module temperature for each hour of the year. The program then calculates the DC energy for each hour based on the radiation and the DC rating of the PV module. In order to calculate the AC output of the system, PV WATTS multiplies the DC values by the *AC Derate Factor*, which has been previously specified by the user. The previously specified inverter efficiency is adjusted for each hour as a function of the output load. After calculating the hourly

values of AC energy, these values are then summarised as monthly and annual energy generation estimates.

PV WATTS Results

Input parameters were chosen that best represent the set-up. The chosen UK location was Aughton near Ormskirk, (53.55° Latitude, –2.92° Longitude), at a distance of approximately 15 miles from the test site. The derate factor was chosen at 0.86 in order to use the same value as for the PV GIS simulation (which used a value of 14% for system losses).

PV SYST

PV SYST is a stand-alone program, requiring installation and licensing. The full license is available for 900CHF (around £450) from the Swiss University of Geneva. The weather data, which can be selected from many sources, consists of hourly intervals. As a unique feature it also allows weather data to be imported manually. The following input is required:

- Location, can be chosen from a list or created using a separate tool
- Weather data, which can be selected from one of many databases or imported manually
- Horizon, where the user can manually specify any terrain (or building) shading
- System, where information including size, tilt and orientation are specified
- Module type and technology
- Mounting type and ventilation

Although not standard input options, some calculation parameters can also be adjusted by the user, including:

- Standard module efficiency for different module types
- Temperature correction factors
- Wiring losses
- Inverter efficiency

With this many input options PV SYST is very flexible, albeit not quite as user-friendly as the two web-based estimation tools. Like PV GIS, this tool is also able to

calculate the optimum inclination and orientation, as well as given the effective losses incurred by moving away from this optimum.

PV SYST Method

Using global solar radiation as a basis, an hourly model is used to calculate in-plane direct beam radiation and the diffuse component, the module temperature and the DC generation. A model validation[323] using measurements found the following range of errors:

- up to 10% for beam / diffuse model
- ± 4°C for module temperature
- Root mean square error up to 2.24% for DC output

With the DC generation determined, an inverter model is used to simulate to provide AC output. Inverters can be modelled based on user specifications, a tool for this approach is provided.

Based on the independent validation, the creators of PV SYST are confident that the error margin of the final results of the simulation is in the order of 2-3%.

PV SYST Results

Again, all parameters were specified to best represent the set-up. A location was created with exact Latitude and Longitude, and the artificial horizon specified based on observations. Standard NASA satellite weather data was selected to simulate a case where little data is available. For better accuracy determination, a second test was carried out for the Malvern building, where imported weather data was used. Settings for system losses were kept at default values.

PV Estimation Tools – Qualitative Comparison

After the accuracy of all tools has been established, some other factors are also considered. These are outlined below.

Accuracy: All tools provide acceptable accuracy, where PV WATTS appears to have an inherent flaw when converting angles. PV GIS benefits from its high flexibility, giving the most accurate results after adjusting losses to real values. PV SYST can be very accurate if recent local weather data is imported. PV WATTS does not appear to account for any shading, while this is automatically calculated by PV GIS.

Weather Data: PV GIS uses the comprehensive ESRA database, which is further interpolated to give a refined and accurate spread of data. PV SYST excels in this area, providing a choice of several data bases and providing an import option. However, this may also make it hard to find the most accurate data set. PV WATTS was designed for use in North America, only providing 9 fixed locations for UK weather samples. For better comparison, the standard weather is compared to the CIBSE Test Reference Year for the near-by location of Manchester. The comparison, giving good correlation of within 6% for all sets, is shown in Figure 17.1.

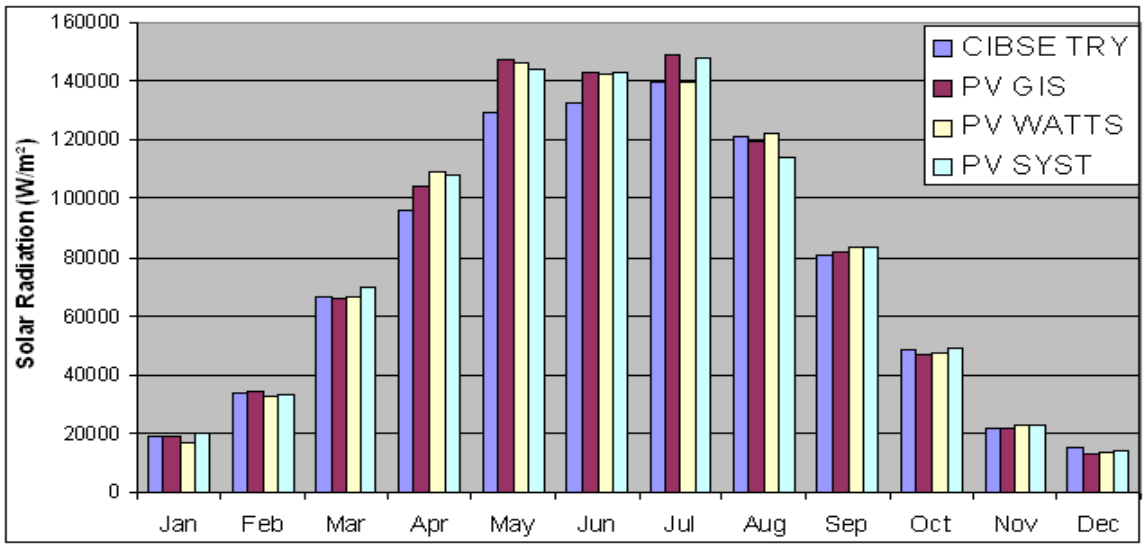

Figure 17.1: Monthly comparison of solar radiation on horizontal surface between CIBSE test reference year and solar estimation tools

Output: PV GIS and PV SYST are able to provide very comprehensive and detailed sets of results, including optimum PV angles. In particular for PV GIS all losses are specified, and in-plane irradiance presented in numeric and graphical form. PV WATTS is purely focussed on providing a numerical generation estimate, but similar to PV SYST it is also able to estimate financial savings.

Ease of Use: PV GIS has a very user-friendly and flexible interface incorporating Google Maps. Data entry is done on one page and can be done very quickly. The PV WATTS locations choices are somewhat ambiguous, but good advice provided for estimating errors. PV SYST provides many input options that can be challenging and confusing for inexperienced user. The incorporation of tools provides flexibility but results in an overall lengthy process before getting a result.

Adjustability: PV GIS allows adjusting system losses, explore a system with sun-tracking capabilities, obtained detailed meteorological data for the given location

and optimum PV angles. A unique consideration for building-integrated systems is also given. PV WATTS has similar flexibility. While unable to obtain the optimum system set-up, it provides a comprehensive 'AC derate factor calculator'. Not having an option to choose between different PV technologies can be limiting. PV SYST is a very powerful tool, allowing the user to adjust the PV estimates for almost any possible scenario.

Accessibility and Cost: PV GIS and PV WATTS are free web-based software tools. Assuming an Internet connection, they are accessible anywhere around the world. PV SYST on the other hand is a stand-alone program, which requires a local installation as well as licensing. A full license costs £450. However, the software is available for download from the internet and has a 10-day trial period.

B. Visitor Feedback Questionnaire

BARRATT ECO SMART SHOW VILLAGE

We are very interested in learning which of the innovative 'green' technologies used in this village are of most interest to you and which you would like Barratt to introduce in new homes in the future. To assist us, please complete this questionnaire as you look around the Show Village and return it to the Information Centre.
Thank you for your assistance.

Rainwater Harvesting System
(for example in THE MALVERN, house number 1)

This system recycles rainwater for washing machines, toilets and the garden, saving a large percentage of mains water use. This would cost around £2,000 extra on a new home and save around £60 per year.

1) Setting aside thoughts on price, how **appealing** is having a Rainwater Harvesting System in a new home?

- Extremely ☐
- Slightly ☐
- Undecided ☐
- Not at all ☐

2) Considering the price and the potential savings, would you be prepared to pay this amount to have this Rainwater Harvesting system in a new home?

Definitely ☐ Probably ☐ Undecided ☐ Probably not ☐ Definitely not ☐

Please answer Q3

3) If not, what is the maximum price you would be prepared to pay for the Rainwater Harvesting System?

£ _____ (Please write in)

Small Wind Turbine
(for example in THE WINDERMERE, house number 2)

Electricity produced by these wind turbines reduces the amount of conventional electricity required and therefore reduces carbon dioxide emissions (by around 283kg per year) and fuel bills. It would cost around £2,250 extra on a new home and save around £53 per year.

1) Setting aside thoughts on price, how **appealing** is having a Small Wind Turbine System in a new home?

- Extremely ☐
- Slightly ☐
- Undecided ☐
- Not at all ☐

2) Considering the price and the potential savings, would you be prepared to pay this amount to have this Small Wind Turbine system in a new home?

Definitely ☐ Probably ☐ Undecided ☐ Probably not ☐ Definitely not ☐

Please answer Q3

3) If not, what is the maximum price you would be prepared to pay for the Small Wind Turbine System?

£ _____ (Please write in)

Solar Thermal Energy Collector Panels
(for example in THE ALDERNEY, house number 3)

These panels use the sun's heat to provide hot water, and can reduce the need for conventional water heating by about two thirds and therefore reduce carbon dioxide emissions (by around 1007kg per year). This would cost around £3,500 extra on a new home and would save around £111 per year.

1) Setting aside thoughts on price, how **appealing** is having a Solar Thermal Energy Collector Panel System in a new home?

- Extremely ☐
- Slightly ☐
- Undecided ☐
- Not at all ☐

2) Considering the price and the potential savings, would you be prepared to pay this amount to have this Solar Thermal Energy Collector Panel system in a new home?

Definitely ☐ Probably ☐ Undecided ☐ Probably not ☐ Definitely not ☐

Please answer Q3

3) If not, what is the maximum price you would be prepared to pay for the Solar Thermal Energy Collector Panel System?

£ _____ (Please write in)

Geothermal Heating System
(for example in THE PALMERSTON, house number 4)

This system transfers natural heat from the ground into the home, for hot water or underfloor heating and therefore reduces carbon dioxide emissions (by around 1224kg per year). This would cost around £7,800 extra on a new home and save around £79 per year.

1) Setting aside thoughts on price, how **appealing** is having a Geothermal Heating System in a new home?

- Extremely ☐
- Slightly ☐
- Undecided ☐
- Not at all ☐

2) Considering the price and the potential savings, would you be prepared to pay this amount to have this Geothermal Heating system in a new home?

Definitely ☐ Probably ☐ Undecided ☐ Probably not ☐ Definitely not ☐

Please answer Q3

3) If not, what is the maximum price you would be prepared to pay for the Geothermal Heating System?

£ _____ (Please write in)

Micro Combined Heat and Power Unit
(for example in THE EDINBURGH, house number 6)

This system typically uses 35% less energy than conventional systems to produce electricity and hot water, and therefore reduces carbon dioxide emissions (by around 750kg per year) and gas consumption. This would cost around £2,700 extra in a new home and save around £108 per year

1) Setting aside thoughts on price, how **appealing** is having a Micro Combined Heat and Power Unit System in a new home?

- Extremely ☐
- Slightly ☐
- Undecided ☐
- Not at all ☐

2) Considering the price and the potential savings, would you be prepared to pay this amount to have this Micro Combined Heat and Power Unit system in a new home?

Definitely ☐ Probably ☐ Undecided ☐ Probably not ☐ Definitely not ☐

Please answer Q3

3) If not, what is the maximum price you would be prepared to pay for the Micro Combined Heat and Power System in a new home?

£ _____ (Please write in)

Based on the systems you have viewed today, we would now like you to rank the 5 systems below in order of importance, i.e. which you would most like to be introduced into new homes, with 1 being most important and 5 being least important.

Rainwater Harvesting System	_____	Geothermal Heating Systems	_____
Small Wind Turbine	_____	Micro Combined Heat and Power Unit	_____
Solar Thermal Energy Collector Panels	_____		

Below is a list of statements about being environmentally friendly. Please indicate for each statement how much you agree or disagree.

	Strongly Agree	Agree	Neither Agree nor Disagree	Disagree	Strongly Disagree
I would pay extra for my home to be more environmentally friendly, even if I might not make the costs back in savings on energy bills.	☐	☐	☐	☐	☐
I would like my home to be environmentally friendly, but only if I made the extra cost back in savings.	☐	☐	☐	☐	☐
I would not spend extra on environmentally friendly technology, even if it might be cheaper in the long term.	☐	☐	☐	☐	☐
I would be prepared to make lifestyle compromises, e.g. not have a power shower, if it meant my home was more environmentally friendly.	☐	☐	☐	☐	☐

The next set of questions are used to divide our responses into groups

Please indicate your gender: **Male** ☐ **Female** ☐

Please indicate your age:

Under 18 years	☐	**45 to 54 years**	☐
18 to 24 years	☐	**55 to 64 years**	☐
25 to 34 years	☐	**65 years or over**	☐
35 to 44 years	☐		

What was the key purpose Of your visit to the EcoSmart Show Village today? **(Tick all that apply)**

- **I intend to buy a new house in the near future** ☐
- **I have a particular interest in environmental issues** ☐
- **Other (Please write in):** _____ ☐

Which of the following groups comes closest to your household's yearly income?

£19,999 or under	☐	**£80,000-£99,999**	☐
£20,000-£39,999	☐	**£100,000 or more**	☐
£40,000-£59,999	☐	**Don't Know / Refuse**	☐
£60,000-£79,999	☐		

Thank you for completing this questionnaire. We would welcome any other comments you would like to make or ideas for saving energy in new homes. Please write in below or on a separate sheet of paper.

If you are willing to take part in market research about the EcoSmart Show Village in the future, please provide contact details below. PLEASE NOTE, WE WILL ONLY CONTACT YOU FOR PURPOSES OF RESEARCH NOT FOR THE PURPOSE OF SELLING.

Name: _____

Address: _____

_____

Tel. No. _____

THANK YOU FOR COMPLETING THIS QUESTIONNAIRE
PLEASE RETURN IT TO THE INFORMATION CENTRE

[321] Source: http://rredc.nrel.gov/solar/codes_algs/PVWATTS/

[322] The Renewable Resource Data Center, USA

[323] P. Perez, P. Ineichen, R. Seals, J. Michalsky, R. Steward "Modelling Daylight Availability and Irradiance Component from Direct and Global Irradiance", Solar Energy Vol. 44-5, pg. 271-289, 1990